Food for microbes. The interplay between indigestible carbohydrates, gut microbiota, and cardiometabolic disease

Hoving, L.R.

Citation

Hoving, L. R. (2019, January 31). *Food for microbes. The interplay between indigestible carbohydrates, gut microbiota, and cardiometabolic disease*. Retrieved from https://hdl.handle.net/1887/68263

Cover Page

Universiteit Leiden

Leiden University Repository

The following handle holds various files of this Leiden University dissertation:
http://hdl.handle.net/1887/68263

Author: Hoving, L.R.
Title: Food for microbes. The interplay between indigestible carbohydrates, gut microbiota, and cardiometabolic disease
Issue Date: 2019-01-31

FOOD FOR MICROBES

THE INTERPLAY BETWEEN INDIGESTIBLE
CARBOHYDRATES, GUT MICROBIOTA,
AND CARDIOMETABOLIC DISEASE

Lisa Hoving

FOOD FOR MICROBES

The interplay between indigestible carbohydrates, gut microbiota,
and cardiometabolic disease

Cover design & Layout	Malou-Amber	www.malou-amber.com
Printing	Ridderprint	www.ridderprint.com
ISBN:	978-94-6299-978-7

FOOD FOR MICROBES

THE INTERPLAY BETWEEN INDIGESTIBLE CARBOHYDRATES, GUT MICROBIOTA, AND CARDIOMETABOLIC DISEASE
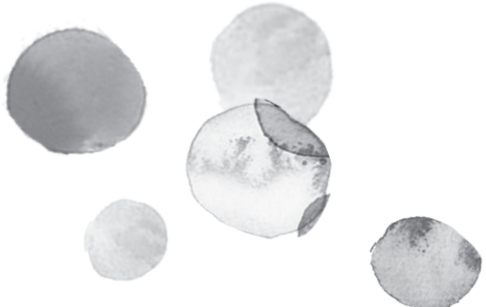
Proefschrift

Ter verkrijging van de graad tot
Doctor aan de Universiteit Leiden, op gezag
van Rector Magnificus prof. mr. C.J.J.M.
Stolker volgens besluit van het College voor
Promoties te verdedigen op donderdag
31 januari 2019 klokke 11:15 uur

Door

Lisa Rianne Hoving
Geboren te Groningen
In 1987
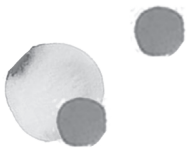
Promotor   Prof. dr. ir. K. Willems van Dijk

Copromotor   Dr. V.J.A. van Harmelen

Leden promotiecommissie

Mw. Prof. dr. M. Yazdanbakhsh

Dr. M. Giera

Prof. dr. ir. S. Kersten

Prof. dr. F. Kuipers

⫷⫷⫷

TABLE OF CONTENTS

————— ❰❰❰❰ —————

GENERAL INTRODUCTION

01

CARDIOMETABOLIC DISEASE

Cardiometabolic disease represents a cluster of metabolic abnormalities that are risk factors for cardiovascular disease (CVD) including atherosclerosis. The world is facing an epidemic increase in atherosclerosis which is currently one of the major leading causes of deaths worldwide [1]. Cardiometabolic disease is predominantly driven by overweight and obesity and is further characterised by insulin-resistant glucose metabolism, dyslipidemia and hypertension which can ultimately lead to atherosclerosis. The mechanisms responsible for developing cardiometabolic disease are intensively investigated, and it is generally acknowledged that hyperlipidemia and inflammation play a prominent role.

HYPERLIPIDEMIA AND INFLAMMATION IN CARDIOMETABOLIC DISEASE

OBESITY AS A PRECURSOR FOR TYPE 2 DIABETES AND ATHEROSCLEROSIS

Obesity develops as a result of a long-term positive energy balance where energy intake exceeds energy expenditure. After a meal, dietary triglycerides (TG) and cholesterol are taken up by intestinal cells, which assemble the lipids into TG-rich lipoproteins named chylomicrons, that subsequently travel via the lymph to the blood. From the blood, chylomicrons can provide skeletal muscle and white adipose tissue (WAT) TG-derived fatty acids (FA). The TG-depleted chylomicrons or chylomicron-remnants are cleared by the liver. The majority of the cholesterol in the chylomicrons is ultimately used as a component of cell membranes and as precursor for synthesis of bile acids (BAs), steroid hormones, and vitamin D.

Excess energy intake that is not used for the production of energy in various tissues will be stored primarily in WAT, causing WAT to expand. However, excessive WAT expansion lead to dysfunctional WAT that renders a pro-atherogenic profile (reviewed in [2]). In brief, the balance between TG storage and TG removal from adipocytes determines WAT mass. The removal of TG from WAT is dependent on intracellular lipolysis in which TG are broken down to FA and released from the adipocytes into the circulation. In healthy conditions, circulating free fatty acids (FFA) can be oxidised in other organs such as muscle, liver and brown adipose

tissue. Obesity on the other hand is characterised by hypertrophy of white adipocytes together with increased release of FA into the circulation due to both elevated basal lipolytic rate as well as a reduced regulated lipolysis response to insulin [3,4]. The decreased response of expanded WAT to insulin can be a result of increased WAT inflammation. For example, extensive WAT hypertrophy stresses adipocytes and induces the secretion of inflammatory proteins (adipokines) which subsequently attract pro-inflammatory leukocytes that also release pro-inflammatory cytokines and chemokines into the circulation [5,6]. In the presence of WAT inflammation, the inflammatory cytokines tumour necrosis factor α (*Tnf-α*) and interleukin-6 (*IL-6*) have been shown to directly inhibit the insulin signalling pathway and thereby induce insulin resistance predominately in WAT itself, liver, and muscle [7–10]. The numbers of pro-inflammatory M1 macrophages and cytotoxic T cells in expanded WAT are increased, whereas the numbers of anti-inflammatory M2 macrophages and regulatory T cells are reduced [11,12]. In addition to macrophages and T cells, increased abundance of B cells and neutrophils and reduced abundance of eosinophils are also hallmarks of WAT inflammation [13–15]. This increased pro-inflammatory state in expanded WAT is also associated with the development of glucose intolerance and type 2 diabetes. After a meal, plasma glucose levels rise and in response insulin is released by the pancreas. Insulin acts on its target tissues including muscle, liver and adipose tissues and induces the uptake of glucose by these tissues which subsequently lowers plasma glucose again [16]. However, inhibition of insulin signalling by e.g. dysfunctional expanded WAT leads to hyperglycemia, signalling the pancreas to produce more insulin. Progressive insulin resistance and compensatory increases in insulin production will ultimately result in failure of the pancreas and the development of type 2 diabetes [9,17,18].

The combination of insulin resistance and the rise in circulating FFA in obesity leads to reduced FFA oxidation and therefore decreased clearance of FFA from the circulation by other organs [19]. The excess FFA that cannot be oxidised by other organs build up in plasma and can serve as a substrate for hepatic TG-rich very-low-density lipoprotein (VLDL) production [20]. Hepatic TG-VLDL are either synthesised *de novo*, extracted from the circulation as non-esterified FA, or recycled from lipoprotein remnants cleared by hepatic

receptors. As a consequence, plasma levels of TG-VLDL are increased, called hypertrigly-ceridemia. TG-VLDL particles carry 90% of the plasma TG in the fasted state. TG-VLDL are substrates for the lipolytic enzyme lipoprotein lipase (LPL) mediating TG removal, which finally renders smaller lipoprotein particles with a low density of TG and relatively high in cholesterol, called low-density lipoproteins (LDL). High levels of plasma cholesterol is called hypercholesterolemia. WAT Inflammation, systemic inflammation, hypertriglyceridemia, and hypercholesterolemia form major risk factors for the development of atherosclerosis.

ATHEROSCLEROSIS

The development of atherosclerosis is thought to start with some form of damage of the arterial wall, for example due to high shear stress caused by the blood flow, allowing for the retention of LDL to infiltrate and accumulate in the sub-endothelial space of the arterial wall. These trapped lipoproteins are subject to oxidation resulting in oxidised LDL (oxLDL)[21]. The presence of oxLDL activates endothelial cells to express adhesion molecules. Adhesion molecules form the entry point for monocytes to invade the arterial wall where they differentiate towards macrophages. These macrophages scavenge oxLDL which under chronic conditions results in the formation of lipid-laden foam cells and a fatty streak in the arterial wall. This fatty streak is the hallmark of atherosclerosis development [22]. Activated endothelial cells and foam cells also produce pro-inflammatory cytokines and chemokines, leading to proliferation of vascular smooth muscle cells (VMCs) that produce a collagen cap, and attraction of more immune cells towards the lesion. Due to cell death within the lesion, a necrotic core may be formed, containing dead cell debris and cholesterol crystals that are released from foam cells.

The shape and cellular composition of arteries is dynamic and the arterial wall can respond to the presence of lesions by vascular remodelling. Inward vascular remodelling in arteries results in lumen loss, whereas outward vascular remodelling can compensate for lumen loss due to plaque accumulation in the arterial wall [23]. Outward remodelling together with a preserved luminal area often indicates a plaque phenotype that is more vulnerable to rupture [24]. A stable plaque phenotype is defined by a thick collagen cap and a small necrotic core. In

contrast, an unstable plaque is characterised by a low collagen content and thin cap [25], a large necrotic core and a high amount of macrophages within the lesion [21]. An unstable plaque prone to rupture might cause a local thrombotic event and the formation of a thrombus that will stop the blood flow at the site of the lesion, or at some distant site. Occlusion of arteries in the heart can cause an infarction and in the brain it can cause a stroke [21].

Taken together, hyperlipidemia and inflammation play an important role in the development of cardiometabolic disease, including atherosclerosis. Therapeutic interventions that can both decrease hyperlipidemia and inflammation may help to mitigate the underlying pathologies of cardiometabolic disease. Although relatively efficient drugs are available that inhibit the development of atherosclerosis by targeting plasma cholesterol levels and inflammation directly, additional strategies that reduce inflammation and hyperlipidemia are urgently required. Recently, it has become clear that factors deriving from the intestinal tract play a role in the initiation and progression of cardiometabolic disease [26,27].

GUT MICROBIOTA

GASTROINTESTINAL TRACT AND GUT MICROBIOTA COMPOSITION

The gastrointestinal tract comprises the entire path from mouth to stomach, duodenum, jejunum, ileum, cecum, and colon. The major functions of the gastrointestinal tract are to extract and absorb energy and nutrients from food we ingest, and excrete the remaining waste as feces [28]. Although the digestive process starts in the mouth, a substantial part of the enzymatic digestion of food takes place in the small intestine, whereas the remainder of the food components that cannot be digested in the small intestine will reach the cecum and colon of the large intestine. Predominantly complex carbohydrates, but also proteins, which are not digested by host enzymes in the upper gut, are metabolised by gut bacteria in the distal gut [29].

Microorganisms that specifically live within the intestinal tract are collectively known as gut microbiota. This gut microbiota harbours bacteria, viruses, fungi, archaea, and protozoa.

New molecular techniques such as next generation sequencing have made it possible to further identify and study the composition of the human gut microbiota [30–32]. It is estimated that the gut microbiota harbour some 10^{14} bacteria and consists of more than 1000 different bacterial species [33,34]. In the jejunum and ileum, the diversity of the microbiota composition is greater than in the duodenum and is composed of mainly anaerobic bacteria. The gut microbiota can be classified using phylogenetic trees, ranging from kingdom, phylum, class, order, family, genus, to species level. The dominant phyla in human gut microbiota are *Bacteroidetes* and *Firmicutes* [35], but many other phyla are present, including *Actinobacteria*, *Proteobacteria*, and *Verrucomicrobia* [36]. Most of the species are difficult or impossible to cultivate *in vitro*, due to required anaerobic conditions and unknown substrate requirements. However, exploitation of new analytical techniques based on genomics, proteomics and metabolomics approaches, makes it possible to obtain more insight into the diversity of the gut microbiota, their metabolic activities, and their functions and effects on the host [37–39].

GUT MICROBIOTA SYMBIOSIS AND DYSBIOSIS

Babies acquire intestinal microbiota from the mother and environment during and after birth and are thus affected by mode of delivery and neonatal nutrition. The gut microbiota composition diversifies after the first few years of life, and will eventually converge an adult-like phylogenetic structure [40,41]. Although gut microbiota composition within each individual has been reported to be relatively stable over time [42,43], the intestinal microbiota composition varies greatly between individuals [36,44]. Major differences in gut microbiota composition can be caused by changes in environmental factors such as diet, exercise, medication use, hygiene as well as by specific diseases [39,45–47].

In a symbiotic relationship, interactions between the host and the gut microbiota play a crucial role in the maintenance of normal physiology by extracting remaining energy from food components, shaping the immune system, offering protection against invading pathogens, and by producing essential vitamins [48,49]. Despite strictly controlled interactions between host and gut microbiota, the symbiotic relationship of the host and intestinal microbiota can

become impaired. Dysbiosis is a term for gut microbiota imbalance or maladaptation inside the body and is thought to be associated with disease. Abundant scientific evidence indicates that the increased prevalence of obesity, type 2 diabetes, and atherosclerosis cannot be attributed solely to changes in the human genome, nutritional habits, or reduced physical activity in our daily lives [50], but by the gut microbiota as well [51–55].

GUT MICROBIOTA DYSBIOSIS, OBESITY AND TYPE 2 DIABETES

The mechanisms linking gut microbiota and cardiometabolic disease are under intense investigation. The role of gut microbiota in energy homeostasis and obesity development has been pioneered by Bäckhed *et al.* They found that mice raised in the absence of microorganisms, i.e. germ-free (GF) mice, had about 40% less total body fat than mice with normal gut microbiota, even though GF mice ate 30% more than the conventional mice [56]. When GF mice were conventionalised again with a normal gut microbiota harvested from the cecum of a "normal" mouse, body fat content was increased by 60% and fasting glucose and insulin levels were elevated despite a significantly lower food intake compared to unconventionalised GF mice [56]. The mechanisms behind the weight gain in the conventionalised mice may be ascribed to energy extraction from indigestible food components by the acquired microbiota, an increase in intestinal carbohydrate absorption, and concomitant increase in *de novo* hepatic lipogenesis which are associated risk factors for the development of obesity and type 2 diabetes.

Besides affecting energy homeostasis, the gut microbiota also influence local and systemic immune responses [57,58]. It has been suggested that high-fat diet (HFD) feeding leads to gut microbiota dysbiosis and inflammation in the small intestine, characterised by activation of specific immune cells and production of pro-inflammatory cytokines [9,59]. These pro-inflammatory factors may contribute to increased intestinal permeability and leakage of lipopolysaccharides (LPS) from the lumen into the circulation. Systemic LPS may lead to activation of circulating immune cells and to infiltration of macrophages in adipose tissue, liver, and muscle. As mentioned previously, increased infiltration of macrophages in e.g. WAT may contribute to the development of systemic inflammation and insulin resistance.

Furthermore, short chain fatty acids (SCFA) produced by the gut microbiota also play a role in the inflammatory phenotype, which will be described in the section '*Short-chain fatty acids*'. Together, this suggests that HFD-induced gut microbiota dysbiosis may also play an indirect role in the development of cardiometabolic disease.

GUT MICROBIOTA DYSBIOSIS AND ATHEROSCLEROSIS

Gut microbiota dysbiosis is not only associated with insulin resistance, but recent studies also indicate a prominent role for gut microbiota in the development of atherosclerosis. The gut microbiota may affect atherosclerosis development via different mechanisms, e.g. by affecting the immune system and/or by affecting cholesterol metabolism [60,61].

During bacterial infections, it was found that bacteria can translocate from the intestinal lumen to the site prone to atherosclerotic lesion development, as evidenced by the presence of bacterial DNA in human atherosclerotic plaques [62,63]. Moreover, some infectious microorganisms have been shown to be potentially associated with atherosclerosis. For example, microorganisms such as *A. actinomycetemcomitans*, *C. pneumoniae*, *Helicobacter pylori*, and *P. gingivalis* might contribute to atherosclerosis by increasing atherosclerotic lesion areas in various experimental models [64]. However, although the presence of bacterial DNA in human atherosclerotic plaques is established, it is uncertain whether an infection initiates or promotes atherosclerosis development in humans.

Despite the site of infection (local or systemic), the immune system responds to microbial-derived components, leading to the activation of several inflammatory pathways. For instance, several studies demonstrated that low levels of LPS are detectable in the circulation of healthy humans [65,66], suggesting that LPS can translocate from the intestinal lumen into the bloodstream. It was found that LPS leads to the recruitment of adaptor proteins e.g. MYD88 to the cytoplasmic domain of Toll-like receptors (TLRs). After recruitment of adaptor proteins, downstream signalling cascades can be triggered that lead to the production of pro-inflammatory cytokines and chemokines [67]. It has been suggested that LPS may lead to the induction of a low-grade inflammatory state and can aggravate the progression

of atherosclerosis [61,68].

  In addition to affecting inflammation in atherosclerotic plaques, the gut microbiota may also affect atherosclerosis development by influencing the enterohepatic circulation of BAs and therefore cholesterol metabolism. BA metabolism and cholesterol metabolism are inter regulated. In the liver, the BAs cholic acid (CA) and xenodeoxycholic acid (CDCA) are synthesised from cholesterol. In rodent liver, most of the CDCA is converted to α-muricholic acid (α-MCA) and β-muricholic acid (β-MCA)[69,70]. After formation, BAs are predominantly conjugated in the liver to either glycine in humans, or to taurine in rodents [71,72], after which primary BAs are secreted in the bile canaliculi and directed to the gall bladder. Upon ingestion of a meal, bile is released into the duodenum to facilitate the digestion and absorption of dietary lipids by pancreatic lipase. Approximately 95% of the conjugated BAs are actively reabsorbed by the apical sodium-dependent bile acid transporter (ASBT) in the distal ileum and returned to the liver via enterohepatic circulation. Although the major component of BA absorption is active, some of the absorption of BAs is passive, less intensive compared to active absorption, and occurs along the entire small intestine and colon. BAs that are unconjugated and more lipophilic such as CDCA and deoxycholic acid (DCA) diffuse more readily through the apical membrane than hydrophilic BAs such as CA. On the other hand, active transport via ASBT is primarily responsible for absorbing conjugated BAs in the ileum which are more hydrophilic [73]. A fraction of the BAs that escape active or passive absorption in the small intestine is subject to bacterial modification in the colon. Gut microbiota that possess active bile salt hydrolase (BSH) activity in the colon first deconjugate BAs, followed by a 7α-dehydroxylation reaction leading to the formation of secondary BAs [74,75] including hyocholic acid (HCA), DCA, and ω-muricholic acid (ω-MCA)[76]. The deconjugated secondary BAs may then be either absorbed passively in the colon or excreted in the feces. Both the absorbed primary BAs and the secondary BAs formed by the gut microbiota are recycled back to the liver via the portal vein and again undergo biotransformation through conjugation to glycine or taurine [77,78]. Thus, gut microbial metabolism of BAs increases BA diversity but also contributes to a more hydrophobic and toxic BA pool. To prevent accumulation of potentially cytotoxic

BAs, BA transport and metabolism are tightly regulated within the liver and intestine. As such, hepatic conversion of cholesterol to BAs balances fecal bile excretion, being the major route for cholesterol catabolism and accounting for almost half of the cholesterol eliminated from the body per day [79]. Therefore, differences in fecal BA excretion affect the enterohepatic circulation of cholesterol and may ultimately affect plasma cholesterol levels [80]. Although it is widely accepted that BAs are important regulators of metabolic homeostasis, the exact relationship between BAs and atherosclerosis development is still elusive.

Finally, the gut microbiota interacts with dietary components and synthesise or convert specific metabolites that, when taken up by the host, directly affect physiological processes and promote or prevent CVD. An example of a CVD-promoting metabolite is trimethylamine N-oxide (TMAO). The group of Hazen *et al.,* found that metabolism of dietary phosphatidylcholine and L-carnitine by intestinal microbiota results in the formation of the metabolite trimethylamine (TMA). TMA enters the circulation and is converted in the liver to TMAO. In patients that are vulnerable to a cardiovascular event, increased TMAO was associated with increased risk of cardiometabolic disease and atherosclerosis [81,82]. The same group recently showed that TMAO directly increases platelet hyperreactivity and thus the risk for a thrombotic event [83]. Synthesised metabolites by the gut microbiota that are linked to the prevention of CVD are e.g. SCFAs. The role of SCFAs in the prevention and onset of CVD is described in the section '*Short-chain fatty acids'*.

Taken together, evidence implicates a role for the gut microbiota in the development of obesity, type 2 diabetes, and atherosclerosis via different pathways. Targeting the gut microbiota may be a promising tool for the prevention and treatment of these diseases including the underlying pathology such as inflammation and hyperlipidemia.

DIET AND GUT MICROBIOTA

It has long been known that diet is a major contributor to the risk of developing cardiome-tabolic disease [84]. Not surprisingly, diet and its components are also a main driver of gut microbiota dysbiosis and underlying pathologies [45,85]. The primary source of energy that sustains the gut microbiota composition is obtained via the fermentation of indigestible carbohydrates [86–88]. Previous studies have shown that a diet rich in indigestible carbohy-drates can improve health by increasing bacterial diversity and bacterial richness [89–91]. In contrast, intake of diets rich in fat and sucrose lead to the extinction of several taxa of the gut microbiota [92]. Furthermore, degradation of indigestible carbohydrates by the gut microbiota yields SCFAs, which are acknowledged to have beneficial effects on the intestinal epithelium and gut immune system [93]. Reasonably, this puts indigestible carbohydrates in the spotlight as a tool to modify gut microbiota composition and induce microbial diversity and richness to improve health and prevent disease.

INDIGESTIBLE CARBOHYDRATES

Indigestible carbohydrates are food ingredients considered as 'roughage' material that comprises portions of food that are not broken down by the enzymes of the human digestive tract. They are predominantly plant-derived and abundant in fruits, vegetables, cereals, and legumes.

PREBIOTICS

Based on the growing evidence for a link between the human diet and the gut microbiota composition in the large intestine [94,95], the term prebiotics was introduced for substances that cause specific advantageous shifts in the gut microbial composition. The term prebiotic, first introduced by Gibson and Roberfroid (1995), was defined as "a non-digestible food ingredient that beneficially affects the host by selectively stimulating the growth and/or activity of one or a limited number of bacteria in the colon, and thus improves host health" [96]. This definition was later refined and adjusted with the addition of three criteria: 1) neither hydrolysis

nor absorption in the stomach or small intestine may occur, 2) the ingredient is fermented by intestinal bacteria, and 3) a selective response with regard to beneficial commensal bacteria in the colon is required [97]. Inulin and mannan-oligosaccharides (MOS) are two examples of indigestible carbohydrates with prebiotic activity and/or prebiotic potential that will be discussed below.

INULIN

Inulin is a water-soluble polysaccharide present in >45,000 plant species [98] which belongs to a group of indigestible carbohydrates called fructans. Inulin-type fructans are storage carbohydrates of plants containing 1–70 fructose units in their structure linked to a terminal sucrose molecule. Due to the β-configuration of the fructose monomers, these molecules are not absorbed in the small intestine and resistant to hydrolysis by digestive enzymes in the gastrointestinal tract [99]. Instead, inulin-type fructans are fermented by colonic microbiota stimulating the growth and activity of presumably beneficial gut bacteria. Therefore, inulin is an indigestible carbohydrate that meets the three classification criteria for being considered a prebiotic [96].

Inulin is widely studied for its potential to improve intestinal health. Most of the effects of inulin on the gut microbiota composition and function occur via changes in the prevalence and abundance of *Bifidobacteria*, *Bacteroides*, and *Lactobacilli* [100–102]. In addition, dietary intake of inulin has been associated with a number of health benefits including reduction of gastrointestinal diseases [103], regulation of food intake and appetite [104], but also stimulation of the immune system [105,106], and decreasing hyperlipidemia [107–110]. As immune-related inflammation and increased hyperlipidemia are important risk factors in the development of cardiometabolic disease and its underlying pathology, dietary inulin is an interesting tool for prevention and or treatment of cardiometabolic disease via interactions with the gut microbiota.

MANNAN OLIGOSACCHARIDES

Another important potential, but relatively unknown type of prebiotic, are MOS. MOS can be derived from the outer cell-wall membrane of yeast, plants, or bacteria [111]. The main constituents of the outer cell wall of yeast consists of ß(1→3)-D-glucan, ß(1→6)-D-glucan, chitin, mannan and proteins [112], which cannot be hydrolysed by host digestive enzymes. MOS obtained from the yeast *Saccharomyces cerevisiae* generally consist of glucomannan complexes [113].

Yeast *Saccharomyces cerevisiae*-derived MOS have been widely used in livestock industry as an alternative to antibiotics and as food supplementation to ameliorate performance by reducing pathogenic contamination [114–116]. However, the mechanism by which MOS exert their effect on the immune system is not fully established. One suggested mode of action by which MOS may improve inflammation is via interaction and modification of the gut microbiota. According to Spring *et al.,* MOS bind to type-1 fimbriae of pathogenic bacteria and prevent their adherence to the intestinal mucosa [117], thereby reducing pathogen-induced inflammation. Although the majority of the studies using MOS were conducted in species such as chickens [118,119], juvenile rainbow trout [120], or turkeys [121], it has been shown that MOS can decrease inflammation both within the gastro-intestinal tract [122] as well as systemically [123,124].

Moreover, in different studies using a variety of experimental animal models, it was shown that dietary supplementation with MOS lowered plasma cholesterol levels [125–127]. Similar to inulin, as inflammation and hyperlipidemia are associated with the onset of cardiometabolic disease, this warrants further research on the effect of MOS in the development of cardiometabolic disease and its underlying pathology.

SHORT-CHAIN FATTY ACIDS

Via interaction with specific gut bacteria, fermentation of indigestible carbohydrates leads to the production of SCFAs. When indigestible carbohydrates reach the colon to be fermented and metabolised by gut microbiota, they form SCFAs. SCFAs can serve as energy substrates,

directly activate G-protein coupled receptors (GPRs), inhibit histone deacetylases (HDAC) [128]. SCFAs consist of 1-6 carbons, of which acetate (C:2), propionate (C:3) and butyrate (C:4) are the most abundant (≥95%) [87,129,130]. Generally, acetate, propionate and butyrate are present in an approximate molar ratio of 60:20:20 in cecum content and feces [87,131]. The production rate and amount of SCFAs depend on the composition and density of the gut microbiota in combination with the type of indigestible carbohydrates available for microbial fermentation [97]. For example, when there is shortage in the supply of indigestible carbohydrates, gut microbes can switch to other sources to support their growth, such as amino acids or dietary fats [95,132]. These less favourable sources of energy lead to reduced fermentative activity of the microbiota and reduced SCFAs as end products [133]. However, supplementation of diets rich in protein or fat with additional indigestible carbohydrates, restores the levels of beneficial gut microbes, and increases SCFAs [134]. SCFAs in turn can be utilised by other bacterial species, or can be readily absorbed by the host. In the cecum and large intestine, 95% of the produced SCFAs are absorbed by the colonocytes, while the remaining 5% is excreted in the feces [135–138].

TRANSPORT OF SHORT-CHAIN FATTY ACIDS

Studies that investigated SCFA transport have been performed mostly in colonocytes, which are physiologically exposed to the highest concentrations of SCFAs. SCFAs can be transported across the apical and the basolateral membranes of colonocytes either via passive diffusion or via active transport mediated by a number of different transporters, including MCT1 and SMCT1 for transport across the apical membrane, and MCT4 and MCT5 for the basolateral membrane [139]. Depending on the strength of acidity (pK_a) and pH in the gut lumen, either passive diffusion or active transport of SCFAs takes place [139].

Currently, it is still elusive which transporters are exactly responsible for the uptake of SCFAs from the circulation into the tissues. However, OAT2 and OAT7 were identified to transport propionate and butyrate, respectively, across the membranes of hepatocytes [140,141]. Further research is needed to investigate the uptake of SCFA by different organs in order to

better understand the role of SCFAs in various tissues.

SHORT-CHAIN FATTY ACIDS AS A SUBSTRATE AND THEIR REGULATION OF GLUCOSE AND LIPID METABOLISM

When SCFAs are taken up, a large part can be used as a substrate for energy. For instance, it is known that humans can use SCFAs for approximately 10% of their daily caloric requirements [142]. Furthermore, around 60-70% of oxidised butyrate is used for the provision of energy in colonocytes [143,144]. Once absorbed, the SCFAs that are produced by gut microbiota in the cecum and colon will end up in the portal vein, the liver, peripheral blood, and in other peripheral tissues [87,145]. For example, while butyrate is hardly absorbed and mainly used as an energy source for colonocytes, acetate and propionate produced after colonic fermentation enter the portal vein of which the majority is taken up by the liver [87,146,147]. In general it is believed that the liver clears a large fraction of propionate from the portal circulation, but absolute values are still unknown. The remainder of the SCFAs will enter the peripheral blood circulation where they will be taken up by other organs and tissues such as adipose tissue, heart, muscle, and kidneys [148].

SCFAs play a role in the regulation of lipid and glucose metabolism [149–153]. For instance, acetate can be used as a substrate for hepatic *de novo* cholesterol and fatty acid synthesis [147], while propionate inhibits cholesterol synthesis and can be used as a substrate for gluconeogenesis [153]. Variation in the ratio of propionate:acetate can therefore be used to determine either hepatic stimulation or inhibition of lipogenesis which may consequently affect plasma lipid levels [154]. However, the extent to which propionate contributes to energy metabolism in humans is largely unknown due to the lack of data on actual production rates of propionate. SCFAs are able to regulate glucose metabolism by normalising plasma glucose levels and increasing glucose handling via activation of the hepatic AMPK pathway and by increasing the gut hormones peptide YY (PYY) and glucagon-like peptide-1 (GLP-1)[139]. Thus, when SCFAs are taken up and absorbed by various tissues and organs, they play an important role as a substrate in lipid en glucose metabolism.

SHORT-CHAIN FATTY ACIDS AS SIGNALLING MOLECULES

SCFA can serve as signalling molecules either as HDACs inhibitors or via activation of GPRs. Predominantly butyrate and, to a lesser extent, propionate are known to act as HDAC inhibitors, changing the expression of multiple genes with various functions, including proliferation, differentiation, apoptosis, and inhibiting inflammation (reviewed in [128]). Besides its function as HDAC inhibitors, SCFAs predominantly act via activation of the G-protein coupled receptors (GPR) GPR41 and GPR43 [155,156]. They are expressed on various cells residing in the intestine, but also on extra-intestinal cells like adipocytes, pancreatic cells, renal smooth muscle cells, enteric neuronal cells [157,158] and to a lower extend on hepatocytes [159]. Immune cells that can be activated by SCFA are granulocytes, some myeloid cells, macrophages, and dendritic cells [160–163]. SCFAs are well known for their potential to beneficially affect the immune system either directly or via indirect activation their receptors (reviewed in [164,165]). The possible immune-modulatory functions of SCFAs are revealed by a recent study in Gpr43$^{-/-}$ mice [166]. This study showed exacerbated inflammation in various models including colitis, arthritis and asthma. The underlying mechanisms on how SCFAs can modulate the immune system in obesity and atherosclerosis is via the effects of SCFAs on reducing chemotaxis and adhesion of immune cells. By preventing chemotaxis and cell adhesion, SCFAs might prevent infiltration of monocytes in adipose tissue and atherosclerotic lesions and can have a protective effect against systemic inflammation.

1

THESIS OUTLINE

As the occurrence of cardiometabolic disease is still increasing, strategies to target the underlying risk factors inflammation and hyperlipidemia are urgently needed.

As evident from **chapter 1** of this thesis, the gut microbiota have been strongly associated with the development of cardiometabolic risk factors and disease, including obesity, type 2 diabetes, and atherosclerosis. Since gut microbiota composition and function is highly susceptible to modification via dietary intervention, insight in the role of different dietary components in the modulation of the gut microbiota is crucial. This is a prerequisite for the development of novel strategies to modify risk factors associated with cardiometabolic disease.

Since we exploited the use of high fat and high cholesterol diets in the development of cardiometabolic disease, it was important to have the ability to determine blood lipid composition. Therefore in **chapter 2**, we describe a method to determine the medium- and long chain fatty acid composition of blood of mice using gas chromatography-mass spectrometry (GC-MS) analysis. Simultaneously, we have exploited the use of indigestible carbohydrates to modulate microbiota activity and composition. The potential role of SCFAs in mediating the beneficial role of plant-derived indigestible carbohydrates necessitates the development of comprehensive, sensitive, and reliable methodologies to quantify the SCFA composition in biological samples such as blood, cecum content and feces. For that reason, in **chapter 3** we established a method to determine SCFAs in blood, cecum, and feces samples using GC-MS analysis.

To examine the effects of indigestible carbohydrates on cardiometabolic risk outcome, we performed two mouse studies in which we investigated the effect of the prebiotic inulin on atherosclerosis development. In **chapter 4** we investigated the effect of the prebiotic inulin on accelerated atherosclerosis after placement of a non-constrictive perivascular cuff around the femoral artery. In **chapter 5** we studied the effect of the prebiotic inulin on cholesterol-driven long-term atherosclerosis development.

Dietary MOS have proven effective at improving growth performance, while also reducing inflammation and hyperlipidemia in livestock. In this thesis, two studies are included

that focus on the effect of dietary supplementation with MOS on diet-induced obesity and atherosclerosis development. In **chapter 6** we investigated the effect of MOS on innate immune composition in mesenteric white adipose tissue and liver as well as on diet-induced obesity and glucose intolerance. The effects of MOS on hyperlipidemia and atherosclerosis development were studied in **chapter 7**.

Finally, in **chapter 8**, methods to map gut microbiota composition and function, SCFAs as markers for gut microbial function, factors that determine gut microbiota function, the role of the gut microbiota in the development of atherosclerosis, the translatability of mouse models in gut microbiota research, and implications for prebiotics will be discussed.

1

REFERENCES

1. World Health Organization WHO | Cardiovascular diseases (CVDs) :Fact sheet Available online: http://www.who.int/mediacentre/factsheets/fs317/en/ (accessed on Aug 29, *2017*).

2. van Dam, A. D.; Boon, M. R.; Berbée, J. F. P.; Rensen, P. C. N.; van Harmelen, V. Targeting white, brown and perivascular adipose tissue in atherosclerosis development. *Eur. J. Pharmacol.* **2017**, *816*, 82–92, doi:10.1016/j.ejphar.2017.03.051.

3. Rydén, M.; Arner, P. Tumour necrosis factor-alpha in human adipose tissue -- from signalling mechanisms to clinical implications. *J. Intern. Med.* **2007**, *262*, 431–8, doi:10.1111/j.1365-2796.2007.01854.x.

4. Langin, D.; Arner, P. Importance of TNFalpha and neutral lipases in human adipose tissue lipolysis. *Trends Endocrinol. Metab.* **2006**, *17*, 314–20, doi:10.1016/j.tem.2006.08.003.

5. Xu, H.; Barnes, G. T.; Yang, Q.; Tan, G.; Yang, D.; Chou, C. J.; Sole, J.; Nichols, A.; Ross, J. S.; Tartaglia, L. A.; Chen, H. Chronic inflammation in fat plays a crucial role in the development of obesity-related insulin resistance. *J. Clin. Invest.* **2003**, *112*, 1821–30, doi:10.1172/JCI19451.

6. Ouchi, N.; Parker, J. L.; Lugus, J. J.; Walsh, K. Adipokines in inflammation and metabolic disease. *Nat. Rev. Immunol.* **2011**, *11*, 85–97, doi:10.1038/nri2921.

7. Cani, P.; Delzenne, N. The Role of the Gut Microbiota in Energy Metabolism and Metabolic Disease. *Curr. Pharm. Des.* **2009**, *15*, 1546–1558, doi:10.2174/138161209788168164.

8. Hotamisligil, G. S.; Peraldi, P.; Budavari, A.; Ellis, R.; White, M. F.; Spiegelman, B. M. IRS-1-mediated inhibition of insulin receptor tyrosine kinase activity in TNF-alpha- and obesity-induced insulin resistance. *Science* **1996**, *271*, 665–8, doi:10.1126/science.271.5249.665.

9. Hotamisligil, G.; Shargill, N.; Spiegelman, B. Adipose expression of tumour necrosis factor-alpha: direct role in obesity-linked insulin resistance. *Science (80-.)*. **1993**, *259*, 87–91, doi:10.1126/science.7678183.

10. Dandona, P.; Aljada, A.; Bandyopadhyay, A. Inflammation: The link between insulin

resistance, obesity and diabetes. *Trends Immunol.* **2004**, *25*, 4–7.

11.   Acosta, J. R.; Douagi, I.; Andersson, D. P.; Bäckdahl, J.; Rydén, M.; Arner, P.; Lau-rencikiene, J. Increased fat cell size: a major phenotype of subcutaneous white adipose tissue in non-obese individuals with type 2 diabetes. *Diabetologia* **2016**, *59*, 560–570, doi:10.1007/s00125-015-3810-6.

12.   Wu, H.; Ghosh, S.; Perrard, X. D.; Feng, L.; Garcia, G. E.; Perrard, J. L.; Sweeney, J. F.; Peterson, L. E.; Chan, L.; Smith, C. W.; Ballantyne, C. M. T-cell accumulation and regulated on activation, normal T cell expressed and secreted upregulation in adipose tissue in obesity. *Circulation* **2007**, *115*, 1029–1038, doi:10.1161/CIRCULATIONA-HA.106.638379.

13.   Huh, J. Y.; Park, Y. J.; Ham, M.; Kim, J. B. Crosstalk between adipocytes and immune cells in adipose tissue inflammation and metabolic dysregulation in obesity. *Mol Cells* **2014**, *37*, 365–371, doi:10.14348/molcells.2014.0074.

14.   Nijhuis, J.; Rensen, S. S.; Slaats, Y.; van Dielen, F. M. H.; Buurman, W. A.; Greve, J. W. M. Neutrophil Activation in Morbid Obesity, Chronic Activation of Acute Inflam-mation. *Obesity* **2009**, *17*, 2014–2018, doi:10.1038/oby.2009.113.

15.   Wu, D.; Molofsky, A. B.; Liang, H.-E.; Ricardo-Gonzalez, R. R.; Jouihan, H. A.; Bando, J. K.; Chawla, A.; Locksley, R. M. Eosinophils Sustain Adipose Alternatively Activated Macrophages Associated with Glucose Homeostasis. *Science (80-.).* **2011**, *332*, 243–247, doi:10.1126/science.1201475.

16.   White, M. F. The insulin signalling system and the IRS proteins. In *Diabetologia*; **1997**; Vol. 40, pp. S2-17.

17.   Shoelson, S. E.; Lee, J.; Goldfine, A. B. Inflammation and insulin resistance. *J. Clin. Invest.* **2006**, *116*, 1793–1801, doi:10.1172/JCI29069.

18.   Wellen, K. E.; Hotamisligil, G. S. di. *J. Clin. Invest.* **2005**, *115*, 1111–1119, doi:10.1172/JCI25102.

19.   Frayn, K. N. Visceral fat and insulin resistance--causative or correlative? *Br. J. Nutr.* **2000**, *83 Suppl 1*, S71-7.

20. Kissebah, A. H.; Adams, P. W.; Wynn, V. Plasma free fatty acid and triglyceride transport kinetics in man. *Clin. Sci. Mol. Med.* **1974**, *47*, 259–78.

21. Libby, P. Inflammation in atherosclerosis. *Nature* **2002**, *420*, 868–74, doi:10.1038/nature01323.

22. Biessen, E. A. L.; Wouters, K. Macrophage complexity in human atherosclerosis. *Curr. Opin. Lipidol.* **2017**, *28*, 419–426, doi:10.1097/MOL.0000000000000447.

23. Glagov, S.; Weisenberg, E.; Zarins, C. K.; Stankunavicius, R.; Kolettis, G. J. Compensatory Enlargement of Human Atherosclerotic Coronary Arteries. *N. Engl. J. Med.* **1987**, *316*, 1371–1375, doi:10.1056/NEJM198705283162204.

24. Pasterkamp, G.; Smits, P. C. Imaging of atherosclerosis. Remodelling of coronary arteries. *J. Cardiovasc. Risk* **2002**, *9*, 229–35.

25. Galis, Z. S.; Sukhova, G. K.; Lark, M. W.; Libby, P. Increased expression of matrix metalloproteinases and matrix degrading activity in vulnerable regions of human atherosclerotic plaques. *J. Clin. Invest.* **1994**, *94*, 2493–2503, doi:10.1172/JCI117619.

26. Ding, S.; Chi, M. M.; Scull, B. P.; Rigby, R.; Schwerbrock, N. M. J.; Magness, S.; Jobin, C.; Lund, P. K. High-fat diet: bacteria interactions promote intestinal inflammation which precedes and correlates with obesity and insulin resistance in mouse. *PLoS One* **2010**, *5*, e12191, doi:10.1371/journal.pone.0012191.

27. Lam, Y. Y.; Ha, C. W. Y.; Campbell, C. R.; Mitchell, A. J.; Dinudom, A.; Oscarsson, J.; Cook, D. I.; Hunt, N. H.; Caterson, I. D.; Holmes, A. J.; Storlien, L. H. Increased gut permeability and microbiota change associate with mesenteric fat inflammation and metabolic dysfunction in diet-induced obese mice. *PLoS One* **2012**, *7*, e34233, doi:10.1371/journal.pone.0034233.

28. Goodman, B. E. Insights into digestion and absorption of major nutrients in humans. *AJP Adv. Physiol. Educ.* **2010**, *34*, 44–53, doi:10.1152/advan.00094.2009.

29. Macfarlane, G. T.; Macfarlane, S. Bacteria, colonic fermentation, and gastrointestinal health. *J. AOAC Int.* **2012**, *95*, 50–60, doi:10.5740/jaoacint.SGE-Macfarlane.

30. Hooper, L. V; Gordon, J. I. Commensal host-bacterial relationships in the gut. *Science*

2001, *292*, 1115–8.

31.   Turnbaugh, P. J.; Ley, R. E.; Hamady, M.; Fraser-Liggett, C. M.; Knight, R.; Gordon, J. I. The human microbiome project. *Nature* **2007**, *449*, 804–10, doi:10.1038/nature06244.

32.   The Integrative Human Microbiome Project: dynamic analysis of microbiome-host omics profiles during periods of human health and disease. *Cell Host Microbe* **2014**, *16*, 276–89, doi:10.1016/j.chom.2014.08.014.

33.   Xu, J.; Gordon, J. I. Honor thy symbionts. *Proc. Natl. Acad. Sci. U. S. A.* **2003**, *100*, 10452–9, doi:10.1073/pnas.1734063100.

34.   Savage, D. C. Microbial ecology of the gastrointestinal tract. *Annu. Rev. Microbiol.* **1977**, *31*, 107–33, doi:10.1146/annurev.mi.31.100177.000543.

35.   Qin, J.; Li, R.; Raes, J.; Arumugam, M.; Burgdorf, K. S.; Manichanh, C.; Nielsen, T.; Pons, N.; Levenez, F.; Yamada, T.; Mende, D. R.; Li, J.; Xu, J.; Li, S.; Li, D.; Cao, J.; Wang, B.; Liang, H.; Zheng, H.; Xie, Y.; Tap, J.; Lepage, P.; Bertalan, M.; Batto, J.-M.; Hansen, T.; Le Paslier, D.; Linneberg, A.; Nielsen, H. B.; Pelletier, E.; Renault, P.; Sicheritz-Ponten, T.; Turner, K.; Zhu, H.; Yu, C.; Li, S.; Jian, M.; Zhou, Y.; Li, Y.; Zhang, X.; Li, S.; Qin, N.; Yang, H.; Wang, J.; Brunak, S.; Doré, J.; Guarner, F.; Kristiansen, K.; Pedersen, O.; Parkhill, J.; Weissenbach, J.; Antolin, M.; Artiguenave, F.; Blottiere, H.; Borruel, N.; Bruls, T.; Casellas, F.; Chervaux, C.; Cultrone, A.; Delorme, C.; Denariaz, G.; Dervyn, R.; Forte, M.; Friss, C.; van de Guchte, M.; Guedon, E.; Haimet, F.; Jamet, A.; Juste, C.; Kaci, G.; Kleerebezem, M.; Knol, J.; Kristensen, M.; Layec, S.; Le Roux, K.; Leclerc, M.; Maguin, E.; Melo Minardi, R.; Oozeer, R.; Rescigno, M.; Sanchez, N.; Tims, S.; Torrejon, T.; Varela, E.; de Vos, W.; Winogradsky, Y.; Zoetendal, E.; Bork, P.; Ehrlich, S. D.; Wang, J. A human gut microbial gene catalogue established by metagenomic sequencing. *Nature* **2010**, *464*, 59–65, doi:10.1038/nature08821.

36.   Eckburg, P. B.; Bik, E. M.; Bernstein, C. N.; Purdom, E.; Dethlefsen, L.; Sargent, M.; Gill, S. R.; Nelson, K. E.; Relman, D. A. Diversity of the human intestinal microbial flora. *Science* **2005**, *308*, 1635–8, doi:10.1126/science.1110591.

37.   Clemente, J. C.; Ursell, L. K.; Parfrey, L. W.; Knight, R. The impact of the gut microbiota on human health: An integrative view. *Cell* **2012**, *148*, 1258–1270.

38.   Sekirov, I.; Russell, S. L.; Caetano, L.; Antunes, M.; Finlay, B. B. Gut Microbiota in Health and Disease. *Physiol. Rev.* **2009**, *120*, 859–904, doi:10.1161/CIRCRESAHA.117.309715.

39.   Sommer, F.; Bäckhed, F. The gut microbiota--masters of host development and physiology. *Nat. Rev. Microbiol.* **2013**, *11*, 227–38, doi:10.1038/nrmicro2974.

40.   Palmer, C.; Bik, E. M.; DiGiulio, D. B.; Relman, D. A.; Brown, P. O. Development of the Human Infant Intestinal Microbiota. *PLoS Biol.* **2007**, *5*, e177, doi:10.1371/journal.pbio.0050177.

41.   Yatsunenko, T.; Rey, F. E.; Manary, M. J.; Trehan, I.; Dominguez-Bello, M. G.; Contreras, M.; Magris, M.; Hidalgo, G.; Baldassano, R. N.; Anokhin, A. P.; Heath, A. C.; Warner, B.; Reeder, J.; Kuczynski, J.; Caporaso, J. G.; Lozupone, C. A.; Lauber, C.; Clemente, J. C.; Knights, D.; Knight, R.; Gordon, J. I. Human gut microbiome viewed across age and geography. *Nature* **2012**, *486*, 222–7, doi:10.1038/nature11053.

42.   Faith, J. J.; Guruge, J. L.; Charbonneau, M.; Subramanian, S.; Seedorf, H.; Goodman, A. L.; Clemente, J. C.; Knight, R.; Heath, A. C.; Leibel, R. L.; Rosenbaum, M.; Gordon, J. I. The long-term stability of the human gut microbiota. *Science* **2013**, *341*, 1237439, doi:10.1126/science.1237439.

43.   Lozupone, C. A.; Stombaugh, J. I.; Gordon, J. I.; Jansson, J. K.; Knight, R. Diversity, stability and resilience of the human gut microbiota. *Nature* **2012**, *489*, 220–30, doi:10.1038/nature11550.

44.   Turnbaugh, P. J.; Hamady, M.; Yatsunenko, T.; Cantarel, B. L.; Duncan, A.; Ley, R. E.; Sogin, M. L.; Jones, W. J.; Roe, B. A.; Affourtit, J. P.; Egholm, M.; Henrissat, B.; Heath, A. C.; Knight, R.; Gordon, J. I. A core gut microbiome in obese and lean twins. *Nature* **2009**, *457*, 480–4, doi:10.1038/nature07540.

45.   David, L. A.; Maurice, C. F.; Carmody, R. N.; Gootenberg, D. B.; Button, J. E.; Wolfe, B. E.; Ling, A. V.; Devlin, A. S.; Varma, Y.; Fischbach, M. A.; Biddinger, S. B.; Dutton, R. J.; Turnbaugh, P. J. Diet rapidly and reproducibly alters the human gut microbiome.

1

Nature **2014**, *505*, 559–63, doi:10.1038/nature12820.

46.   Shen, W.; Gaskins, H. R.; McIntosh, M. K. Influence of dietary fat on intestinal microbes, inflammation, barrier function and metabolic outcomes. *J. Nutr. Biochem.* **2014**, *25*, 270–80, doi:10.1016/j.jnutbio.2013.09.009.

47.   Wen, L.; Duffy, A. Factors Influencing the Gut Microbiota, Inflammation, and Type 2 Diabetes. *J. Nutr.* **2017**, *147*, 1468S–1475S, doi:10.3945/jn.116.240754.

48.   Macpherson, A. J.; Harris, N. L. Opinion: Interactions between commensal intestinal bacteria and the immune system. *Nat. Rev. Immunol.* **2004**, *4*, 478–485, doi:10.1038/nri1373.

49.   Ubeda, C.; Djukovic, A.; Isaac, S. Roles of the intestinal microbiota in pathogen protection. *Clin. Transl. Immunol.* **2017**, *6*, e128, doi:10.1038/cti.2017.2.

50.   Kahn, S. E.; Hull, R. L.; Utzschneider, K. M. Mechanisms linking obesity to insulin resistance and type 2 diabetes. *Nature* **2006**, *444*, 840–846, doi:10.1038/nature05482.

51.   Ley, R. R. E.; Turnbaugh, P. P. J.; Klein, S.; Gordon, J. I. J. Microbial ecology: human gut microbes associated with obesity. *Nature* **2006**, *444*, 1022–3, doi:10.1038/4441022a.

52.   Festi, D.; Schiumerini, R.; Eusebi, L. H.; Marasco, G.; Taddia, M.; Colecchia, A. Gut microbiota and metabolic syndrome. *World J. Gastroenterol.* **2014**, *20*, 16079–16094, doi:10.3748/wjg.v20.i43.16079.

53.   Kau, A. L.; Ahern, P. P.; Griffin, N. W.; Goodman, A. L.; Gordon, J. I. Human nutrition, the gut microbiome and the immune system. *Nature* **2011**, *474*, 327–336, doi:10.1038/nature10213.

54.   Qin, J.; Li, Y.; Cai, Z.; Li, S.; Zhu, J.; Zhang, F.; Liang, S.; Zhang, W.; Guan, Y.; Shen, D.; Peng, Y.; Zhang, D.; Jie, Z.; Wu, W.; Qin, Y.; Xue, W.; Li, J.; Han, L.; Lu, D.; Wu, P.; Dai, Y.; Sun, X.; Li, Z.; Tang, A.; Zhong, S.; Li, X.; Chen, W.; Xu, R.; Wang, M.; Feng, Q.; Gong, M.; Yu, J.; Zhang, Y.; Zhang, M.; Hansen, T.; Sanchez, G.; Raes, J.; Falony, G.; Okuda, S.; Almeida, M.; LeChatelier, E.; Renault, P.; Pons, N.; Batto, J.-M.; Zhang, Z.; Chen, H.; Yang, R.; Zheng, W.; Li, S.; Yang, H.; Wang, J.; Ehrlich, S. D.; Nielsen, R.; Pedersen, O.; Kristiansen, K.; Wang, J. A metagenome-wide association

study of gut microbiota in type 2 diabetes. *Nature* **2012**, *490*, 55–60, doi:10.1038/nature11450.

55.   Tang, W. H. W.; Hazen, S. L. The contributory role of gut microbiota in cardiovascular disease. *J. Clin. Invest.* **2014**, *124*, 4204–11, doi:10.1172/JCI72331.

56.   Bäckhed, F.; Ding, H.; Wang, T.; Hooper, L. V; Koh, G. Y.; Nagy, A.; Semenkovich, C. F.; Gordon, J. I. The gut microbiota as an environmental factor that regulates fat storage. *Proc. Natl. Acad. Sci. U. S. A.* **2004**, *101*, 15718–23, doi:10.1073/pnas.0407076101.

57.   Wellen, K. E.; Hotamisligil, G. S. Inflammation, stress, and diabetes. *J. Clin. Invest.* **2005**, *115*, 1111–9, doi:10.1172/JCI25102.

58.   Hotamisligil, G. S. Inflammation and metabolic disorders. *Nature* **2006**, *444*, 860–867, doi:10.1038/nature05485.

59.   Weisberg, S. P.; McCann, D.; Desai, M.; Rosenbaum, M.; Leibel, R. L.; Ferrante, A. W. Obesity is associated with macrophage accumulation in adipose tissue. *J. Clin. Invest.* **2003**, *112*, 1796–1808, doi:10.1172/JCI19246.

60.   Yamashita, T. Intestinal Immunity and Gut Microbiota in Atherogenesis. *J. Atheroscler. Thromb.* **2016**, *24*, 110–119, doi:10.5551/jat.38265.

61.   Caesar, R.; Fåk, F.; Bäckhed, F. Effects of gut microbiota on obesity and atherosclerosis via modulation of inflammation and lipid metabolism: Review. *J. Intern. Med.* **2010**, *268*, 320–328.

62.   Koren, O.; Spor, A.; Felin, J.; Fåk, F.; Stombaugh, J.; Tremaroli, V.; Behre, C. J.; Knight, R.; Fagerberg, B.; Ley, R. E.; Bäckhed, F. Human oral, gut, and plaque microbiota in patients with atherosclerosis. *Proc. Natl. Acad. Sci. U. S. A.* **2011**, *108 Suppl*, 4592–8, doi:10.1073/pnas.1011383107.

63.   Mitra, S.; Drautz-Moses, D. I.; Alhede, M.; Maw, M. T.; Liu, Y.; Purbojati, R. W.; Yap, Z. H.; Kushwaha, K. K.; Gheorghe, A. G.; Bjarnsholt, T.; Hansen, G. M.; Sillesen, H. H.; Hougen, H. P.; Hansen, P. R.; Yang, L.; Tolker-Nielsen, T.; Schuster, S. C.; Givskov, M. In silico analyses of metagenomes from human atherosclerotic plaque samples. *Microbiome* **2015**, *3*, 38, doi:10.1186/s40168-015-0100-y.

1

64.   Rosenfeld, M. E.; Campbell, L. A. Pathogens and atherosclerosis: update on the potential contribution of multiple infectious organisms to the pathogenesis of atherosclerosis. *Thromb. Haemost.* **2011**, *106*, 858–67, doi:10.1160/TH11-06-0392.

65.   Nádházi, Z.; Takáts, A.; Offenmüller, K.; Bertók, L. Plasma endotoxin level of healthy donors. *Acta Microbiol. Immunol. Hung.* **2002**, *49*, 151–157, doi:10.1556/AMicr.49.2002.1.15.

66.   Wiedermann, C. J.; Kiechl, S.; Dunzendorfer, S.; Schratzberger, P.; Egger, G.; Oberhollenzer, F.; Willeit, J. Association of endotoxemia with carotid atherosclerosis and cardiovascular disease: prospective results from the Bruneck Study. *J. Am. Coll. Cardiol.* **1999**, *34*, 1975–81.

67.   Akira, S. Pathogen recognition by innate immunity and its signalling. *Proc. Jpn. Acad. Ser. B. Phys. Biol. Sci.* **2009**, *85*, 143–56.

68.   Ostos, M. A.; Recalde, D.; Zakin, M. M.; Scott-Algara, D. Implication of natural killer T cells in atherosclerosis development during a LPS-induced chronic inflammation. *FEBS Lett.* **2002**, *519*, 23–9.

69.   Russell, D. W. The enzymes, regulation, and genetics of bile acid synthesis. *Annu. Rev. Biochem.* **2003**, *72*, 137–74, doi:10.1146/annurev.biochem.72.121801.161712.

70.   Botham, K. M.; Boyd, G. S. The metabolism of chenodeoxycholic acid to beta-muricholic acid in rat liver. *Eur. J. Biochem.* **1983**, *134*, 191–6.

71.   Chiang, J. Y. L. Bile acids: regulation of synthesis. *J. Lipid Res.* **2009**, *50*, 1955–66, doi:10.1194/jlr.R900010-JLR200.

72.   Pircher, P. C.; Kitto, J. L.; Petrowski, M. L.; Tangirala, R. K.; Bischoff, E. D.; Schulman, I. G.; Westin, S. K. Farnesoid X Receptor Regulates Bile Acid-Amino Acid Conjugation. *J. Biol. Chem.* **2003**, *278*, 27703–27711, doi:10.1074/jbc.M302128200.

73.   Boron, W. F.; Boulpaep, E. L. *Medical Physiology: A Cellular and Molecular Approach*; **2003**; ISBN 0721632564.

74.   Sayin, S. I.; Wahlström, A.; Felin, J.; Jäntti, S.; Marschall, H.-U.; Bamberg, K.; Angelin, B.; Hyötyläinen, T.; Orešič, M.; Bäckhed, F. Gut Microbiota Regulates Bile Acid Metabolism by Reducing the Levels of Tauro-beta-muricholic Acid, a Naturally Occurring FXR

Antagonist. *Cell Metab.* **2013**, *17*, 225–235, doi:10.1016/j.cmet.2013.01.003.

75. Ridlon, J. M.; Kang, D.-J.; Hylemon, P. B. Bile salt biotransformations by human intestinal bacteria. *J. Lipid Res.* **2006**, *47*, 241–59, doi:10.1194/jlr.R500013-JLR200.

76. Li, T.; Chiang, J. Y. L. Bile acids as metabolic regulators. *Curr. Opin. Gastroenterol.* **2015**, *31*, 159–65, doi:10.1097/MOG.0000000000000156.

77. Dawson, P. A.; Lan, T.; Rao, A. Bile acid transporters. *J. Lipid Res.* **2009**, *50*, 2340–57, doi:10.1194/jlr.R900012-JLR200.

78. Dawson, P. A.; Karpen, S. J. Intestinal transport and metabolism of bile acids. *J. Lipid Res.* **2015**, *56*, 1085–1099, doi:10.1194/jlr.R054114.

79. Dietschy, J. M.; Turley, S. D.; Spady, D. K. Role of liver in the maintenance of cholesterol and low density lipoprotein homeostasis in different animal species, including humans. *J. Lipid Res.* **1993**, *34*, 1637–1659.

80. Out, C.; Groen, A. K.; Brufau, G. Bile acid sequestrants: more than simple resins. *Curr. Opin. Lipidol.* **2012**, *23*, 43–55, doi:10.1097/MOL.0b013e32834f0ef3.

81. Koeth, R. A.; Wang, Z.; Levison, B. S.; Buffa, J. A.; Org, E.; Sheehy, B. T.; Britt, E. B.; Fu, X.; Wu, Y.; Li, L.; Smith, J. D.; DiDonato, J. A.; Chen, J.; Li, H.; Wu, G. D.; Lewis, J. D.; Warrier, M.; Brown, J. M.; Krauss, R. M.; Tang, W. H. W.; Bushman, F. D.; Lusis, A. J.; Hazen, S. L. Intestinal microbiota metabolism of L-carnitine, a nutrient in red meat, promotes atherosclerosis. *Nat. Med.* **2013**, *19*, 576–85, doi:10.1038/nm.3145.

82. Brown, J. M.; Hazen, S. L. The Gut Microbial Endocrine Organ: Bacterially Derived Signals Driving Cardiometabolic Diseases. *Annu. Rev. Med.* **2015**, *66*, 343–359, doi:10.1146/annurev-med-060513-093205.

83. Zhu, W.; Gregory, J. C.; Org, E.; Buffa, J. A.; Gupta, N.; Wang, Z.; Li, L.; Fu, X.; Wu, Y.; Mehrabian, M.; Sartor, R. B.; McIntyre, T. M.; Silverstein, R. L.; Tang, W. H. W.; DiDonato, J. A.; Brown, J. M.; Lusis, A. J.; Hazen, S. L. Gut Microbial Metabolite TMAO Enhances Platelet Hyperreactivity and Thrombosis Risk. *Cell* **2016**, doi:10.1016/j.cell.2016.02.011.

84. Yu, E.; Rimm, E.; Qi, L.; Rexrode, K.; Albert, C. M.; Sun, Q.; Willett, W. C.; Hu, F.

B.; Manson, J. E. Diet, Lifestyle, Biomarkers, Genetic Factors, and Risk of Cardiovascular Disease in the Nurses' Health Studies. *Am. J. Public Health* **2016**, *106*, 1616–1623, doi:10.2105/AJPH.2016.303316.

85.   Donaldson, G. P.; Lee, S. M.; Mazmanian, S. K. Gut biogeography of the bacterial microbiota. *Nat. Rev. Microbiol.* **2015**, *14*, 20–32, doi:10.1038/nrmicro3552.

86.   Macfarlane, G. T.; Macfarlane, S. Fermentation in the human large intestine: its physiologic consequences and the potential contribution of prebiotics. *J. Clin. Gastroenterol.* **2011**, *45 Suppl*, S120-7, doi:10.1097/MCG.0b013e31822fecfe.

87.   Cummings, J. H.; Pomare, E. W.; Branch, W. J.; Naylor, C. P.; Macfarlane, G. T. Short chain fatty acids in human large intestine, portal, hepatic and venous blood. *Gut* **1987**, *28*, 1221–1227, doi:10.1136/gut.28.10.1221.

88.   Leser, T. D.; Mølbak, L. Better living through microbial action: the benefits of the mammalian gastrointestinal microbiota on the host. *Environ. Microbiol.* **2009**, *11*, 2194–206, doi:10.1111/j.1462-2920.2009.01941.x.

89.   Walker, A. W.; Ince, J.; Duncan, S. H.; Webster, L. M.; Holtrop, G.; Ze, X.; Brown, D.; Stares, M. D.; Scott, P.; Bergerat, A.; Louis, P.; McIntosh, F.; Johnstone, A. M.; Lobley, G. E.; Parkhill, J.; Flint, H. J. Dominant and diet-responsive groups of bacteria within the human colonic microbiota. *ISME J.* **2011**, *5*, 220–30, doi:10.1038/ismej.2010.118.

90.   Le Chatelier, E.; Nielsen, T.; Qin, J.; Prifti, E.; Hildebrand, F.; Falony, G.; Almeida, M.; Arumugam, M.; Batto, J.-M.; Kennedy, S.; Leonard, P.; Li, J.; Burgdorf, K.; Grarup, N.; Jørgensen, T.; Brandslund, I.; Nielsen, H. B.; Juncker, A. S.; Bertalan, M.; Levenez, F.; Pons, N.; Rasmussen, S.; Sunagawa, S.; Tap, J.; Tims, S.; Zoetendal, E. G.; Brunak, S.; Clément, K.; Doré, J.; Kleerebezem, M.; Kristiansen, K.; Renault, P.; Sicheritz-Ponten, T.; de Vos, W. M.; Zucker, J.-D.; Raes, J.; Hansen, T.; Bork, P.; Wang, J.; Ehrlich, S. D.; Pedersen, O.; Guedon, E.; Delorme, C.; Layec, S.; Khaci, G.; van de Guchte, M.; Vandemeulebrouck, G.; Jamet, A.; Dervyn, R.; Sanchez, N.; Maguin, E.; Haimet, F.; Winogradski, Y.; Cultrone, A.; Leclerc, M.; Juste, C.; Blottière, H.; Pelletier, E.; LePaslier, D.; Artiguenave, F.; Bruls, T.; Weissenbach, J.; Turner, K.;

Parkhill, J.; Antolin, M.; Manichanh, C.; Casellas, F.; Boruel, N.; Varela, E.; Torrejon, A.; Guarner, F.; Denariaz, G.; Derrien, M.; van Hylckama Vlieg, J. E. T.; Veiga, P.; Oozeer, R.; Knol, J.; Rescigno, M.; Brechot, C.; M'Rini, C.; Mérieux, A.; Yamada, T. Richness of human gut microbiome correlates with metabolic markers. *Nature* **2013**, *500*, 541–6, doi:10.1038/nature12506.

91.   Schnorr, S. L.; Candela, M.; Rampelli, S.; Centanni, M.; Consolandi, C.; Basaglia, G.; Turroni, S.; Biagi, E.; Peano, C.; Severgnini, M.; Fiori, J.; Gotti, R.; De Bellis, G.; Luiselli, D.; Brigidi, P.; Mabulla, A.; Marlowe, F.; Henry, A. G.; Crittenden, A. N. Gut microbiome of the Hadza hunter-gatherers. *Nat. Commun.* **2014**, *5*, 3654, doi:10.1038/ncomms4654.

92.   Sonnenburg, E. D.; Smits, S. A.; Tikhonov, M.; Higginbottom, S. K.; Wingreen, N. S.; Sonnenburg, J. L. Diet-induced extinctions in the gut microbiota compound over generations. *Nature* **2016**, *529*, 212–215, doi:10.1038/nature16504.

93.   Lee, W.-J.; Hase, K. Gut microbiota-generated metabolites in animal health and disease. *Nat. Chem. Biol.* **2014**, *10*, 416–24, doi:10.1038/nchembio.1535.

94.   Cummings, J. H.; Englyst, H. N. Fermentation in the human large intestine and the available substrates. *Am. J. Clin. Nutr.* **1987**, *45*, 1243–55.

95.   Cummings, J. H.; Macfarlane, G. T. The control and consequences of bacterial fermentation in the human colon. *J. Appl. Bacteriol.* **1991**, *70*, 443–59.

96.   Gibson, G. R.; Roberfroid, M. B. Dietary modulation of the human colonic microbiota: introducing the concept of prebiotics. *J. Nutr.* **1995**, *125*, 1401–12.

97.   Gibson, G. R.; Probert, H. M.; Loo, J. Van; Rastall, R. A.; Roberfroid, M. B. Dietary modulation of the human colonic microbiota: updating the concept of prebiotics. *Nutr. Res. Rev.* **2004**, *17*, 259–75, doi:10.1079/NRR200479.

98.   Van Laere, A.; Van den Ende, W. Inulin metabolism in dicots: Chicory as a model system. *Plant, Cell Environ.* **2002**, *25*, 803–813, doi:10.1046/j.1365-3040.2002.00865.x.

99.   Gibson, G. R.; Scott, K. P.; Rastall, R. a.; Tuohy, K. M.; Hotchkiss, A.; Dubert-Ferrandon, A.; Gareau, M.; Murphy, E. F.; Saulnier, D.; Loh, G.; Macfarlane, S.; Delzenne,

N.; Ringel, Y.; Kozianowski, G.; Dickmann, R.; Lenoir-Wijnkook, I.; Walker, C.; Buddington, R. Dietary prebiotics: current status and new definition. *Food Sci. Technol. Bull. Funct. Foods* **2010**, *7*, 1–19, doi:10.1616/1476-2137.15880.

100. Bouhnik, Y.; Raskine, L.; Champion, K.; Andrieux, C.; Penven, S.; Jacobs, H.; Simoneau, G. Prolonged administration of low-dose inulin stimulates the growth of bifidobacteria in humans. *Nutr. Res.* **2007**, *27*, 187–193, doi:10.1016/j.nutres.2007.01.013.

101. Kolida, S.; Meyer, D.; Gibson, G. R. A double-blind placebo-controlled study to establish the bifidogenic dose of inulin in healthy humans. *Eur. J. Clin. Nutr.* **2007**, *61*, 1189–1195, doi:10.1038/sj.ejcn.1602636.

102. Roberfroid, M.; Gibson, G. R.; Hoyles, L.; McCartney, A. L.; Rastall, R.; Rowland, I.; Wolvers, D.; Watzl, B.; Szajewska, H.; Stahl, B.; Guarner, F.; Respondek, F.; Whelan, K.; Coxam, V.; Davicco, M.-J.; Léotoing, L.; Wittrant, Y.; Delzenne, N. M.; Cani, P. D.; Neyrinck, A. M.; Meheust, A. Prebiotic effects: metabolic and health benefits. *Br. J. Nutr.* **2010**, *104 Suppl*, S1-63, doi:10.1017/S0007114510003363.

103. Guarner, F. Inulin and oligofructose: impact on intestinal diseases and disorders. *Br. J. Nutr.* **2007**, *93*, S61, doi:10.1079/BJN20041345.

104. Heap, S.; Ingram, J.; Law, M.; Tucker, A. J.; Wright, A. J. Eight-day consumption of inulin added to a yogurt breakfast lowers postprandial appetite ratings but not energy intakes in young healthy females: a randomised controlled trial. *Br. J. Nutr.* **2016**, *115*, 262–70, doi:10.1017/S0007114515004432.

105. Vogt, L.; Meyer, D.; Pullens, G.; Faas, M.; Smelt, M.; Venema, K.; Ramasamy, U.; Schols, H. A.; De Vos, P. Immunological properties of inulin-type fructans. *Crit. Rev. Food Sci. Nutr.* **2015**, *55*, 414–36, doi:10.1080/10408398.2012.656772.

106. Dehghan, P.; Pourghassem Gargari, B.; Asghari Jafar-Abadi, M.; Aliasgharzadeh, A. Inulin controls inflammation and metabolic endotoxemia in women with type 2 diabetes mellitus: a randomized-controlled clinical trial. *Int. J. Food Sci. Nutr.* **2014**, *65*, 117–123, doi:10.1016/j.nut.2013.09.005.

107. Brighenti, F. Dietary fructans and serum triacylglycerols: a meta-analysis of randomized

controlled trials. *J. Nutr.* **2007**, *137*, 2552S–2556S.

108. Brighenti, F.; Casiraghi, M. C.; Canzi, E.; Ferrari, A. Effect of consumption of a ready-to-eat breakfast cereal containing inulin on the intestinal milieu and blood lipids in healthy male volunteers. *Eur. J. Clin. Nutr.* **1999**, *53*, 726–33.

109. Davidson, M. H.; Maki, K. C.; Synecki, C.; Torri, S. A.; Drennan, K. B. Effects of dietary inulin on serum lipids in men and women with hypercholesterolemia. *Nutr. Res.* **1998**, *18*, 503–517, doi:10.1016/S0271-5317(98)00038-4.

110. Aliasgharzadeh, A.; Khalili, M.; Mirtaheri, E.; Gargari, B. P.; Tavakoli, F.; Farhangi, M. A.; Babaei, H.; Dehghan, P. A combination of prebiotic inulin and oligofructose improve some of cardiovascular disease risk factors in women with type 2 diabetes: A randomized controlled clinical trial. *Adv. Pharm. Bull.* **2015**, *5*, 507–514, doi:10.15171/apb.2015.069.

111. Abbott, D. W.; Martens, E. C.; Gilbert, H. J.; Cuskin, F.; Lowe, E. C. Coevolution of yeast mannan digestion: Convergence of the civilized human diet, distal gut microbiome, and host immunity. *Gut Microbes* **2015**, *6*, 334–9, doi:10.1080/19490976.2015.1091913.

112. Maru, V.; Hewale, S.; Mantri, H.; Ranade, V. Partial Purification and Characterization of Mannan Oligosaccharides from Cell Wall of Saccharomyces cerevisiae. *Int. J. Curr. Microbiol. Appl. Sci.* **2015**, *4*, 705–711.

113. Dimitroglou, A.; Merrifield, D. L.; Moate, R.; Davies, S. J.; Spring, P.; Sweetman, J.; Bradley, G. Dietary mannan oligosaccharide supplementation modulates intestinal microbial ecology and improves gut morphology of rainbow trout, Oncorhynchus mykiss (Walbaum). *J. Anim. Sci.* **2009**, *87*, 3226–34, doi:10.2527/jas.2008-1428.

114. Torrecillas, S.; Montero, D.; Izquierdo, M. Improved health and growth of fish fed mannan oligosaccharides: Potential mode of action. *Fish Shellfish Immunol.* **2014**, *36*, 525–544, doi:10.1016/j.fsi.2013.12.029.

115. Berge, A. C.; Wierup, M. Nutritional strategies to combat Salmonella in mono-gastric food animal production. *animal* **2012**, *6*, 557–564, doi:10.1017/S1751731111002217.

1

116.   Munyaka, P. M.; Echeverry, H.; Yitbarek, A.; Camelo-Jaimes, G.; Sharif, S.; Guenter, W.; House, J. D.; Rodriguez-Lecompte, J. C. Local and systemic innate immunity in broiler chickens supplemented with yeast-derived carbohydrates. *Poult. Sci.* **2012**, *91*, 2164–72, doi:10.3382/ps.2012-02306.

117.   Spring, P.; Wenk, C.; Dawson, K. A.; Newman, K. E. The effects of dietary mannanoligosaccharides on cecal parameters and the concentrations of enteric bacteria in the ceca of Salmonella-challenged broiler chicks. *Poult. Sci.* **2000**, *79*, 205–211, doi:10.1093/ps/79.2.205.

118.   Pourabedin, M.; Xu, Z.; Baurhoo, B.; Chevaux, E.; Zhao, X. Effects of mannan oligosaccharide and virginiamycin on the cecal microbial community and intestinal morphology of chickens raised under suboptimal conditions. *Can. J. Microbiol.* **2014**, *60*, 255–66, doi:10.1139/cjm-2013-0899.

119.   Corrigan, A.; de Leeuw, M.; Penaud-Frézet, S.; Dimova, D.; Murphy, R. A. Phylogenetic and functional alterations in bacterial community compositions in broiler ceca as a result of mannan oligosaccharide supplementation. *Appl. Environ. Microbiol.* **2015**, *81*, 3460–70, doi:10.1128/AEM.04194-14.

120.   Gonçalves, A. T.; Gallardo-Escárate, C. Microbiome dynamic modulation through functional diets based on pre- and probiotics (mannan-oligosaccharides and Saccharomyces cerevisiae) in juvenile rainbow trout (Oncorhynchus mykiss). *J. Appl. Microbiol.* **2017**, *122*, 1333–1347, doi:10.1111/jam.13437.

121.   Corrigan, A.; Horgan, K.; Clipson, N.; Murphy, R. A. Effect of dietary prebiotic (mannan oligosaccharide) supplementation on the caecal bacterial community structure of turkeys. *Microb. Ecol.* **2012**, *64*, 826–36, doi:10.1007/s00248-012-0046-6.

122.   Wang, W.; Li, Z.; Han, Q.; Guo, Y.; Zhang, B.; D'inca, R. Dietary live yeast and mannan-oligosaccharide supplementation attenuate intestinal inflammation and barrier dysfunction induced by Escherichia coli in broilers. *Br. J. Nutr.* **2016**, *116*, 1878–1888, doi:10.1017/S0007114516004116.

123.   Che, T. M.; Johnson, R. W.; Kelley, K. W.; Van Alstine, W. G.; Dawson, K. A.; Moran,

C. A.; Pettigrew, J. E. Mannan oligosaccharide modulates gene expression profile in pigs experimentally infected with porcine reproductive and respiratory syndrome virus. *J. Anim. Sci.* **2011**, *89*, 3016–29, doi:10.2527/jas.2010-3366.

124. Che, T. M.; Johnson, R. W.; Kelley, K. W.; Dawson, K. A.; Moran, C. A.; Pettigrew, J. E. Effects of mannan oligosaccharide on cytokine secretions by porcine alveolar macrophages and serum cytokine concentrations in nursery pigs. *J. Anim. Sci.* **2012**, *90*, 657–668, doi:10.2527/jas.2011-4310.

125. Yalcinkaya, I.; Guengoer, T.; Basalan, M.; Erdem, E. Mannan oligosaccharides (MOS) from Saccharomyces cerevisiae in broilers: Effects on performance and blood biochemistry. *TURKISH J. Vet. Anim. Sci.* **2008**, *32*, 43–48.

126. Sohail, M. U.; Ijaz, A.; Yousaf, M. S.; Ashraf, K.; Zaneb, H.; Aleem, M.; Rehman, H. Alleviation of cyclic heat stress in broilers by dietary supplementation of mannan-oligosaccharide and Lactobacillus-based probiotic: Dynamics of cortisol, thyroid hormones, cholesterol, C-reactive protein, and humoral immunity. *Poult. Sci.* **2010**, *89*, 1934–1938, doi:10.3382/ps.2010-00751.

127. M. Kannan, R. Karunakaran, V. Balakrishnan, T. G. P. Influence of Prebiotics Supplementation on Lipid Profile of Broilers. *Int. J. Poult. Sci.* **2005**, *4*, 994–997.

128. Koh, A.; De Vadder, F.; Kovatcheva-Datchary, P.; Bäckhed, F. From dietary fiber to host physiology: Short-chain fatty acids as key bacterial metabolites. *Cell* **2016**, *165*, 1332–1345.

129. Roy, C. C.; Kien, C. L.; Bouthillier, L.; Levy, E. Short-Chain Fatty Acids: Ready for Prime Time? *Nutr. Clin. Pract.* **2006**, *21*, 351–366, doi:10.1177/0115426506021004351.

130. Cook, S. I.; Sellin, J. H. Review article: short chain fatty acids in health and disease. *Aliment. Pharmacol. Ther.* **1998**, *12*, 499–507.

131. Hijova, E.; Chmelarova, A. Short chain fatty acids and colonic health. *Bratisl. Lek. Listy* **2007**, *108*, 354–8.

132. Wall, R.; Ross, R. P.; Shanahan, F.; O'Mahony, L.; O'Mahony, C.; Coakley, M.; Hart,

O.; Lawlor, P.; Quigley, E. M.; Kiely, B.; Fitzgerald, G. F.; Stanton, C. Metabolic activity of the enteric microbiota influences the fatty acid composition of murine and porcine liver and adipose tissues. *Am. J. Clin. Nutr.* **2009**, *89*, 1393–1401, doi:10.3945/ajcn.2008.27023.

133. Russell, W. R.; Gratz, S. W.; Duncan, S. H.; Holtrop, G.; Ince, J.; Scobbie, L.; Duncan, G.; Johnstone, A. M.; Lobley, G. E.; Wallace, R. J.; Duthie, G. G.; Flint, H. J. High-protein, reduced-carbohydrate weight-loss diets promote metabolite profiles likely to be detrimental to colonic health. *Am. J. Clin. Nutr.* **2011**, *93*, 1062–72, doi:10.3945/ajcn.110.002188.

134. Sanchez, J. I.; Marzorati, M.; Grootaert, C.; Baran, M.; Van Craeyveld, V.; Courtin, C. M.; Broekaert, W. F.; Delcour, J. A.; Verstraete, W.; Van de Wiele, T. Arabinoxylan-oligosaccharides (AXOS) affect the protein/carbohydrate fermentation balance and microbial population dynamics of the Simulator of Human Intestinal Microbial Ecosystem. *Microb. Biotechnol.* **2009**, *2*, 101–13, doi:10.1111/j.1751-7915.2008.00064.x.

135. Topping, D. L.; Clifton, P. M. Short-Chain Fatty Acids and Human Colonic Function: Roles of Resistant Starch and Nonstarch Polysaccharides. *Physiol Rev* **2001**, *81*, 1031–1064.

136. Ruppin, H.; Bar-Meir, S.; Soergel, K. H.; Wood, C. M.; Schmitt, M. G. Absorption of short-chain fatty acids by the colon. *Gastroenterology* **1980**, *78*, 1500–7.

137. Dawson, A. M.; Holdsworth, C. D.; Webb, J. Absorption of Short Chain Fatty Acids in Man. *Exp. Biol. Med.* **1964**, *117*, 97–100, doi:10.3181/00379727-117-29505.

138. Rechkemmer, G.; Rönnau, K.; Engelhardt, W. . Fermentation of polysaccharides and absorption of short chain fatty acids in the mammalian hindgut. *Comp. Biochem. Physiol. Part A Physiol.* **1988**, *90*, 563–568, doi:10.1016/0300-9629(88)90668-8.

139. den Besten, G.; van Eunen, K.; Groen, A. K.; Venema, K.; Reijngoud, D.-J.; Bakker, B. M. The role of short-chain fatty acids in the interplay between diet, gut microbiota, and host energy metabolism. *J. Lipid Res.* **2013**, *54*, 2325–40, doi:10.1194/jlr.R036012.

140. Islam, R.; Anzai, N.; Ahmed, N.; Ellapan, B.; Jin, C. J.; Srivastava, S.; Miura, D.;

Fukutomi, T.; Kanai, Y.; Endou, H. Mouse organic anion transporter 2 (mOat2) mediates the transport of short chain fatty acid propionate. *J. Pharmacol. Sci.* **2008**, *106*, 525–8.

141.   Shin, H. J.; Anzai, N.; Enomoto, A.; He, X.; Kim, D. K.; Endou, H.; Kanai, Y. Novel liver-specific organic anion transporter OAT7 that operates the exchange of sulfate conjugates for short chain fatty acid butyrate. *Hepatology* **2007**, *45*, 1046–55, doi:10.1002/hep.21596.

142.   Bergman, E. N. Energy contributions of volatile fatty acids from the gastrointestinal tract in various species. *Physiol. Rev.* **1990**, *70*, 567–90.

143.   Binder, H. J. Role of colonic short-chain fatty acid transport in diarrhea. *Annu. Rev. Physiol.* **2010**, *72*, 297–313, doi:10.1146/annurev-physiol-021909-135817.

144.   Roediger, W. E. Utilization of nutrients by isolated epithelial cells of the rat colon. *Gastroenterology* **1982**, *83*, 424–9.

145.   Murase, M.; Kimura, Y.; Nagata, Y. Determination of portal short-chain fatty acids in rats fed various dietary fibers by capillary gas chromatography. *J. Chromatogr. B Biomed. Sci. Appl.* **1995**, *664*, 415–420, doi:10.1016/0378-4347(94)00491-M.

146.   Ballard, F. J. Supply and utilization of acetate in mammals. *Am. J. Clin. Nutr.* **1972**, *25*, 773–779, doi:10.1093/ajcn/25.8.773.

147.   Bloemen, J. G.; Venema, K.; van de Poll, M. C.; Olde Damink, S. W.; Buurman, W. A.; Dejong, C. H. Short chain fatty acids exchange across the gut and liver in humans measured at surgery. *Clin. Nutr.* **2009**, *28*, 657–61, doi:10.1016/j.clnu.2009.05.011.

148.   Knowles, S. E.; Jarrett, I. G.; Filsell, O. H.; Ballard, F. J. Production and utilization of acetate in mammals. *Biochem. J.* **1974**, *142*, 401–11.

149.   Gao, Z.; Yin, J.; Zhang, J.; Ward, R. E.; Martin, R. J.; Lefevre, M.; Cefalu, W. T.; Ye, J. Butyrate improves insulin sensitivity and increases energy expenditure in mice. *Diabetes* **2009**, *58*, 1509–17, doi:10.2337/db08-1637.

150.   Fushimi, T.; Suruga, K.; Oshima, Y.; Fukiharu, M.; Tsukamoto, Y.; Goda, T. Dietary acetic acid reduces serum cholesterol and triacylglycerols in rats feda cholesterol-rich

diet. *Br. J. Nutr.* **2006**, *95*, 916–924, doi:10.1079/BJN20061740.

151.   Demigné, C.; Morand, C.; Levrat, M. A.; Besson, C.; Moundras, C.; Rémésy, C. Effect of propionate on fatty acid and cholesterol synthesis and on acetate metabolism in isolated rat hepatocytes. *Br. J. Nutr.* **1995**, *74*, 209–19.

152.   Todesco, T.; Rao, A. V; Bosello, O.; Jenkins, D. J. Propionate lowers blood glucose and alters lipid metabolism in healthy subjects. *Am. J. Clin. Nutr.* **1991**, *54*, 860–5.

153.   Wolever, T. M.; Spadafora, P.; Eshuis, H. Interaction between colonic acetate and propionate in humans. *Am. J. Clin. Nutr.* **1991**, *53*, 681–7.

154.   Pereira, D. I. A.; Gibson, G. R. Effects of consumption of probiotics and prebiotics on serum lipid levels in humans. *Crit. Rev. Biochem. Mol. Biol.* **2002**, *37*, 259–81, doi:10.1080/10409230290771519.

155.   Brown, A. J.; Goldsworthy, S. M.; Barnes, A. A.; Eilert, M. M.; Tcheang, L.; Daniels, D.; Muir, A. I.; Wigglesworth, M. J.; Kinghorn, I.; Fraser, N. J.; Pike, N. B.; Strum, J. C.; Steplewski, K. M.; Murdock, P. R.; Holder, J. C.; Marshall, F. H.; Szekeres, P. G.; Wilson, S.; Ignar, D. M.; Foord, S. M.; Wise, A.; Dowell, S. J. The Orphan G protein-coupled receptors GPR41 and GPR43 are activated by propionate and other short chain carboxylic acids. *J. Biol. Chem.* **2003**, *278*, 11312–9, doi:10.1074/jbc.M211609200.

156.   Le Poul, E.; Loison, C.; Struyf, S.; Springael, J.-Y.; Lannoy, V.; Decobecq, M.-E.; Brezillon, S.; Dupriez, V.; Vassart, G.; Van Damme, J.; Parmentier, M.; Detheux, M. Functional characterization of human receptors for short chain fatty acids and their role in polymorphonuclear cell activation. *J. Biol. Chem.* **2003**, *278*, 25481–9, doi:10.1074/jbc.M301403200.

157.   Xiong, Y.; Miyamoto, N.; Shibata, K.; Valasek, M. A.; Motoike, T.; Kedzierski, R. M.; Yanagisawa, M. Short-chain fatty acids stimulate leptin production in adipocytes through the G protein-coupled receptor GPR41. *Proc. Natl. Acad. Sci.* **2004**, *101*, 1045–1050, doi:10.1073/pnas.2637002100.

158.   Zaibi, M. S.; Stocker, C. J.; O'Dowd, J.; Davies, A.; Bellahcene, M.; Cawthorne, M.

A.; Brown, A. J. H.; Smith, D. M.; Arch, J. R. S. Roles of GPR41 and GPR43 in leptin secretory responses of murine adipocytes to short chain fatty acids. *FEBS Lett.* **2010**, *584*, 2381–6, doi:10.1016/j.febslet.2010.04.027.

159.   Lu, Y.; Fan, C.; Li, P.; Lu, Y.; Chang, X.; Qi, K. Short Chain Fatty Acids Prevent High-fat-diet-induced Obesity in Mice by Regulating G Protein-coupled Receptors and Gut Microbiota. *Sci. Rep.* **2016**, *6*, 37589, doi:10.1038/srep37589.

160.   Sina, C.; Gavrilova, O.; Förster, M.; Till, A.; Derer, S.; Hildebrand, F.; Raabe, B.; Chalaris, A.; Scheller, J.; Rehmann, A.; Franke, A.; Ott, S.; Häsler, R.; Nikolaus, S.; Fölsch, U. R.; Rose-John, S.; Jiang, H.-P.; Li, J.; Schreiber, S.; Rosenstiel, P. G protein-coupled receptor 43 is essential for neutrophil recruitment during intestinal inflammation. *J. Immunol.* **2009**, *183*, 7514–22, doi:10.4049/jimmunol.0900063.

161.   Voltolini, C.; Battersby, S.; Etherington, S. L.; Petraglia, F.; Norman, J. E.; Jabbour, H. N. A Novel Antiinflammatory Role for the Short-Chain Fatty Acids in Human Labor. *Endocrinology* **2012**, *153*, 395–403, doi:10.1210/en.2011-1457.

162.   Thangaraju, M.; Cresci, G. A.; Liu, K.; Ananth, S.; Gnanaprakasam, J. P.; Browning, D. D.; Mellinger, J. D.; Smith, S. B.; Digby, G. J.; Lambert, N. A.; Prasad, P. D.; Ganapathy, V. GPR109A is a G-protein-coupled receptor for the bacterial fermentation product butyrate and functions as a tumour suppressor in colon. *Cancer Res.* **2009**, *69*, 2826–32, doi:10.1158/0008-5472.CAN-08-4466.

163.   Millard, A. L.; Mertes, P. M.; Ittelet, D.; Villard, F.; Jeannesson, P.; Bernard, J. Butyrate affects differentiation, maturation and function of human monocyte-derived dendritic cells and macrophages. *Clin. Exp. Immunol.* **2002**, *130*, 245–55.

164.   Meijer, K.; de Vos, P.; Priebe, M. G. Butyrate and other short-chain fatty acids as modulators of immunity: what relevance for health? *Curr. Opin. Clin. Nutr. Metab. Care* **2010**, *13*, 715–21, doi:10.1097/MCO.0b013e32833eebe5.

165.   Brestoff, J. R.; Artis, D. Commensal bacteria at the interface of host metabolism and the immune system. *Nat. Immunol.* **2013**, *14*, 676–84, doi:10.1038/ni.2640.

166.   Maslowski, K. M.; Vieira, A. T.; Ng, A.; Kranich, J.; Sierro, F.; Yu, D.; Schilter, H.

1

C.; Rolph, M. S.; Mackay, F.; Artis, D.; Xavier, R. J.; Teixeira, M. M.; Mackay, C. R. Regulation of inflammatory responses by gut microbiota and chemoattractant receptor GPR43. *Nature* **2009**, *461*, 1282–6, doi:10.1038/nature08530.

1
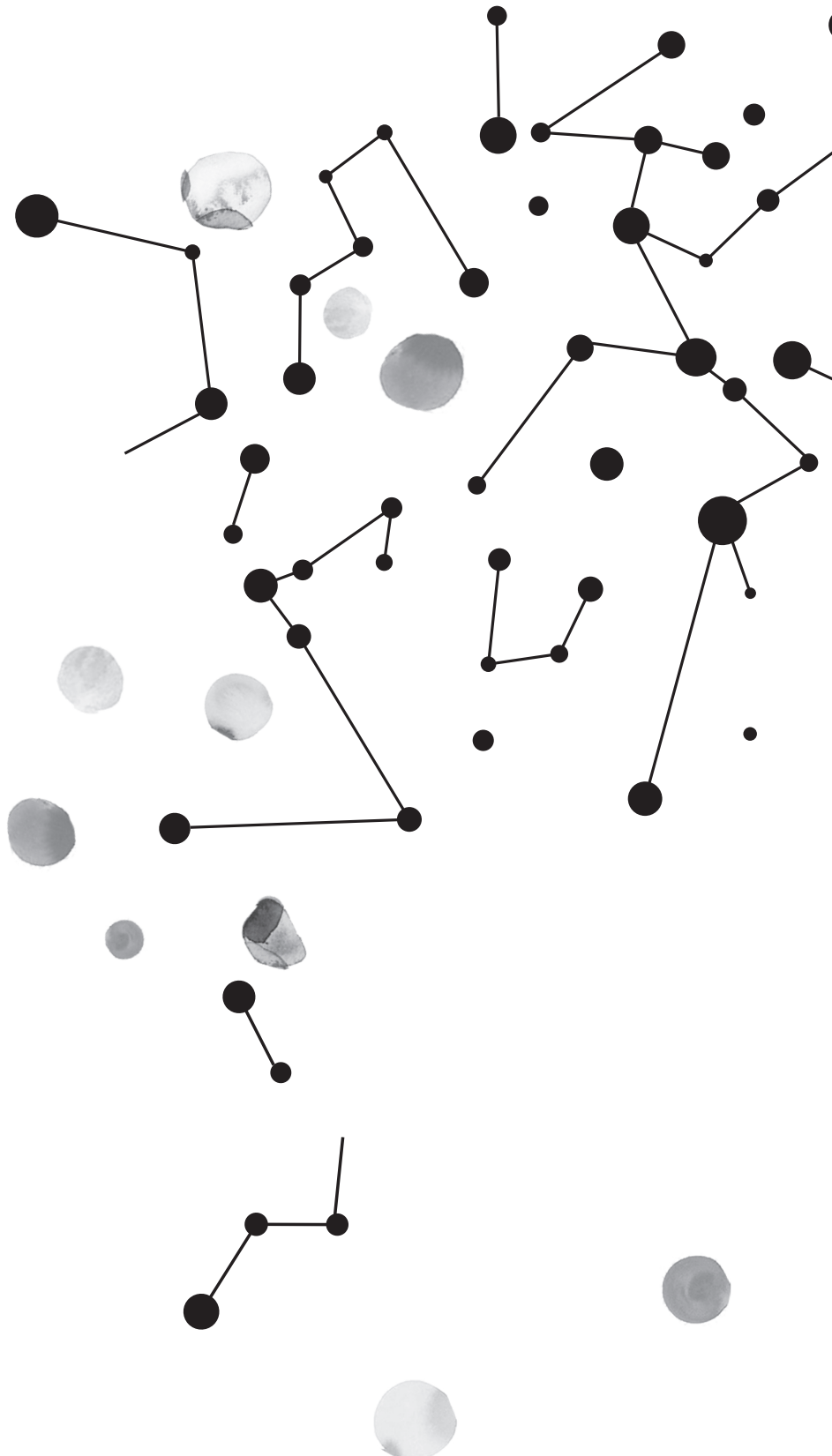
GC-MS ANALYSIS
OF MEDIUM- AND LONG-CHAIN
FATTY ACIDS IN BLOOD SAMPLES

02

Lisa R. Hoving,

Marieke Heijink,

Vanessa van Harmelen,

Ko Willems van Dijk, and

Martin Giera

ABSTRACT

Our body contains a wide variety of fatty acids that differ in chain length, the degree of unsaturation, and location of the double bonds. As the various fatty acids play distinct roles in health and disease, methods that can specifically determine the fatty acid profile are needed for fundamental and clinical studies. Here we describe a method for the separation and quantification of fatty acids ranging from 8 to 24 carbon chain lengths in blood samples using gas chromatography-mass spectrometry following derivatization using pentafluorobenzyl bromide. This method quantitatively monitors fatty acid composition in a manner that satisfies the requirements for comprehensiveness, sensitivity, and accuracy.

2

INTRODUCTION

Lipids and fatty acids (FAs) are present in all organisms and constitute essential structural elements of biological membranes, regulate and control cellular function, and are involved in the onset and progression of various diseases [1]. The majority of FAs are present as esters in lipids, such as triacylglycerols, sterol esters, and phospholipids. Only a small fraction is nonesterified, generally termed free FAs (FFAs) [2]. The role of FAs in health and disease has gained extensive interest. FAs differ in chain length, the degree of unsaturation, and location of the double bond(s). As various types of FAs have different associations with disease outcomes, the assessment of the FA composition in biological samples may provide suitable information. Therefore, great effort has been put in the development of comprehensive, sensitive, and reliable methodologies to quantify the FA composition. Here we describe step-by-step the quantitative analysis of the FA profile in plasma using GC-MS, measuring FAs with a chain length ranging from 8 to 24 carbons.

GC-MS is an analytical technique that is well-suited for the analysis of the total amount of FAs as well as the FA composition within a sample [3]. As blood contains both esterified FAs and FFAs, a separate hydrolysis step is required during sample preparation to determine the total FA composition. For the analysis of FAs by GC-MS, it is of importance to convert FAs into suitable volatile derivatives by derivatization (e.g., alkylation or silylation) [4]. Traditionally in GC-MS analysis, FAs were being transformed into their methyl ester or trimethylsilyl ester derivatives [5]. Alternatively, pentafluorobenzyl bromide (PFBBr) can be used to derivatize FAs. It has been successfully applied for the analysis of FAs with different chain lengths [6–9]. The benzyl bromide group reacts with the carboxylic acid group to form a pentafluorobenzyl ester. In addition, this pentafluorobenzyl ester contains ideal properties for electron capture negative ionisation (ECNI), a highly selective and sensitive ionisation technique. The combination of PFBBr derivatization and ECNI ionisation allows for the analysis of negatively charged molecular ions. These ions are usually detected in the single ion monitoring (SIM) mode on quadrupole-based mass spectrometers. Isotopically labelled internal standards (IS) have to be used for quantitative analysis of FAs by GC-MS. The addition of IS

in GC-MS analysis enables quantitative analysis of biological samples and greatly improves detection specificity [10].

MATERIALS

Use only high-purity solvents (preferably LC-MS grade) in order to prevent increased background signals (*see* **Note 1**). If vendors from different materials are mentioned in this method section, the use of these chemicals is recommended based on our previous experiences. The use of 10 M NaOH forms an exception. In order for the method to succeed, it is urged to use the specific items mentioned in the Materials section. An overview of the amount of materials and chemicals is provided in Table 1.

MATERIALS FOR SAMPLE PREPARATION

1. Glass autosampler vials, inserts, and caps. It is recommended to use Agilent certified 2 mL vials with screw top; Agilent certified 250 μL inserts with polymer feet; and Agilent screw caps with PTFE/red silicone septum.

2. 1 μg/mL IS solution in ethanol (EtOH) (*see* **Note 2**): accurately weigh decanoic acid-d19, palmitic acid-d31, and arachidonic acid-d8, and dissolve in EtOH to a final concentration of 1 μg/mL. Store at −80°C.

3. Concentration series of FA standards in EtOH: use GLC reference standard 85 mix (Nu-Chek Prep), eicosapentaenoic acid (Cayman), docosapentaenoic acid (Cayman), and docosahexaenoic acid (Cayman), and serially dilute using EtOH. Prepare concentrations ranging from the lower limit of quantification (LLOQ) (*see* Table 2) to 50 μg/mL. Store at −80°C.

4. 172 mM PFBBr in acetone: add 26.8 μL PFBBr to 1 mL acetone. Prepare fresh daily.

5. 10 M NaOH in water. In order for the method to succeed, it is urged to use a prepared solution from Sigma-Aldrich (Art. No. 72068) (*see* **Note 3**).

Table 1. Chemicals and materials needed per sample for the quantification of FAs

Chemical / material	Calibration series per sample	Plasma / serum sample
Plasma / serum	-	10 μL
Acetone	250 μL	250 μL
10 M NaOH	-	10 μL
1 μg/mL IS solution	10 μL	10 μL
Standards in EtOH	10 μL[a]	-
EtOH	-	10 μL
172 mM PFBBr	100 μL	100 μL
n-hexane	500 μL	500 μL
Water	250 μL	250 μL
Glass autosampler vials	2	2
Glass autosampler inserts	1	1
Glass autosampler caps	2	2

For every batch of samples, take along three blank samples. Blank samples should be processed in exactly the same way as biological samples

[a] For every individual sample of the calibration series, a specific concentration of standards in EtOH is used

MATERIALS FOR GC-MS

1. GC with split/splitless injector, coupled to a quadrupole mass spectrometer with chemical ionisation source.

2. Injection: autosampler (recommended).

3. GC column: use an Agilent VF-5 ms column (5% phenylmethyl; 25 m × 0.25 mm internal diameter; 0.25 μm film thickness).

4. Pure helium (99.9990%) and methane (99.9995%) are used as carrier and chemical ionisation gas, respectively.

METHODS

Palmitic acid and stearic acid are ubiquitous. Hence, extra care has to be taken to prevent sample contamination. Sources of contamination include low-quality plastics and (low-purity) solvents (*see* **Note 1**).

SAMPLE PREPARATION

1. Facilitate rapid sampling. Store samples at −80°C upon collection if the samples are not prepared immediately (*see* **Note 4**).

2. Prepare a glass autosampler vial for every sample: for calibration samples, add 250 µL acetone and 10 µL of your calibration series FA standards at the desired concentration. An indication of the expected LLOQ for every FA is provided in Table 2. For biological samples, add 250 µL acetone (*see* **Note 5**), 10 µL EtOH (*see* **Note 6**), and 10 µL plasma or serum into a glass autosampler vial. For blank samples, add 250 µL acetone and 10 µL EtOH into a glass autosampler vial. For every experiment, three blank samples should be included.

3. Hydrolyse the biological and blank samples (*see* **Note 7**): add 10 µL 10 M NaOH to the biological and blank samples. Vortex all samples. Heat the biological and blank samples at 60°C for 30 min in a laboratory stove. Let the samples cool down to room temperature (approximately 15 min).

4. Add 10 µL 1 µg/mL IS solution (*see* **Notes 2** and **8**) to every sample and vortex all samples.

5. Add 100 µL 172mM PFBBr in acetone (*see* **Note 9**). Vortex the samples.

6. Heat the samples at 60°C for 30 min in a laboratory stove. Let the samples cool down to room temperature (approximately 15 min) (*see* **Note 10**).

7. Add 500 µL *n*-hexane and 250 µL water to the samples. Shake vigorously in vertical direction of the vial for 10 sec. Let the samples rest for 1 min at room temperature.

8. Prepare a new empty glass autosampler vial with a glass insert for every sample. Transfer 250 µL of the *n*-hexane (upper layer) into the glass insert.

Table 2. Overview of FAs

FA	Name	RT (min)	Monitored m/z (M⁻)	LLOQ (ng/mL)[a]	IS
FA 08:0	Octanoic acid	10.14	143.1	200	FA 10:0-d19
FA 10:0	Decanoic acid	11.01	171.1	50	FA 10:0-d19
FA 10:0-d19	Decanoic acid-d19	10.92	190.3	N/A	N/A
FA 11:0	Undecanoic acid	11.42	185.2	50	FA 10:0-d19
FA 12:0	Lauric acid	11.87	199.2	100	FA 10:0-d19
FA 13:0	Tridecanoic acid	12.40	213.2	50	FA 10:0-d19
FA 14:0	Myristic acid	13.03	227.2	50	FA 16:0-d31
FA 14:1 (n-5)	Myristoleic acid	12.97	225.2	20	FA 16:0-d31
FA 15:0	Pentadecanoic acid	13.78	241.2	50	FA 16:0-d31
FA 15:1 (n-5)	10-Pentadecenoic acid	13.72	239.2	10	FA 16:0-d31
FA 16:0	Palmitic acid	14.68	255.2	500	FA 16:0-d31
FA 16:0-d31	Palmitic acid-d31	14.43	286.4	N/A	N/A
FA 16:1 (n-7)	Palmitoleic acid	14.50	253.2	50	FA 16:0-d31
FA 17:0	Heptadecanoic acid	15.72	269.3	20	FA 16:0-d31
FA 17:1 (n-7)	10-Heptadecenoic acid	15.53	267.2	10	FA 16:0-d31
FA 18:0	Stearic acid	16.54	283.3	500	FA 16:0-d31
FA 18:1 (n-9) cis	Oleic acid	16.37	281.3	100	FA 16:0-d31
FA 18:1 (n-9) trans	Elaidic acid	16.41	281.3	50	FA 16:0-d31
FA 18:2 (n-6)	Linoleic acid	16.34	279.2	50	FA 16:0-d31
FA 18:3 (n-6)	Gamma linolenic acid (GLA)	16.15	277.2	50	FA 16:0-d31
FA 18:3 (n-3)	Alpha linolenic acid (ALA)	16.40	277.2	50	FA 16:0-d31
FA 20:0	Arachidic acid	17.66	311.3	50	FA 20:4-d8
FA 20:1 (n-9)	11-Eicosenoic acid	17.55	309.3	20	FA 20:4-d8
FA 20:2 (n-6)	11,14-Eicosadienoic acid	17.54	307.3	10	FA 20:4-d8
FA 20:3 (n-6)	Homo-Gamma linolenic acid (DGLA)	17.43	305.3	10	FA 20:4-d8
FA 20:3 (n-3)	11,14,17-Eicosatrienoaic acid	17.58	305.3	10	FA 20:4-d8
FA 20:4 (n-6)	Arachidonic acid (AA)	17.28	303.2	10	FA 20:4-d8

(Continued)

Table 2. *Continued*

FA	Name	RT (min)	Monitored *m/z* (M⁻)	LLOQ (ng/mL)ᵃ	IS
FA 20:4-d8	Arachidonic acid-d8 (AA-d8)	17.26	311.3	N/A	N/A
FA 20:5 (n-3)	Eicosapentaenoic acid (EPA)	17.33	301.2	10	FA 20:4-d8
FA 22:0	Behenic acid	18.48	339.3	50	FA 20:4-d8
FA 22:1 (n-9)	Erucic acid	18.40	337.3	20	FA 20:4-d8
FA 22:2 (n-6)	13,16-Docosadienoic acid	18.39	335.3	10	FA 20:4-d8
FA 22:4 (n-6)	Adrenic acid (AdA)	18.21	331.3	10	FA 20:4-d8
FA 22:5 (n-3)	Docosapentaenoic acid (DPA)	18.25	329.3	10	FA 20:4-d8
FA 22:6 (n-3)	Docosahexaenoic acid (DHA)	18.15	327.2	20	FA 20:4-d8
FA 24:1 (n-9)	Nervonic acid	19.28	365.4	20	FA 20:4-d8

For each FA, an indication of the retention time (RT), the *m*/z value, an indication of the LLOQ, and the IS to be used are shown.

N/A not applicable

ᵃ An indication of the lowest concentration to be included in the calibration series. This LLOQ is determined for every individual experiment. The calibration series samples are measured twice. A specific concentration is included if signal/noise >10 and if the accuracy based on the calibration obtained ≥80 and ≤120% for both measurements

GC-MS ANALYSIS

1. Inject 1 µL in the GC-MS, splitless at 280°C.

2. Use helium as carrier gas at a constant flow rate of 1.20 mL/min.

3. Use the following temperature gradient: 1 min at 50°C, linear increase at 40°C/min to 60°C, held for 3 min at 60°C, linear increase at 25°C/min to 237°C, linear increase at 3°C/min to 250°C, linear increase at 25°C/min to 315°C, held for 1.55 min at 315°C.

4. Set the transfer line temperature at 280°C.

5. Keep the ionisation source temperature at 280°C.

6. Use methane as chemical ionisation gas at approximately 15 psi.

7. Detect ions obtained in the negative mode using SIM analysis (*see* **Notes 11** and **12**). Table 2 provides the *m*/z values to be monitored and an indication of retention times (RT).

As a consequence of small chromatographic differences (e.g., GC column length), the exact RT varies between various GC systems. Hence, calibration using external standards is mandatory.

DATA ANALYSIS

1. Integrate the obtained signal (*see* **Note 13**).

2. Calculate the relative retention times (RRT) and area ratios using the respective IS (*see* Table 2) (*see* **Notes 14** and **15**).

3. Determine the slope and LLOQ for every FA by performing linear regression. It is recommended to use a weighing factor of $1/x^2$ [11].

4. Calculate the FA concentrations by using the area ratios obtained from the biological samples, average signal of the blank samples as intercept (*see* **Note 16**), and the slopes obtained from the analysis of the calibration series samples.

NOTES

1. Palmitic acid and stearic acid usually give high background signals, resulting in a relatively high LLOQ (Fig. 1). Sources of these FAs include solvents and plastic containers of inferior quality. Background signals of these FAs can be diminished by using high-purity solvents (preferably LC-MS grade). Additionally, use glass vials for organic solvents.

2. The IS signal should be present in every sample. The IS are used to correct for differences in sample preparation between the samples. Use exactly the same batch of 1 μg/mL IS solution in EtOH for the entire experiment, as minor differences in IS composition might translate into systematic under or overestimation of FAs in samples.

3. Sodium hydroxide pellets can be heavily contaminated by FAs.

4. Collect the biological samples as quickly as possible, and store the samples at −80°C. Levels of FAs can change upon sample collection if the collection is performed slowly or when samples are stored improperly by auto-oxidation of polyunsaturated FAs and enzymatic hydroxylation.
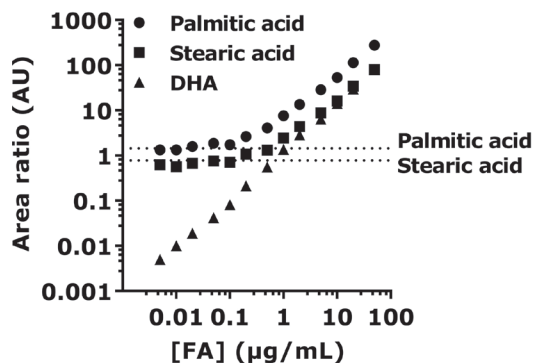
Fig. 1 Background signal of palmitic acid and stearic acid. Palmitic acid and stearic acid usually show a high background signal. As a consequence, the LLOQ for these FAs is higher than for FAs which do not show a high background signal like docosahexaenoic acid (DHA). The dashed lines in the graph show the size of the background signals.

5.   Acetone facilitates the precipitation of proteins.

6.   The addition of 10 μL EtOH to the samples ensures that the solvents of the biological samples are matched to the solvents in the calibration samples.

7.   No esterified FAs are present in the calibration series samples. Therefore, no hydrolysation step is needed.

8.   Under highly alkaline conditions, risk of hydrogen–deuterium exchange exists [12]. Therefore, the IS need to be added after hydrolysis.

9.   Within this protocol no base is added to catalyse the derivatization reaction, since the addition of base can severely increase FA background [7].

10. *n*-Hexane is added after the samples have been cooled down in order to prevent evaporation and spilling.

11. Sensitivity is higher when the mass spectrometer is operated in SIM mode as compared to the full scan mode. However, the full scan mode can be very useful to detect FAs that are not incorporated in the SIM method or to determine the RT of a specific FA. If one

decides to operate in full scan mode, an m/z range of 100-400 can be used.

12. For isotopologue analysis, either m/z values corresponding to isotopologues can be added to the SIM method (e.g., M0, M1, M2, etc. for every FA) [7] or the MS can be operated in scheduled scan mode (e.g., scan window including m/z values corresponding to M0, M1, M2, etc., for every FA).

13. Oleic and elaidic acids have equal masses and are not baseline separated. In some cases, it is therefore not possible to accurately and precisely quantify one or both of these two FAs within the same sample. FA 20:1 (n-9) and FA 22:1 (n-9), co-elute with, respectively, FA 20:2 (n-6) and FA 22:2 (n-6). As a consequence, the M2 isotopes (containing $2 \times {}^{13}C$ instead of ${}^{12}C$) of FA 20:2 (n-6) and FA 22:2 (n-6) might contaminate the FA 20:1 (n-9) and FA 22:1 (n-9) signal.

14. $\mathrm{RRT} = \dfrac{\text{retention time analyte}}{\text{retention time IS}}$

15. $\text{Area ratio} = \dfrac{\text{area analyte}}{\text{area IS}}$

16. The blank samples reflect the background signal of the biological samples more accurately than the intercept obtained from the linear regression of the calibration series samples. Therefore, use the average area ratio of the blank samples as background signal/intercept to calculate the concentrations of the biological samples. Use the following formula:

$\text{concentration} = \dfrac{\text{area ratio - average area ratio blank samples}}{\text{slope}}$

REFERENCES

1. Siri-Tarino, P. W.; Chiu, S.; Bergeron, N.; Krauss, R. M. Saturated Fats Versus Polyunsaturated Fats Versus Carbohydrates for Cardiovascular Disease Prevention and Treatment. *Annu. Rev. Nutr.* **2015**, *35*, 517–43, doi:10.1146/annurev-nutr-071714-034449.

2. van Meer, G.; Voelker, D. R.; Feigenson, G. W. Membrane lipids: where they are and how they behave. *Nat. Rev. Mol. Cell Biol.* **2008**, *9*, 112–124, doi:10.1038/nrm2330.

3. Dołowy, M.; Pyka, A. Chromatographic Methods in the Separation of Long-Chain Mono- and Polyunsaturated Fatty Acids. *J. Chem.* **2015**, *2015*.

4. Gao, P.; Xu, G. Mass-spectrometry-based microbial metabolomics: recent developments and applications. *Anal. Bioanal. Chem.* **2015**, *407*, 669–80, doi:10.1007/s00216-014-8127-7.

5. Kloos, D.-P.; Gay, E.; Lingeman, H.; Bracher, F.; Müller, C.; Mayboroda, O. A.; Deelder, A. M.; Niessen, W. M. A.; Giera, M. Comprehensive gas chromatography-electron ionisation mass spectrometric analysis of fatty acids and sterols using sequential one-pot silylation: quantification and isotopologue analysis. *Rapid Commun. Mass Spectrom.* **2014**, *28*, 1507–14, doi:10.1002/rcm.6923.

6. Quehenberger, O.; Armando, A. M.; Dennis, E. A. High sensitivity quantitative lipidomics analysis of fatty acids in biological samples by gas chromatography-mass spectrometry. *Biochim. Biophys. Acta - Mol. Cell Biol. Lipids* **2011**, *1811*, 648–656, doi:10.1016/j.bbalip.2011.07.006.

7. Tomcik, K.; Ibarra, R. A.; Sadhukhan, S.; Han, Y.; Tochtrop, G. P.; Zhang, G. F. Isotopomer enrichment assay for very short chain fatty acids and its metabolic applications. *Anal. Biochem.* **2011**, *410*, 110–117, doi:10.1016/j.ab.2010.11.030.

8. Quehenberger, O.; Armando, A.; Dumlao, D.; Stephens, D. L.; Dennis, E. A. Lipidomics analysis of essential fatty acids in macrophages. *Prostaglandins, Leukot. Essent. Fat. Acids* **2008**, *79*, 123–129, doi:10.1016/j.plefa.2008.09.021.

9. Pawlosky, R. J.; Sprecher, H. W.; Salem, N. High sensitivity negative ion GC-MS method for detection of desaturated and chain-elongated products of deuterated linoleic and linolenic acids. *J. Lipid Res.* **1992**, *33*, 1711–7.

10. Kloos, D.; Lingeman, H.; Mayboroda, O. A.; Deelder, A. M.; Niessen, W. M. A.; Giera,

2

M. Analysis of biologically-active, endogenous carboxylic acids based on chromatography-mass spectrometry. *TrAC - Trends Anal. Chem.* **2014**, *61*, 17–28.

11. Gu, H.; Liu, G.; Wang, J.; Aubry, A. F.; Arnold, M. E. Selecting the correct weighting factors for linear and quadratic calibration curves with least-squares regression algorithm in bioanalytical LC-MS/MS assays and impacts of using incorrect weighting factors on curve stability, data quality, and assay perfo. *Anal. Chem.* **2014**, *86*, 8959–8966, doi:10.1021/ac5018265.

12. Lee, J.; Jang, E.-S.; Kim, B. Development of isotope dilution-liquid chromatography/mass spectrometry combined with standard addition techniques for the accurate determination of tocopherols in infant formula. *Anal. Chim. Acta* **2013**, *787*, 132–139, doi:10.1016/j.aca.2013.05.034.
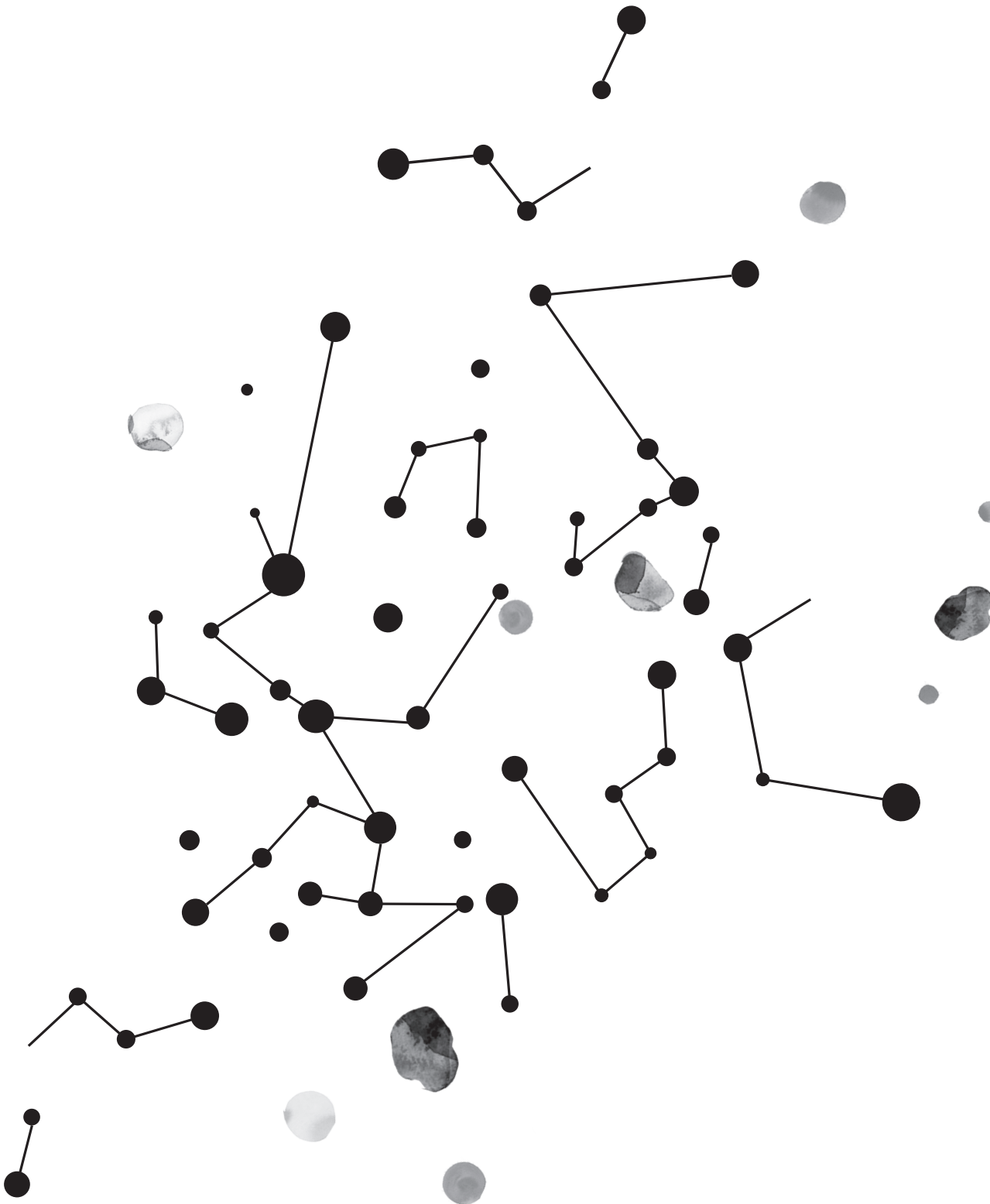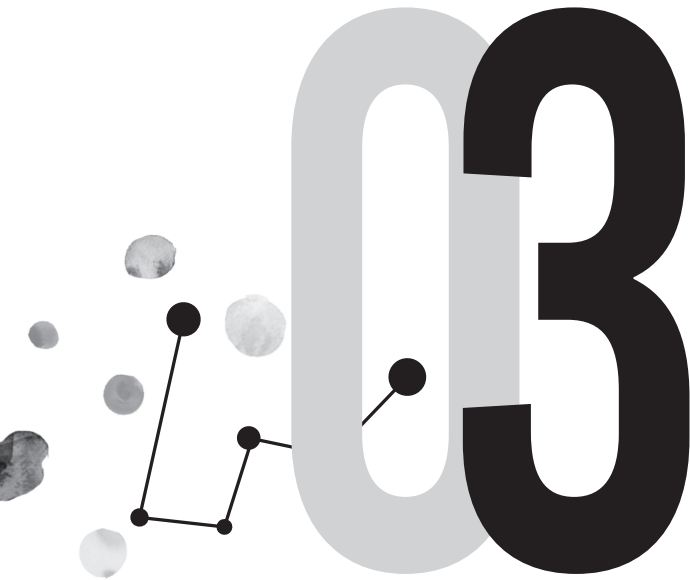
2

GC-MS ANALYSIS OF SHORT-CHAIN FATTY ACIDS IN FECES, CECUM CONTENT, AND BLOOD SAMPLES

03

Lisa R. Hoving,

Marieke Heijink,

Vanessa van Harmelen,

Ko Willems van Dijk, and

Martin Giera

ABSTRACT

Short-chain fatty acids, the end products of fermentation of dietary fibers by the gut microbiota, have been shown to exert multiple effects on mammalian metabolism. For the analysis of short-chain fatty acids, gas chromatography–mass spectrometry is a very powerful and reliable method. Here, we describe a fast, reliable, and reproducible method for the separation and quantification of short-chain fatty acids in mouse feces, cecum content, and blood samples (i.e., plasma or serum) using gas chromatography–mass spectrometry. The short-chain fatty acids analysed include acetic acid, propionic acid, butyric acid, valeric acid, hexanoic acid, and heptanoic acid.

3

INTRODUCTION

Lipids and fatty acids (FAs) are essential molecules in the regulation and control of various biological functions and play a role in the onset and progression of disease [1]. FAs with less than 8 carbon atoms are considered short-chain fatty acids (SCFAs) [2]. SCFAs (predominantly acetic acid, propionic acid, and butyric acid with respectively 2, 3, and 4 carbon atoms) are mainly produced in the colonic lumen after anaerobic fermentation of indigestible carbohydrates by saccharolytic gut bacteria [3]. The link between diet, the gut microbiota, the production of SCFAs and their role in human health and disease is an active area of research [4]. This requires suitable analytical techniques for sensitive and accurate quantification of SCFAs. One technique traditionally used for the analysis of small, volatile molecules is gas chromatography–mass spectrometry (GC-MS). Here, were describe step by step the quantitative analysis of the SCFAs acetic acid, propionic acid, butyric acid, valeric acid, hexanoic acid, and heptanoic acid using GC-MS in feces, cecum content, as well as in blood samples (i.e., plasma or serum).

GC-MS is an analytical technique, well suited for the analysis of SCFAs and other (longer) FAs [5]. However, one critical step in the GC-MS analysis of FAs is their conversion into suitable volatile derivatives by derivatization (e.g., by alkylation or silylation) [6]. Traditionally, FAs are being transformed into their methyl ester, or trimethylsilyl ester derivatives in GC-MS analysis [7]. While both approaches work well for longer chain FAs, the intrinsically low boiling point of the SCFA methyl ester or trimethylsilyl ester derivatives results in some issues with their GC-MS based analysis. For example, the trimethylsilyl ester of acetic acid roughly presents the same boiling point as the commonly used derivatization reagents, leading to severe signal overlap.

Alternatively, for SCFA analysis FAs can be derivatized by the alkylation reagent pentafluorobenzyl bromide (PFBBr) [8,9]. The benzyl bromide group reacts with the carboxylic acid group to form an ester, allowing analysis as pentafluorobenzyl ester. Additionally, this so-formed ester presents ideal properties for electron-capture negative ionisation (ECNI), which is a highly selective and sensitive ionisation technique. ECNI allows analysis of the

negatively charged molecular ions, usually detected in the single ion monitoring mode (SIM) on quadrupole based mass spectrometers.

For targeted analysis of SCFAs, ideally isotopically labelled internal standards (IS) should be used. The use of IS enables quantitative analysis of biological samples and greatly improves specificity [7,9].

Apart from GC-MS, Nuclear magnetic resonance (NMR) spectroscopy can be used to analyse SCFAs in feces or cecum content. An interplatform comparison performed in our lab, comparing GC-MS and NMR spectroscopy, showed good correlations for the measurements of SCFA concentrations. However, the advantage of GC-MS over NMR is its higher sensitivity, which is essential for the analysis of SCFAs at low concentrations such as SCFAs present in blood.

MATERIALS

Use only high purity solvents (preferably LC-MS grade) in order to prevent elevated background signals (*see* **Note 1**). An overview of the amount of materials and chemicals is provided in Table 1. If vendors of different materials are specifically mentioned in this section, the use of these materials are recommended based on our previous experiences.

MATERIALS FOR SAMPLE PREPARATION

1. Glass autosampler vials, inserts, and caps. It is important to use the highest quality glass ware. We recommend to use the following items: Agilent certified 2 mL vials with screw top; Agilent certified 250 µL inserts with polymer feet; Agilent screw caps with PTFE/red silicone septum.

2. 1 µg/mL IS solution in ethanol (EtOH) (*see* **Note 2**): mix acetic acid-d4, propionic acid-d6 and butyric acid-d8 and dissolve in EtOH to a final concentration of 1 µg/mL. Store at −80°C. Apart from butyric acid, butyric acid-d8 is also used as the IS for valeric acid, hexanoic acid, and heptanoic acid.

Table 1. Chemicals and materials required per sample for the quantification of SCFAs. For every type of biological matrix, take along three blank samples. Blank samples should be processed in exactly the same way as biological samples

Chemical/material	Calibration series sample	Biological sample		
		Feces	**Cecum content**	**Plasma/ serum**
Biological sample	-	± 50 mg	± 10 mg	10 μL
Water	250 μL	550 μL	690 μL	250 μL
Acetone	250 μL	250 μL	250 μL	250 μL
1 μg/mL IS solution	10 μL	10 μL	10 μL	10 μL
Standards in EtOH	10 μL[a]	-	-	-
EtOH	-	10 μL	10 μL	10 μL
172 mM PFBBr	100 μL	100 μL	100 μL	100 μL
n-hexane	500 μL	500 μL	500 μL	500 μL
1.5 mL plastic tubes	-	2	3	-
Clean steel beads	-	2	2	-
Glass autosampler vials	2	2	2	2
Glass autosampler inserts	1	1	1	1
Glass autosampler caps	2	2	2	2

[a] For every individual sample of the calibration series, a specific concentration of standards in EtOH is used

3. Concentration series of SCFA standards in EtOH: use the SCFA standard mixture (Sigma-Aldrich) and dilute with EtOH. Prepare concentrations ranging from the lower limit of quantification (LLOQ) (*see* Table 2) to 1000 μM. Store at −80°C.

4. 172 mM PFBBr in acetone: add 26.8 μL PFBBr to 1 mL acetone. Prepare fresh daily.

5. Clean steel beads (only for fibrous biological matrices): rinse 3.2 mm stainless steel beads with methanol and dry at room temperature.

MATERIALS FOR GC-MS

1. GC with split/splitless injector, coupled to a quadrupole mass spectrometer with chemical ionisation source.

2. Injection: autosampler (recommended).

75

3. GC column: use an Agilent VF-5 ms column (5% phenylmethyl; 25 m × 0.25 mm internal diameter; 0.25 μm film thickness).

4. Pure helium (99.9990%) and methane (99.9995%) should be used as carrier and as chemical ionisation gas, respectively.

Table 2. Overview of FAs. For each SCFA, an indication of the retention time (RT), the *m/z*-value, an indication of the LLOQ, and the IS to be used are shown

FA	Name	RT (min)	Monitored *m/z* (M⁻)	LLOQ (μM)[a]	IS
FA 2:0-d4	acetic acid-d4	7.19	62	N/A	N/A
FA 2:0	acetic acid	7.22	59	20	FA 2:0-d4
FA 3:0-d6	propionic acid-d6	7.86	78	N/A	N/A
FA 3:0	propionic acid	7.89	73	5	FA 3:0-d6
FA 4:0-d8	butyric acid-d8	8.41	94	N/A	N/A
FA 4:0	butyric acid	8.44	87	2	FA 4:0-d8
FA 5:0	valeric acid	8.99	101	1	FA 4:0-d8
FA 6:0	hexanoic acid	9.51	115	5	FA 4:0-d8
FA 7:0	heptanoic acid	9.99	129	1	FA 4:0-d8

[a] An indication of the lowest concentration to be included in the calibration series. This LLOQ is determined for every individual experiment. The calibration series samples are measured twice. A specific concentration is included if signal/noise >10 and if the accuracy based on the calibration obtained ≥80 and ≤120% for both measurements

N/A not applicable.

METHODS

SCFAs are ubiquitous. Hence, extra care has to be taken to prevent sample contamination. Possible sources of contamination include environmental air, pipettes, pipette tips, low quality plastics, and (low purity) solvents (*see* **Note 1**). Interday and intraday repeatability of the method, validated in fetal calf serum (FCS), is provided in Table 3.

Table 3. Interday and intraday repeatability data in FCS. FCS was spiked with 5 µM and 100 µM SCFA. Acetic acid, propionic acid and butyric acid in these samples were quantified in triplicate on three different days using the described method

FA	Day	FCS		FCS + 5 µM SCFA		FCS + 100 µM SCFA		
		Mean (µM)	RSD	Mean (µM)	RSD	Mean (µM)	RSD	RE[a]
Acetic acid	intraday 1	108.5	0,12	113.4	0,12	204.4	0,03	-0,04
	intraday 2	126.5	0,05	120.8	0,04	180.2	0,03	-0,46
	intraday 3	117.8	0,11	121.4	0,06	192.5	0,06	-0,25
	interday	117.6	0,08	118.5	0,04	192.4	0,06	-0,25
Propionic acid	intraday 1	<LLOQ	N/A	10.5	0,18	101.3	0,02	-0,04
	intraday 2	<LLOQ	N/A	9.3	0,08	89.4	0,04	-0,16
	intraday 3	8.1	0,24	13.5	0,08	96.5	0,02	-0,13
	interday	N/A	N/A	11.1	0,19	95.7	0,06	-0,11
Butyric acid	intraday 1	<LLOQ	N/A	7.3	0,24	96.7	0,05	-0,06
	intraday 2	<LLOQ	N/A	5.7	0,09	87.9	0,07	-0,14
	intraday 3	<LLOQ	N/A	6.7	0,06	80.8	0,1	-0,22
	interday	<LLOQ	N/A	6.6	0,12	88.5	0,09	-0,14

[a] RE, based on the difference in the determined concentrations. For acetic acid, the RE is determined based on the difference between the FCS and FCS + 100 µM SCFA sample. For propionic acid and butyric acid, the RE is determined based on the difference between the FCS +5 µM SCFA and FCS + 100 µM SCFA sample.

N/A not applicable, *RE* relative error, *RSD* relative standard deviation

SAMPLE PREPARATION OF FECES, CECUM CONTENT, AND BLOOD

1. Facilitate rapid sampling. Store the samples at −80 °C upon collection if the samples are not prepared immediately (*see* **Note 3**).

2. Matrix dependent pre-processing of feces:

    Prepare an aqueous extract of feces. Weigh feces (approximately 50 mg mouse feces) (*see* **Note 4**) in a 1.5 mL plastic tube with 0.1 mg accuracy and add 300 µL water. Homogenise the sample using a bullet blender: add two clean 3.2 mm steel beads and blend the sample for 5 min. Centrifuge at $1400 \times g$ for 10 min. Transfer the supernatant to a fresh 1.5 mL plastic tube.

3. Matrix dependent pre-processing of cecum content:

   Weigh cecum content (approximately 10 mg mouse cecum content) (*see* **Note 4**) in a 1.5 mL plastic tube with 0.1 mg accuracy and add 400 µL water. Homogenise by vortexing. Use a bullet blender if the material is fibrous: add two clean 3.2 mm steel beads and blend the sample for 5 min. Centrifuge at 1400 × *g* for 10 min. Transfer the supernatant to a fresh 1.5 mL plastic tube. Dilute the supernatant 1:5 with water in a total volume of 50 µL using a fresh 1.5 mL plastic tube.

4. Matrix dependent preprocessing of blood:

   Obtain plasma and/or serum. No further pre-processing is needed.

5. Prepare a glass autosampler vial for every sample:

6. For calibration samples, add 250 µL acetone, 10 µL 1 µg/mL IS solution, and 10 µL of the calibration series SCFA standards at the desired concentration. In case of feces or cecum content analysis, add 10 µL water which is pre-processed exactly the same as the biological samples. This includes bullet blending if necessary.

7. For biological samples, add 250 µL acetone (*see* **Note 5**), 10 µL 1 µg/mL IS solution in EtOH (*see* **Note 2**), 10 µL EtOH (*see* **Note 6**), and 10 µL aqueous feces, 10 µL cecum content extract, or 10 µL plasma/serum into a glass autosampler vial.

8. For blank samples, add 250 µL acetone, 10 µL 1 µg/mL IS solution, and 10 µL EtOH into a glass autosampler vial. In case of feces or cecum content analysis, 10 µL water should be added which is pre-processed in exact the same way as the biological samples. This includes bullet blending if necessary. For every type of biological matrix used in an experiment, three blank samples should be included.

9. Vortex all samples.

10. Add 100 µL 172mM PFBBr in acetone (*see* **Note 7**). Vortex all samples.

11. Heat the samples at 60°C for 30 min in a laboratory stove. Let the samples cool down to room temperature (approximately 15 min) (*see* **Note 8**).

12. Add 500 µL *n*-hexane and 250 µL water to the samples. Shake the vial in vertical direction for approximately 10 sec. Let the samples rest for 1 min at room temperature.

13. Prepare a new empty glass autosampler vial with a glass insert for every sample. Transfer 250 μL of the *n*-hexane (upper layer) into the glass insert.

GC-MS ANALYSIS

1. Inject 1 μL in the GC-MS, splitless at 280°C.

2. Use helium as carrier gas at a constant flow rate of 1.20 mL/min.

3. Use the following temperature gradient: 1 min at 40°C, linear increase at 40°C/min to 60°C, held for 3 min at 60°C, linear increase at 25°C/min to 210°C, linear increase at 40°C/min to 315°C, and held for 3 min at 315°C.

4. Set the transfer line temperature at 280°C.

5. Keep the ionisation source temperature at 280°C.

6. Use methane as chemical ionisation gas at approximately 15 psi.

7. Detect ions obtained in the negative mode using SIM (*see* **Notes 9** and **10**). Table 2 provides the *m/z*-values to be monitored and an indication of retention times (RT). As a consequence of small chromatographic differences (e.g., GC column length), the exact RT varies between various GC systems. Hence, calibration using external standards is mandatory.

DATA ANALYSIS

1. Integrate the obtained signal (*see* **Note 11**).

2. Calculate the relative retention time (RRT) and area ratios using the respective IS (*see* Table 2) (*see* **Notes 12** and **13**).

3. Determine the slope and LLOQ for every SCFA by performing linear regression. It is recommended to use a weighing factor of $1/x^2$ [10].

4. Calculate the SCFA concentrations by using the area ratios obtained from the biological samples, average signal of the blank samples as intercept (*see* **Note 14**), and the slopes obtained from the analysis of the calibration series samples. Take into account the sample dilution for feces and cecum content.

NOTES

1. SCFAs (especially acetic acid and propionic acid) usually show high background signals, resulting in a relatively high LLOQ (*see* Fig. 1). SCFA background signals can be diminished by using high purity solvents (preferably LC-MS grade). Additionally, use glass vials for organic solvents. For plastic tubes, we strongly recommend to use Eppendorf polypropylene tubes.
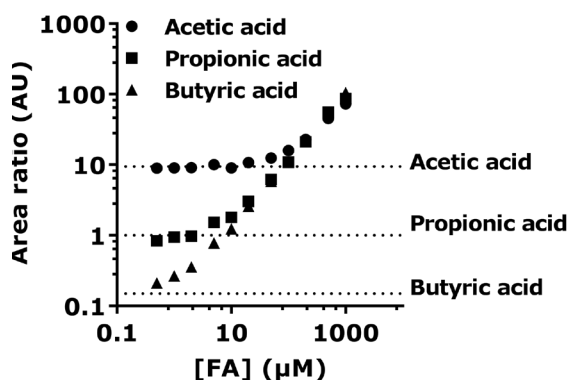

Fig. 1 Background signal of SCFAs. Several SCFAs usually show a high background signal. As a consequence, the LLOQ for these SCFAs is dependent on the background obtained. In our experience, the background signal of acetic acid is higher than that of propionic acid, which in turn is higher than the background signal of butyric acid. The dashed lines in the graph show the extent of the background signals.

2. The IS signal should be present in every sample. The IS is used to correct for differences in sample preparation between the samples. Use exactly the same batch of 1 μg/mL IS solution in EtOH for the entire experiment, as minor differences in IS composition potentially translate into systematic under- or overestimation of SCFAs in samples.

3. Collect the biological samples as quick as possible and store the samples at −80°C. Levels of SCFAs within biological samples are vulnerable for change, especially when the collection is performed slowly or when samples are improperly stored. SCFAs can evaporate from the samples or SCFAs from the air can contaminate the samples.

4. The amount of sample that is required for the analysis of SCFAs might vary between biological samples from different species.

5. Acetone facilitates the precipitation of proteins.

6. The addition of 10 µL EtOH to the samples ensures that the solvents of the biological samples are matched to the solvents in the calibration samples.

7. Within this protocol no base is added to catalyse the derivatization reaction, since the addition of base can severely increase SCFA background signal [8].

8. *n*-Hexane is added after the samples have been cooled down in order to prevent evaporation and spilling.

9. Sensitivity is higher when the MS is operated in SIM mode as compared to the full scan mode. However, the full scan mode can be useful to detect FAs that are not incorporated in the SIM method, or to determine the RT of a specific SCFA. If one decides to operate in full scan mode, an *m/z*-range of 50–150 is recommended to be used.

10. For isotopolog analysis, either *m/z*-values corresponding to isotopologs can be added to the SIM method (e.g., M0, M1, M2, etc. for every SCFA) [8], or the MS can be operated in scheduled scan mode (e.g., scan window including *m/z*-values corresponding to M0, M1, M2, etc., for every SCFA).

11. Pyruvic acid has the same mass and almost the same RT as butyric acid and both acids are derivatized by PFBBr. Consecutively, care has to be taken when both analytes are simultaneously present in the sample (*see* Fig. 2). Particularly in plasma and serum samples, pyruvic acid and butyric acid are simultaneously present. In feces and cecum content, pyruvic acid is usually not detected.
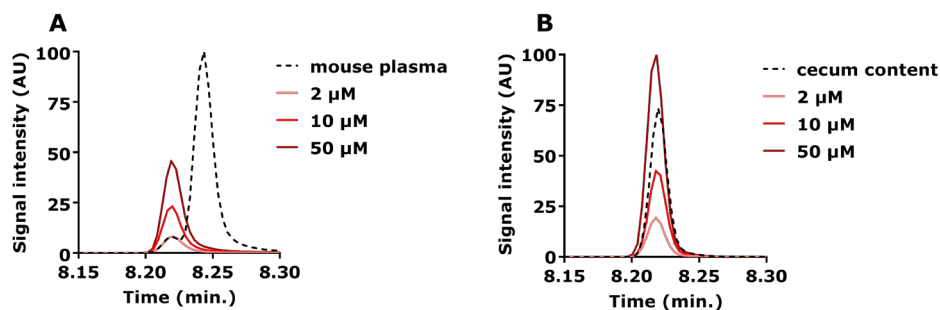
3

Fig. 2 Signal interference between butyric acid (RT = 8.22 min) and pyruvic acid (RT = 8.25 min). Butyric acid and pyruvic acid are eluting closely while being monitored in the same SIM trace. Particularly in plasma (a) and serum samples, pyruvic acid and butyric acid are simultaneously present. In feces and cecum content (b), pyruvic acid is usually not detected.

12. $\text{RRT} = \dfrac{\text{retention } time\ analyte}{\text{retention } time\ IS}$

13. $\text{Area ratio} = \dfrac{\text{area analyte}}{\text{area IS}}$

14. The blank samples reflect the background signal of the biological samples more accurately than the intercept obtained from the linear regression of the calibration series samples. Therefore, use the average area ratio of the blank samples as background signal/intercept to calculate the concentrations of the biological samples. Use the following formula:

$$\text{Concentration} = \dfrac{\text{area ratio} - \text{average area ratio blank samples}}{\text{slope}}$$

REFERENCES

1. Siri-Tarino, P. W.; Chiu, S.; Bergeron, N.; Krauss, R. M. Saturated Fats Versus Poly-unsaturated Fats Versus Carbohydrates for Cardiovascular Disease Prevention and Treatment. *Annu. Rev. Nutr.* **2015**, *35*, 517–43, doi:10.1146/annurev-nutr-071714-034449.

2. Desbois, A. P.; Smith, V. J. Antibacterial free fatty acids: Activities, mechanisms of action and biotechnological potential. *Appl. Microbiol. Biotechnol.* **2010**, *85*, 1629–1642.

3. Cummings, J. H.; Pomare, E. W.; Branch, W. J.; Naylor, C. P.; Macfarlane, G. T. Short chain fatty acids in human large intestine, portal, hepatic and venous blood. *Gut* **1987**, *28*, 1221–1227, doi:10.1136/gut.28.10.1221.

4. O'Keefe, S. J. D. Diet, microorganisms and their metabolites, and colon cancer. *Nat. Rev. Gastroenterol. Hepatol.* **2016**, *13*, 691–706, doi:10.1038/nrgastro.2016.165.

5. Dołowy, M.; Pyka, A. Chromatographic Methods in the Separation of Long-Chain Mono- and Polyunsaturated Fatty Acids. *J. Chem.* **2015**, *2015*.

6. Gao, P.; Xu, G. Mass-spectrometry-based microbial metabolomics: recent developments and applications. *Anal. Bioanal. Chem.* **2015**, *407*, 669–80, doi:10.1007/s00216-014-8127-7.

7. Kloos, D.-P.; Gay, E.; Lingeman, H.; Bracher, F.; Müller, C.; Mayboroda, O. A.; Deelder, A. M.; Niessen, W. M. A.; Giera, M. Comprehensive gas chromatography-electron ionisation mass spectrometric analysis of fatty acids and sterols using sequential one-pot silylation: quantification and isotopologue analysis. *Rapid Commun. Mass Spectrom.* **2014**, *28*, 1507–14, doi:10.1002/rcm.6923.

8. Tomcik, K.; Ibarra, R. A.; Sadhukhan, S.; Han, Y.; Tochtrop, G. P.; Zhang, G. F. Isotopomer enrichment assay for very short chain fatty acids and its metabolic applications. *Anal. Biochem.* **2011**, *410*, 110–117, doi:10.1016/j.ab.2010.11.030.

9. Quehenberger, O.; Armando, A. M.; Dennis, E. A. High sensitivity quantitative lipidomics analysis of fatty acids in biological samples by gas chromatography-mass spectrometry. *Biochim. Biophys. Acta - Mol. Cell Biol. Lipids* **2011**, *1811*, 648–656, doi:10.1016/j.bbalip.2011.07.006.

3

10.   Gu, H.; Liu, G.; Wang, J.; Aubry, A. F.; Arnold, M. E. Selecting the correct weighting factors for linear and quadratic calibration curves with least-squares regression algorithm in bioanalytical LC-MS/MS assays and impacts of using incorrect weighting factors on curve stability, data quality, and assay perfo. *Anal. Chem.* **2014**, *86*, 8959–8966, doi:10.1021/ac5018265.

3

THE PREBIOTIC INULIN AGGRAVATES ACCELERATED ATHEROSCLEROSIS IN HYPERCHOLESTEROLEMIC APOE*3-LEIDEN MICE

04

Lisa R. Hoving,

Margreet R. de Vries,

Rob C. M. de Jong,

Saeed Katiraei,

Amanda Pronk,

Paul H. A. Quax,

Vanessa van Harmelen, and

Ko Willems van Dijk

ABSTRACT

The prebiotic inulin has proven effective at lowering inflammation and plasma lipid levels. As atherosclerosis is provoked by both inflammation and hyperlipidemia, we aimed to determine the effect of inulin supplementation on atherosclerosis development in hypercholesterolemic APOE*3-Leiden (*E3L*) mice. Male *E3L* mice were fed a high-cholesterol (1%) diet, supplemented with or without 10% inulin for 5 weeks. At week 3, a non-constrictive cuff was placed around the right femoral artery to induce accelerated atherosclerosis. At week 5, vascular pathology was determined by lesion thickness, vascular remodelling, and lesion composition. Throughout the study, plasma lipids were measured and in week 5, blood monocyte subtypes were determined using flow cytometry analysis. In contrast to our hypothesis, inulin exacerbated atherosclerosis development, characterised by increased lesion formation and outward vascular remodelling. The lesions showed increased number of macrophages, smooth muscle cells, and collagen content. No effects on blood monocyte composition were found. Inulin significantly increased plasma total cholesterol levels and total cholesterol exposure. In conclusion, inulin aggravated accelerated atherosclerosis development in hypercholesterolemic *E3L* mice, accompanied by adverse lesion composition and outward remodelling. This process was not accompanied by differences in blood monocyte composition, suggesting that the aggravated atherosclerosis development was driven by increased plasma cholesterol.

4

INTRODUCTION

Atherosclerosis is a chronic inflammatory disease of the arteries, which may ultimately prevent adequate blood flow to target tissues leading to cardiovascular complications including heart attack and stroke. In modern society, atherosclerosis is a leading cause of death [1]. An important risk factor for atherosclerosis is increased plasma low-density lipoprotein (LDL) cholesterol. Accumulation and modification of LDL in the arterial wall lead to activation of endothelial cells and increased influx of monocytes. These processes initiate local inflammation characterised by production of pro-inflammatory chemokines and cytokines leading to foam cell formation [2,3]. Foam cell formation leads to proliferation and migration of vascular smooth muscle cells (SMCs) and extracellular matrix deposition. These events ultimately result in intimal hyperplasia and vascular remodelling [4].

Atherosclerosis development can be attenuated by reducing LDL levels and inflammation pharmacologically, for instance, by using statins [5]. However, statin treatment prevents roughly 30% of all cardiovascular events [6], leaving ample opportunities for additional treatment strategies. Epidemiological studies have shown that diets rich in fibers are associated with reductions in the risk of cardiovascular diseases and atherosclerosis development [7–10].

A category of dietary fibers that received great attention in the last decade is inulin-type fructans. Inulin is a dietary fiber that meets the three classification criteria for being considered as a prebiotic [11], i.e., it is resistant to hydrolysis by human enzymes and therefore minimally absorbed in the gastrointestinal tract, it is fermented by colonic microbiota, and it selective stimulates the growth and/or activity of beneficial colonic bacteria.

Evidence is increasingly indicating that inulin exerts favourable effects on a variety of immune-related diseases, such as inflammatory bowel disease [12,13], rheumatoid arthritis [14], and on low-grade chronic inflammation that is associated with cardiovascular disease in humans [15,16]. Furthermore, there are indications that inulin has beneficial effects on hyperlipidemia in rodents [17,18]. However, data on the effects of inulin on lipid metabolism in humans are inconsistent [19–24]. The previous studies in rodents showing beneficial effects of inulin on hyperlipidemia and atherosclerosis were performed in LDL-receptor knockout

mice and APOE-deficient mice, which are both models characterised by severely hampered lipoprotein remnant metabolism.

We extended these findings and investigated whether inulin may delay or prevent development of atherosclerosis in APOE*3-Leiden (*E3L*) transgenic mice [25]. *E3L* mice are a well-established preclinical mouse model to study interventions aimed to improve lipid metabolism and to decrease atherosclerosis development [26,27]. We studied accelerated atherosclerosis development in these mice after placement of a non-constrictive polyethylene cuff around the femoral artery. The ensuing vascular pathology has been shown to be sensitive to both modulation of plasma cholesterol levels and inflammation, and may thus also be affected by inulin.

MATERIALS AND METHODS

MICE AND DIET

Male transgenic APOE*3-Leiden (*E3L*) mice (12–17 weeks of age) were fed a high cholesterol diet containing 1% cholesterol and 0.05% cholic acid (DietW; AB-Diets,Woerden, The Netherlands) 10% inulin (FrutaFit HD; Sensus, Roosendaal, The Netherlands) for a total period of 5 weeks (n = 11–13 mice per group). Before the experiment, mice were randomised based on age, body weight, and plasma cholesterol levels. During the experiment, 2 mice of the control group (n = 13 at the start of the experiment) and 1 mouse of the inulin group (n = 14 at the start of the experiment) died due to unspecified reasons unrelated to the study. Mice were housed under temperature- and humidity-controlled conditions with a 12:12 h light-dark cycle and free access to food and water. During the diet intervention, body weight and food intake were measured weekly. Mouse experiments were performed in compliance with Dutch government guidelines and the Directive 2010/63/EU of the European Parliament and had received approval from the University Ethical Review Board (Leiden University Medical Center, Leiden, The Netherlands).

CUFF-INDUCED ATHEROSCLEROTIC LESION FORMATION

After 3 weeks on diet W ±10% inulin, mice were subjected to femoral arterial cuff placement to induce accelerated atherosclerosis development as described previously [27,28]. Briefly, before surgery mice were anesthetised with an intraperitoneal injection of 5 mg/kg Midazolam (Roche, Woerden, The Netherlands), 0.5 mg/kg Medetomidine (Orion, Helsinki, Finland), and 0.05 mg/kg Fentanyl (Janssen, Beerse, Belgium). The right femoral artery was exposed from surrounding tissue, and sheathed with a rigid non-constrictive polyethylene cuff (Portex, 0.40 mm inner diameter, 0.80 mm outer diameter, and an approximate length of 2.0 mm). After the surgery, the anaesthesia of the mice was antagonised with Atipamezol (1.7 mg/kg, Orion) and Fluminasenil (0.3 mg/kg, Fresenius Kabi). Buprenorphine (0.1 mg/kg, MSD Animal Health) was given after surgery to relieve pain. Mice were sacrificed after 5 weeks of dietary intervention, which was 2 weeks after perivascular cuff placement when profound intima formation with signs of atherosclerosis had developed. Before sacrifice, mice were anesthetised with intraperitoneal injection containing a mixture of Midazolam (8 mg/kg)/Fentanyl (0.08 mg/kg)/Dexdomiter (0.8 mg/kg)/NaCl (0.9%) and subsequently euthanised. Orbital blood was obtained for plasma isolation, which was stored at −20°C until further analysis. The thorax was opened and mild pressure-perfusion (100 mmHg) was performed with ice-cold PBS for 10 min by cardiac puncture in the left ventricle. After perfusion, the cuffed femoral artery was harvested, fixed overnight in 4% formaldehyde in PBS, and finally paraffin-embedded. Serial cross sections (5 µm thick) were used throughout the entire length of the cuffed femoral artery for (immuno)histochemical analysis.

(IMMUNO)HISTOCHEMICAL STAINING

As used previously [27,28], histological Weigert's elastin staining was used to visualise elastic laminae, and a Sirius red staining was performed to quantify the collagen content within the atherosclerotic lesion. The composition of the thickened atherosclerotic lesion was visualised and evaluated by immunohistochemical stainings. Primary antibodies for MAC3 (for macrophages; Rat Anti-Mouse (#550292, BD-Pharmigen, San Diego, CA, USA) 1:300 in 1% PBSA) or

α-smooth muscle cell actin (α-SMC) (for smooth muscle cells; Mouse Anti-Human (clone 1A4, #M0851, Dako, Agilent, Amstelveen, The Netherlands) 1:1000 in 1% PBSA) were applied on tissue sections and incubated overnight. After washing with PBS, secondary antibodies for MAC3 (Goat Anti-Rat (#BA-9401, Vector, Burlingame, CA, USA) 1:300 in 1% PBSA) or α-SMC (HRP Horse Anti-Mouse (#PI-2000, Vector, Burlingame, CA, USA) 1:300 in 1% PBSA) were applied, both developed with 3,3'-diaminobenzidine (DAB, #K4007, Dako Agilent, Amstelveen, The Netherlands), and counterstained with hematoxylin.

ATHEROSCLEROTIC LESION ANALYSIS

Six sequential sections were used per vessel segment to quantify atherosclerotic lesion formation based on Weigert's elastin staining. Using image analysis software (Leica Qwin,Wetzlar, Germany) total cross-sectional lumen area, total cross-sectional medial area between the external- and internal elastic lamina, and total cross-sectional intimal area between the endothelial cell monolayer and the internal elastic lamina were measured. The intensities of staining for macrophages, SMCs, and collagen content within intimal tissue and medial layers were quantified as the average over 6 consecutive cross-sections and were expressed as a percentage of the total surface area per cuffed section.

FLOW CYTOMETRY

Circulating granulocytes and monocytes were analysed using flow cytometry. After lysis of red blood cells, pelleted cells were re-suspended in FACS buffer and stained for 30 min at 4°C in the dark with fluorescently labelled antibodies listed in Table 1. Cells were measured on an LSR II flow cytometer using Diva 6 software (BD Biosciences, San Jose, CA, USA). Data were analysed using FlowJo software (Treestar, Ashland, OR, USA). Representative gating schemes are shown in Figure 1.

Table 1. Antibodies used for flow cytometry

Antibody	Fluorochrome	Dilution	Clone, Supplier
CD45.2	FITC	1:100	104, BioLegend
CD11b	Pacific Blue	1:150	M1/70, BioLegend
CD115-Biotin	n.a.	1:00	AFS98, eBioScience
Streptavidin	PeCy5	1:00	SAV, eBioScience
Gr-1	PeCy7	1:1500	RB6-8C5

PLASMA TOTAL CHOLESTEROL

Blood samples were collected in week 0, 3, and 5 after 4 h fasting (from 8:00 to 12:00 AM) via tail vein bleeding into chilled capillaries, and isolated plasma was assayed for total cholesterol (TC) using a commercially available kit (Roche Diagnostics, Mannheim, Germany). Cholesterol exposure was calculated as the cumulative exposure over the number of weeks fed either the control or the inulin-supplemented diet.
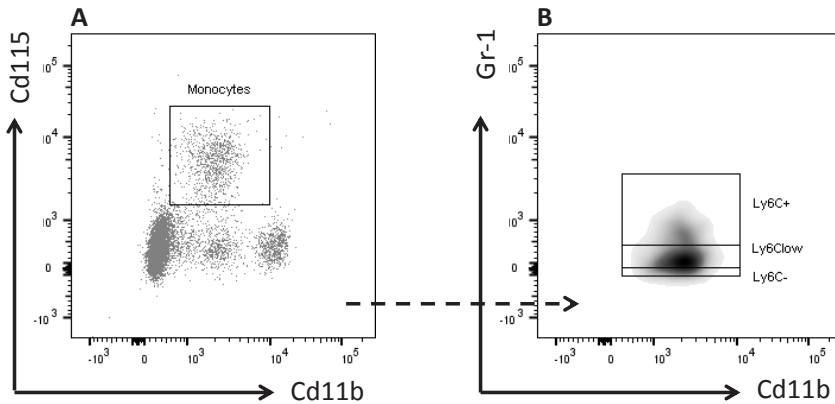

Figure 1. Gating strategy. Gating strategies for the analysis of (A) granulocytes, total monocytes; and (B) Ly6C[+,] Ly6C^{low}, and Ly6C^{-} monocyte subsets in whole blood.

STATISTICAL ANALYSIS

Data are presented as means ± SEM. Normal distribution of the data was tested using D'Agostino-Pearson omnibus normality test, and data were compared in case of normal distribution with the unpaired Student's *t*-test or in the case of not normally distributed data with the nonparametric Mann–Whitney *U* test. Differences in body weight and food intake were evaluated for statistical significance by two-way ANOVA followed by Sidak's post hoc multiple comparison test. Correlation analysis was performed using linear regression analysis. The regression lines of the inulin supplemented mice versus control mice were compared to identify whether the correlations differed between the groups. First it was tested whether slopes of the lines differed and then whether intercepts of the lines differed. When the slopes and intercepts were not significantly different, linear regression analyses was performed on pooled data of both groups. p<0.05 was considered as statistically significant. Analyses were performed using Graph Pad Prism version 7.0 (GraphPad Software, San Diego, CA, USA).

RESULTS

INULIN INCREASED ATHEROSCLEROTIC LESION FORMATION AND OUTWARD VASCULAR REMODELLING

We examined the effect of inulin on vascular pathology 14 days after polyethylene cuff placement around the femoral artery. Figure 2A shows a representative picture of lesion formation in control and inulin supplemented mice. Quantification of the intimal lesion demonstrated that inulin increased lesion surface area (μm^2) by 72% compared to the control group (p=0.01; Figure 2B). Since the total surface area (μm^2) of the media was similar for both groups (Table 2), inulin significantly increased the intima/media ratio by 91% compared to controls (p=0.01; Figure 2C). Outward vascular remodelling took place after inulin supplementation, as shown by increased external (+40% vs. control; p=0.01; Figure 2D) and internal (+73% vs. control; p=0.01; Figure 2E) surface areas. The percentage of luminal stenosis was not affected by inulin (Figure 2F). Compared to the control group, the surface area of the lumen was not changed by inulin (Table 2), which further indicates that inulin did not lead to inward vascular remodelling but rather induced outward vascular remodelling.
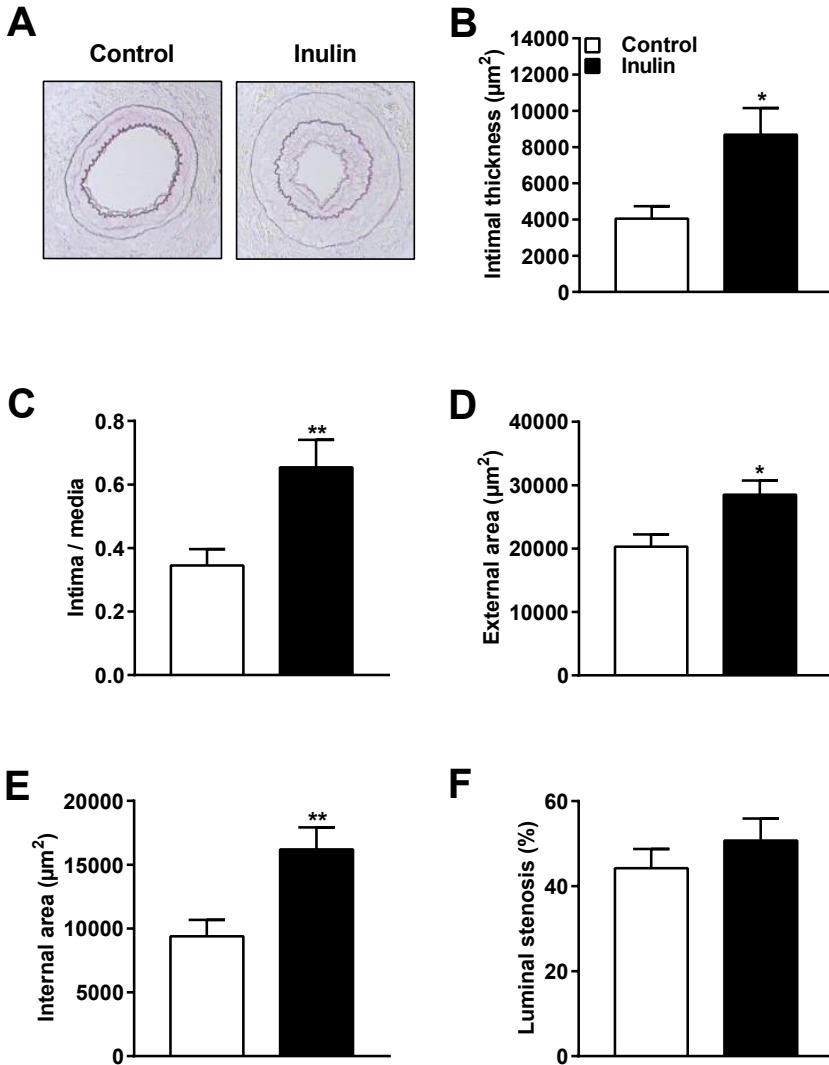
Figure 2. Inulin increased atherosclerotic lesion formation and outward vascular remodelling.
(A) Representative cross-sections of the cuffed femoral arteries of *E3L* mice stained with Weigert's elastin staining visualising the elastic laminae; (B) Quantification of intimal lesion thickening; (C) Intima/media ratio; (D) External surface area; (E) Internal surface area; and (F) Percentage of luminal stenosis. Values are presented as means ± SEM (n = 11–13 mice per group). * $p<0.05$, ** $p<0.01$ vs. control.

Table 2. Experimental measurements including vascular pathology, plasma monocytes, plasma cholesterol, body weight, and food intake.

Vascular pathology	Control (n=11) (mean ± SEM)	Inulin (n=13) (mean ± SEM)	P-value
Intimal thickness (μm^2)	4043 ± 689.5	8685 ± 1462	0.013*
Intima / media	0.35 ± 0.05	0.65 ± 0.09	0.008*
External area (μm^2)	20303 ± 1942	28515 ± 2225	0.012*
Internal area (μm^2)	9383 ± 1288	16203 ± 1715	0.005*
Luminal stenosis (%)	44.21 ± 4.56	50.72 ± 5.21	0.367
Lumen area (μm^2)	5340 ± 961.1	7518 ± 1376	0.224
Medial area (μm^2)	10920 ± 723.1	12312 ± 755	0.201
Medial collagen area (%)	54.88 ± 3.67	56.69 ± 2.76	0.692
Intimal collagen area (%)	33.79 ± 2.62	45.6 ± 2.74	0.011*
Medial SMC area (%)	29.74 ± 4.29	30.1 ± 4.88	0.958
Intimal SMC area (%)	25.31 ± 2.81	41.93 ± 2.57	0.001*
Medial macrophages (%)	4.299 ± 1.92	14.85 ± 2.43	0.001*
Intimal macrophages (%)	1.73 ± 0.78	6.06 ± 1.33	0.002*
Plasma monocytes	Control (n=11) (mean ± SEM)	Inulin (n=11) (mean ± SEM)	P-value
Granulocytes (%)	10.55 ± 1.19	10.64 ± 1.14	0.956
Monocytes (%)	4.91 ± 0.39	6 ± 0.71	0.319
$Ly6C^+$ (%)	0.18 ± 0.12	0.36 ± 0.15	0.635
$LyC6^-$ (%)	1 ± 0.14	1.36 ± 0.24	0.23
$Ly6C^{low}$ (%)	3.18 ± 0.26	3.63 ± 0.51	0.737
Plasma cholesterol	Control (n=11) (mean ± SEM)	Inulin (n=13) (mean ± SEM)	P-value
Plasma TC t=0 (mM)	3.83 ± 0.29	3.79 ± 0.26	0.924
Plasma TC t=3 (mM)	13.28 ± 1	16.33 ± 0.85	0.024*
Plasma TC t=5 (mM)	13.12 ± 0.5	14.65 ± 1.14	0.738
TC exposure (mM*Weeks)	63.54 ± 3.20	72.55 ± 2.38	0.03*

(Continued)

Table 2. *Continued*

Body weight and Food intake	Control (n=11)	Inulin (n=13)	
	(mean ± SEM)	*(mean ± SEM)*	*P-value*
Body weight t=0 (g)	28.42 ± 0.46	27.53 ± 0.54	0.832
Body weight t=1 (g)	28.35 ± 0.49	27.61 ± 0.56	0.921
Body weight t=2 (g)	28.12 ± 0.55	27.49 ± 0.55	0.962
Body weight t=3 (g)	28.28 ± 0.54	27.47 ± 0.56	0.884
Body weight t=4 (g)	28.01 ± 0.49	27.02 ± 0.55	0.754
Body weight t=5 (g)	29.35 ± 0.54	28.59 ± 0.61	0.907
Cumulative food intake t=1 (g)	24.81 ± 0.78	24.4 ± 1.7	>0.999
Cumulative food intake t=2 (g)	47.56 ± 1.51	46.3 ± 2.4	>0.999
Cumulative food intake t=3 (g)	81.33 ± 3.22	68.16 ± 2.71	0.035*
Cumulative food intake t=4 (g)	109.94 ± 6.11	87.39 ± 2.76	<0.0001*
Cumulative food intake t=5 (g)	131.43 ± 6.52	105.81 ± 2.78	<0.0001*

*$P<0.05$ Control vs. Inulin. SMC=smooth muscle cell; TC=Total cholesterol exposure

4

INULIN INDUCED CHANGES IN LESION COMPOSITION

To investigate whether inulin affected lesion composition, we examined the medial and intimal lesion phenotype using (immuno)histochemical analysis. Consecutive cross-sections of the cuffed femoral arteries were stained with Sirius red for collagen, α-actin for SMCs, and MAC3 for the presence of macrophages in the surface area of the plaques.

Representative cross-sections of the cuffed femoral arteries stained for collagen are shown for both the control and the inulin group (Figure 3A). Inulin did not affect medial collagen area (Figure 3B), but increased the intimal collagen area (+35% vs. control; p=0.01; Figure 3C). Figure 3D shows representative cross-sections of the cuffed femoral arteries stained for SMCs in both intervention groups. Likewise, inulin did not affect SMCs in the medial area (Figure 3E), but increased the area of intimal SMCs (+66% vs. control; p=0.001; Figure 3F). Representative cross-sections stained for macrophages are shown in Figure 3G. Inulin substantially increased the intensity stained for macrophages of both the medial area (+247% vs. control; p=0.001; Figure 3H) as well as the intimal lesion

area (+259% vs. control; p=0.002; Figure 3I). These data showed that inulin adversely affected lesion composition in hypercholesterolemic mice after perivascular cuff placement.
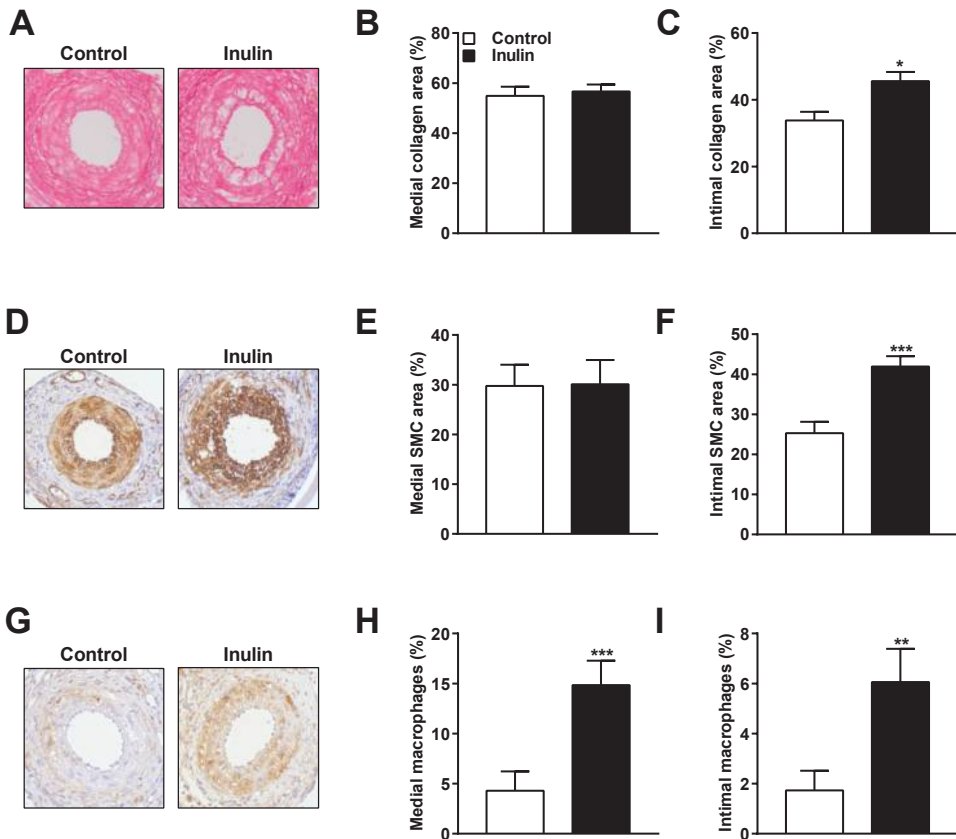

Figure 3. Inulin-induced changes in lesion composition. Representative cross-sections and quantitative analysis for medial and intimal lesion areas of the cuffed femoral arteries of *E3L* mice stained with (A–C) Sirius red for collagen; (D–F) α-actin for SMCs; and (G–I) MAC3 for macrophages. Values are presented as means ± SEM (n = 11–13 mice per group). * p<0.05, ** p<0.01, *** p<0.001 vs. control.

INULIN DID NOT AFFECT BLOOD MONOCYTE COMPOSITION BUT INCREASED TOTAL CHOLESTEROL EXPOSURE

The effect of inulin on blood monocyte composition was determined by flow cytometry. Inulin did not alter the percentages of circulating granulocytes, monocytes, and the monocyte subsets $Ly6C^+$, $Ly6C^{low}$, and $Ly6C^-$ (Figure 4A). However, inulin increased plasma TC levels in week 3 (+23% vs. control; P=0.02; Figure 4B), which overall led to an increased cholesterol exposure over the entire intervention period of 5 weeks (+14% vs. control; p=0.03; Figure 4C). We performed regression analysis on TC exposure versus intimal thickness. Comparison of the regression lines indicated that slopes (F_{slopes}=0.49; p=NS) and intercepts ($F_{intercepts}$=3.98; p=NS) were similar for the control group and the inulin group (pooled data R^2=0.17; p=0.04; Figure 4D). This suggests that the aggravated lesion formation after inulin supplementation was driven by plasma TC. Finally, inulin decreased food intake (up to −17% in week 5 vs. control; p<0.0001; Figure 4E) without affecting body weight (Figure 4F). Together, these data indicate that the mechanism behind the aggravated lesion formation seemed to be driven by cholesterol exposure.
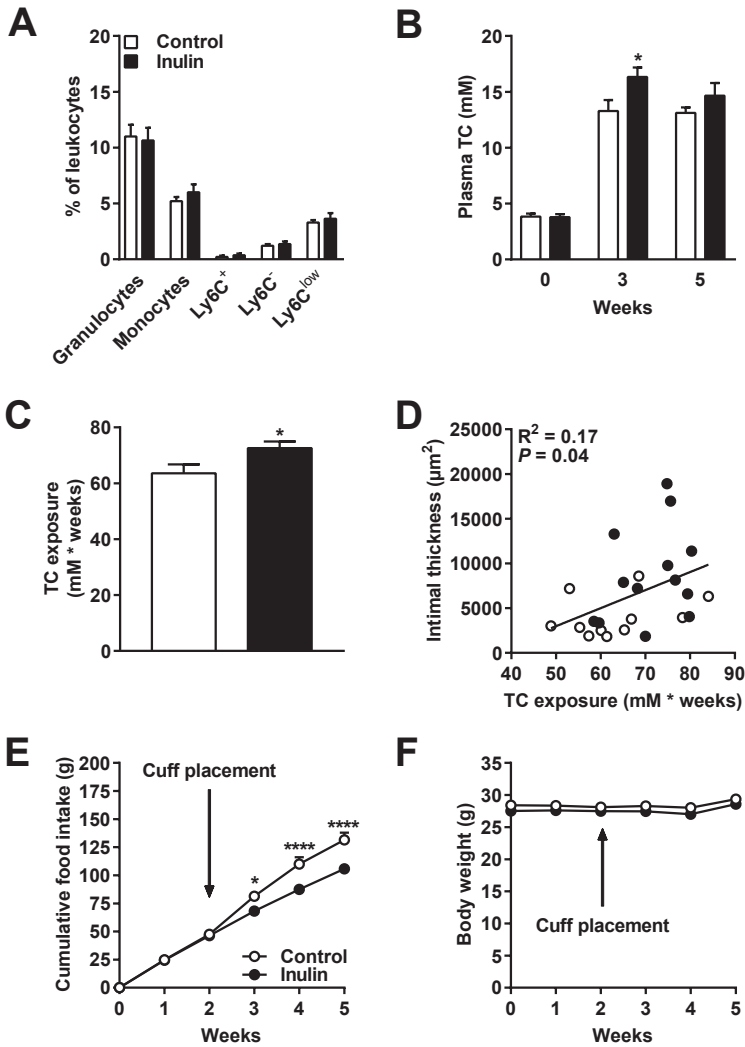
4

Figure 4. Inulin did not affect blood monocyte composition but increased total cholesterol exposure.
(A) Circulating granulocytes, monocytes, and monocyte subsets $Ly6C^+$, $Ly6C^{low}$, and $Ly6C^-$ are shown as a percentage of circulating leukocytes; (B) Plasma TC was analysed in week 0, 3, and 5; and (C) Cumulative TC exposure was calculated over the entire intervention period of 5 weeks; (D) TC exposure was plotted against intimal thickness; (E) Cumulative food intake and (F) Body weight over the 5-week intervention period. The arrow indicates the time point at which the cuff was placed around the femoral artery. Values are presented as means ± SEM (n = 11–13 mice per group). * p<0.05 vs. control.

DISCUSSION

There are clear indications that dietary fibers, and specifically the prebiotic inulin, reduce cardiovascular risk factors such as systemic inflammation and hyperlipidemia [15,16,22–24]. However, in contrast to our expectations, we found that inulin aggravated atherosclerosis development in *E3L* mice. Inulin enlarged the intimal lesion thickness area as well as the collagen content and the percentages of macrophages and SMCs within the lesion. Furthermore, inulin increased outward vascular remodelling in these mice. The aggravated atherosclerosis development was likely explained by increased cholesterol exposure but not by alterations in blood monocyte composition.

In contrast to our results, Rault-Nania *et al.* [17] found that inulin-type fructans reduced atherosclerotic plaque formation by 35% in hypercholesterolemic male mice. However, this study was performed in APOE-deficient mice. Complete deficiency of APOE is associated with a systemic pro-inflammatory state [29]. In addition, APOE-deficient mice are characterised by severely disrupted LDL-receptor mediated lipoprotein remnant clearance and severe hypercholesterolemia [30]. In contrast, *E3L* mice express a dominant variant of human APOE characterised by a moderately disturbed LDL receptor mediated clearance [25]. These mice are highly responsive to diet-induced hyperlipidemia and atherosclerosis development and have been extensively used as preclinical model (review, see [31]). The differential effect of inulin on atherosclerosis development in APOE-deficient mice versus *E3L* mice is therefore likely mouse model-specific. Since *E3L* mice respond similarly as patients to a variety of anti-atherosclerotic interventions [31], we interpret our data to indicate caution with the application of inulin in humans.

We are not the first ones to show adverse effects of inulin on disease outcome. Miles *et al.* [32] reported that diets enriched with inulin did not protect, but further exacerbated the severity of dextran sulfate sodium (DSS)-induced colitis in mice. Two large randomised-controlled trials were performed in which patients with Crohn's disease received either 15 g [33] or 20 g [34] oligofructose/inulin per day. They revealed increased severity of disease in the first study and withdrawal of 30% of patients in the second study due to adverse side effects.

4

These studies suggested that the adverse effects of inulin were likely to be mediated via diverse interactions of inulin with the gut microbiota. However, the adverse effects of inulin were mainly found in combination with severe intestinal/colonic inflammation. This indicates that the effect of inulin on disease outcome might be context dependent. Moreover, it has previously been shown that exposure to diets high in cholesterol are able to serve as a precursor for intestinal inflammation in epithelial cells [35]. It therefore remains possible that a high-cholesterol diet facilitates intestinal inflammation and is associated with the detrimental effects of inulin on atherosclerosis in mice. The consideration that the context of diet affects disease outcome is supported by Goto *et al.* [36], demonstrating that inulin can either positively or negatively affect diarrhea and weight loss in mice, depending on the type of chow diet the mice were fed. It remains to be investigated whether the adverse effects of inulin are a consequence of different context dependent factors, e.g., diet and microbiota composition.

The mode of action of inulin has been shown to depend on inulin chain length. Vogt *et al.* [37] reported that short-chain inulin compared to long-chain inulin induced a more anti-inflammatory phenotype in PBMCs *in vitro* as determined by IL10/IL-12 cytokine production. In our study, we used long-chain inulin, but observed no effects on blood monocyte composition. The effects of short-chain versus long-chain inulin on atherosclerosis development *in vivo* remain to be investigated.

In addition to inulin chain-length, the concentration of inulin added to the diet might influence disease outcome. We fed the mice a high-cholesterol diet supplemented with 10% inulin, which is a relatively high concentration of inulin. However, in another study by Parnell and Reimer [38], obese hyperlipidemic rats were given 10% inulin for a total period of 10 weeks, in which they established a decrease of 24% in circulating cholesterol levels. Although we cannot exclude different effects of inulin within various species, it remains to be determined whether other percentages of dietary inulin will result in lower plasma cholesterol levels in *E3L* mice.

We observed increased outward vascular remodelling of the femoral artery in the inulin group. Inward vascular remodelling in arteries is an important determinant for lumen

loss, whereas outward vascular remodelling can compensate for plaque accumulation in the arterial lumen [39]. Outward remodelling together with a preserved luminal area as observed in our study often indicates a more vulnerable plaque phenotype [40]. The plaque phenotype is determined by collagen turnover [41] and inflammation [42]. Indeed, inulin in our study resulted in changes in the composition of both the media and intima of the plaques, which indicates that the increased lesion formation after inulin supplementation was accompanied by more vulnerable plaques. The adverse effects of inulin on atherosclerosis development could not be explained by changes in blood monocyte composition. However, we cannot exclude the possibility that inulin might have modulated other systemic immune markers or that it has affected the immune status more subtly.

We found that inulin significantly increased plasma cholesterol levels and as a consequence exacerbated atherosclerosis development. The effect of inulin on plasma cholesterol levels might be mediated via interactions with the gut microbiota, by stimulating growth and/or activity of selective bacteria in the gut. We speculate that inulin can increase plasma cholesterol levels via modifications in the production of short-chain fatty acids (SCFAs) by the gut microbiota as suggested by previous studies [43,44]. In the colon, the SCFAs acetate and propionate are produced, absorbed, and transported via the portal vein to the liver [45]. In the liver, acetate is used as a substrate for *de novo* cholesterol and TG synthesis, while propionate inhibits cholesterol synthesis [46]. Variation in the propionate:acetate ratio that reaches the liver might therefore affect either hepatic stimulation or inhibition of *de novo* cholesterol and TG synthesis, resulting in differences in plasma cholesterol levels [47]. The notion that propionate:acetate ratios determine lipid metabolism is supported by a study by Weitkanut *et al.* [48], who found that an increased propionate:acetate ratio was associated with decreased hepatic expression of genes involved in lipogenesis and fatty acid elongation/desaturation of inulin-fed animals. Whether inulin in our study led to a decreased propionate:acetate ratio and therefore adversely affected plasma cholesterol levels and atherosclerosis development, remains to be investigated.

In conclusion, we found that inulin aggravated atherosclerosis development after placement of a cuff around the femoral artery in hypercholesterolemic *E3L* mice. This effect

4

was accompanied by adverse changes in composition of both medial and intimal lesion areas, as well as increased outward vascular remodelling. The adverse effects of inulin on atherosclerosis development were mainly a result of increased plasma total cholesterol levels. Previous studies together with our data therefore raise the concern that inulin not always exert beneficial effects. It will be of importance for future research to decipher potential pathways and mechanisms induced by inulin under various conditions.

ACKNOWLEDGEMENTS

REFERENCES

1.   WHO *WHO | The top 10 causes of death.*; World Health Organization, **2017**;

2.   Hansson, G. K.; Libby, P. The immune response in atherosclerosis: a double-edged sword. *Nat. Rev. Immunol.* **2006**, *6*, 508–519, doi:10.1038/nri1882.

3.   Hansson, G. K. Inflammation, atherosclerosis, and coronary artery disease. *N. Engl. J. Med.* **2005**, *352*, 1685–95, doi:10.1056/NEJMra043430.

4.   Orford, J. L.; Selwyn, A. P.; Ganz, P.; Popma, J. J.; Rogers, C. The comparative pathobiology of atherosclerosis and restenosis. *Am. J. Cardiol.* **2000**, *86*, 6H–11H, doi:10.1016/S0002-9149(00)01094-8.

5.   Tousoulis, D.; Psarros, C.; Demosthenous, M.; Patel, R.; Antoniades, C.; Stefanadis, C. Innate and adaptive inflammation as a therapeutic target in vascular disease: The emerging role of statins. *J. Am. Coll. Cardiol.* **2014**, *63*, 2491–2502, doi:10.1016/j.jacc.2014.01.054.

6.   Jukema, J. W.; Cannon, C. P.; de Craen, A. J. M.; Westendorp, R. G. J.; Trompet, S. The Controversies of Statin Therapy: Weighing the Evidence. *J. Am. Coll. Cardiol.* **2012**, *60*, 875–881, doi:10.1016/j.jacc.2012.07.007.

7.   Wu, H.; Dwyer, K. M.; Fan, Z.; Shircore, A.; Fan, J.; Dwyer, J. H. Dietary fiber and progression of atherosclerosis: the Los Angeles Atherosclerosis Study. *Am. J. Clin. Nutr.* **2003**, *78*, 1085–91.

8.   Liu, S.; Stampfer, M. J.; Hu, F. B.; Giovannucci, E.; Rimm, E.; Manson, J. E.; Hennekens, C. H.; Willett, W. C. Whole-grain consumption and risk of coronary heart disease: results from the Nurses' Health Study. *Am. J. Clin. Nutr.* **1999**, *70*, 412–9.

9.   Bazzano, L. A.; He, J.; Ogden, L. G.; Loria, C. M.; Whelton, P. K.; National Health and Nutrition Examination Survey I Epidemiologic Follow-up Study Dietary Fiber Intake and Reduced Risk of Coronary Heart Disease in US Men and Women. *Arch. Intern. Med.* **2003**, *163*, 1897, doi:10.1001/archinte.163.16.1897.

10. Petersen, K. S.; Clifton, P. M.; Keogh, J. B. The association between carotid intima media thickness and individual dietary components and patterns. *Nutr. Metab. Cardiovasc.*

4

Dis. **2014**, *24*, 495–502, doi:10.1016/j.numecd.2013.10.024.

11.   Gibson, G. R.; Roberfroid, M. B. Dietary modulation of the human colonic microbiota: introducing the concept of prebiotics. *J. Nutr.* **1995**, *125*, 1401–12.

12.   Videla, S.; Vilaseca, J.; Antolin, M.; Garcia-Lafuente, A.; Guarner, F.; Crespo, E.; Casalots, J.; Salas, A.; Malagelada, J. R. Dietary inulin improves distal colitis induced by dextran sodium sulfate in the rat. *Am. J. Gastroenterol.* **2001**, *96*, 1486–1493, doi:10.1111/j.1572-0241.2001.03802.x.

13.   Casellas, F.; Borruel, N.; Torrejón, A.; Varela, E.; Antolin, M.; Guarner, F.; Malagelada, J.-R. Oral oligofructose-enriched inulin supplementation in acute ulcerative colitis is well tolerated and associated with lowered faecal calprotectin. *Aliment. Pharmacol. Ther.* **2007**, *25*, 1061–7, doi:10.1111/j.1365-2036.2007.03288.x.

14.   Abhari, K.; Shekarforoush, S. S.; Hosseinzadeh, S.; Nazifi, S.; Sajedianfard, J.; Eskandari, M. H. The effects of orally administered Bacillus coagulans and inulin on prevention and progression of rheumatoid arthritis in rats. *Food Nutr. Res.* **2016**, *60*, 30876.

15.   Vogt, L.; Meyer, D.; Pullens, G.; Faas, M.; Smelt, M.; Venema, K.; Ramasamy, U.; Schols, H. A.; De Vos, P. Immunological properties of inulin-type fructans. *Crit. Rev. Food Sci. Nutr.* **2015**, *55*, 414–36, doi:10.1080/10408398.2012.656772.

16.   Dehghan, P.; Gargari, B. P.; Jafar-Abadi, M. A.; Aliasgharzadeh, A. Inulin controls inflammation and metabolic endotoxemia in women with type 2 diabetes mellitus: a randomized-controlled clinical trial. *Int. J. Food Sci. Nutr.* **2014**, *65*, 117–123, doi:10.3109/09637486.2013.836738.

17.   Rault-Nania, M.-H.; Gueux, E.; Demougeot, C.; Demigné, C.; Rock, E.; Mazur, A. Inulin attenuates atherosclerosis in apolipoprotein E-deficient mice. *Br. J. Nutr.* **2007**, *96*, 840–844, doi:10.1017/BJN20061913.

18.   Mortensen, A.; Poulsen, M.; Frandsen, H. Effect of a long-chained fructan Raftiline HP on blood lipids and spontaneous atherosclerosis in low density receptor knockout mice. *Nutr. Res.* **2002**, *22*, 473–480, doi:10.1016/S0271-5317(02)00358-5.

19.   Pedersen, A.; Sandström, B.; Van Amelsvoort, J. M. The effect of ingestion of inulin

on blood lipids and gastrointestinal symptoms in healthy females. *Br. J. Nutr.* **1997**, *78*, 215–22.

20. van Dokkum, W.; Wezendonk, B.; Srikumar, T. S.; van den Heuvel, E. G. Effect of nondigestible oligosaccharides on large-bowel functions, blood lipid concentrations and glucose absorption in young healthy male subjects. *Eur. J. Clin. Nutr.* **1999**, *53*, 1–7, doi:10.1038/sj.ejcn.1600668.

21. Letexier, D.; Diraison, F.; Beylot, M. Addition of inulin to a moderately high-carbohydrate diet reduces hepatic lipogenesis and plasma triacylglycerol concentrations in humans. *Am J Clin Nutr* **2003**, *77*, 559–564.

22. Brighenti, F.; Casiraghi, M. C.; Canzi, E.; Ferrari, A. Effect of consumption of a ready-to-eat breakfast cereal containing inulin on the intestinal milieu and blood lipids in healthy male volunteers. *Eur. J. Clin. Nutr.* **1999**, *53*, 726–33, doi:http://dx.doi.org/10.1038/sj.ejcn.1600841.

23. Davidson, M. H.; Maki, K. C.; Synecki, C.; Torri, S. A.; Drennan, K. B. Effects of dietary inulin on serum lipids in men and women with hypercholesterolemia. *Nutr. Res.* **1998**, *18*, 503–517, doi:10.1016/S0271-5317(98)00038-4.

24. Aliasgharzadeh, A.; Khalili, M.; Mirtaheri, E.; Gargari, B. P; Tavakoli, F.; Farhangi, M. A.; Babaei, H.; Dehghan, P. A combination of prebiotic inulin and oligofructose improve some of cardiovascular disease risk factors in women with type 2 diabetes: A randomized controlled clinical trial. *Adv. Pharm. Bull.* **2015**, *5*, 507–514, doi:10.15171/apb.2015.069.

25. van den Maagdenberg, A. M.; Hofker, M. H.; Krimpenfort, P. J.; de Bruijn, I.; van Vlijmen, B.; van der Boom, H.; Havekes, L. M.; Frants, R. R. Transgenic mice carrying the apolipoprotein E3-Leiden gene exhibit hyperlipoproteinemia. *J. Biol. Chem.* **1993**, *268*, 10540–5.

26. Quax, P. H.; Lamfers, M. L.; Lardenoye, J. H.; Grimbergen, J. M.; de Vries, M. R.; Slomp, J.; de Ruiter, M. C.; Kockx, M. M.; Verheijen, J. H.; van Hinsbergh, V. W. Adenoviral expression of a urokinase receptor-targeted protease inhibitor inhibits

4

neointima formation in murine and human blood vessels. *Circulation* **2001**, *103*, 562–9.

27. Lardenoye, J. H.; Delsing, D. J.; de Vries, M. R.; Deckers, M. M.; Princen, H. M.; Havekes, L. M.; van Hinsbergh, V. W.; van Bockel, J. H.; Quax, P. H. Accelerated atherosclerosis by placement of a perivascular cuff and a cholesterol-rich diet in ApoE*3Leiden transgenic mice. *Circ. Res.* **2000**, *87*, 248–53.

28. Pires, N. M. M.; Pols, T. W. H.; De Vries, M. R.; Van Tiel, C. M.; Bonta, P. I.; Vos, M.; Arkenbout, E. K.; Pannekoek, H.; Jukema, J. W.; Quax, P. H. A.; De Vries, C. J. M. Activation of nuclear receptor Nur77 by 6-mercaptopurine protects against neointima formation. *Circulation* **2007**, *115*, 493–500, doi:10.1161/CIRCULATIO-NAHA.106.626838.

29. Grainger, D. J.; Reckless, J.; McKilligin, E. Apolipoprotein E modulates clearance of apoptotic bodies in vitro and in vivo, resulting in a systemic proinflammatory state in apolipoprotein E-deficient mice. *J. Immunol.* **2004**, *173*, 6366–75.

30. Zhang, S. H.; Reddick, R. L.; Piedrahita, J. A.; Maeda, N. Spontaneous hypercholesterolemia and arterial lesions in mice lacking apolipoprotein E. *Science* **1992**, *258*, 468–71.

31. Zadelaar, S.; Kleemann, R.; Verschuren, L.; de Vries-Van der Weij, J.; van der Hoorn, J.; Princen, H. M.; Kooistra, T. Mouse models for atherosclerosis and pharmaceutical modifiers. *Arterioscler. Thromb. Vasc. Biol.* **2007**, *27*, 1706–21, doi:10.1161/ATVBAHA.107.142570.

32. Miles, J. P.; Zou, J.; Kumar, M.-V.; Pellizzon, M.; Ulman, E.; Ricci, M.; Gewirtz, A. T.; Chassaing, B. Supplementation of Low- and High-fat Diets with Fermentable Fiber Exacerbates Severity of DSS-induced Acute Colitis. *Inflamm. Bowel Dis.* **2017**, *23*, 1133–1143, doi:10.1097/MIB.0000000000001155.

33. Benjamin, J. L.; Hedin, C. R. H.; Koutsoumpas, A.; Ng, S. C.; McCarthy, N. E.; Hart, A. L.; Kamm, M. A.; Sanderson, J. D.; Knight, S. C.; Forbes, A.; Stagg, A. J.; Whelan, K.; Lindsay, J. O. Randomised, double-blind, placebo-controlled trial of fructo-oligosaccharides in active Crohn's disease. *Gut* **2011**, *60*, 923–929, doi:10.1136/

gut.2010.232025.

34. Joossens, M.; De Preter, V.; Ballet, V.; Verbeke, K.; Rutgeerts, P.; Vermeire, S. Effect of oligofructose-enriched inulin (OF-IN) on bacterial composition and disease activity of patients with Crohn's disease: results from a double-blinded randomised controlled trial. *Gut* **2012**, *61*, 958, doi:10.1136/gutjnl-2011-300413.

35. Progatzky, F.; Sangha, N. J.; Yoshida, N.; McBrien, M.; Cheung, J.; Shia, A.; Scott, J.; Marchesi, J. R.; Lamb, J. R.; Bugeon, L.; Dallman, M. J. Dietary cholesterol directly induces acute inflammasome-dependent intestinal inflammation. *Nat. Commun.* **2014**, *5*, 5864, doi:10.1038/ncomms6864.

36. Goto, H.; Takemura, N.; Ogasawara, T.; Sasajima, N.; Watanabe, J.; Ito, H.; Morita, T.; Sonoyama, K. Effects of fructo-oligosaccharide on DSS-induced colitis differ in mice fed nonpurified and purified diets. *J. Nutr.* **2010**, *140*, 2121–7, doi:10.3945/jn.110.125948.

37. Vogt, L.; Ramasamy, U.; Meyer, D.; Pullens, G.; Venema, K.; Faas, M. M.; Schols, H. A.; de Vos, P. Immune modulation by different types of β2→1-fructans is toll-like receptor dependent. *PLoS One* **2013**, *8*, e68367, doi:10.1371/journal.pone.0068367.

38. Parnell, J. A.; Reimer, R. A. Effect of prebiotic fibre supplementation on hepatic gene expression and serum lipids: a dose–response study in JCR:LA-cp rats. *Br. J. Nutr.* **2010**, *103*, 1577–1584, doi:10.1017/S0007114509993539.

39. Glagov, S.; Weisenberg, E.; Zarins, C. K.; Stankunavicius, R.; Kolettis, G. J. Compensatory Enlargement of Human Atherosclerotic Coronary Arteries. *N. Engl. J. Med.* **1987**, *316*, 1371–1375, doi:10.1056/NEJM198705283162204.

40. Pasterkamp, G.; Smits, P. C. Imaging of atherosclerosis. Remodelling of coronary arteries. *J. Cardiovasc. Risk* **2002**, *9*, 229–35.

41. Galis, Z. S.; Sukhova, G. K.; Lark, M. W.; Libby, P. Increased expression of matrix metalloproteinases and matrix degrading activity in vulnerable regions of human atherosclerotic plaques. *J. Clin. Invest.* **1994**, *94*, 2493–2503, doi:10.1172/JCI117619.

42. Libby, P. Inflammation in atherosclerosis. *Nature* **2002**, *420*, 868–74, doi:10.1038/

4

nature01323.

43.   Tarini, J.; Wolever, T. M. S. The fermentable fibre inulin increases postprandial serum short-chain fatty acids and reduces free-fatty acids and ghrelin in healthy subjects. *Appl. Physiol. Nutr. Metab.* **2010**, *35*, 9–16, doi:10.1139/H09-119.

44.   Gibson, G. R.; Beatty, E. R.; Wang, X.; Cummings, J. H. Selective stimulation of bifidobacteria in the human colon by oligofructose and inulin. *Gastroenterology* **1995**, *108*, 975–82.

45.   den Besten, G.; Lange, K.; Havinga, R.; van Dijk, T. H.; Gerding, A.; van Eunen, K.; Müller, M.; Groen, A. K.; Hooiveld, G. J.; Bakker, B. M.; Reijngoud, D.-J. Gut-derived short-chain fatty acids are vividly assimilated into host carbohydrates and lipids. *Am. J. Physiol. Gastrointest. Liver Physiol.* **2013**, *305*, G900-10, doi:10.1152/ajpgi.00265.2013.

46.   Wolever, T. M.; Spadafora, P.; Eshuis, H. Interaction between colonic acetate and propionate in humans. *Am. J. Clin. Nutr.* **1991**, *53*, 681–7.

47.   Pereira, D. I. A.; Gibson, G. R. Effects of consumption of probiotics and prebiotics on serum lipid levels in humans. *Crit. Rev. Biochem. Mol. Biol.* **2002**, *37*, 259–81, doi:10.1080/10409230290771519.

48.   Weitkunat, K.; Schumann, S.; Petzke, K. J.; Blaut, M.; Loh, G.; Klaus, S. Effects of dietary inulin on bacterial growth, short-chain fatty acid production and hepatic lipid metabolism in gnotobiotic mice. *J. Nutr. Biochem.* **2015**, doi:10.1016/j.jnutbio.2015.03.010.

THE PREBIOTIC INULIN MODULATES GUT MICROBIOTA BUT DOES NOT AMELIORATE ATHEROSCLEROSIS IN HYPERCHOLESTEROLEMIC APOE*3-LEIDEN.CETP MICE

05

Lisa R. Hoving,

Saeed Katiraei,

Amanda Pronk,

Marieke Heijink,

Kelly K.D. Vonk,

Fatiha Amghar-el Bouazzaoui,

Rosalie Vermeulen,

Lizette Drinkwaard,

Martin Giera,

Vanessa van Harmelen, and

Ko Willems van Dijk

ABSTRACT

Gut microbiota have been implicated in the development of atherosclerosis and cardiovascular disease. Since the prebiotic inulin is thought to beneficially affect gut microbiota, we aimed to determine the effect of inulin supplementation on atherosclerosis development in APOE*3-Leiden.CETP (*E3L.CETP*) mice. Female *E3L.CETP* mice were fed a western-type diet containing 0.1% or 0.5% cholesterol with or without 10% inulin. The effects of inulin were determined on: microbiota composition, cecal short-chain fatty acid (SCFA) levels, plasma lipid levels, atherosclerosis development, hepatic morphology and hepatic inflammation. Inulin with 0.5% dietary cholesterol increased specific bacterial genera and elevated levels of cecal SCFAs, but did not affect plasma cholesterol levels or atherosclerosis development. Surprisingly, inulin resulted in mild hepatic inflammation as shown by increased expression of inflammation markers. However, these effects were not accompanied by increased hepatic macrophage number. Analogously, inulin induced mild steatosis and increased hepatocyte size, but did not affect hepatic triglyceride content. Inulin with 0.1% dietary cholesterol did not affect hepatic morphology, nor hepatic expression of inflammation markers. Overall, inulin did not reduce hypercholesterolemia or atherosclerosis development in *E3L.CETP* mice despite showing clear prebiotic activity, but resulted in manifestations of hepatic inflammation when combined with a high percentage of dietary cholesterol.

5

INTRODUCTION

Atherosclerosis is a narrowing of arteries due to accumulation of lipids and cells in the intima, leading to cardiovascular diseases (CVD) including heart attack and stroke. CVD are a leading cause of morbidity and mortality in Western Society [1]. Hypercholesterolemia is one of the main underlying risk factors of atherosclerosis development, and is routinely treated by prescription of statins. However, statin treatment lowers total plasma cholesterol levels by approximately 30% [2] and only prevents 25-45% of all cardiovascular events [3], indicating the demand for additional therapies. The gut microbiota have been discovered as an important player in the onset of atherosclerosis and CVD [4]. Disturbances in lipid metabolism, the precursor for the development of atherosclerosis and CVD, have also been associated with gut microbiota dysbiosis in both rodents [5] and humans [6]. A well-known factor that modulates the gut microbiota composition and function are dietary fibers or prebiotics. Inulin supplementation is a widely studied prebiotic that has been shown to beneficially modify gut microbiota composition and function [7]. Inulin is fermented by specific bacteria in the gut, leading to outgrowth of these bacteria and short-chain fatty acid (SCFA) production [8], which is thought to improve colonic and systemic health [9]. Inulin has been shown to exert multiple beneficial effects on the host, including lowering inflammation [10,11], as well as decreasing hyperlipidemia [12–15]. Whether inulin affects the development of atherosclerosis is currently underexplored. Therefore, we set out to determine the effect of inulin on the development of atherosclerosis in hypercholesterolemic APOE*3-Leiden.CETP (*E3L.CETP*) mice, a model that is charac-terised by a human-like lipoprotein metabolism and that is susceptible to the development of atherosclerosis. Particularly female *E3L.CETP* mice are highly sensitive to dietary cholesterol and they respond in a human-like manner to lipid-lowering anti-atherogenic therapies [16]. We found that inulin drastically altered gut microbiota composition and function. However, inulin neither decreased hypercholesterolemia nor ameliorated atherosclerosis development in this mouse model. Notably, inulin in combination with a high percentage of dietary cholesterol resulted in manifestations of hepatic inflammation.

MATERIALS AND METHODS

MICE AND DIET

In two experiments, female *E3L.CETP* mice were fed a WTD containing 0.1% or 0.5% cholesterol (Diet T 0.1 (Diet T 4022.16) or Diet T 0.5 (Diet T 4022.17); AB Diets, The Netherlands)(Table 1). This WTD diet was supplemented with or without 10% inulin (FrutaFit HD, Sensus, The Netherlands) for a total period of 11 weeks in which 10% of cellulose was replaced with 10% inulin. At baseline, after a run-in of 3 weeks with WTDs, randomisation of the mice was performed based on plasma total cholesterol (TC) levels, plasma triglyceride (TG) levels, and body weight. During the intervention period, body weight and food intake were measured weekly. After 11 weeks, non-fasted mice were sacrificed using CO_2 inhalation. Orbital bleeding was performed to collect blood and mice were subsequently perfused with ice-cold PBS through the heart. Cecum content, heart, and liver were collected for further analysis. Mice were housed under temperature- and humidity-controlled conditions with a 12:12h light-dark cycle and free access to food and water. A schematic of the experimental study protocol is provided in Figure 1. Mouse experiments were performed in compliance with Dutch government guidelines and the Directive 2010/63/EU of the European Parliament and had received approval from the University Ethical Review Board (Leiden University Medical Center, The Netherlands).

16S RIBOSOMAL RNA GENE SEQUENCING AND PROFILING

16S rRNA sequencing in cecum samples of *E3L.CETP* mice fed with a WTD (0.5% cholesterol) ± inulin was performed as described previously [17]. Relative bacterial abundance was determined. For statistical significance, biological relevance and visualisation linear discriminant analysis (LDA) effect size (LEfSe) method (https://bitbucket.org/biobakery/biobakery/wiki/lefse)[18] and ANCOM analysis were used as described previously (https://www.niehs.nih.gov/research/resources/software/biostatistics/ancom/index.cfm)[19].
Prior to LEfSe analysis low abundant taxa were filtered out, applying a two-step filtering.

Table 1. Diet composition (% of total weight)

| Dietary substitute (%)	Control/Inulin 0.1%	Control/Inulin 0.5%
Inulin	0/10	0/10
Cholesterol	0.1	0.5
Magnesium oxide	0.2	0.2
Methionine	0.2	0.2
Standard trace elements premix	0.25	0.25
Standard vitamin premix	0.25	0.25
Salt	0.3	0.3
Magnesium sulphate heptahydate	0.4	0.4
Potassium hydrogen phosphate	0.7	0.7
Potassium chloride	0.7	0.7
Calcium carbonate	1	1
Corn oil	1	1
Calcium hydrogen phosphate	1.3	1.3
Choline chloride	2	2
Corn starch	10	10
Cacoa butter	15	15
Cellulose	16.1/6.1	16/6
Sour casein	20	20
Sugar/sucrose	30.5	30.2
Total	*100*	*100*

5
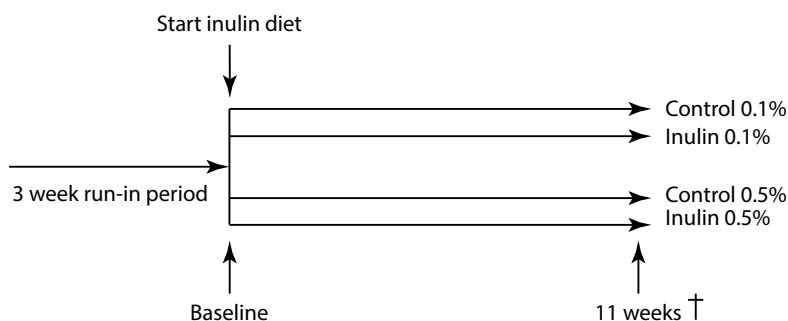
Figure 1. Experimental study protocol.

First, taxa that were present in less than half of the group size were filtered out. In a second step, very rare taxa that were abundant less than 0.5% of total group taxa were filtered out. At baseline and after 11 weeks (wks) of intervention, jack-knifed β-diversity of unweighted UniFrac distances, with 10 jack-knifed replicates was measured at rarefaction depth of 22000 reads per sample, based on the unfiltered OTU table.

CECAL SHORT-CHAIN FATTY ACID ANALYSIS
Cecum SCFA content was analysed using gas chromatography mass spectrometry (GC-MS) as described previously [20].

PLASMA PARAMETERS
Plasma TG and TC were measured in 4 hour fasted mice as described previously [17]. Plasma cholesterol exposure was calculated as the cumulative exposure over the number of weeks where mice were fed a WTD ± inulin.

ATHEROSCLEROSIS QUANTIFICATION

Atherosclerosis quantification using histological staining with hematoxylin-phloxyin-saffron (HPS) was performed in hearts of *E3L.CETP* mice fed a WTD (0.5% cholesterol) ± inulin as described previously [17]. Image J Software (NIH, USA) was used for the quantification of atherosclerotic lesion areas.

LIVER (IMMUNO)HISTOCHEMISTRY

Livers were removed, fixed in 4% paraformaldehyde, dehydrated in 70% ethanol, embedded in paraffin and sectioned (5µm). Paraffin-embedded liver sections were stained with haematoxylin and eosin (H&E) using standard protocols. From H&E-stained sections, hepatocyte size (hepatic hypertrophy) was quantified as the average number of hepatocytes per total microscopic field (mm^2) per section. H&E-stained liver sections were scored for hepatic steatosis on the level of microvesicular and macrovesicular steatosis [21], expressed as the percentage of the total liver section area affected. Immunohistochemical detection of the macrophage marker *F4/80* was done on paraffin-embedded sections that were treated with proteinase K, using a primary Rat Anti-Mouse *F4/80* monoclonal Ab (MCA497; 1:600, Serotec, UK) and a secondary Goat Anti-Rat immunoglobulin peroxidase (MP-7444, Vector Laboratories Inc., USA). All histological and histochemical analysis were analysed using Image J software (NIH, USA).

LIVER LIPIDS

Lipids were extracted from the liver according to a protocol from Bligh and Dyer [22] and modified as described previously [17]. TG content was assayed as described above.

RNA ISOLATION AND QUANTITATIVE RT-PCR

Snap-frozen liver samples were used for the extraction of RNA using a NucleoSpin RNA kit (Machery-Nagel, Germany). NanoDrop ND-1000 spectrophotometer (Isogen, The Netherlands) was used to determine concentrations and purity of RNA. Reverse transcription of RNA was done using Moloney Murine Leukemia Virus Reverse Transcriptase (Promega, The Netherlands).

5

Gene expression levels were determined using qRT-PCR, SYBR green supermix (Biorad, The Netherlands), and gene-specific primers (Table 2). Expression of mRNA was normalised to cyclophilin (*CypA*) and ribosomal protein large P0 (*Rplp0*) RNA, and expressed as fold change versus control using the ΔΔ CT method.

Table 2. Primer sequences of forward and reverse primers (5' > 3')

Gene	Sense	Antisense
CypA	ACTGAATGGCTGGATGGCAA	TGTCCACAGTCGGAAATGGT
Rplp0	GGACCCGAGAAGACCTCCTT	GCACATCACTCAGAATTTCAATGG
IL-10	GACAACATACTGCTAACCGACTC	ATCACTCTTCACCTGCTCCACT
IL-6	AAGAAATGATGGATGCTACCAAACTG	GTACTCCAGAAGACCAGAGGAAATT
Mcp-1	CACTCACCTGCTGCTACTCA	GCTTGGTGACAAAAACTACAGC
Tnf-α	GATCGGTCCCCAAAGGGATG	CACTTGGTGGTTTGCTACGAC
F4/80	CTTTGGCTATGGGCTTCCAGTC	GCAAGGAGGACAGAGTTTATCGTG

STATISTICAL ANALYSIS

Data are presented as means ± SEM. Normal distribution of the data was tested using D'Agostino-Pearson omnibus normality test, and data were analysed with the unpaired Student's *t*-test in case of normal distribution or with the nonparametric Mann–Whitney *U* test in case of not normally distributed data. Differences in body weight over time were evaluated for statistical significance by two-way ANOVA followed by Sidak's post hoc multiple comparison test. $P < 0.05$ was considered as statistically significant. Analyses were performed using Graph Pad Prism version 7.0 (GraphPad Software, USA).

RESULTS

INULIN MODIFIED GUT MICROBIOTA COMPOSITION AND FUNCTION

To determine the effects of inulin on gut microbiota in mice fed a WTD with 0.5% cholesterol, 16S rRNA gene sequencing was used to assess the effect of inulin on gut microbiota composition and relative abundance of specific gut microbial taxa. Cluster analysis based on unweighted UniFrac distances revealed a clear difference between the control group and the inulin group after 11 weeks of intervention, while the control group did not change after 11 weeks compared to the baseline measurement (Figure 2A).

Further analysis of the gut microbiota revealed clear differences in the composition of the microbial community between the control group and the inulin group. Figure 2B schematically depicts LEfSe's results included in a cladogram showing the significant differences on each taxonomic level with a maximum depth to genus level. Table 3 shows the relative abundances (%) of genera in the control and the inulin group and the percentage difference between the two groups based on LEfSe and ANCOM analyses. Based on LEfSe analysis, inulin significantly increased the relative abundance of the genera *Coprococcus* (+409%), and *Allobaculum* (+833%), whereas the genera *Bacteroides* (-59%), *Parabacteroides* (-60%), *Prevotella* (-88%), *Micispirillum* (-100%), *Clostridium* (-100%), and *Coprobacillus* (-100%) were reduced compared to control mice (Table 3). Based on ANCOM analysis, inulin increased the relative abundance of the genera *Coprococcus* (+409%), *Ruminococcus* (+52%), *Allobaculum* (+833%), and *Sutterella* (+12%), whereas the genera *Mucispirillum* (-100%) and *Coprobacillus* (-100%) were decreased compared to control mice (Table 3). The overlapping genera that significantly increased after inulin supplementation compared to control mice according to both analyses were *Allobaculum* and *Coprococcus*.

Subsequently, we determined the effects of inulin on SCFA levels in the cecum. Inulin increased cecal levels of propionate (+57% vs. control; P=0.0005) and butyrate (+146% vs. control; P=0.0002), but not of acetate (Figure 2C). These data indicate that dietary inulin supplementation modulated both microbial composition and function in *E3L.CETP* mice.
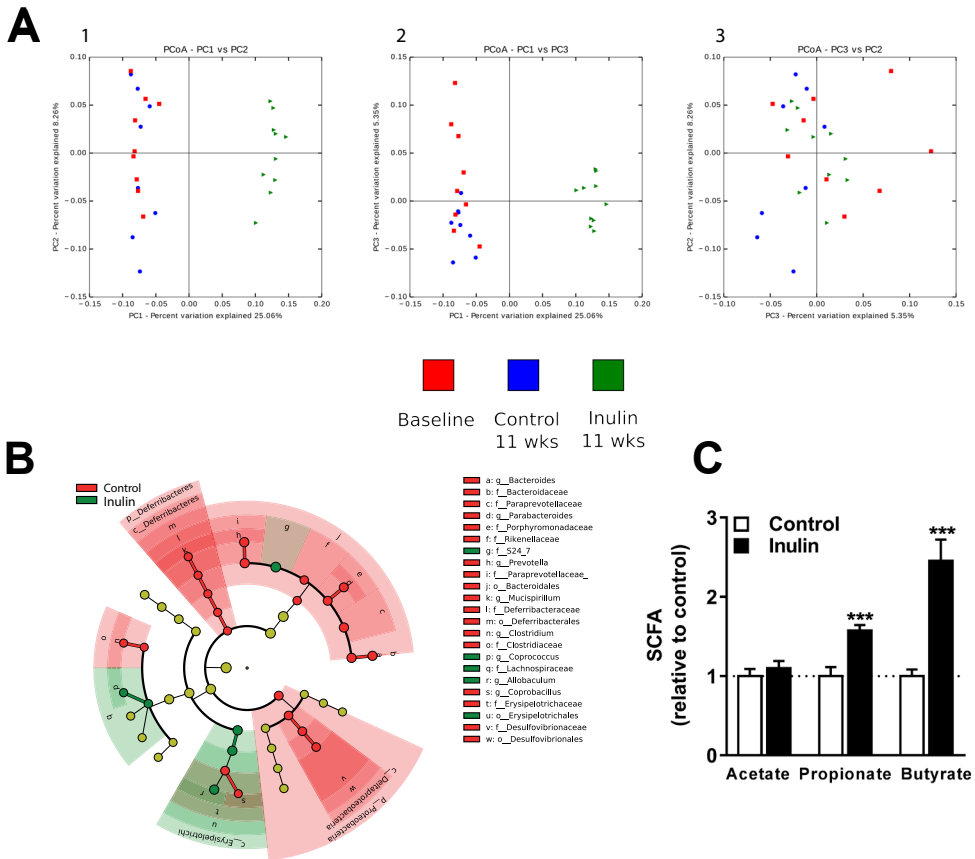
Figure 2. Inulin modified gut microbiota composition and function. The effect of inulin supplementation on microbiota composition and function in mice fed a WTD containing 0.5% cholesterol ± inulin. (A) Principal coordinates analysis (PCoA) plot of unweighted UniFrac distances metric of 16S rRNA gene sequences at baseline (depicted in red) and for the subsequent control group (depicted in blue) and inulin group (depicted in green) after 11 weeks (wks) of treatment. To evaluate similarities between bacterial communities, graphs 1, 2, and 3 were generated using OTU's based on the unweighted UniFrac distance metrics PC1 and PC2, PC1 and PC3, and PC3 and PC2, respectively, and are shown on multiple two-dimensional arrays. (B) The cladogram report the taxa (highlighted by small circles and by shading) showing significant different relative abundance values with a maximum depth till genus level (according to LEfSe). Differences are represented in the colour of the most abundant genus (red indicating the control group, green indicating the inulin group; yellow indicates differences between the inulin and control group which are not significant). The taxonomic level is indicated by letter preceding the underscore: o, order; f, family; g, genus. The central point in the cladogram represents the taxonomic domain 'bacteria' and each ring outward represents

the next lower taxonomic level (phylum to genus). The darker the shading of the red or green colours, the higher the abundance (n = 8-10 mice per group). (C) Finally, the cecal SCFAs acetate, propionate, and butyrate were determined (n = 10 mice per group). Values are presented as means ± SEM. * P<0.05, **P<0.01, ***P<0.001 vs. control.

INULIN NEITHER DECREASED HYPERLIPIDEMIA NOR AMELIORATED ATHEROSCLEROSIS DEVELOPMENT

Given the potential beneficial effects of inulin on plasma lipid parameters, we determined the effect of inulin on plasma TG and TC levels in *E3L.CETP* mice fed a Western-type diet (WTD) containing 0.5% cholesterol ± inulin. Surprisingly, inulin did not affect plasma TG levels (Figure 3A), plasma TC levels (Figure 3B), or TC exposure (Figure 3C). In order to determine whether inulin affected atherosclerosis development, we measured atherosclerosis progression in the aortic root of the heart after 11 weeks of inulin supplementation. Representative images (Figure 3D) illustrate that inulin did not affect mean atherosclerotic lesion area throughout the aortic root (Figure 3E). Finally, there was no effect of inulin on body weight (Figure 3F) or food intake (Figure 3G) in these mice. These data show that inulin did not beneficially lower plasma lipid levels and did not affect atherosclerosis development in hypercholesterolemic *E3L.CETP* mice.

Table 3. Relative abundance and the percentage difference of the inulin group (n=10) and the control group (n=8) for each genera at 11 weeks of intervention.

Phylum Class Order Family Genus	Control	Inulin	Inulin / Control	
	Abundance (%)	Abundance (%)	% Difference	
	Mean ± SEM	*Mean ± SEM*	*Mean ± SEM*	
Bacteroidetes				
Bacteroidia				
Bacteroidales				
Bacteroidaceae				
Bacteroides	15.53 ± 1.87	6.33 ± 1.00	-59%	*
Porphyromonadaceae				
Parabacteroides	8.88 ± 1.60	3.52 ± 0.71	-60%	*
Paraprevotellaceae				
Prevotella	17.2 ± 6.29	2.1 ± 2.03	-88%	*
Rikenellaceae				
Unidentified	3.28 ± 0.90	0.06 ± 0.02	-98%	
S24-7				
Unidentified	5.54 ± 0.90	44.88 ± 2.76	710%	
Unidentified				
Unidentified	3.21 ± 0.68	0.03 ± 0.02	-99%	
Deferribacteres				
Deferribacteres				
Deferribacterales				
Deferribacteraceae				
Mucispirillum	1.83 ± 0.75	0 ± 0	-100%	* $

(Continued)

Table 3. *Continued*

Phylum	Class	Order	Family	Genus	Control	Inulin	Inulin / Control	
					Abundance (%)	Abundance (%)	% Difference	
					Mean ± SEM	*Mean ± SEM*	*Mean ± SEM*	
Firmicutes								
	Bacilli							
		Lactobacillales						
			Lactobacillaceae					
				Lactobacillus	5.69 ± 2.06	3.27 ± 0.76	-43%	
	Clostridia							
		Clostridiales						
			Clostridiaceae					
				Clostridium	1.52 ± 0.70	0 ± 0	-100%	*
			Lachnospiraceae					
				Coprococcus	0.38 ± 0.12	1.91 ± 0.45	403%	* $
				Ruminococcus	1.08 ± 0.36	1.64 ± 0.44	52%	$
			Ruminococcaceae					
				Oscillospira	2.08 ± 0.60	0.96 ± 0.21	-54%	
				Unidentified	1.48 ± 0.85	0.48 ± 0.11	-68%	
			Unidentified					
				Unidentified	14.65 ± 3.37	12.85 ± 2.46	-12%	
	Erysipelotrichi							
		Erysipelotrichales						
			Erysipelotrichaceae					
				Allobaculum	1.88 ± 0.55	17.50 ± 2.30	831%	* $
				Coprobacillus	1.17 ± 0.44	0 ± 0	-100%	* $
				Unidentified	5.86 ± 1.93	0 ± 0	-100%	

5

(Continued)

Table 3. *Continued*

Phylum Class Order Family Genus	Control	Inulin	Inulin / Control	
	Abundance (%)	Abundance (%)	% Difference	
	Mean ± SEM	*Mean ± SEM*	*Mean ± SEM*	
Proteobacteria				
Betaproteobacteria				
Burkholderiales				
Alcaligenaceae				
Sutterella	2.34 ± 0.80	2.63 ± 0.55	12%	$
Deltaproteobacteria				
Desulfovibrionale				
Desulfovibrionaceae				
Unidentified	4.78 ± 1.54	1.52 ± 0.71	-68%	
Gammaproteobacteri				
Enterobacteriales				
Enterobacteriaceae				
Unidentified	1.61 ± 0.75	0.32 ± 0.17	-80%	

Data are presented as mean ± standard error of the mean (SEM). *P<0.05 according to LEfSe analysis; $P<0.05 according to
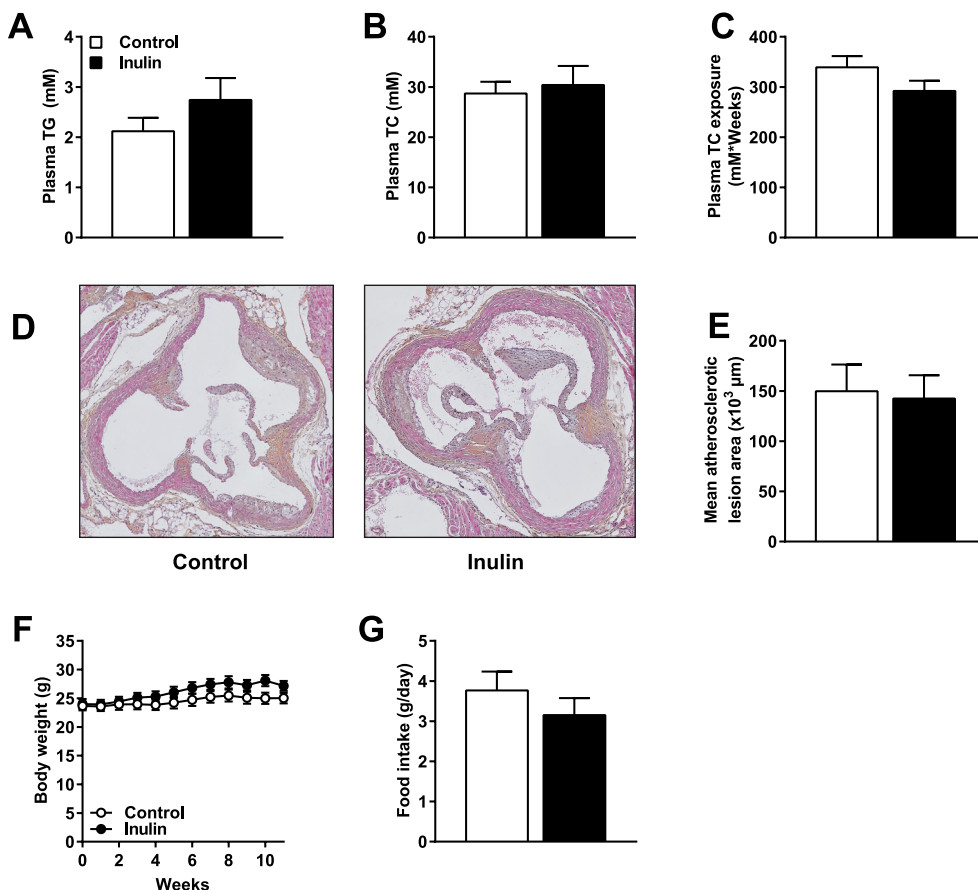
ANCOM analysis.

Figure 3. Inulin neither decreased hyperlipidemia nor ameliorated atherosclerosis development.
Mice were fed a WTD containing 0.5% cholesterol ± inulin for 11 weeks. (A) Plasma TG levels, (B) plasma TC levels, and (C) cumulative TC exposure were determined in 4 hour fasted mice. (D) Representative cross-sections are shown of the valve area of the aortic root of the heart stained with HPS, and (E) the mean atherosclerotic lesion area from the four consecutive cross-sections. Finally, (F) body weight, and (G) food intake were determined. Values are presented as means ± SEM (n = 10 mice per group). P<0.05 was considered as statistically significant.

INULIN ADVERSELY AFFECTED THE LIVER BY MANIFESTATIONS OF HEPATIC INFLAMMATION

Although inulin did not affect hyperlipidemia and atherosclerosis, we found that inulin increased liver weight in mice fed a WTD containing 0.5% cholesterol (+34% vs. control; P=0.003; Figure 4A). We observed notable hepatic morphological derangement in the inulin group (Figure 4B). Inulin significantly increased hepatic hypertrophy as indicated by increased hepatocyte size (+20% vs. control; P=0.008; Figure 4C). Inulin increased microvesicular steatosis (+37% vs. control; P=0.006) and macrovesicular steatosis (+167% vs. control; P=0.03) (Figure 4D), but did not affect hepatic TG content (Figure 4E). Hepatic gene expression of *F4/80* (+65% vs. control; P=0.002), *Mcp-1* (+186% vs. control; P=0.0009), *Tnf-a* (+139% vs. control; P=0.008), and *IL-6* (+67% vs. control; P=0.04) were higher in the inulin group without any effect on *IL-10* expression, indicating a pro-inflammatory phenotype in the mice fed inulin (Figure 4F). However, inulin did not lead to changes in the macrophage marker *F4/80* as quantified by immunohistochemical staining (Figure 4G). These data indicate that inulin in combination with 0.5% dietary cholesterol adversely affected liver morphology and resulted in manifestations of hepatic inflammation in hypercholesterolemic *E3L.CETP* mice.
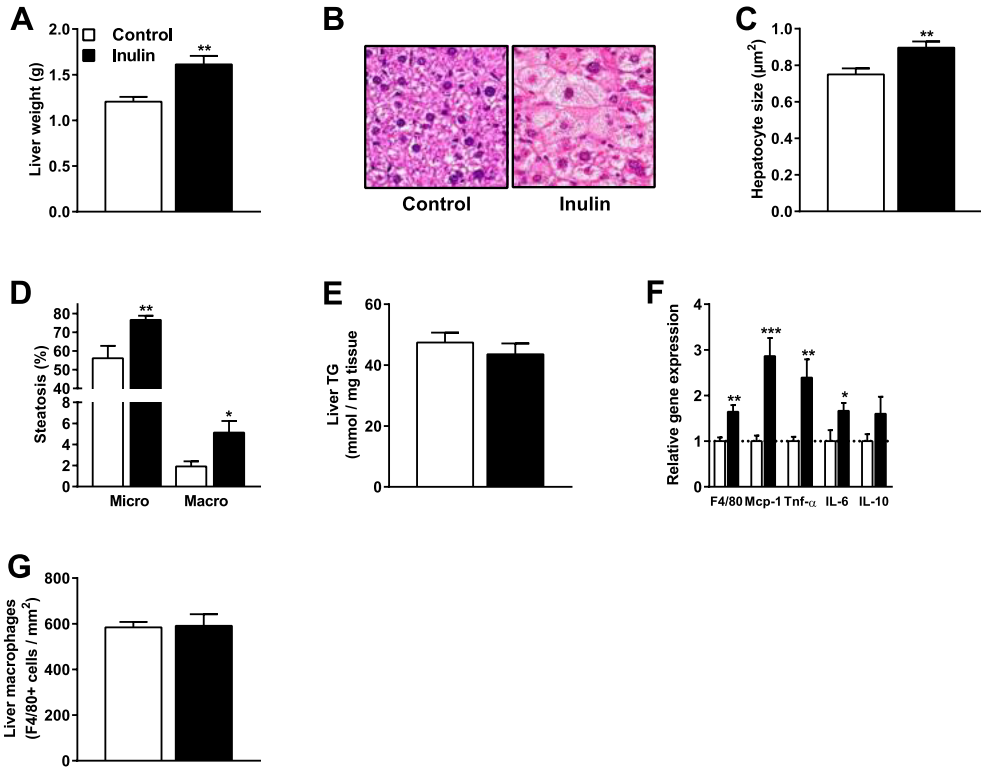
Figure 4. Inulin adversely affected the liver by manifestations of hepatic inflammation. Mice were fed a WTD containing 0.5% cholesterol ± inulin for 11 weeks. (A) Liver weight, (B) liver morphology, (C) hepatocyte size as a marker for hepatic hypertrophy, (D) microvesicular and macrovesicular steatosis, (E) liver TG content, (F) qRT-PCR analysis of *F4/80*, *Mcp-1*, *Tnf-a*, *IL-6*, *IL-10*, and (G) immunohistochemical analysis of hepatic *F4/80* were determined. Values are presented as means ± SEM (n = 10 mice per group). *P<0.05, **P<0.01, ***P<0.001 vs. control.

INULIN IN COMBINATION WITH 0.1% DIETARY CHOLESTEROL INCREASED SHORT-CHAIN FATTY ACIDS IN CECUM CONTENT, BUT DID NOT AFFECT HYPERLIPIDEMIA OR HEPATIC INFLAMMATION

We subsequently determined whether inulin in combination with a more moderate percentage of dietary cholesterol (0.1%) would lead to different outcomes. Using this lower percentage of dietary cholesterol, hypercholesterolemia is induced to a lower extent compared with 0.5% dietary cholesterol. Indeed, 0.5% dietary cholesterol resulted in final plasma TC levels of 27.6 ± 1.5 mM, while 0.1% dietary cholesterol resulted in plasma TC levels of 15.6 ± 0.3 mM (Figure 5A). Similar to mice fed 0.5% cholesterol, inulin in combination with 0.1% dietary cholesterol significantly elevated levels of propionate (+188% vs. control; $P<0.0001$) and butyrate (+344% vs. control; $P<0.0001$) in cecum content (Figure 5B). However, 0.1% dietary cholesterol with inulin also increased levels of acetate in cecum content (+90%; $P<0.0001$; Figure 5B). Inulin in combination with 0.1% cholesterol did not affect plasma TG levels (Figure 5C), plasma TC levels (Figure 5D), or liver TG content (Figure 5E), but increased liver weight (Figure 5F) which was similar to mice fed 0.5% cholesterol. However, in contrast to mice fed inulin with 0.5% cholesterol, inulin combined with 0.1% cholesterol did not affect hepatic morphology (Figure 5G), hepatocyte size (Figure 5H), microvesicular or macrovesicular steatosis (Figure 5I), or hepatic gene expression of inflammatory markers (Figure 5J). Finally, there was neither an effect of inulin on body weight (Figure 5K) nor on food intake (Figure 5L) in these mice.

These results show that inulin in combination with 0.1% cholesterol also modulated gut microbiota function, did also not affect hypercholesterolemia, but in contrast to inulin with 0.5% cholesterol did not affect liver inflammation.
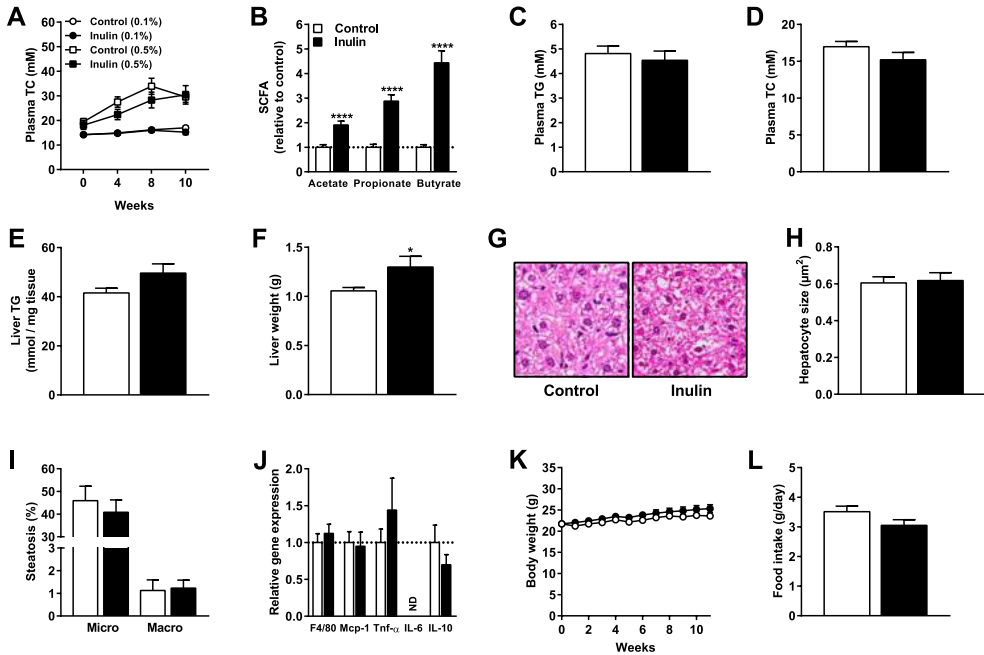
Figure 5. Inulin in combination with 0.1% dietary cholesterol increased SCFAs in cecum content, but did not affect hyperlipidemia or hepatic inflammation. Mice were fed a WTD containing 0.1% cholesterol ± inulin for 11 weeks (n = 17 mice per group). (A) Plasma TC levels for control and inulin fed mice on both 0.5% dietary cholesterol (n = 10 mice per group) and 0.1% dietary cholesterol for 0, 4, 8, and 10 weeks of dietary intervention. (B) The cecal SCFAs acetate, propionate, and butyrate, (C) plasma TG levels, (D) plasma TC levels, (E) liver TG content, (F) liver weight, (G) liver morphology, (H) hepatocyte size, (I) microvesicular and macrovesicular steatosis, (J) qRT-PCR analysis of *F4/80*, *Mcp-1*, *Tnf-α*, *IL-6*, and *IL-10*, (K) body weight, and (L) food intake were determined. Values are presented as means ± SEM. *P<0.05, **P<0.01, ***P<0.001, ***P<0.0001 vs. control.

5

DISCUSSION

Our data show that dietary inulin did not reduce atherosclerosis in *E3L.CETP* mice fed a WTD with 0.5% cholesterol. This may not have been surprising, since plasma lipid levels were not decreased by inulin supplementation. In contrast, inulin in combination with 0.5% cholesterol was associated with manifestations of hepatic inflammation. To further investigate the interaction between dietary cholesterol and inulin on plasma lipid levels and inflammation, we analysed the effect of inulin in combination with 0.1% cholesterol. In this experiment, we found no clear signs of hepatic inflammation but again no effects of inulin on plasma lipid levels. Thus, inulin appears not to have a cholesterol lowering or anti-atherogenic effect in hypercholesterolemic *E3L.CETP* mice.

Rault-Nania *et al.*, [23] found a 35% reduction in atherosclerotic plaque formation in hypercholesterolemic APOE-deficient mice. APOE-deficient mice are characterised by severe hypercholesterolemia due to a virtually completely blocked LDL-receptor mediated lipoprotein remnant clearance [24]. In contrast, *E3L.CETP* mice express a dominant variant of human APOE, which results in a moderately disrupted LDL-receptor mediated lipoprotein remnant clearance [25]. *E3L.CETP* mice are highly responsive to diet-induced hyperlipidemia and atherosclerosis development and have been widely used as preclinical model to study the effects and underlying mechanisms of various human drugs [16]. Furthermore, the APOE-deficient mice in the study of Rault-Nania *et al.* were fed a semi-purified diet based on sucrose, whereas the *E3L.CETP* mice in our study were fed a WTD. Both mouse models are based on C57BL/6 genetic background. However, whether the differential effects of inulin on atherosclerosis development in APOE-deficient mice versus *E3L.CETP* mice are mouse model-specific and/or a result of differences in dietary composition and/or housing conditions remain to be determined.

Nevertheless, inulin led to elevations of the SCFAs propionate and butyrate on both 0.1% and 0.5% cholesterol diets in *E3L.CETP* mice. Both propionate and butyrate have been suggested to have beneficial effects on cholesterol metabolism. Propionate is absorbed in the colon and transported via the portal vein to the liver where it can inhibit cholesterol synthesis [26]. Butyrate is mainly used as energy substrate for colonocytes, and studies in rats have

suggested that ingestion of butyrate may lead to reduced hepatic cholesterol synthesis [27]. Furthermore, Wang *et al.*, [28] recently have shown that butyrate improves energy metabolism by reducing energy intake and enhancing fat oxidation by activating brown adipose tissue in *E3L.CETP* mice. Despite elevations of both propionate and butyrate in our study, no lipid lowering effects of inulin were observed. However, we cannot exclude that prior administration of an inulin containing diet may affect the subsequent response to a cholesterol WTD . This further implies that the effects of administration of inulin prior to cholesterol WTD feeding on SCFAs and atherosclerosis development remains to be further investigated.

Interestingly, inulin in combination with 0.5% dietary cholesterol led to manifestations of hepatic inflammation. This effect seemed to be dependent on the amount of cholesterol in the diet as inulin did not adversely affect the liver when combined with 0.1% cholesterol. We found similar detrimental effects of inulin and cholesterol in an inflammation-driven cuff-induced atherosclerosis model, were inulin in combination with 1% dietary cholesterol even resulted in increased plasma cholesterol levels and aggravated atherosclerosis development [29]. We are not the first ones to show adverse effects of dietary fiber on liver inflammation mediated via gut microbiota interactions. In a previous study by Janssen *et al.*, [30] specific modulation of the gut microbiota by feeding mice the prebiotic indigestible carbohydrate guar gum, promoted liver inflammation and led to worsening of non-alcoholic fatty liver disease (NAFLD) in mice. In this study, the effects of guar gum on liver inflammation could be linked to altered circulating and hepatic levels of bile acids. Whether inulin in our study adversely affected the liver via changes in bile acid metabolism remains to be investigated.

Inulin has been shown to induce inflammation in previous studies, although in these studies inulin mainly exacerbated pre-existing inflammation. For instance Miles *et al.*, [31] reported that diets enriched with inulin further exacerbated the severity of dextran sulfate sodium (DSS)-induced colitis in mice. It is possible that in our study the high-cholesterol diet induced borderline liver inflammation which was exacerbated by inulin.

Inulin is well established to exert bifidogenic effects and the increased abundance of

5

Bifidobacteria in the gut microbiota presumably explains the beneficial effects of inulin on health [32]. Notably, inulin in combination with 0.5% dietary cholesterol led to major shifts in microbial composition but there was no significant increase in the relative abundance of *Bifidobacteria*. Instead, according to both LEfSe and ANCOM analysis, inulin stimulated the relative abundance of the genera *Allobaculum* and *Coprococcus*. Catry *et al.* [33] have previously reported that dietary intervention with inulin-type fructans (ITF) improved endothelial dysfunction in which they found increased abundance of *Allobaculum* in APOE$^{-/-}$ mice. Furthermore, Lee *et al.*, [34] have reported that feeding rats a diet rich in cholesterol specifically increased the abundance of *Allobaculum* and *Coprococcus* compared to a control AIN76A diet. Whether the relative increase in *Allobaculum* in these and our studies was due to inulin supplementation, hypercholesterolemia, or both is not clear. In the study of Lee *et al.*, [34] it was found that *Allobaculum* exhibited a negative correlation with anti-inflammatory genes in the gut, indicating that *Allobaculum* plays a role in inflammation. We found a relative decrease in the abundance of *Bacteroides*, *Parabacteroides*, *Prevotella*, *Mucispirillum*, *Clostridium*, and *Coprobacillus* after inulin supplementation. Whether the absence of *Bifidobacteria*, relative increase of *Allobaculum* and *Coprococcus*, and/or the decrease in relative abundance of certain other genera played a role in the underlying mechanism of the manifestations of liver inflammation after inulin supplementation on a high cholesterol diet, remains to be investigated.

In conclusion, in this study inulin did neither affect hypercholesterolemia nor atherosclerosis development in hypercholesterolemic *E3L.CETP* mice, but rather resulted in manifestations of hepatic inflammation when combined with a high percentage of dietary cholesterol. Although inulin is widely acknowledged as a prebiotic with favourable effects on lipid metabolism and CVD, inulin clearly not always exerts beneficial effects. It will be important for future research to decipher potential adverse pathways and mechanisms that are induced by the interaction of inulin with high dietary cholesterol and the gut microbiota. Although the gut microbiota of mice differ significantly from humans, *E3L.CETP* mice respond similarly as patients to a variety of anti-atherosclerotic interventions [23]. Therefore, we interpret our data to indicate caution with the application of inulin to reduce lipid levels in humans.

ACKNOWLEDGEMENTS

5

REFERENCES

1. World Health Organization WHO | Cardiovascular diseases (CVDs) :Fact sheet Available online: http://www.who.int/mediacentre/factsheets/fs317/en/ (accessed on Aug 29, **2017**).

2. Chan, D. C.; Barrett, P. H. R.; Watts, G. F. The metabolic and pharmacologic bases for treating atherogenic dyslipidaemia. *Best Pract. Res. Clin. Endocrinol. Metab.* **2014**, *28*, 369–85, doi:10.1016/j.beem.2013.10.001.

3. Jukema, J. W.; Cannon, C. P.; de Craen, A. J. M.; Westendorp, R. G. J.; Trompet, S. The Controversies of Statin Therapy: Weighing the Evidence. *J. Am. Coll. Cardiol.* **2012**, *60*, 875–881, doi:10.1016/j.jacc.2012.07.007.

4. Karlsson, F. H.; Fåk, F.; Nookaew, I.; Tremaroli, V.; Fagerberg, B.; Petranovic, D.; Bäckhed, F.; Nielsen, J. Symptomatic atherosclerosis is associated with an altered gut metagenome. *Nat. Commun.* **2012**, *3*, 1245, doi:10.1038/ncomms2266.

5. Turnbaugh, P. J.; Ley, R. E.; Mahowald, M. A.; Magrini, V.; Mardis, E. R.; Gordon, J. I. An obesity-associated gut microbiome with increased capacity for energy harvest. *Nature* **2006**, *444*, 1027–31, doi:10.1038/nature05414.

6. Ley, R. R. E.; Turnbaugh, P. P. J.; Klein, S.; Gordon, J. I. J. Microbial ecology: human gut microbes associated with obesity. *Nature* **2006**, *444*, 1022–3, doi:10.1038/4441022a.

7. Wilson, B.; Whelan, K. Prebiotic inulin-type fructans and galacto-oligosaccharides: definition, specificity, function, and application in gastrointestinal disorders. *J. Gastroenterol. Hepatol.* **2017**, *32*, 64–68, doi:10.1111/jgh.13700.

8. Tremaroli, V.; Bäckhed, F. Functional interactions between the gut microbiota and host metabolism. *Nature* **2012**, *489*, 242–9, doi:10.1038/nature11552.

9. Peng, M.; Biswas, D. Short Chain and Polyunsaturated Fatty Acids in Host Gut Health and Foodborne Bacterial Pathogen Inhibition. *Crit. Rev. Food Sci. Nutr.* **2016**, 0, doi:10.1080/10408398.2016.1203286.

10. Vogt, L.; Meyer, D.; Pullens, G.; Faas, M.; Smelt, M.; Venema, K.; Ramasamy, U.; Schols, H. A.; De Vos, P. Immunological Properties of Inulin-Type Fructans. *Crit. Rev.*

Food Sci. Nutr. **2015**, *55*, 414–436, doi:10.1080/10408398.2012.656772.

11.   Dehghan, P.; Gargari, B. P.; Jafar-Abadi, M. A.; Aliasgharzadeh, A. Inulin controls inflammation and metabolic endotoxemia in women with type 2 diabetes mellitus: a randomized-controlled clinical trial. *Int. J. Food Sci. Nutr.* **2014**, *65*, 117–23, doi:10.31 09/09637486.2013.836738.

12.   Brighenti, F. Dietary fructans and serum triacylglycerols: a meta-analysis of randomized controlled trials. *J. Nutr.* **2007**, *137*, 2552S–2556S.

13.   Brighenti, F.; Casiraghi, M. C.; Canzi, E.; Ferrari, A. Effect of consumption of a ready-to-eat breakfast cereal containing inulin on the intestinal milieu and blood lipids in healthy male volunteers. *Eur. J. Clin. Nutr.* **1999**, *53*, 726–33, doi:http://dx.doi. org/10.1038/sj.ejcn.1600841.

14.   Davidson, M. H.; Maki, K. C.; Synecki, C.; Torri, S. A.; Drennan, K. B. Effects of dietary inulin on serum lipids in men and women with hypercholesterolemia. *Nutr. Res.* **1998**, *18*, 503–517, doi:10.1016/S0271-5317(98)00038-4.

15.   Aliasgharzadeh, A.; Khalili, M.; Mirtaheri, E.; Gargari, B. P.; Tavakoli, F.; Farhangi, M. A.; Babaei, H.; Dehghan, P. A combination of prebiotic inulin and oligofructose improve some of cardiovascular disease risk factors in women with type 2 diabetes: A randomized controlled clinical trial. *Adv. Pharm. Bull.* **2015**, *5*, 507–514, doi:10.15171/ apb.2015.069.

16.   Zadelaar, S.; Kleemann, R.; Verschuren, L.; de Vries-Van der Weij, J.; van der Hoorn, J.; Princen, H. M.; Kooistra, T. Mouse models for atherosclerosis and phar-maceutical modifiers. *Arterioscler. Thromb. Vasc. Biol.* **2007**, *27*, 1706–21, doi:10.1161/ ATVBAHA.107.142570.

17.   R. Hoving, L.; Katiraei, S.; Heijink, M.; Pronk, A.; van der Wee-Pals, L.; Streefland, T.; Giera, M.; Willems van Dijk, K.; van Harmelen, V. Dietary Mannan Oligosaccharides Modulate Gut Microbiota, Increase Fecal Bile Acid Excretion, and Decrease Plasma Cholesterol and Atherosclerosis Development. *Mol. Nutr. Food Res.* **2018**, *62*, 1700942, doi:10.1002/mnfr.201700942.

18. Segata, N.; Izard, J.; Waldron, L.; Gevers, D.; Miropolsky, L.; Garrett, W. S.; Huttenhower, C. Metagenomic biomarker discovery and explanation. *Genome Biol.* **2011**, *12*, R60, doi:10.1186/gb-2011-12-6-r60.

19. Mandal, S.; Van Treuren, W.; White, R. A.; Eggesbø, M.; Knight, R.; Peddada, S. D. Analysis of composition of microbiomes: a novel method for studying microbial composition. *Microb. Ecol. Health Dis.* **2015**, *26*, 27663.

20. Hoving, L. R.; Heijink, M.; van Harmelen, V.; Willems van Dijk, K.; Giera, M. GC-MS Analysis of Short-Chain Fatty Acids in Feces, Cecum Content, and Blood Samples. In *Clinical Metabolomics*; Giera, M., Ed.; Springer, **2018** ISBN 978-1-4939-7592-1.

21. Liang, W.; Menke, A. L.; Driessen, A.; Koek, G. H.; Lindeman, J. H.; Stoop, R.; Havekes, L. M.; Kleemann., R.; Van Den Hoek, A. M. Establishment of a general NAFLD scoring system for rodent models and comparison to human liver pathology. *PLoS One* **2014**, *9*, e115922, doi:10.1371/journal.pone.0115922.

22. Bligh, E.; Dyer, W. a Rapid Method of Total Lipid Extraction and Purification. *Can. J. Biochem. Physiol.* **1959**, *37*, 911–917, doi:10.1139/o59-099.

23. Rault-Nania, M.-H.; Gueux, E.; Demougeot, C.; Demigné, C.; Rock, E.; Mazur, A. Inulin attenuates atherosclerosis in apolipoprotein E-deficient mice. *Br. J. Nutr.* **2007**, *96*, 840–844, doi:10.1017/BJN20061913.

24. Zhang, S. H.; Reddick, R. L.; Piedrahita, J. A.; Maeda, N. Spontaneous hypercholesterolemia and arterial lesions in mice lacking apolipoprotein E. *Science* **1992**, *258*, 468–71.

25. van den Maagdenberg, A. M.; Hofker, M. H.; Krimpenfort, P. J.; de Bruijn, I.; van Vlijmen, B.; van der Boom, H.; Havekes, L. M.; Frants, R. R. Transgenic mice carrying the apolipoprotein E3-Leiden gene exhibit hyperlipoproteinemia. *J. Biol. Chem.* **1993**, *268*, 10540–5.

26. Wolever, T. M.; Spadafora, P.; Eshuis, H. Interaction between colonic acetate and propionate in humans. *Am. J. Clin. Nutr.* **1991**, *53*, 681–7.

27. Hara, H.; Haga, S.; Aoyama, Y.; Kiriyama, S. Short-chain fatty acids suppress cholesterol

5

synthesis in rat liver and intestine. *J. Nutr.* **1999**, *129*, 942–8.

28.   Li, Z.; Yi, C.-X.; Katiraei, S.; Kooijman, S.; Zhou, E.; Chung, C. K.; Gao, Y.; van den Heuvel, J. K.; Meijer, O. C.; Berbée, J. F. P.; Heijink, M.; Giera, M.; Willems van Dijk, K.; Groen, A. K.; Rensen, P. C. N.; Wang, Y. Butyrate reduces appetite and activates brown adipose tissue via the gut-brain neural circuit. *Gut* **2017**, gutjnl-2017-314050, doi:10.1136/gutjnl-2017-314050.

29.   Hoving, L. R.; de Vries, M.; de Jong, R.; Katiraei, S.; Pronk, A.; Quax, P.; van Harmelen, V.; Willems van Dijk, K. The Prebiotic Inulin Aggravates Accelerated Atherosclerosis in Hypercholesterolemic APOE*3-Leiden Mice. *Nutrients* **2018**, *10*, 172, doi:10.3390/nu10020172.

30.   Janssen, A. W.; Houben, T.; Katiraei, S.; Dijk, W.; Boutens, L.; van der Bolt, N.; Wang, Z.; Brown, J. M.; Hazen, S. L.; Mandard, S.; Shiri-Sverdlov, R.; Kuipers, F.; Willems van Dijk, K.; Vervoort, J.; Stienstra, R.; Hooiveld, G. J.; Kersten, S. Modulation of the gut microbiota impacts non-alcoholic fatty liver disease: a potential role for bile acids. *J. Lipid Res.* **2017**, jlr.M075713, doi:10.1194/jlr.M075713.

31.   Miles, J. P.; Zou, J.; Kumar, M.-V.; Pellizzon, M.; Ulman, E.; Ricci, M.; Gewirtz, A. T.; Chassaing, B. Supplementation of Low- and High-fat Diets with Fermentable Fiber Exacerbates Severity of DSS-induced Acute Colitis. *Inflamm. Bowel Dis.* **2017**, *23*, 1133–1143, doi:10.1097/MIB.0000000000001155.

32.   Meyer, D.; Stasse-Wolthuis, M. The bifidogenic effect of inulin and oligofructose and its consequences for gut health. *Eur. J. Clin. Nutr.* **2009**, *63*, 1277–1289.

33.   Catry, E.; Bindels, L. B.; Tailleux, A.; Lestavel, S.; Neyrinck, A. M.; Goossens, J.-F.; Lobysheva, I.; Plovier, H.; Essaghir, A.; Demoulin, J.-B.; Bouzin, C.; Pachikian, B. D.; Cani, P. D.; Staels, B.; Dessy, C.; Delzenne, N. M. Targeting the gut microbiota with inulin-type fructans: preclinical demonstration of a novel approach in the management of endothelial dysfunction. *Gut* **2017**, gutjnl-2016-313316, doi:10.1136/gutjnl-2016-313316.

34.   Lee, S.-M.; Han, H. W.; Yim, S. Y. Beneficial effects of soy milk and fiber on high

cholesterol diet-induced alteration of gut microbiota and inflammatory gene expression in rats. *Food Funct.* **2015**, *6*, 492–500, doi:10.1039/c4fo00731j.
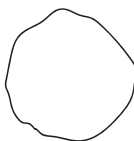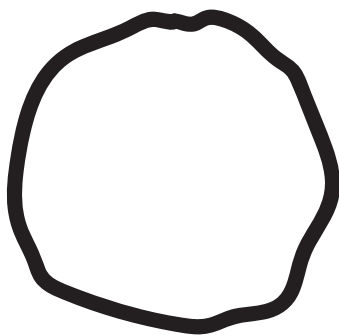
5

DIETARY YEAST-DERIVED MANNAN OLIGOSACCHARIDES HAVE IMMUNE-MODULATORY PROPERTIES BUT DO NOT IMPROVE HIGH FAT DIET-INDUCED OBESITY AND GLUCOSE INTOLERANCE

06

Lisa R. Hoving,

Hendrik J. P. van der Zande,

Amanda Pronk,

Bruno Guigas,

Ko Willems van Dijk, and

Vanessa van Harmelen

ABSTRACT

The indigestible mannan oligosaccharides (MOS) derived from the outer cell wall of yeast *Saccharomyces cerevisiae* have shown potential to reduce inflammation. Since inflammation is one of the underlying mechanisms involved in the development of obesity-associated metabolic dysfunctions, we aimed to determine the effect of dietary supplementation with MOS on inflammation and metabolic homeostasis in lean and diet-induced obese mice. Male C57BL/6 mice were fed either a low fat diet (LFD) or a high fat diet (HFD) with, respectively, 10% or 45% energy derived from lard fat, with or without 1% MOS for 17 weeks. Body weight and composition were measured throughout the study. After 12 weeks of intervention, whole-body glucose tolerance was assessed and in week 17 immune cell composition was determined in mesenteric white adipose tissue (mWAT) and liver by flow cytometry and RT-qPCR. In LFD-fed mice, MOS supplementation induced a significant increase in the abundance of macrophages and eosinophils in mWAT. A similar trend was observed in hepatic macrophages. Although HFD feeding induced a classical shift from the anti-inflammatory M2-like macrophages towards the pro-inflammatory M1-like macrophages in both mWAT and liver from control mice, MOS supplementation had no effect on this obesity-driven immune response. Finally, MOS supplementation did not improve whole-body glucose homeostasis in both lean and obese mice. Altogether, our data showed that MOS had extra-intestinal immune modulatory properties in mWAT and liver. However these effects were not substantial enough to significantly ameliorate HFD-induced glucose intolerance or inflammation.

6

INTRODUCTION

Obesity is associated with chronic low-grade inflammation. Obesity induces a phenotypic switch in the expanding white adipose tissue (WAT) from an anti-inflammatory towards a pro-inflammatory state which is characterised by an increase in M1-like macrophages, cytotoxic T cells, B cells, and neutrophils, whereas the numbers of M2-like macrophages, regulatory T cells, and eosinophils are reduced [1–5].

WAT inflammation results in the release of pro-inflammatory cytokines and fatty acids in the circulation, which are key mediators in inducing insulin resistance and inflammation in other organs, including the liver [6]. Inflammation in the insulin resistant liver is mainly characterised by high numbers of hepatic pro-inflammatory macrophages [7]. Obesity-associated inflammation is thought to eventually lead to the development of type 2 diabetes [8].

Dietary supplementation with mannan-oligosaccharides (MOS) has been suggested to modulate inflammation [9,10]. MOS are derived from the outer cell-wall membrane of bacteria, plants, or yeast and have been shown to be resistant to hydrolysis by the action of digestive enzymes in the human gut [11]. They are widely used in the animal industry as food supplements to reduce pathogenic contamination and to improve economic performance [12,13].

MOS supplementation was reported to lower the ileal gene expression of pro-inflammatory cytokines while increasing anti-inflammatory cytokines after challenging broilers with *Escherichia coli* [14]. Interestingly, there are also indications that MOS have extra-intestinal immune modulatory properties. Indeed, alveolar macrophages from pigs fed a MOS diet for two weeks showed reduced secretion of the pro-inflammatory cytokine *Tnf-α* and increased secretion of the anti-inflammatory cytokine *IL-10* in response to *ex vivo* stimulation by lipopolysaccharide (LPS) [15]. In addition, MOS improved immune responses and growth efficiency of nursery pigs after experimental respiratory virus infection [16].

Since inflammation is one of the underlying mechanisms involved in the development of obesity-associated dysfunctions, we hypothesised that dietary MOS have extra-intestinal immune modulating properties and reduce inflammation in WAT and liver of

6

obese mice. Therefore, we aimed to determine the effect of dietary supplementation with *Saccharomyces cerevisiae*-derived MOS on inflammation in metabolic tissues and whole-body glucose tolerance in both lean and HFD-induced obese mice.

Altogether, we report that MOS supplementation slightly altered the immune cell composition of mesenteric WAT (mWAT) and liver in lean mice, but did not ameliorate HFD-induced glucose intolerance or inflammation.

MATERIALS AND METHODS

MICE AND DIET

Male C57BL/6J mice were purchased from Charles River (Maastricht, The Netherlands) and housed under temperature- and humidity-controlled conditions with a 12:12h light-dark cycle and free access to food and water. At the start of the experiment mice were 10 weeks of age. Mice (n = 10 per group) were fed a LFD or HFD (10% or 45% kcal derived from lard fat, respectively; D12450B and D12451, Research Diet Services, Wijk bij Duurstede, The Netherlands) supplemented with 1% MOS (LFD-M and HFD-M) or without (LFD and HFD). The rationale behind the usage of 1% MOS was based on a study performed in C57BL/6 mice, where addition of 1% MOS to the diet led to decreased fat accumulation in adipose tissue and liver [17]. MOS used in this study was derived from the outer cell wall of yeast *S. cerevisiae* (Actigen®, Alltech, Ridderkerk, Netherlands). After 17 weeks, mice were sedated, perfused with ice-cold PBS through the heart and mWAT, liver, as well as thymus, and spleen were dissected for further analysis. Mouse experiments were performed in accordance with the Institute for Laboratory Animal Research Guide for the Care and Use of Laboratory Animals and had received approval from the University Ethical Review Board (Leiden University Medical Center, The Netherlands; permit no. 131031).

BODY WEIGHT, FOOD INTAKE, AND BODY COMPOSITION

During the diet intervention, body weight and food intake were measured weekly. Lean and

fat mass were monitored every 4 weeks up to 12 weeks by using an EchoMRI-100 analyser (Echo MRI, TX, USA).

STROMAL VASCULAR CELL ISOLATION FROM MESENTERIC WHITE ADIPOSE TISSUE

mWAT was dissected, rinsed in PBS and minced. Stromal vascular fraction (SVF) cells from mWAT were isolated as described previously [18]. Briefly, tissues were digested in a collagenase mixture (0.5 g/L collagenase [Type 1] in DMEM/F12 [pH 7.4] with 20 g/L of dialysed bovine serum albumin [BSA, fraction V; Sigma, St Louis, USA]) for 1 hour at 37°C, and filtered through a 236-µm nylon mesh. Upon centrifugation of the suspension (10 min, 200 g), the pelleted SVF was treated with red blood cell lysis buffer (BD Biosciences, CA, USA), stained with Aqua fixable live/dead stain (Invitrogen, Carlsbad, CA, USA) and fixed in 1.9% paraformaldehyde (Sigma-Aldrich). Cells were stored in FACS buffer (2 mM EDTA and 0.5% BSA in PBS) at 4°C until analyses.

ISOLATION OF IMMUNE CELLS FROM LIVER

Livers were dissected, washed in PBS and collected in RPMI 1640 GlutaMAX medium (Life Technologies, Grand Island, NY, USA). Immune cells from liver were isolated as described previously [19]. In brief, after mincing, tissues were digested for 20 minutes at 37°C in RPMI 1640 GlutaMAX (Life Technologies) supplemented with 1 mg/mL collagenase type IV from *C. hystolyticum* (Sigma-Aldrich), 2000 U/mL DNAse type I (Sigma-Aldrich) and 1 mM $CaCl_2$ to activate the enzymes. Digestion was stopped by adding ice cold wash buffer (1% FCS and 2.5 mM EDTA in PBS) and digested tissues were filtered through a 100 µm cell strainer (Corning, Corning, NY, USA). Following pelleting cells twice at 1,500 rpm for 5 minutes at 4°C, hepatocytes were pelleted by spinning at $50 \times g$ for 3 minutes at 4°C. Supernatant was collected, centrifuged at 1,500 rpm for 5 minutes at 4°C, and pellet was treated with 5 mL red blood cell lysis buffer. Cells were manually counted, stained and fixed as described above.

FLOW CYTOMETRY

Stromal vascular cells and liver immune cells were stained for 30 minutes at 4°C in the dark with the fluorescently-labelled antibodies listed in S1 Table. To assess the macrophage M2-like phenotype, cells were first permeabilised with eBioscience permeabilisation/wash buffer (San Diego, CA, USA) and stained with a biotin-conjugated Ym1 antibody (R&D systems, Minneapolis, MN, USA). All flow cytometry analyses were done within 3 days following cell fixation. Cells were measured by use of the FACSCanto flow cytometer (BD Bioscience, CA, USA) and analysed using FlowJo software (Treestar, OR, USA). Representative gating schemes are shown in S1 Fig.

INTRAPERITONEAL GLUCOSE TOLERANCE TEST

At 12 weeks LFD or HFD feeding, an intraperitoneal glucose tolerance test (ipGTT) was performed. Prior to the ipGTT, mice were fasted for 6 hours (from 8:00 AM to 14:00 PM). Blood samples were collected by tail vein bleeding immediately at baseline (t = 0 min) and 5, 15, 30, 60, 90 and 120 minutes after intraperitoneal injection with glucose (2 g/kg body weight). Plasma glucose concentrations were quantified using the Glucose Start Reagent Method according to manufacturer's instructions (Instruchemie, Delftzijl, The Netherlands).

PLASMA PARAMETERS

6 hour-fasted (from 8:00 AM to 14:00 PM) blood samples were collected by tail vein bleeding into chilled capillaries and isolated plasma was assayed for glucose and insulin at week 0, 4, and 8. Glucose was measured using an enzymatic kit from Instruchemie (Delfzijl, the Netherlands), and insulin by ELISA (Crystal Chem Inc., Downers Grove, IL).

RNA ISOLATION AND QUANTITATIVE RT-PCR

RNA was extracted from snap-frozen mWAT and liver samples using the NucleoSpin RNA kit according to manufacturer's instructions (Machery-Nagel, Düren, Germany). Concentrations and purity of RNA were determined on a NanoDrop ND-1000 spectrophotometer (Isogen,

Maarssen, The Netherlands) and RNA was reverse transcribed using Moloney Murine Leukemia Virus Reverse Transcriptase (Promega, The Netherlands). Expression levels of genes were determined by qRT-PCR, using SYBR green supermix (Biorad, The Netherlands) and gene specific primers (S2 Table). mRNA expression was normalised to cyclophilin (*CypA*) RNA and expressed as fold change versus control mice using the ΔΔCT method.

STATISTICAL ANALYSIS

Data are presented as means ± SEM. Statistical significance of differences was assessed by two-way ANOVA analysis of variance followed by a Tukey's post hoc multiple comparison test to determine Interaction effect, HFD effect, and MOS effect. Body weight gain, fat mass gain, lean mass gain, cumulative food intake, plasma glucose, plasma insulin, and ipGTT were analysed using two-way ANOVA for repeated measured, followed by a Tukey's post hoc multiple comparison test. The results were considered statistically significant at P<0.05. Analyses were performed using Graph Pad Prism version 7.0 (GraphPad Software, San Diego, CA, USA).

6

RESULTS

MOS SUPPLEMENTATION DID NOT AFFECT BODY WEIGHT, FAT MASS, ORGAN WEIGHT, AND FOOD INTAKE

To assess the effect of MOS supplementation on diet-induced obesity, mice were fed a LFD or HFD supplemented with or without MOS for 17 weeks. As expected, HFD induced a time-dependent increase in body weight (P<0.0001; Fig 1A; Table 1), fat mass gain (P<0.0001; Fig 1B; Table 1), mWAT weight (P<0.0001; Fig 1C; Table 1), and lean mass gain (P<0.0001; Table 1; S2A Fig) when compared with LFD-fed mice. Furthermore, HFD significantly increased liver weight (P=0.014; Fig 1D; Table 1) and thymus weight (P=0.001; Fig 1D; Table 1). MOS supplementation did not affect body weight (Fig 1A; Table 1), fat mass (Fig 1B; Table 1), and lean mass (Table 1; S2A Fig) when compared to control diets. Accordingly, the weights of mWAT (Fig 1C; Table 1), liver, spleen, and thymus (Fig 1D; Table 1) were not affected by MOS supplementation.

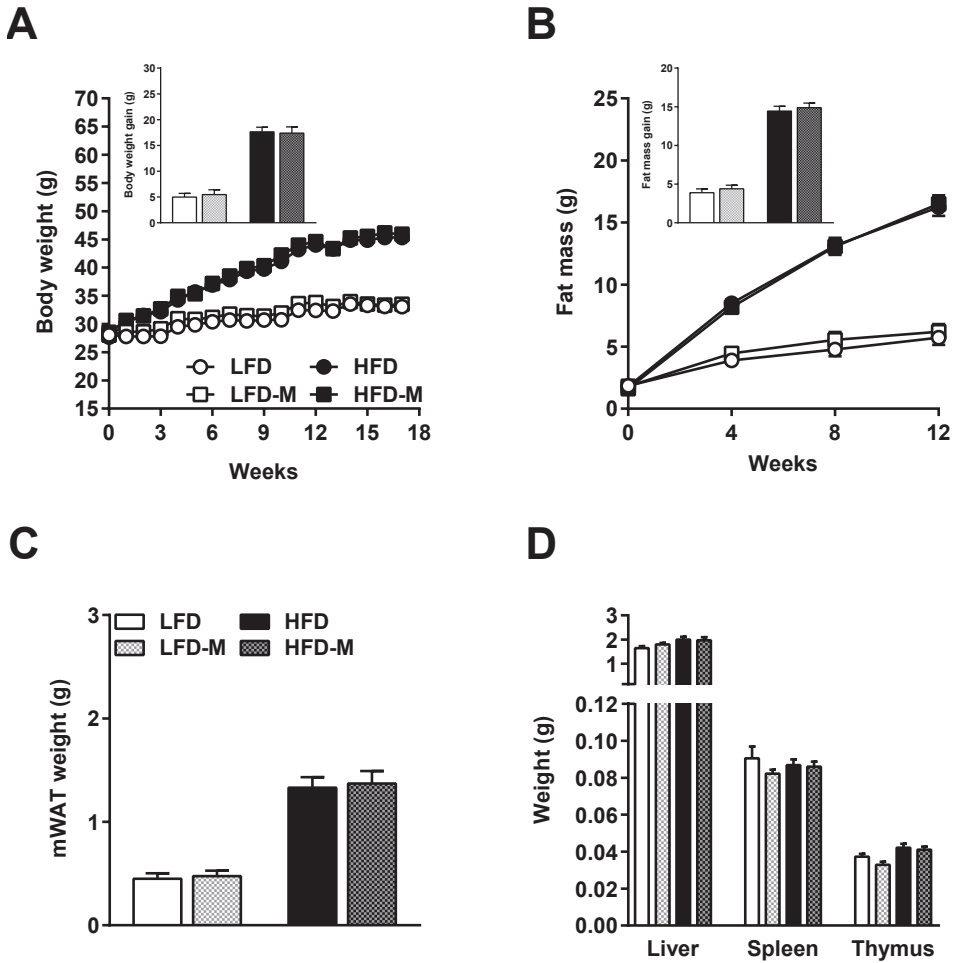Finally, neither HFD feeding nor MOS supplementation affected cumulative food intake (Table 1; S2B Fig).

Fig 1. MOS supplementation did not affect body weight, fat mass, organ weight, and food intake. Body weight [A], fat mass [B], mWAT weight [C], organ weight of liver, spleen, and thymus weight [D] of mice fed a LFD or HFD with or without MOS for 17 weeks. Values are presented as means ± SEM (n = 10 mice/group). Differences were evaluated for statistical significance by two-way ANOVA or two-way ANOVA for repeated measurements, both followed by a Tukey's post hoc multiple comparison test and provided in Table 1. mWAT, mesenteric white adipose tissue.

Table 1. Body weight, organ weight, and food intake characteristics

Body weight and organ weight	LFD (n=10) (mean ± SEM)	LFD-M (n=10) (mean ± SEM)	HFD (n=10) (mean ± SEM)	HFD-M (n=10) (mean ± SEM)	Interaction effect P-value	HFD effect P-value	MOS effect P-value	Time point effect P-value
Body weight gain (g)	4.99 ± 0.7165	5.48 ± 0.93	17.64 ± 0.89	17.39 ± 1.21	0.700	**<0.0001**	0.900	**<0.0001**
Fat mass gain (g)	3.88 ± 0.49	4.4 ± 0.47	14.45 ± 0.61	14.89 ± 0.59	0.945	**<0.0001**	0.387	**<0.0001**
mWAT weight (g)	0.45 ± 0.05	0.48 ± 0.05	1.33 ± 0.1	1.37 ± 0.12	0.944	**<0.0001**	0.706	n.a.
Liver weight (g)	1.64 ± 0.09	1.8 ± 0.06	2 ± 0.12	1.97 ± 0.13	0.354	**0.014**	0.523	n.a.
Spleen weight (g)	0.09 ± 0.01	0.08 ± 0.002	0.09 ± 0.003	0.09 ± 0.003	0.368	0.993	0.276	n.a.
Thymus weight (g)	0.04 ± 0.001	0.03 ± 0.002	0.04 ± 0.002	0.04 ± 0.002	0.348	**0.001**	0.140	n.a.
Lean mass gain (g)	1.26 ± 0.29	1.46 ± 0.38	2.63 ± 0.23	1.85 ± 0.35	0.129	**0.008**	0.370	**<0.0001**
Cumulative food intake week 17 (g / mouse)	52.7 ± 1.65	54.02 ± 1.70	49.96 ± 1.55	54.2 ± 2.77	0.472	0.527	0.179	**<0.0001**

$P < 0.05$ was considered significant determined by two-way ANOVA or two-way ANOVA for repeated measurements, both followed by a Tukey's post hoc multiple comparison test; Bold=(trend toward) significance; mWAT=mesenteric white adipose tissue

6

157

MOS SUPPLEMENTATION REDUCED THE ABUNDANCE OF M2-LIKE MONOCYTES AND INCREASED EOSINOPHILS IN MWAT

The immune cell composition of WAT, specifically the balance between M1-like and M2-like macrophages and the abundance of eosinophils, has been shown to play a crucial role in the maintenance of adipocyte insulin sensitivity and whole-body metabolic homeostasis [20,21]. To assess whether MOS supplementation has extra-intestinal immune modulatory effects in WAT, the SVF was isolated from mWAT and the immune cell composition of the mWAT SVF was determined using flow cytometry (see S1 Fig for the gating scheme). The expression of *CD11c* and *Ym1* within the total macrophage population allowed to discriminate between M1-like (Ym1$^-$ CD11c$^+$) and M2-like (Ym1$^+$ CD11c$^-$) macrophages, respectively [22].

HFD feeding did not affect the total Ly6C^{hi} monocyte population in mWAT (Fig 2A; Table 2). However, a trend towards a diet effect (LFD/HFD) was observed for M1-like (CD11c$^+$ Ly6C^{hi})(P=0.052; Table 2) and M2-like (Ym1$^+$ LyC6^{hi}) monocytes (P=0.098; Fig 2B; Table 2). The total Ly6C^{hi} monocyte population in mWAT of MOS supplemented mice was not affected (Fig 2A; Table 2). However, mice that received MOS displayed a decrease in M2-like monocytes (P=0.039; Fig 2B; Table 2). MOS did not affect M1-like monocytes (Table 2).

HFD feeding did not change the total abundance of macrophages (Fig 2C; Table 2). Although HFD did not affect the total abundance of macrophages in mWAT, HFD feeding induced a significant increase in M1-like macrophages (P<0.0001; Fig 2D; Table 2), a decrease in M2-like macrophages (P=0.038; Fig 2D; Table 2), and a decreased M2/M1 ratio (P=0.013; Table 2) in mWAT. MOS supplementation did not affect the total abundance of macrophages (Fig 2C; Table 2) and neither resulted in changes in M1-like and M2-like macrophage subsets (Fig 2D; Table 2), nor M2/M1 ratio (Table 2) in mWAT.

We further investigated whether granulocyte percentages within the CD45$^+$ population of mWAT were affected by either HFD feeding or MOS supplementation. HFD did not significantly change eosinophils (Fig 2E; Table 2) or neutrophils (Table 2) in mWAT. MOS supplementation did not affect the neutrophil population (Table 2) in mWAT of both LFD- and HFD-fed mice. However, with respect to eosinophils in mWAT there was a tendency

towards an interaction of MOS with diet (P=0.052; Fig 2E; Table 2) as MOS doubled the percentage of eosinophils in LFD but not in HFD-fed mice (5.08% and 1.59% respectively, P=0.047; Fig 2E; Table 2).

Finally, the effect of MOS supplementation on lymphocyte percentages within the CD45^{+} population was determined. HFD did not affect percentages of T cells, CD4^{+} T cells, CD8^{+} T cells, NK T cells, and B cells (Table 2), but lowered NK cells in (P=0.011; Table 2). There were no effects of MOS supplementation on any of these cells, except for a trend toward decreased T cells (P=0.062; Table 2).

Analysis of the mWAT mRNA gene expression showed that both the macrophage marker *F4/80* (P=0.023; Fig 2F; Table 2) and the M1-like macrophage marker *CD11c* (P=0.042; Fig 2F; Table 2) were increased in response to HFD. The relative mRNA expression of *CD11c*, *Ym1*, *Mcp1*, *Tnf*-α, *IL-6*, and *IL-10* was not affected by MOS supplementation (Fig 2F; Table 2). However, MOS showed a trend toward a decreased *F4/80* expression mainly on HFD (P=0.066; Fig 2F; Table 2) which was likely due to an interaction with diet (LFD/HFD) (P=0.086; Fig 2F; Table 2).

Taken together, these results showed that MOS supplementation has extra-intestinal immune modulatory properties by reducing M2-like monocytes on both diets and increasing eosinophils on LFD, whilst showing a trend toward reduced T cells on both diets and *F4/80* expression on HFD in mWAT.
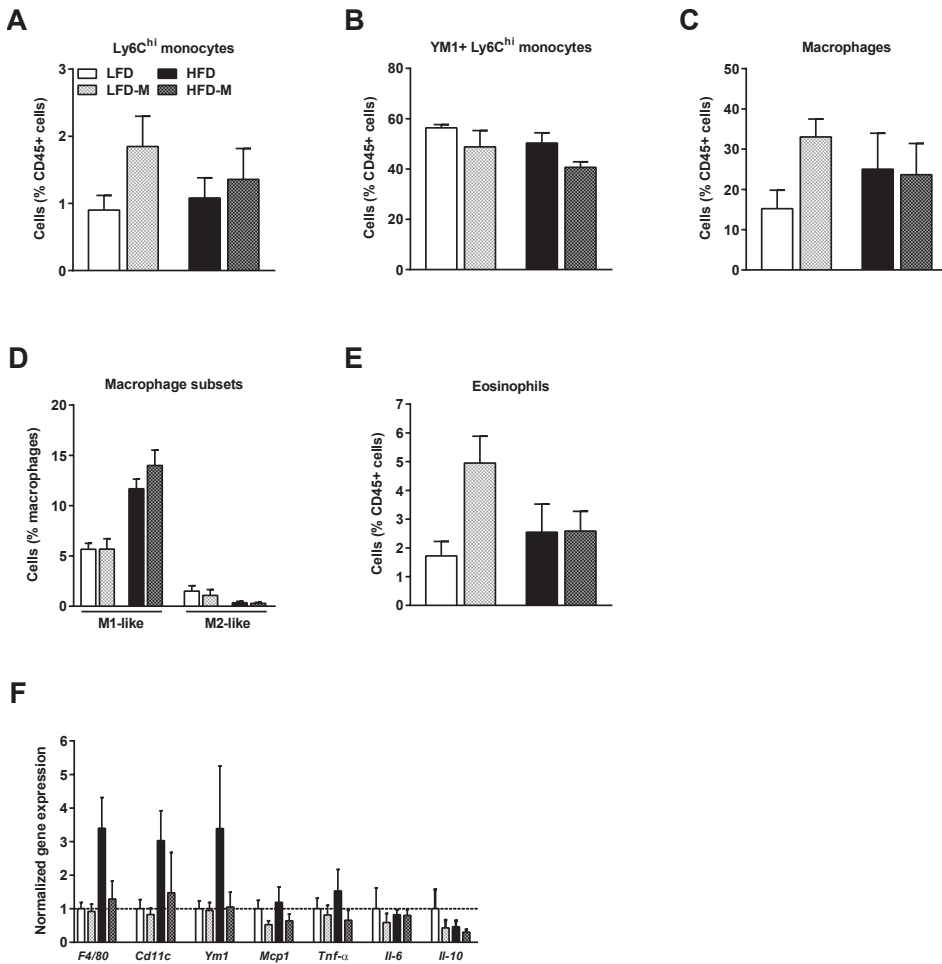
6

Fig 2. MOS supplementation reduced the abundance of M2-like monocytes and increased eosinophils in mWAT. Extra-intestinal immune modulatory properties of MOS were assessed in mWAT of mice fed a LFD or HFD with or without MOS for 17 weeks. Percentages of $Ly6C^{hi}$ monocytes [A], $Ym1^+$ $Ly6C^{hi}$ monocytes [B] macrophages [C], macrophage M1-like and M2-like subsets [D], and eosinophils [E] within $CD45^+$ cells in SVF of mWAT. mRNA expression of the inflammatory markers *F4/80, CD11c, Ym1, Mcp1, Tnf-α, IL-6*, and *IL-10* was determined [F]. Values are presented as means ± SEM (n = 6-7 mice/group). Differences were evaluated for statistical significance by two-way ANOVA, followed by a Tukey's post hoc multiple comparison test and provided in Table 2. For information on the immunological cell markers used in flow cytometry analysis, see Method section and Table 2.

Table 2. Innate immune cells, lymphocytes, and relative gene expression characteristics in mWAT

Innate immune cells mWAT	Immunological cell markers	LFD (n=7) (mean ± SEM)	LFD-M (n=6) (mean ± SEM)	HFD (n=5) (mean ± SEM)	HFD-M (n=6) (mean ± SEM)	Interaction effect P-value	HFD effect P-value	MOS effect P-value
Ly6C^{hi} monocytes (%CD45)	CD45+ Siglec-F- CD11b+ Ly6C^{hi} F4/80-	0.9 ± 0.2	1.85 ± 0.41	1.08 ± 0.27	1.36 ± 0.42	0.376	0.680	0.114
CD11c+ Ly6C^{hi} monocytes (%)	CD45+ Siglec-F- CD11b+ Ly6C^{hi} F4/80- CD11c+	50.6 ± 4.35	40 ± 6.47	35.6 ± 4.32	32.5 ± 4.18	0.503	**0.053**	0.224
Ym1+ Ly6C^{hi} monocytes (%)	CD45+ Siglec-F- CD11b+ Ly6C^{hi} F4/80- Ym1+	56.4 ± 1.16	48.8 ± 5.95	50.3 ± 3.65	40.7 ± 2.02	0.794	**0.085**	**0.039***
Macrophages (%CD45)	CD45+ Siglec-F- Ly6C- CD11b+ F4/80+	15.2 ± 4.27	33 ± 4.07	25.1 ± 7.99	23.7 ± 7.1	0.151	0.973	0.217
M1-like macrophages (%)	CD45+ Siglec-F- Ly6C- CD11b+ F4/80+ Ym1- CD11c+	5.67 ± 0.54	5.68 ± 1	11.7 ± 0.85	14 ± 1.4	0.295	**<0.0001***	0.292
M2-like macrophages (%)	CD45+ Siglec-F- Ly6C- CD11b+ F4/80+ Ym1+ CD11c-	1.51 ± 0.5	1.08 ± 0.53	0.34 ± 0.13	0.29 ± 0.09	0.667	**0.038***	0.590
M2/M1 ratio		0.28 ± 0.10	0.26 ± 0.12	0.03 ± 0.01	0.02 ± 0.004	0.960	**0.013***	0.853
Eosinophils (% CD45)	CD45+ Siglec-F+ (F4/80+)§	1.72 ± 0.46	4.95 ± 0.86	2.55 ± 0.88	2.59 ± 0.63	**0.052**	0.329	**0.047***
Neutrophils (% CD45)	CD45+ Siglec-F- CD11b^{hi} Ly6C+ F4/80- Ym1^{hi}	0.52 ± 0.13	1.17 ± 0.49	1.05 ± 0.63	0.27 ± 0.07	**0.093**	0.655	0.879

(Continued)

6

CHAPTER 6

Table 2. *Continued*

Lymphocytes mWAT	Immunological cell markers	LFD (n=9) (mean ± SEM)	LFD-M (n=6) (mean ± SEM)	HFD (n=5) (mean ± SEM)	HFD-M (n=6) (mean ± SEM)	Interaction effect P-value	HFD effect P-value	MOS effect P-value
T cells (% CD45)	CD45+ NK1.1- CD3+	27.3 ± 3.44	18.8 ± 2.87	24.3 ± 4.03	17.1 ± 3.77	0.878	0.567	**0.062**
CD4+ T cells (%)	CD45+ NK1.1- CD3+ CD4+ CD8-	53.2 ± 2.59	46.2 ± 7.91	54.7 ± 1.62	30.8 ± 9.93	0.893	0.912	0.187
CD25+ CD4+ T cells (%)	CD45+ NK1.1- CD3+ CD4+ CD8- CD25+	1839 ± 49.5	1884 ± 92.1	1919 ± 83.9	2029 ± 90.3	0.709	0.197	0.369
CD8+ T cells (%)	CD45+ NK1.1- CD3+ CD8+ CD4-	29.7 ± 3.65	20.9 ± 2.87	31 ± 4.7	39.2 ± 8.42	0.153	0.102	0.951
CD25+ CD8+ T cells (%)	CD45+ NK1.1- CD3+ CD8+ CD4- CD25+	2084 ± 63	2069 ± 113.6	2002 ± 58.8	1857 ± 117.1	0.522	0.156	0.435
NK T cells (% CD45)	CD45+ NK1.1+ CD3+	6.5 ± 0.91	8.26 ± 0.86	6.86 ± 1.39	9.94 ± 2.03	0.654	0.492	0.110
NK cells (% CD45)	CD45+ NK1.1+ CD3-	4.2 ± 0.85	5.80 ± 0.72	2.91 ± 0.66	2.55 ± 0.35	0.248	**0.011***	0.462
B cells (% CD45)	CD45+ CD19+ CD3- NK1.1-	34.9 ± 3.2	26.1 ± 4.82	36.3 ± 5.88	33.4 ± 5.77	0.576	0.413	0.277

(Continued)

162

Table 2. *Continued*

Gene expression mWAT	LFD (n=8) (mean ± SEM)	LFD-M (n=7) (mean ± SEM)	HFD (n=7) (mean ± SEM)	HFD-M (n=4) (mean ± SEM)	Interaction effect P-value	HFD effect P-value	MOS effect P-value
F4/80	0.45 ± 0.09	0.46 ± 0.11	1.69 ± 0.46	0.64 ± 0.26	**0.086**	**0.023***	**0.066**
CD11c	0.19 ± 0.05	0.15 ± 0.04	0.9 ± 0.36	0.27 ± 0.22	0.277	**0.042***	0.177
Ym1	0.27 ± 0.06	0.26 ± 0.06	1.32 ± 0.56	0.29 ± 0.12	0.175	0.142	0.158
Mcp1	0.68 ± 0.17	0.36 ± 0.08	0.81 ± 0.31	0.436 ± 0.13	0.902	0.634	0.120
Tnf-α	0.69 ± 0.22	0.56 ± 0.2	1.06 ± 0.44	0.46 ± 0.21	0.458	0.684	0.256
IL-6	0.3 ± 0.19	0.18 ± 0.08	0.25 ± 0.04	0.24 ± 0.05	0.662	0.965	0.629
IL-10	0.33 ± 0.19	0.14 ± 0.08	0.15 ± 0.06	0.1 ± 0.03	0.620	0.423	0.380

*P<0.05 was considered significant determined by two-way ANOVA followed by a Tukey's post hoc multiple comparison test; $ Specific for mWAT Bold=(trend toward) significance; mWAT=mesenteric white adipose tissue

6

MOS SUPPLEMENTATION SLIGHTLY AFFECTED HEPATIC MONOCYTES AND MACROPHAGE SUBSETS

Classical activation of Kupffer cells, the liver-resident macrophages, has been observed in diet-induced obesity [7]. Therefore, we determined the effect of MOS supplementation on hepatic immune cell composition using flow cytometry (see S1 Fig for the gating scheme).

As expected, HFD feeding increased Ly6C^{hi} monocytes (P=0.001; Fig 3A; Table 3) and macrophages (P=0.032; Fig 3B; Table 3) in the liver, indicating enhanced recruitment of pro-inflammatory monocytes. After MOS supplementation, a trend towards decreased Ly6C^{hi} monocytes were observed (P=0.093; Fig 3A; Table 3). Accordingly, an interaction was found between MOS supplementation and diet (LFD/HFD) on the total percentage of macrophages in the liver (P=0.05; Fig 3B; Table 3).

HFD-feeding increased predominantly M1-like macrophage subsets (P=0.003; Fig 3C; Table 3), while MOS supplementation resulted in a tendency toward decreased M1-like macrophages (P=0.095; Fig 3C; Table 3). No effects were found on M2-like macrophages (Fig 3C; Table 3) and on the M2/M1 ratio (Table 3) either with HFD or MOS.

We further investigated whether MOS supplementation affected granulocyte percentages within the CD45$^+$ population of the liver. A tendency toward increased eosinophils was found after HFD feeding (P=0.061; Fig 3D; Table 3), while neutrophils remained unaffected (Table 3). However, MOS-supplementation did not affect hepatic neutrophils (Table 3) or eosinophils (Fig 3D; Table 3).

Finally, we determined the effect of MOS on lymphocyte percentages within the CD45$^+$ population. HFD did not affect percentages of total T cells, CD4$^+$ T cells, CD8$^+$ T cells, NK T cells, and NK cells (Table 3). However, B cells were found to be significantly lower in HFD-fed mice (P=0.006; Table 3). MOS did not affect any of these lymphocytes, although a significant interaction was found between diet (LFD/HFD) and MOS on CD25$^+$ CD8$^+$ expressing T cells (P=0.013; Fig 3E; Table 3).

Analysis of the liver mRNA gene expression showed an increase in the expression of *Ym1* (P=0.012; Fig 3F; Table 3) in HFD-fed mice indicating M2-like macrophages, and we found a tendency towards an increase in *CD11c* (P=0.098; Fig 3F; Table 3) indicating M1-like

macrophages in HFD-fed mice. On the other hand, MOS decreased hepatic expression of *Ym1* (P=0.021; Fig 3F; Table 3) and a tendency towards decreased expression of *CD11c* (P=0.099; Fig 3F; Table 3). A trend towards interaction between diet (LFD/HFD) and MOS was found for the expression of *CD11c* (P=0.092; Fig 3C; Table 3). Finally, HFD tended to decrease the expression of *IL-6* (P=0.072; Fig 3F; Table 3), and an interaction between diet (LFD/HFD) and MOS supplementation was found for *IL-6* (P=0.08; Fig 3F; Table 3). Gene expression of *F4/80*, *Mcp1*, *Tnf-α*, and *IL-10* remained unaffected by diet or MOS (Fig 3F; Table 3).

Overall, MOS supplementation modestly affected the liver with tendencies to decrease Ly6C^{hi} monocytes and M1-like macrophages.
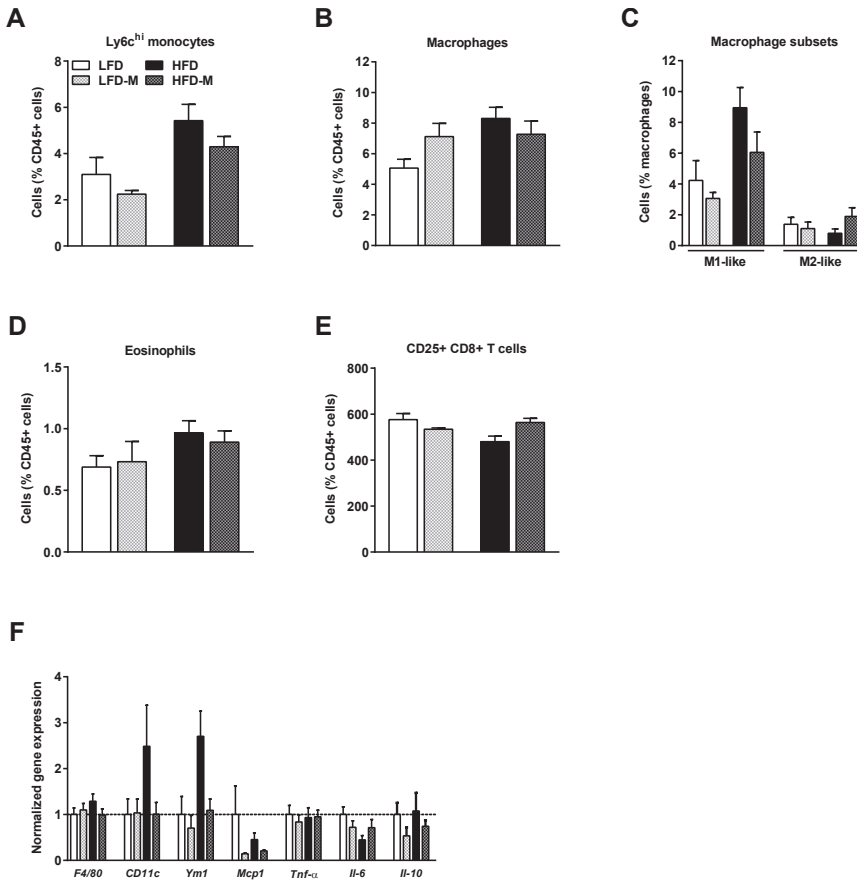
Fig 3. MOS supplementation slightly affected hepatic monocytes and macrophage subsets.

Hepatic extra-intestinal immune modulatory properties of MOS were assessed in mice fed a LFD or HFD with or without MOS for 17 weeks. Percentages of Ly6C^{hi} monocytes [A], macrophages [B], macrophage M1-like and M2-like subsets [C], eosinophils [D] and CD25$^+$ CD8$^+$ expressing T cells [E] within CD45$^+$ cells in the liver. mRNA expression of the inflammatory markers *F4/80, CD11c, Ym1, Mcp1, Tnf-a, IL-6,* and *IL-10* was determined [F]. Values are presented as means ± SEM (n = 4-10 mice/group). Differences were evaluated for statistical significance by two-way ANOVA, followed by a Tukey's post hoc multiple comparison test and provided in Table 3. For information on the immunological cell markers used in flow cytometry analysis, see Method section and Table 3.

Table 3. Innate immune cells, lymphocytes, and relative gene expression characteristics in liver

Innate immune cells Liver	Immunological cell markers	LFD (n=10) (mean ± SEM)	LFD-M (n=9) (mean ± SEM)	HFD (n=10) (mean ± SEM)	HFD-M (n=10) (mean ± SEM)	Interaction effect P-value	HFD effect P-value	MOS effect P-value
Ly6C^{hi} monocytes (% CD45)	CD45+ Siglec-F- CD11b+ Ly6C^{hi} F4/80+	3.10 ± 0.69	2.24 ± 0.15	5.42 ± 0.67	4.29 ± 0.43	0.812	**0.001***	**0.093**
CD11c+ Ly6C^{hi} monocytes (%)	CD45+ Siglec-F- CD11b+ Ly6C^{hi} F4/80- CD11c+	9.52 ± 1.57	8.17 ± 0.76	8.88 ± 0.77	10.9 ± 1.14	0.164	0.384	0.778
Ym1+ Ly6C^{hi} monocytes (%)	CD45+ Siglec-F- CD11b+ Ly6C^{hi} F4/80- Ym1+	20.6 ± 4.48	13.1 ± 2.79	15.8 ± 5	27 ± 6.24	**0.078**	0.378	0.724
Macrophages (% CD45)	CD45+ Siglec-F- Ly6C- CD11b+ F4/80+	5.06 ± 0.54	7.12 ± 0.82	8.30 ± 0.69	7.27 ± 0.81	**0.050***	**0.032***	0.502
M1-like macrophages (%)	CD45+ Siglec-F- Ly6C- CD11b+ F4/80+ Ym1- CD11c+	4.23 ± 1.23	3.06 ± 0.34	8.94 ± 1.25	6.05 ± 1.26	0.469	**0.003***	**0.095**
M2-like macrophages (%)	CD45+ Siglec-F- Ly6C- CD11b+ F4/80+ Ym1+ CD11c-	1.38 ± 0.43	1.1 ± 0.4	0.80 ± 0.26	1.9 ± 0.54	0.131	0.809	0.366
M2/M1 ratio		0.68 ± 0.3	0.45 ± 0.2	0.13 ± 0.06	0.62 ± 0.2	0.108	0.398	0.552
Eosinophils (% CD45)	CD45+ Siglec-F+ (F4/80+)	0.69 ± 0.09	0.73 ± 0.15	0.97 ± 0.09	0.89 ± 0.09	0.599	**0.061**	0.888
Neutrophils (% CD45)	CD45+ Siglec-F- CD11b^{hi} Ly6C+ F4/80- Ym1^{hi}	6.20 ± 1.44	7.01 ± 1.48	5.04 ± 1.41	6.23 ± 1.33	0.875	0.539	0.491

(Continued)

6

Table 3. *Continued*

Lymphocytes Liver	Immunological cell markers	LFD (n=6) *(mean ± SEM)*	LFD-M (n=4) *(mean ± SEM)*	HFD (n=5) *(mean ± SEM)*	HFD-M (n=6) *(mean ± SEM)*	Interaction effect *P-value*	HFD effect *P-value*	MOS effect *P-value*
T cells (% CD45)	CD45+ NK1.1- CD3+	10.8 ± 0.79	9.29 ± 0.42	11.9 ± 1.45	10.2 ± 0.86	0.915	0.369	0.172
CD4+ T cells (%)	CD45+ NK1.1- CD3+ CD4+ CD8-	54.1 ± 1.43	55.6 ± 1.27	56.4 ± 6.04	56.1 ± 0.99	0.800	0.698	0.866
CD25+ CD4+ T cells (%)	CD45+ NK1.1- CD3+ CD4+ CD8- CD25+	367.8 ± 14.11	363.8 ± 21.85	338.2 ± 18.87	364 ± 6.95	0.395	0.403	0.534
CD8+ T cells (%)	CD45+ NK1.1- CD3+ CD8+ CD4-	37.6 ± 1.76	34.1 ± 2.91	34.8 ± 5.83	34.8 ± 0.83	0.635	0.769	0.624
CD25+ CD8+ T cells (%)	CD45+ NK1.1- CD3+ CD8+ CD4- CD25+	576 ± 24.6	534.3 ± 5.14	480 ± 21.88	563.5 ± 16.95	**0.013***	0.159	0.370
NK T cells (% CD45)	CD45+ NK1.1+ CD3+	10.4 ± 0.83	10.2 ± 0.62	7.56 ± 1.29	10.7 ± 0.76	0.126	0.265	0.189
NK cells (% CD45)	CD45+ NK1.1+ CD3-	3.46 ± 0.27	3.88 ± 0.67	3.32 ± 0.5	3.56 ± 0.25	0.853	0.623	0.482
B cells (% CD45)	CD45+ CD19+ CD3- NK1.1-	35.6 ± 1.41	34.1 ± 0.53	23 ± 4.98	28.3 ± 1.06	0.268	**0.006***	0.523

*P<0.05 was considered significant determined by two-way ANOVA followed by a Tukey's post hoc multiple comparison test; Bold=(trend toward) significance

MOS SUPPLEMENTATION DID NOT IMPROVE WHOLE-BODY GLUCOSE INTOLERANCE

We next studied whether MOS affected whole-body glucose homeostasis in lean and diet-induced obese mice. As expected, HFD feeding increased fasting plasma glucose (P<0.0001; Fig 4A; Table 4) and insulin (P<0.0001; Fig 4B; Table 4) levels over time as compared to LFD feeding. In week 12, whole-body glucose tolerance was measured using ipGTT. HFD deteriorated glucose tolerance over time as compared to LFD-fed mice (P<0.0001; Fig 4C and 4D; Table 4). MOS supplementation did neither affect fasting plasma glucose (Fig 4A; Table 4) or insulin (Fig 4B; Table 4) levels, nor altered glucose tolerance (Fig 4C and 4D; Table 4). These data indicate that MOS supplementation did not affect whole-body glucose homeostasis.

6

A

B

C

D
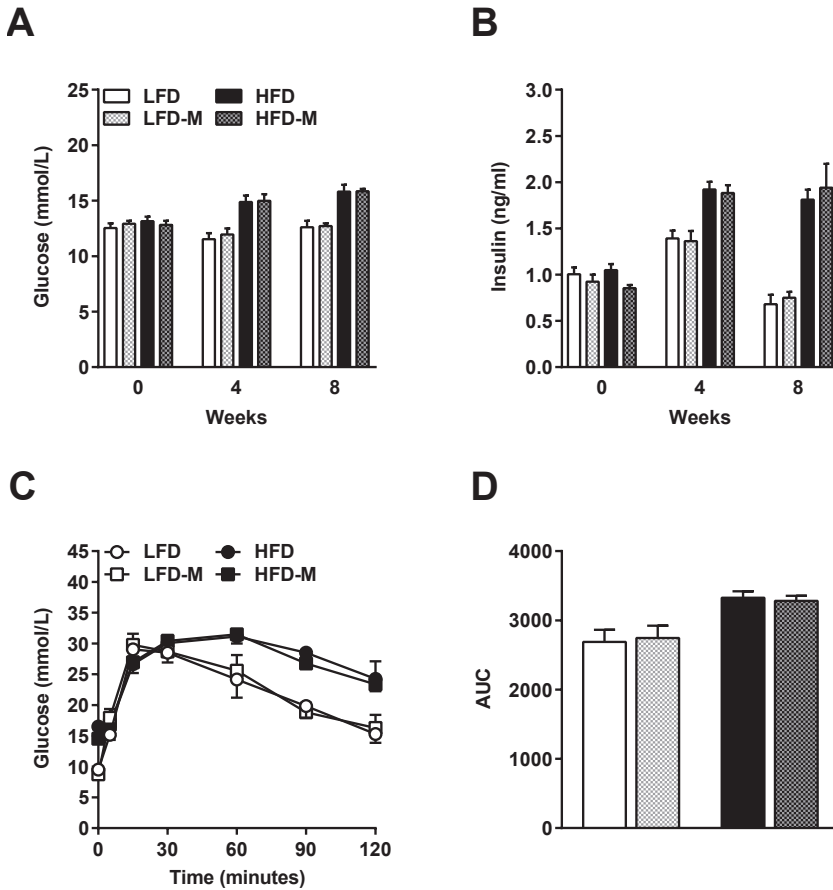
Fig 4. MOS supplementation did not improve whole-body glucose intolerance. Whole-body glucose homeostasis was assessed in mice fed a LFD or HFD with or without MOS for 17 weeks. Fasting plasma glucose [A] and insulin levels [B] were determined in 6-hour fasted mice in week 0, 4, and 8. An ipGTT was performed in 6-hour fasted mice at week 12. Blood glucose levels were measured at the indicated minutes [C], and the area under the curve (AUC) of the glucose excursion curve was calculated as a measure for glucose tolerance [D]. Values are presented as means ± SEM (n = 10 mice/group). Differences were evaluated for statistical significance by two-way ANOVA or two-way ANOVA for repeated measurements, both followed by a Tukey's post hoc multiple comparison test and provided in Table 4.

Table 4. Glucose, insulin, and ipGTT characteristics

Glucose, insulin, and ipGTT analysis	LFD (n=10) (mean ± SEM)	LFD-M (n=10) (mean ± SEM)	HFD (n=10) (mean ± SEM)	HFD-M (n=10) (mean ± SEM)	Interaction effect P-value	HFD effect P-value	MOS effect P-value	Time point effect P-value
Glucose (mmol/L)	12.6 ± 0.58	12.71 ± 0.25	15.82 ± 0.62	15.85 ± 0.20	0.930	<0.0001*	0.876	**<0.0001**
Insulin (ng/ml)	0.68 ± 0.1	0.751 ± 0.06	1.81 ± 0.11	1.94 ± 0.26	0.850	<0.0001*	0.525	**<0.0001**
ipGTT (AUC)	2687 ± 175.1	2745 ± 179.3	3327 ± 91.7	3281 ± 73.7	0.710	0.0001*	0.968	**<0.0001**

*P<0.05 was considered significant determined by two-way ANOVA or two-way ANOVA for repeated measurements followed, both by a Tukey's post hoc multiple comparison test; Bold=(trend toward) significance; AUC=area under curve; ipGTT=intraperitoneal glucose tolerance test

6

DISCUSSION

The immune modulatory properties of MOS have been exploited to increase the economic yields of livestock [12,13]. In the present study, we investigated the effect of MOS supplementation on body weight and composition, food intake, immune composition of mWAT and liver, and whole-body glucose tolerance in both LFD-fed lean and HFD-induced obese mice. We showed that MOS supplementation mildly altered immune cell composition in both mWAT and liver, which was not accompanied by amelioration in HFD-induced obesity or whole-body glucose intolerance. Our data confirm the potential extra-intestinal modulatory properties of MOS on immune composition as reported previously [9,14–16], although the effects are relatively modest.

Specifically, MOS increased eosinophils in mWAT of LFD-fed mice. Eosinophils have been shown previously to beneficially reduce inflammation in WAT by promoting M2-like macrophage polarisation [5,20]. However, the observed increase in eosinophils with MOS did not lead to skewing toward M2-like macrophages as there were no alterations in macrophage subpopulations after MOS supplementation in mWAT. As a matter of fact, MOS even led to a decrease in M2-like monocytes in mWAT. The effects of MOS on eosinophils were therefore probably too small to induce beneficial effects on macrophage polarisation. Whether MOS is able to induce more substantial effects in other fat depot regions remains to be investigated. As whole-body glucose tolerance was not affected by MOS supplementation in both lean and obese mice in our study, we suggest that MOS will not affect inflammation in any of the fat depots.

In livers of these mice, HFD feeding increased both the total amount of monocytes and macrophages. However, no significant effect of MOS was found on reducing these parameters although MOS tended to reduce monocytes and M1-like macrophages in the liver. This may imply that MOS supplementation in this setting steers towards beneficial M2/M1 ratios in the liver, although the observed effects were minor. Additionally, the data obtained from the flow cytometry data were not in direct line with the gene expression data. Although we do not have a clear explanation for this, it is likely that this discrepancy is a result of the markers measured on specific cell types on protein level in flow cytometry analysis versus markers measured on

the total pool of cells on gene expression level.

Given that MOS supplementation did not affect diet-induced obesity and whole-body glucose tolerance, leads us to speculate that the observed alterations in immune cell compositions were insufficient to achieve a significant effect. Another possibility is that the concentration of supplemented MOS in the diet was not high enough. However, in previous studies where MOS supplementation showed intra-intestinal and extra-intestinal effects on the immune system, concentrations of 0.005% to 0.5% of MOS were used in the diet [10,14,23]. However, these studies were performed in broiler chickens or pigs, and it is possible that different species respond differently to MOS. Another study performed in mice also used 1% MOS supplementation and found a decreased fat accumulation in the parametrial adipose tissue and in the liver [17]. However, this latter study MOS derived from coffee mannan which is different from the yeast-derived MOS that we used in this study. Whether the origin of MOS may determine the effect of MOS on fat accumulation remains to be determined. The limited effects of MOS supplementation on diet-induced obesity in our mice did not seem to be due to inappropriate dosages of MOS.

Alternatively, other factors within the experimental setting might explain the relatively limited effects of MOS in our experiments. In previous studies, MOS showed anti-inflammatory effects in experimentally viral or bacterial infected animals [9,14–16]. In order for MOS to reduce inflammation, a strong pro-inflammatory trigger may first be needed, e.g. by bacteria or bacterial components such as LPS. Importantly, the experimental mice used in our study are guaranteed free of particular pathogens. The mechanistic action of MOS to improve performance in animal industry is thought to occur via the ability of MOS to inhibit attachment of pathogens with type-1 fimbriae to the intestinal wall of animals [24]. In our facility, the presence of type-1 fimbriae containing pathogenic bacteria residing in the gut of the mice is probably very limited. Further research needs to be conducted to determine whether *S. cerevisiae*-derived MOS is dependent upon pathogenic stimuli in order to exert its anti-inflammatory function.

Furthermore, the impact of the HFD might be too strong in order for MOS to exert

6

its beneficial function on the intestinal barrier. Intestinal epithelial mucosal surfaces possess a variety of defence mechanisms to prevent adhesion of bacteria, including mucus secretion and sloughing [25,26]. Mucins are major anti-adhesive components of mucus. In order for the epithelial surface to produce mucus, an intact epithelial layer should be present. HFD feeding in mice damages the intestinal barrier integrity, increasing intestinal permeability and increasing LPS leakage (endotoxemia) into the system [27]. It is likely that MOS is not able to restore the intestinal barrier integrity to inhibit bacterial colonisation and reduce systemic inflammation.

The type of MOS used in various studies might also determine the effect of MOS on diet-induced obesity, glucose tolerance, and immune modulation. In our study, we used mannan derived from the yeast *S. cerevisiae*. However, MOS can be derived from various sources with different effects on body weight in mice. For instance, MOS derived from coffee mannan decreased fat accumulation in mice [17], whereas MOS derived from the plant konjac mannan did not have any effect on body weight in mice [28]. Therefore, it remains to be investigated whether MOS derived from different sources also have different immune modulatory effects.

In conclusion, this study showed that MOS supplementation did alter immune composition in mWAT and liver. However, these effects were not accompanied by ameliorations in HFD-induced glucose intolerance or inflammation.

ACKNOWLEDGEMENTS

REFERENCES

1. Acosta, J. R.; Douagi, I.; Andersson, D. P.; Bäckdahl, J.; Rydén, M.; Arner, P.; Laurencikiene, J. Increased fat cell size: a major phenotype of subcutaneous white adipose tissue in non-obese individuals with type 2 diabetes. *Diabetologia* **2016**, *59*, 560–570, doi:10.1007/s00125-015-3810-6.

2. Wu, H.; Ghosh, S.; Perrard, X. D.; Feng, L.; Garcia, G. E.; Perrard, J. L.; Sweeney, J. F.; Peterson, L. E.; Chan, L.; Smith, C. W.; Ballantyne, C. M. T-cell accumulation and regulated on activation, normal T cell expressed and secreted upregulation in adipose tissue in obesity. *Circulation* **2007**, *115*, 1029–1038, doi:10.1161/CIRCULATIONAHA.106.638379.

3. Huh, J. Y.; Park, Y. J.; Ham, M.; Kim, J. B. Crosstalk between adipocytes and immune cells in adipose tissue inflammation and metabolic dysregulation in obesity. *Mol Cells* **2014**, *37*, 365–371, doi:10.14348/molcells.2014.0074.

4. Nijhuis, J.; Rensen, S. S.; Slaats, Y.; van Dielen, F. M. H.; Buurman, W. A.; Greve, J. W. M. Neutrophil Activation in Morbid Obesity, Chronic Activation of Acute Inflammation. *Obesity* **2009**, *17*, 2014–2018, doi:10.1038/oby.2009.113.

5. Wu, D.; Molofsky, A. B.; Liang, H.-E.; Ricardo-Gonzalez, R. R.; Jouihan, H. A.; Bando, J. K.; Chawla, A.; Locksley, R. M. Eosinophils Sustain Adipose Alternatively Activated Macrophages Associated with Glucose Homeostasis. *Science (80-.).* **2011**, *332*, 243–247, doi:10.1126/science.1201475.

6. Ndumele, C. E.; Nasir, K.; Conceiçao, R. D.; Carvalho, J. A. M.; Blumenthal, R. S.; Santos, R. D. Hepatic steatosis, obesity, and the metabolic syndrome are independently and additively associated with increased systemic inflammation. *Arterioscler. Thromb. Vasc. Biol.* **2011**, *31*, 1927–1932, doi:10.1161/ATVBAHA.111.228262.

7. Morinaga, H.; Mayoral, R.; Heinrichsdorff, J.; Osborn, O.; Franck, N.; Hah, N.; Walenta, E.; Bandyopadhyay, G.; Pessentheiner, A. R.; Chi, T. J.; Chung, H.; Bogner-Strauss, J. G.; Evans, R. M.; Olefsky, J. M.; Oh, D. Y. Characterization of distinct subpopulations of hepatic macrophages in HFD/obese mice. *Diabetes* **2015**, *64*, 1120–30, doi:10.2337/

6

db14-1238.

8.	Hotamisligil, G.; Shargill, N.; Spiegelman, B. Adipose expression of tumour necrosis factor-alpha: direct role in obesity-linked insulin resistance. *Science (80-.).* **1993**, *259*, 87–91, doi:10.1126/science.7678183.

9.	Baurhoo, B.; Ferket, P.; Ashwell, C. M.; de Oliviera, J.; Zhao, X. Cell walls of Saccharomyces cerevisiae differentially modulated innate immunity and glucose metabolism during late systemic inflammation. *PLoS One* **2012**, *7*, e30323, doi:10.1371/journal.pone.0030323.

10.	Munyaka, P. M.; Echeverry, H.; Yitbarek, A.; Camelo-Jaimes, G.; Sharif, S.; Guenter, W.; House, J. D.; Rodriguez-Lecompte, J. C. Local and systemic innate immunity in broiler chickens supplemented with yeast-derived carbohydrates. *Poult. Sci.* **2012**, *91*, 2164–72, doi:10.3382/ps.2012-02306.

11.	Gómez, B.; Miguez, B.; Yáñez, R.; Alonso, J. L. Manufacture and Properties of Glucomannans and Glucomannooligosaccharides Derived from Konjac and Other Sources. *J. Agric. Food Chem.* **2017**, *65*, 2019–2031.

12.	Torrecillas, S.; Montero, D.; Izquierdo, M. Improved health and growth of fish fed mannan oligosaccharides: potential mode of action. *Fish Shellfish Immunol.* **2014**, *36*, 525–44, doi:10.1016/j.fsi.2013.12.029.

13.	Berge, A. C.; Wierup, M. Nutritional strategies to combat Salmonella in mono-gastric food animal production. *animal* **2012**, *6*, 557–564, doi:10.1017/S1751731111002217.

14.	Wang, W.; Li, Z.; Han, Q.; Guo, Y.; Zhang, B.; D'inca, R. Dietary live yeast and mannan-oligosaccharide supplementation attenuate intestinal inflammation and barrier dysfunction induced by Escherichia coli in broilers. *Br. J. Nutr.* **2016**, *116*, 1878–1888, doi:10.1017/S0007114516004116.

15.	Che, T. M.; Johnson, R. W.; Kelley, K. W.; Van Alstine, W. G.; Dawson, K. A.; Moran, C. A.; Pettigrew, J. E. Mannan oligosaccharide modulates gene expression profile in pigs experimentally infected with porcine reproductive and respiratory syndrome virus. *J. Anim. Sci.* **2011**, *89*, 3016–29, doi:10.2527/jas.2010-3366.

16. Che, T. M.; Johnson, R. W.; Kelley, K. W.; Dawson, K. A.; Moran, C. A.; Pettigrew, J. E. Effects of mannan oligosaccharide on cytokine secretions by porcine alveolar macrophages and serum cytokine concentrations in nursery pigs. *J. Anim. Sci.* **2012**, *90*, 657–668, doi:10.2527/jas.2011-4310.

17. Takao, I.; Fujii, S.; Ishii, A.; Han, L.-K.; Kumao, T.; Ozaki, K.; Asakawa, A. Effects of Mannooligosaccharides from Coffee Mannan on Fat Storage in Mice Fed a High Fat Diet. *J. Heal. Sci.* **2006**, *52*, 333–337, doi:10.1248/jhs.52.333.

18. van Beek, L.; van Klinken, J. B.; Pronk, A. C. M.; van Dam, A. D.; Dirven, E.; Rensen, P. C. N.; Koning, F.; Willems van Dijk, K.; van Harmelen, V. The limited storage capacity of gonadal adipose tissue directs the development of metabolic disorders in male C57Bl/6J mice. *Diabetologia* **2015**, *58*, 1601–9, doi:10.1007/s00125-015-3594-8.

19. Hussaarts, L.; García-Tardón, N.; van Beek, L.; Heemskerk, M. M.; Haeberlein, S.; van der Zon, G. C.; Ozir-Fazalalikhan, A.; Berbée, J. F. P.; Willems van Dijk, K.; van Harmelen, V.; Yazdanbakhsh, M.; Guigas, B. Chronic helminth infection and helminth-derived egg antigens promote adipose tissue M2 macrophages and improve insulin sensitivity in obese mice. *FASEB J.* **2015**, *29*, 3027–39, doi:10.1096/fj.14-266239.

20. Zhang, Y.; Yang, P.; Cui, R.; Zhang, M.; Li, H.; Qian, C.; Sheng, C.; Qu, S.; Bu, L. Eosinophils Reduce Chronic Inflammation in Adipose Tissue by Secreting Th2 Cytokines and Promoting M2 Macrophages Polarization. *Int. J. Endocrinol.* **2015**, *2015*, 1–5, doi:10.1155/2015/565760.

21. Chawla, A.; Nguyen, K. D.; Goh, Y. P. S. Macrophage-mediated inflammation in metabolic disease. *Nat. Rev. Immunol.* **2011**, *11*, 738–749, doi:10.1038/nri3071.

22. Lumeng, C. N.; Bodzin, J. L.; Saltiel, A. R. Obesity induces a phenotypic switch in adipose tissue macrophage polarization. *J. Clin. Invest.* **2007**, *117*, 175–184, doi:10.1172/JCI29881.

23. Baurhoo, B.; Phillip, L.; Ruiz-Feria, C. A. Effects of purified lignin and mannan oligosaccharides on intestinal integrity and microbial populations in the ceca and litter

6

of broiler chickens. *Poult. Sci.* **2007**, *86*, 1070–1078.

24.   Thomas, W. E.; Nilsson, L. M.; Forero, M.; Sokurenko, E. V.; Vogel, V. Shear-dependent "stick-and-roll" adhesion of type 1 fimbriated Escherichia coli. *Mol. Microbiol.* **2004**, *53*, 1545–1557, doi:10.1111/j.1365-2958.2004.04226.x.

25.   Bavington, C. D.; Lever, R.; Mulloy, B.; Grundy, M. M.; Page, C. P.; Richardson, N. V.; McKenzie, J. D. Anti-adhesive glycoproteins in echinoderm mucus secretions. *Comp. Biochem. Physiol. Part B Biochem. Mol. Biol.* **2004**, *139*, 607–617, doi:10.1016/j.cbpc.2004.07.008.

26.   Bavington, C.; Page, C. Stopping bacterial adhesion: A novel approach to treating infections. *Respiration* **2005**, *72*, 335–344.

27.   Johnson, A. M. F.; Costanzo, A.; Gareau, M. G.; Armando, A. M.; Quehenberger, O.; Jameson, J. M.; Olefsky, J. M. High fat diet causes depletion of intestinal eosinophils associated with intestinal permeability. *PLoS One* **2015**, *10*, e0122195, doi:10.1371/journal.pone.0122195.

28.   Smith, D. L.; Nagy, T. R.; Wilson, L. S.; Dong, S.; Barnes, S.; Allison, D. B. The effect of mannan oligosaccharide supplementation on body weight gain and fat accrual in C57Bl/6J mice. *Obesity (Silver Spring).* **2010**, *18*, 995–9, doi:10.1038/oby.2009.308.

SUPPLEMENT

S1 Table. Antibodies used for flow cytometry

Fluorophore	Antibody	Clone	Vendor
FITC	anti-CD45.2	104	Biolegend
PE	anti-Siglec-F	E50-2440	BD Biosciences
PE	anti-NK1.1	PK136	BD Biosciences
PerCP	Streptavidin	N/A	BD Biosciences
PerCP-Cy5.5	anti-CD25	PC61	BD Biosciences
PE-Cy7	anti-CD11b	M1/70	eBioscience
PE-Cy7	anti-CD4	GK1.5	eBioscience
APC	anti-F4/80	BM8	eBioscience
APC	anti-CD8a	53-6.7	Biolegend
APC-Cy7	anti-Ly6C	HK1.4	Biolegend
APC-Cy7	anti-CD19	1D3	eBioscience
Horizon V450	anti-CD11c	HL3	BD Biosciences
eFluor 450	anti-CD3	17A2	eBioscience

6

S2 Table. Primer sequences of forward and reverse primers (5' > 3').

Gene	Sense	Antisense
CypA	ACTGAATGGCTGGATGGCAA	TGTCCACAGTCGGAAATGGT
F4/80	CTTTGGCTATGGGCTTCCAGTC	GCAAGGAGGACAGAGTTTATCGTG
Cd11c	GCCACCAACCCTTCCTGGCTG	TTGGACACTCCTGCTGTGCAGTTG
Ym1	ACAATTAGTACTGGCCCACCAGGAA	TCCTTGAGCCACTGAGCCTTCA
Mcp1	CACTCACCTGCTGCTACTCA	GCTTGGTGACAAAAACTACAGC
Tnf-α	GATCGGTCCCCAAAGGGATG	CACTTGGTGGTTTGCTACGAC
IL-6	AAGAAATGATGGATGCTACCAAACTG	GTACTCCAGAAGACCAGAGGAAATT
IL-10	GACAACATACTGCTAACCGACTC	ATCACTCTTCACCTGCTCCACT
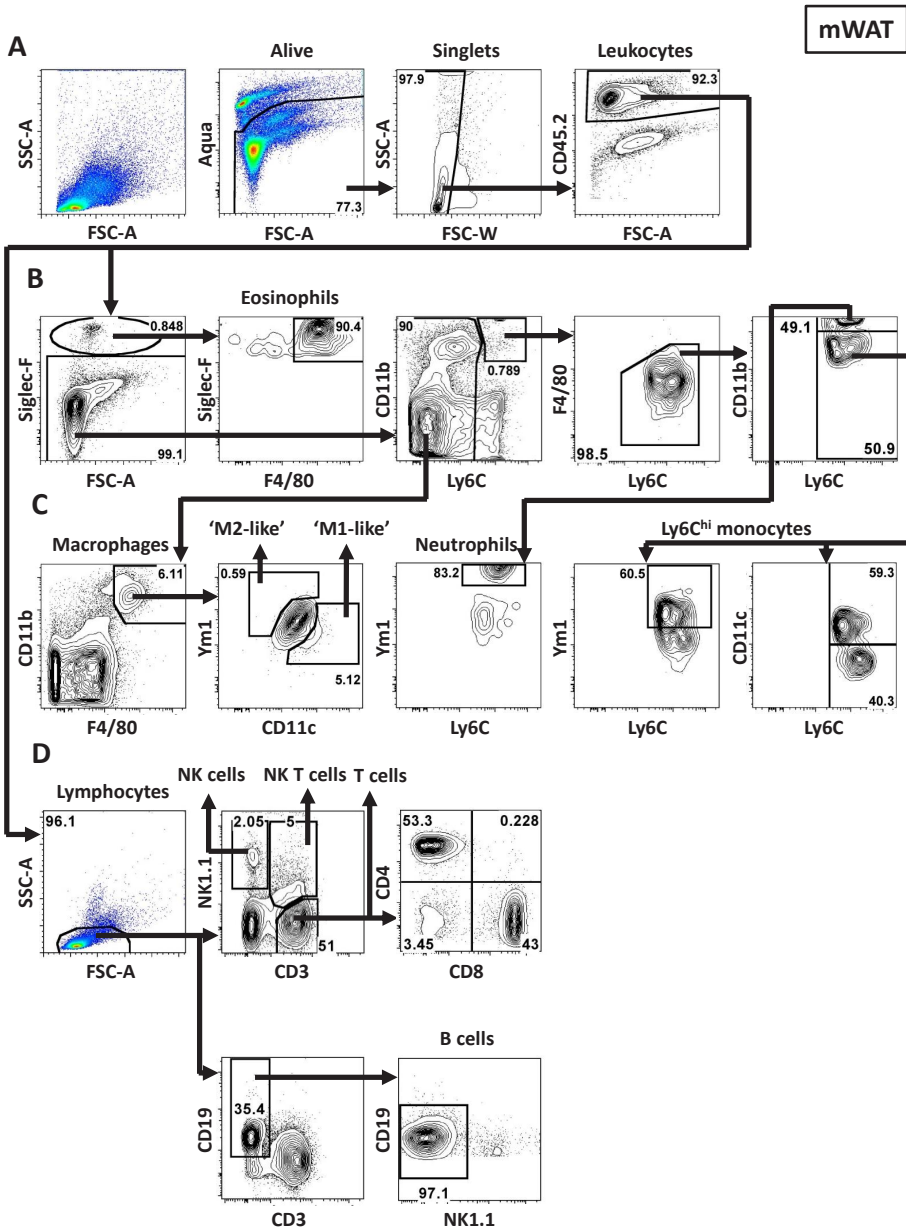
S1 Fig. Gating strategies mWAT and liver. Isolated cells were pre-gated on Aqua-CD45$^+$ single cells. FSC-A, forward scatter area; SSC-A, sideward scatter area; FSC-W, forward scatter width [A]. Gating strategies for the analysis of eosinophils, neutrophils and monocytes [B], macrophages, M1-like (CD11c$^+$ Ym1$^-$)
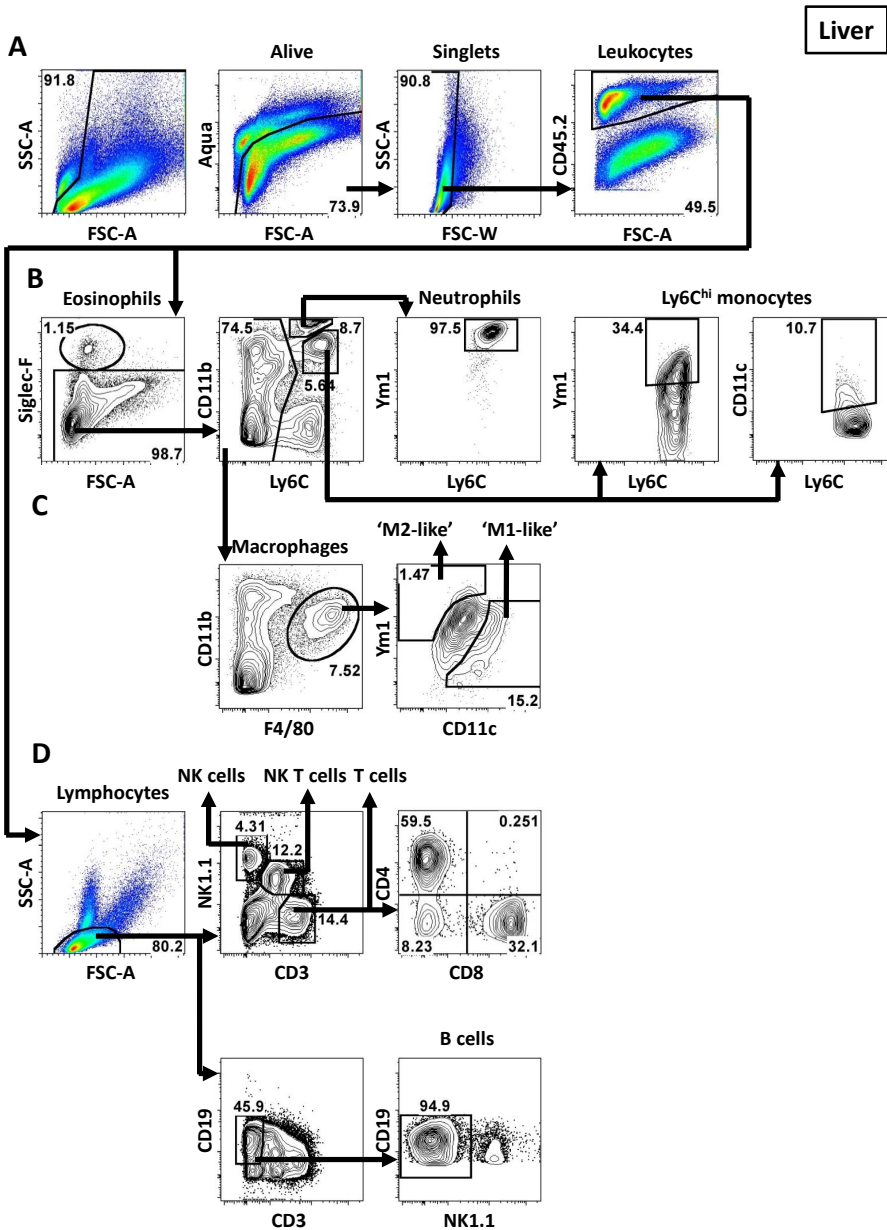
macrophages and M2-like (CD11c⁻ Ym1⁺) macrophages [C], and NK cell, NK T cell, T cell and B cell lymphocyte subsets [D] are given. Gating strategies are shown for representative samples from mWAT and liver.
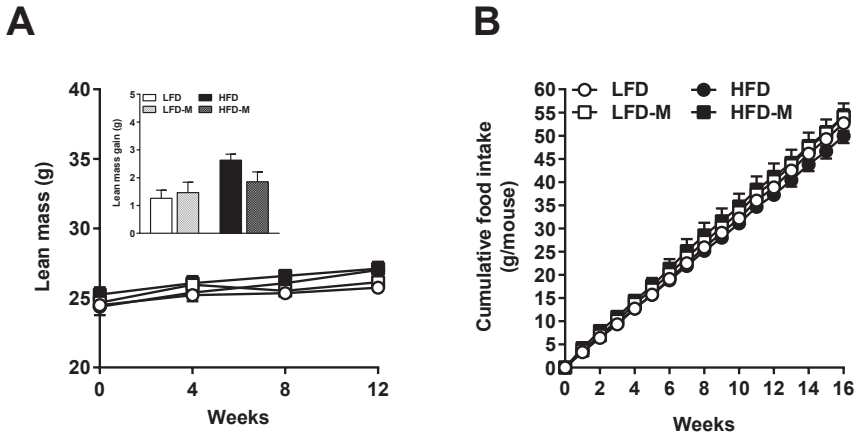
S2 Fig. The effect of MOS supplementation on lean mass and cumulative food intake. Lean mass [A] and food intake [B] of mice fed a LFD or HFD with or without MOS for 17 weeks. Values are presented as means ± SEM (n = 10 mice/group). Differences were evaluated for statistical significance by two-way ANOVA for repeated measures, followed by Tukey's post hoc multiple comparison test and provided in Table 1.
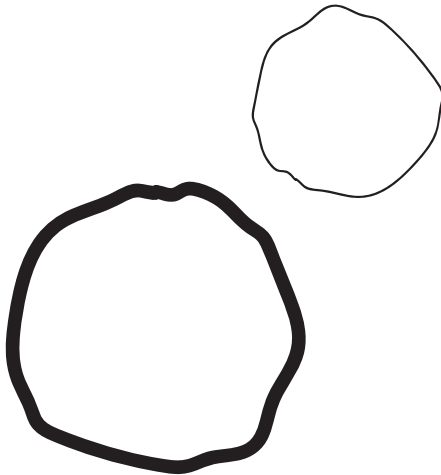
6

DIETARY MANNAN OLIGOSACCHARIDES MODULATE GUT MICROBIOTA, INCREASE FECAL BILE ACID EXCRETION, AND DECREASE PLASMA CHOLESTEROL AND ATHEROSCLEROSIS DEVELOPMENT

07

Lisa R. Hoving,

Saeed Katiraei,

Marieke Heijink,

Amanda Pronk,

Lianne van der Wee-Pals,

Trea Streefland,

Martin Giera,

Ko Willems van Dijk, and

Vanessa van Harmelen

ABSTRACT

Mannan oligosaccharides (MOS) have proven effective at improving growth performance, while also reducing hyperlipidemia and inflammation. As atherosclerosis is accelerated both by hyperlipidemia and inflammation, we aim to determine the effect of dietary MOS on atherosclerosis development in hyperlipidemic ApoE*3-Leiden.CETP (*E3L.CETP*) mice, a well-established model for human-like lipoprotein metabolism.

Female *E3L.CETP* mice were fed a high-cholesterol diet, with or without 1% MOS for 14 weeks. MOS substantially decreased atherosclerotic lesions up to 54%, as assessed in the valve area of the aortic root. In blood, IL-1RA, monocyte subtypes, lipids, and bile acids (BAs) were not affected by MOS. Gut microbiota composition was determined using 16S rRNA gene sequencing and MOS increased the abundance of cecal *Bacteroides Ovatus*. MOS did not affect fecal excretion of cholesterol, but increased fecal BAs as well as butyrate in cecum as determined by gas chromatography mass spectrometry.

MOS decreased the onset of atherosclerosis development via lowering of plasma cholesterol levels. These effects were accompanied by increased cecal butyrate and fecal excretion of BAs, presumably mediated via interactions of MOS with the gut microbiota.

7

INTRODUCTION

Atherosclerosis is a major cause of severe disease in modern society and a leading cause of death [1]. Left untreated, atherosclerosis leads to cardiovascular complications including heart attack and stroke. The development of atherosclerosis is initiated by LDL cholesterol deposition in the arterial wall, oxidation of these lipoproteins, and uptake by macrophages leading to foam cell formation [2]. Accumulation of foam cells is associated with endothelial dysfunction, influx of inflammatory cells, and progression of atherosclerotic lesion formation. This process is further aggravated in the presence of systemic inflammation. Atherosclerosis is thus initiated by the formation of lesions within the arterial wall [3], and is driven by both lipids and by inflammation [4–6].

Although relatively efficient drugs are available to inhibit the development of atherosclerosis, additional strategies that reduce inflammation and hyperlipidemia are urgently required. One potential candidate includes dietary supplementation with mannan oligosaccharides (MOS). MOS can be derived from the outer cell-wall membrane of bacteria, plants, or yeast [7]. Yeast *Saccharomyces cerevisiae*-derived MOS have been widely used in livestock industry as an alternative to antibiotics and as food supplementation to ameliorate performance by reducing pathogenic contamination [8–10].

Several studies demonstrated that MOS is able to inflammation, both within the gastrointestinal tract [11] as well as systemically [12,13]. Additionally, in different studies using a variety of experimental animal models, it was shown that dietary supplementation with MOS lowered plasma cholesterol levels [14–16]. However, the mechanism by which MOS exert their effect is not fully established. A suggested mode of action by which MOS may improve inflammation is via interaction and modification of the gut microbiota. According to Spring *et al.*, MOS bind to type-1 fimbriae of pathogenic bacteria and prevent their adherence to the intestinal mucosa [17], thereby reducing pathogen-induced inflammation. Additionally, cholesterol levels might also be affected by the interaction of MOS with the gut microbiota. Gut microbiota play an important role in regulating bile acid (BA) metabolism by converting primary BAs to secondary BAs [18]. Secondary BAs are relatively less efficiently reabsorbed

7

and excreted more via the feces compared to primary BAs [18–20]. Hepatic conversion of cholesterol to BAs balances fecal excretion, which is the major route for cholesterol catabolism and accounting for almost half of the cholesterol eliminated from the body per day [21]. Therefore, differences in fecal BA excretion affects the enterohepatic circulation of cholesterol and may ultimately affect plasma cholesterol levels [22].

Given the potential anti-inflammatory and cholesterol-lowering effects of MOS, we hypothesised that dietary MOS supplementation will reduce atherosclerosis development via interactions with the gut microbiota. In the present study, we set out to determine the effect of dietary MOS supplementation on systemic inflammation and plasma lipid levels in the progression of atherosclerosis, using female hyperlipidemic ApoE*3-Leiden.CETP (*E3L.CETP*) mice, a well-established mouse model for hyperlipidemia and atherosclerosis development [23,24].

We found that MOS modulated the gut microbiota composition and activity, which was associated with increased fecal BA excretion. Increased BA excretion can explain lowered plasma total cholesterol (TC) levels and subsequently decreased progression of atherosclerosis.

MATERIALS AND METHODS

MICE AND DIET

Female *E3L.CETP* mice of 11–15 weeks of age were fed a control western-type diet (WTD) containing 0.1% cholesterol (Diet T; AB Diets,Woerden, TheNetherlands) or this diet supplemented with 1% MOS derived from *S. cerevisiae* (Actigen, Alltech, Ridderkerk, The Netherlands) for a total period of 14 weeks. After a run-in period of 3 weeks with WTD, mice were randomised according to plasma TC, triglycerides (TG), body weight, and age. Mice were housed under temperature- and humidity-controlled specific pathogen-free (SPF) conditions with a 12:12 h light–dark cycle and free access to food and water. During the diet intervention, body weight and food intake were weekly measured. After 14 weeks of intervention, non-fasted mice were sacrificed using CO_2 inhalation, perfused with ice-cold PBS through the heart, and trunk blood was collected via heart puncture. Livers were collected for further analysis. Mouse experiments

were performed in compliance with Dutch government guidelines and the Directive 2010/63/ EU of the European Parliament and had received approval from the University Ethical Review Board (Leiden University Medical Center, The Netherlands, permission no. 13164).

ATHEROSCLEROSIS QUANTIFICATION AND (IMMUNO)HISTOCHEMICAL ANALYSIS

After 14 weeks of dietary intervention, hearts were collected and fixed in phosphate-buffered 4% formaldehyde, dehydrated in 70% ethanol, embedded in paraffin, and cross-sectioned (5 µm) perpendicular to the axis of the aorta throughout the aortic root area, starting from the appearance of open aortic valve leaflets. Per mouse, four sections with 50 µm intervals were used for atherosclerosis quantification. Obtained sections were stained with hematoxylin phloxin saffron (HPS) for histological analysis. Lesions were visually categorised for lesion severity according to the guidelines of the American Heart Association adapted for mice [25]. Various types of lesions were discerned: mild lesions (types 1−3), severe lesions (types 4 and 5), and the absence of lesions defined as "non-diseased segments." Rat monoclonal anti-mouse antibod MAC3 (1:1000; BD Pharmingen, San Diego, CA, USA) was used to quantify macrophage area. Atherosclerotic lesion area and composition were analysed using ImageJ software (NIH, Bethesda, Maryland, USA).

7

FLOW CYTOMETRY

Circulating monocytes were analysed using flow cytometry. After lysis of red blood cells, pelleted cells were resuspended in FACS buffer and stained for 30 minutes at 4°C in the dark with fluorescently labelled antibodies listed in Table S1, Supporting Information. Cells were measured on an LSR II flow cytometer using Diva 6 software (BD Biosciences, CA, USA). Data were analysed using FlowJo software (Treestar, OR, USA). Representative gating schemes are shown in Figure S1, Supporting Information.

PLASMA PARAMETERS

At the indicated time points, 4 hour fasted (from 8:00 AM to 12:00 PM) blood samples were collected by tail vein bleeding into chilled capillaries and isolated plasma was assayed for TC and TG using commercially available kits (Roche Diagnostics, Germany). For determination of plasma HDL-cholesterol, apoB-containing particles were precipitated from plasma with 20% polyethylene glycol in 200 mM glycine buffer (pH 10) and TC was measured in the supernatant. Non-HDL was calculated by subtracting HDL values from TC values. Cholesterol exposure was calculated as the cumulative exposure over the number of weeks the WTD was fed. The plasma cytokine IL-1RA was measured using the R&D Quantikine kit following the manufacturer's standard protocol (R&D Systems,Minneapolis, USA). Plasma concentrations of total BAs were determined using a colourimetric assay kit (Diazyme Laboratories, Poway, USA).

LIVER LIPIDS

Lipids were extracted from the liver according to a protocol modified from Bligh and Dyer [26]. Liver samples were homogenised in 10 µL ice-cold CH_3OH/mg tissue. Lipids were extracted by the addition of 1800 µL CH_3OH:$CHCl_3$ (3:1 v/v) to 45 µL homogenate and subsequent centrifugation. The homogenate was dried and dissolved in 2% Triton X-100, and TC content was assayed as described above.

16S RIBOSOMAL RNA GENE SEQUENCING AND PROFILING

For 16S rRNA sequencing, genomic DNA was isolated from cecum samples and sent to the Broad Institute of MIT and Harvard (Cambridge, USA). Microbial 16S rRNA gene was amplified targeting the hyper-variable V4 region using forward primer 515F (5'-GTGCCAGCMGCCG-CGGTAA-3') and the reverse primer 806R (5'-GGACTACHVGGGTWTCTAAT-3'). The cycling conditions consisted of an initial denaturation of 94°C for 3 minutes, followed by 25 cycles of denaturation at 94°C for 45 seconds, annealing at 50°C for 60 seconds, extension at 72°C for 5 minutes, and a final extension at 72°C for 10 minutes. Sequencing was performed using the Illumina MiSeq platform generating paired-end reads of 175 bp in length in each

direction. Overlapping paired-end reads were subsequently aligned. Details of this protocol are previously described [27]. Raw sequence data quality was assessed using FastQC, version 0.11.2 (http://www.bioinformatics.babraham.ac.uk/projects/fastqc/). Reads' quality was verified using Sickle version 1.33 (https://github.com/najoshi/sickle) and low-quality reads were removed. For visualising the taxonomic composition of the cecal microbiota and further β-diversity analysis, QIIME, version 1.9.1 was used [28]. In brief, closed reference OTU picking with 97% sequence similarity against GreenGenes 13.8 reference database was performed. Jackknifed β-diversity of unweighted UniFrac distances, with 10 jackknifed replicates was measured at rarefaction depth of 5000 reads per sample.

CECAL SHORT-CHAIN FATTY ACID ANALYSIS

Cecum short-chain fatty acid (SCFA) content was analysed using GC-MS as previously described with additional modifications [29]. Briefly, aqueous extracts of cecal content were prepared and added to acetone along with the internal standards acetate-d4, propionate-d6, and butyrate-d8. Subsequently, SCFAs were derivatized using pentafluorobenzyl bromide (PFBBr) (60°C for 30 minutes). Samples were extracted by the addition of *n*-hexane and water. The *n*-hexane fraction was subjected for further analysis. A Bruker Scion 436 GC coupled to a Bruker Scion TQ MS (Bruker, Bremen, Germany) was employed. Injection was performed using a CTC PAL autosampler (CTC Analytics, Zwingen, Switzerland) splitless at 280°C. The GC was equipped with an Agilent VF-5ms (25 m × 0.25 mm i.d., 0.25 µm film thickness) column (Agilent, Waldbronn, Germany). The following temperature gradient was used: 1 minute constant at 50°C, linear increase at 40°C/minute to 60°C, kept constant for 3 minutes, linear increase of 25°C/minute to 200°C, linear increase at 40°C/minute to 315°C, kept constant for 2 minutes. The transfer line and ionisation source temperature were 280°C. Methane 99.995% was used as chemical ionisation gas and negatively charged molecular ions were detected in the selected ion monitoring mode.

7

FECAL CHOLESTEROL AND BILE ACID ANALYSIS

Feces was collected over a 24 hour period for 3 consecutive days. Fecal samples were dried at room temperature, weighed, and homogenised. Fecal cholesterol, the fecal primary BAs cholic acid (CA), α-muricholic acid (α-MCA), and β-muricholic acid (β-MCA), and the secondary BAs hyocholic acid (HCA), deoxycholic acid (DCA), and ω-muricholic acid (ω-MCA) were determined by capillary gas chromatography on an Agilent gas chromatograph (HP 6890), equipped with a 25 m × 0.25 mm CP-Sil-19-fused silica column (Varian, Middelburg, The Netherlands) and a flame ionisation detector as described previously [30].

RNA ISOLATION AND QUANTITATIVE RT-PCR

RNA was extracted from snap-frozen liver samples using NucleoSpin RNA kit according to the manufacturer's instructions (Machery-Nagel, Germany). Concentrations and purity of RNA were determined on a NanoDrop ND-1000 spectrophotometer (Isogen, The Netherlands) and RNA was reverse-transcribed using Moloney Murine Leukemia Virus Reverse Transcriptase (Promega, The Netherlands). The mRNA expression level of 7-α-hydroxylase (*Cyp7a1*) and sterol 27-hydroxylase (*Cyp27a1*) were determined by qRT-PCR, using SYBR green supermix (Biorad, The Netherlands) and the gene-specific primers for *Cyp7a1* (forward: 5'-CAGG-GAGATGCTCTGTGTTCA-3'; reverse: 5'-AGGCATACATCCCTTCCGTGA-3') and for *Cyp27a1* (forward 5'-TCTGGCTACCTGCACTTCCT-3'; reverse: 5'-CTGGATCTCTGG-GCTCTTTG-3'). mRNA expression was normalised to the housekeeping gene *36b4* (forward: 5'-GGACCCGAGAAGACCTCCTT-3'; reverse: 5'-GCACATCACTCAGAATTTCAAT-GG-3'), and expressed as fold change versus control using the ΔΔCT method.

STATISTICAL ANALYSIS

Data are presented as means ± SEM. Normal distribution of the data was tested using D'Agostino–Pearson omnibus normality test, and data were compared with the unpaired Student's *t*-test in the case of normal distribution or with the non-parametric Mann–Whitney *U* test in the case of not normally distributed data. Correlation analysis was performed using

linear regression analysis. The regression lines of the MOS-supplemented mice versus control mice were compared to identify whether the correlations differed between the groups. First it was tested whether slopes of the lines differed and then whether intercepts of the lines differed. When the slopes and intercepts were not significantly different, linear regression analyses was performed on pooled data of both groups. P<0.05 was considered as statistically significant. Analyses were performed using Graph Pad Prism version 7.0 (GraphPad Software, USA).

RESULTS

MOS DECREASED ATHEROSCLEROSIS DEVELOPMENT

To assess whether MOS affects atherosclerosis, we determined the progression of atherosclerosis in the aortic root after 14 weeks of MOS supplementation. As illustrated by representative images in Figure 1A, MOS markedly reduced the atherosclerotic lesion area throughout the whole aortic root (Figure 1B), which resulted in a 54% reduction of the mean atherosclerotic lesion area (p=0.03; Figure 1C). Although the overall lesion severity was generally profound in both intervention groups, MOS greatly reduced type 5 lesions in the aortic root by 49% (p=0.004; Figure 1D). Concomitantly, the number of non-diseased segments was doubled after MOS supplementation (+147%; p=0.01; Figure 1E). However, MOS did not affect the macrophage content of the atherosclerotic lesions of these mice (Figure 1F). Together, these findings demonstrated that MOS markedly delayed the progression of atherosclerosis and attenuated the severity of atherosclerotic lesions.

7
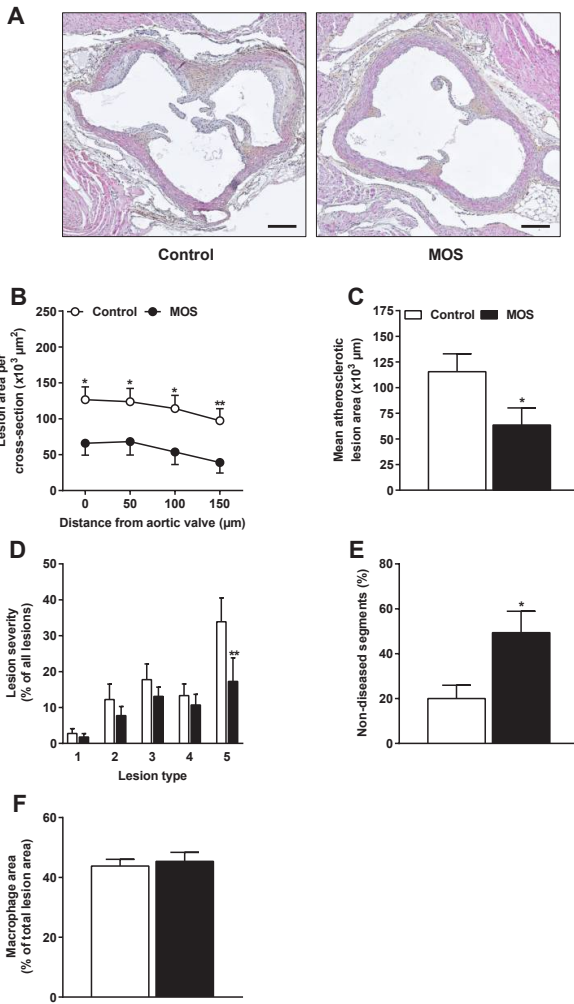
Figure 1. MOS decreased atherosclerosis development. Mice were fed a WTD with or without MOS for 14 weeks. A) Representative cross sections of the valve area of the aortic root stained with HPS are shown. Scale bar, 200 µm. B) Atherosclerotic lesion area was determined as a function of distance (50 µm intervals) starting from the appearance of open aortic valve leaflets covering 150 µm. C) The mean atherosclerotic lesion area was determined from the four consecutive cross sections, D) lesions were categorised according to lesion severity (type 1–5), E) the percentage of non-diseased segments were scored, and F) macrophage area within the atherosclerotic lesions were quantified. Open bars/circles represent the control group and closed bars/circles represent the MOS group. Values are presented as means ± SEM (n = 14–15 mice per group). * $p<0.05$, ** $p<0.01$ versus control.

MOS DID NOT AFFECT MARKERS OF SYSTEMIC INFLAMMATION

We subsequently assessed whether the attenuation of atherosclerosis development and lesion severity after MOS supplementation was related to specific markers of systemic inflammation, such as the percentages of circulating monocytes (Figure 2A) and IL-1RA (Figure 2B) [31]. Circulating monocytes and monocyte subsets (Ly6C$^+$, Ly6C^{low}, and Ly6C$^-$) were not affected by MOS (Figure 2A). Finally, MOS did not alter spleen and thymus weight (Figure 2C). These results indicate that the MOS did not affect specific markers of systemic inflammation after 14 weeks of dietary intervention.
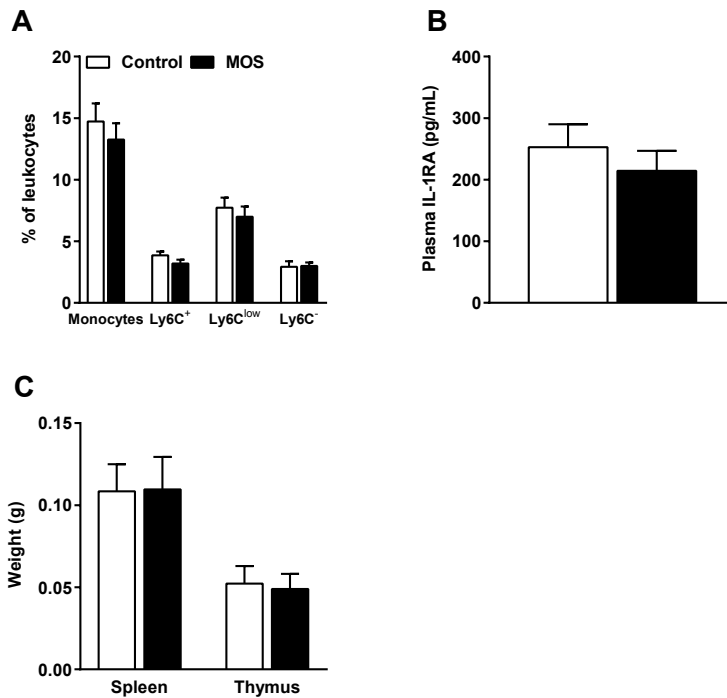
Figure 2. MOS did not affect markers of systemic inflammation. A) Circulating monocytes, Ly6C$^+$, Ly6C^{low}, and Ly6C$^-$ monocyte subsets as a percentage of circulating leukocytes, B) plasma IL-1RA levels, and C) spleen and thymus weight were measured in mice fed a WTD with or without MOS for 14 weeks. Open bars/circles represent the control group and closed bars/circles represent the MOS group. Values are presented as means ± SEM (n = 14–15 mice per group). P<0.05 was considered as statistically significant.

MOS INHIBITED THE GRADUAL INCREASE IN PLASMA TOTAL CHOLESTEROL LEVELS WITHOUT AFFECTING PLASMA TRIGLYCERIDES

As MOS is known to beneficially affect hyperlipidemia, we determined the effect of MOS on plasma lipid levels. From week 4 onward, MOS significantly inhibited the gradual increase in plasma TC levels compared to the control group (Figure 3A) without affecting plasma TG levels (Figure 3B). In terms of cholesterol exposure, this reduction in TC after MOS supplementation was confined to a reduction in the non-HDL cholesterol fraction (-21%; p=0.008; Figure 3C). We performed regression analysis on TC exposure versus mean atherosclerotic lesion area. Comparison of the regression lines indicated that slopes (F_{slopes}=0.34; p=NS) and intercepts ($F_{intercepts}$=0.77; p=NS) were similar for MOS-supplemented mice and control mice (pooled data R^2=0.6; p<0.0001; Figure 3D). This implies that the reduction in atherosclerotic lesion area after MOS supplementation was due to the cholesterol-lowering effect of MOS.

THE CHOLESTEROL-LOWERING EFFECT OF MOS WAS NOT DUE TO DIFFERENCES IN CHOLESTEROL INTAKE, FECAL CHOLESTEROL EXCRETION, OR LIVER CHOLESTEROL LEVELS

Considering that plasma cholesterol levels might be affected by alterations in dietary cholesterol intake or fecal excretion, we assessed whether MOS affected these parameters. MOS did neither affect body weight (Figure 4A) nor food intake (Figure 4B), indicating that both groups ingested similar amounts of food and cholesterol via the diet. Furthermore, the fecal concentration of cholesterol was not different after MOS supplementation (Figure 4C), which demonstrates that fecal cholesterol excretion was comparable between the groups. Additionally, liver weight (Figure 4D) and liver TC (Figure 4E) were similar between the groups. Together, these data illustrate that the plasma cholesterol-lowering effect of MOS was not due to reduced cholesterol intake, liver TC, or increased fecal cholesterol excretion.
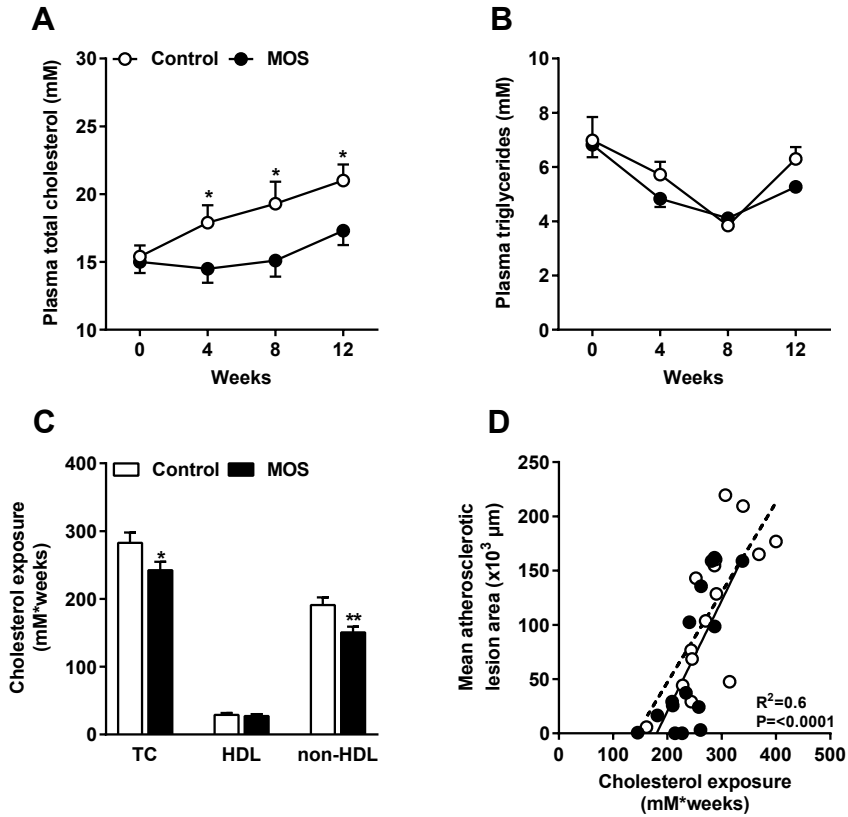
Figure 3. MOS inhibited the gradual increase in plasma total cholesterol levels without affecting plasma triglycerides. Mice were fed a WTD with or without MOS for 14 weeks. A) Plasma TC and B) TG were analysed in 4 hour fasted mice at the indicated time points. C) Cumulative TC, HDL, and non-HDL cholesterol exposure were calculated and TC exposure was plotted against mean atherosclerotic lesion area. D) The dotted line represents the regression line of the control mice and the straight line represents the regression line of the MOS-supplemented mice. Open bars/circles represent the control group and closed bars/circles represent the MOS group. Values are presented as means ± SEM (n = 14–15 mice per group). * $p<0.05$, ** $p<0.01$ versus control.
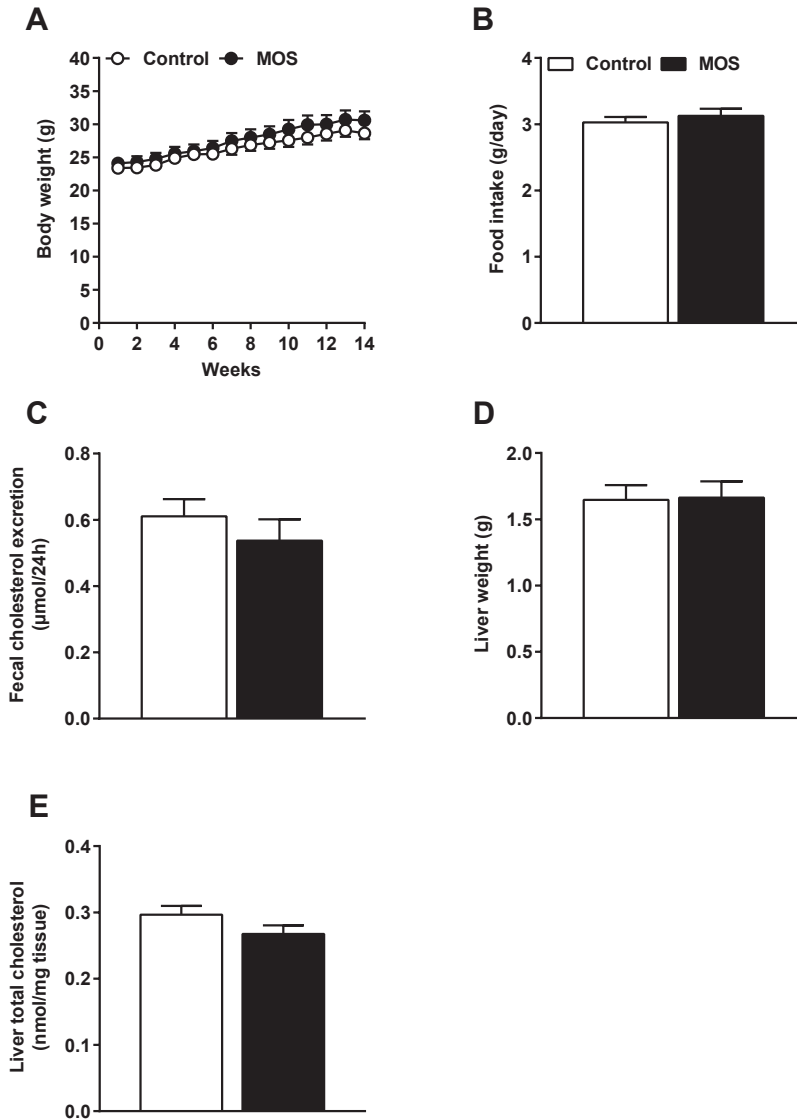
Figure 4. The cholesterol-lowering effect of MOS was not due to differences in cholesterol intake, fecal cholesterol excretion, or liver cholesterol levels. A) Body weight, B) food intake, C) fecal cholesterol excretion, D) liver weight, and E) liver TC were determined in mice fed a WTD with or without MOS for 14 weeks. Open bars/circles represent the control group and closed bars/circles represent the MOS group. Values are presented as means ± SEM (n = 15 mice per group). P<0.05 was considered as statistically significant.

MOS INCREASED THE ABUNDANCE OF CECAL BACTEROIDES OVATUS AND BUTYRATE

MOS is thought to act in the gut via interactions with the gut microbiota. To decipher the effects of MOS on gut microbiota, we first determined the effect of MOS supplementation on gut microbiota composition and the relative abundance of specific microbial taxa by 16S rRNA gene sequencing. Clustering analysis of 16S rRNA gene sequences by unweighted UniFrac distances revealed no clustering based on intervention (Figure 5A), which indicated that the β-diversity did not change after MOS supplementation. However, analysis of the gut microbiota at various taxonomic levels demonstrated that MOS altered the bacterial composition at phylum level, that is, MOS increased the abundance of *Bacteroidetes* (fold-change=1.5; p=0.006; Figure 5B; Table 1) and decreased the abundance of *Firmicutes* (fold-change=−1.1; p=0.03)(Figure 5B; Table 1). At lower taxonomic levels, differences in microbial community between the control mice and the MOS-supplemented mice became more apparent, although significant effects were mainly found on unidentified species (Table 1). One specific identified bacterium in the phylum of *Bacteroidetes* which significantly increased with 95% after MOS supplementation, was *B. Ovatus* (fold-change=29.2; p=0.0001; Figure 5C; Table 1). Therefore, the increase in the abundance of the phylum *Bacteroidetes* was mainly explained by an increase in *B. Ovatus*. The decreased abundance of the phylum *Firmicutes* was mostly explained by a decrease in the order of *Clostridiales* (fold-change=−1.2; p=0.04; Table 1), the family *Lachnospiraceae* (fold-change=−1.4; p=0.03; Table 1), and unidentified taxonomic species in the genera of *Ruminococcus* (fold-change=−2.3; p=0.006; Table 1).

We further assessed bacterial function by analysing SCFAs in cecal content of these mice. MOS elevated cecal concentrations of the SCFA butyrate (+31%; p=0.01; Figure 5C). Collectively, these data revealed that MOS altered the abundance of specific microbial taxa and modulated microbial function by increasing cecal butyrate.

7
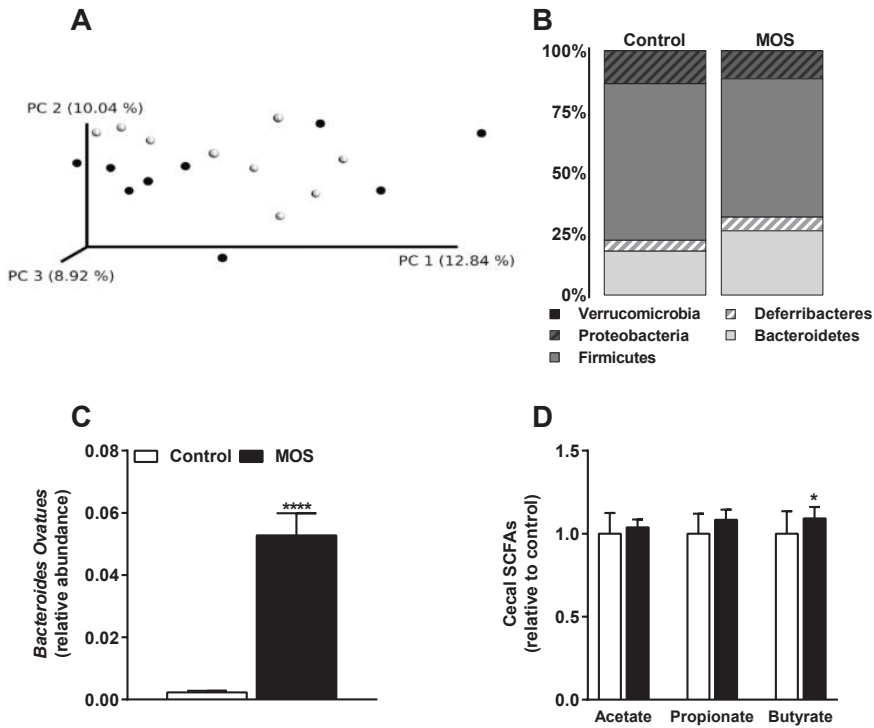
Figure 5. MOS increased the abundance of cecal *Bacteroides Ovatus* and butyrate.
A) Principal coordinates analysis plot of unweighted UniFrac distances of 16S rRNA gene sequences in which each circle represents an individual mouse. B) Microbiota composition at phylum level in cecal samples, C) relative abundance of *B. Ovatus,* and D) the cecal SCFAs acetate, propionate, and butyrate of mice fed a WTD with or without MOS for 14 weeks. Open bars/circles represent the control group and closed bars/circles represent the MOS group. Values are presented as means ± SEM (n = 15 mice per group). * $p<0.05$, ** $p<0.01$, *** $p<0.001$, **** $p<0.0001$ versus control.

Table 1. Relative abundance of cecal microbiota

Phylum	Class	Order	Family	Genus	Species	Control (%)	MOS (%)	Fold change	P-value [a]
Bacteroidetes						17.98	26.31	1.5	0.006
	Bacteroidia					17.98	26.31	1.5	0.006
		Bacteroidales				2.96	5.72	1.9	0.02
			Unidentified			1.63	5.50	3.4	0.0002
				Unidentified		1.83	5.50	3.0	0.0002
					Unidentified	1.83	5.50	3.0	0
			Bacteroidaceae			6.77	10.83	1.6	0.04
				Bacteroides		7.61	10.83	1.4	0.04
					Unidentified	7.38	5.55	-1.3	0.15
					Ovatus	0.23	5.28	22.9	0.0001
			Porphyromonadaceae			0.84	1.54	1.8	0.19
				Parabacteroides		0.95	1.54	1.6	0.19
					Unidentified	0.95	1.54	1.6	0.19
			Rikenellaceae			2.26	5.18	2.3	0.01
				Unidentified		2.54	5.18	2.0	0.01
					Unidentified	2.54	5.18	2.0	0.01
			S24-7			3.13	2.40	-1.3	0.16
				Unidentified		3.52	2.40	-1.5	0.16
					Unidentified	3.52	2.40	-1.5	0.16
			Paraprevotellaceae			1.36	0.86	-1.6	0.62
				Prevotella		1.53	0.86	-1.8	0.62
					Unidentified	1.53	0.86	-1.8	0.62
Deferribacteres						4.44	5.64	1.3	0.39
	Deferribacteres					4.44	5.64	1.3	0.39
		Deferribacterales				4.44	5.64	1.3	0.39
			Deferribacteraceae			3.94	5.64	1.4	0.39
				Mucispirillum		4.44	5.64	1.3	0.39
					Schaedleri	4.44	5.64	1.3	0.39
Firmicutes						64.18	56.64	-1.1	0.03
	Bacilli					0.76	0.38	-2.0	0.16
		Lactobacillales				0.76	0.38	-2.0	0.16
			Lactobacillaceae			0.67	0.38	-1.8	0.16
				Lactobacillus		0.76	0.38	-2.0	0.16
					Unidentified	0.76	0.38	-2.0	0.16

(Continued)

Table 1. *Continued*

Phylum	Class	Order	Family	Genus	Species	Control (%)	MOS (%)	Fold change	P-value [a)]
Firmicutess									
	Clostridia					50.06	43.40	-1.2	0.04
		Clostridiales				50.06	43.40	-1.2	0.04
			Unidentified			31.05	31.46	1.0	0.12
				Unidentified		34.93	31.46	-1.1	0.12
					Unidentified	34.93	31.46	-1.1	0.12
			Lachnospiraceae			4.55	3.16	-1.4	0.03
				Dorea		1.23	0.67	-1.8	0.25
					Unidentified	1.23	0.67	-1.8	0.25
				Ruminococcus		3.89	2.49	-1.6	0.11
					Gnavus	3.89	2.49	-1.6	0.11
			Peptostreptococcaceae			1.04	1.16	1.1	>.999
				Unidentified		1.16	1.16	1.0	>.999
					Unidentified	1.16	1.16	1.0	>.999
			Ruminococcaceae			7.85	7.62	1.0	0.35
				Oscillospira		7.20	6.92	1.0	0.81
					Unidentified	7.20	6.92	1.0	0.81
				Ruminococcus		1.64	0.70	-2.3	0.006
					Unidentified	1.64	0.70	-2.3	0.006
	Erysipelotrichi					13.36	12.86	1.0	0.90
		Erysipelotrichales				13.36	12.86	1.0	0.90
			Erysipelotrichaceae			11.88	12.86	1.1	0.90
				Unidentified		0.71	1.46	2.1	0.23
					Unidentified	0.71	1.46	2.1	0.23
				Allobaculum		12.66	11.40	-1.1	0.74
					Unidentified	12.66	11.40	-1.1	0.74
Proteobacteria						13.37	11.37	-1.2	0.47
	Deltaproteobacteria					13.37	11.37	-1.2	0.47
		Desulfovibrionales				13.37	11.37	-1.2	0.47
			Desulfovibrionaceae			11.89	11.37	1.0	0.47
				Bilophila		7.61	7.92	1.0	0.86
					Unidentified	7.61	7.92	1.0	0.86
				Desulfovibrio		5.76	3.45	-1.7	0.30
					C21_c20	5.76	3.45	-1.7	0.30

(Continued)

Table 1. *Continued*

Phylum	Class	Order	Family	Genus	Species	Control (%)	MOS (%)	Fold change	P-value [a]
Verrucomicrobia						0.03	0.04	1.4	0.54
	Verrucomicrobiae					0.03	0.04	1.4	0.54
		Verrucomicrobiales				0.03	0.04	1.4	0.54
			Verrucomicrobiaceae			0.03	0.04	1.5	0.54
				Akkermansia		0.03	0.04	1.4	0.54
					Muciniphila	0.03	0.04	1.4	0.54

P<0.05 was considered as statistically significant; MOS vs Control

[a] Significance according to Mann-Whitney *U* test

MOS INCREASED FECAL BILE ACID EXCRETION

Plasma cholesterol levels might be affected via changes in fecal BA excretion. Therefore, we determined whether MOS supplementation led to differences in fecal BA excretion. The concentration of the fecal primary BAs CA, α-MCA, and β-MCA were considerably increased after MOS supplementation (Figure 6A). For the secondary BAs, MOS increased the fecal excretion of DCA (Figure 6B). Despite increasing fecal BA excretion, MOS did not affect plasma BA concentrations (Figure 6C). We next performed mRNA analysis on *Cyp7a1* and *Cyp27a1*, the rate limiting enzymes in the major pathways for *de novo* BA synthesis. MOS did neither affect the expression of *Cyp7a1* nor *Cyp27a1* in the liver of these mice. Overall, we found that MOS increased the excretion of both primary and secondary BAs in feces without changing plasma BA levels and without affecting expression of *Cyp7a1* and *Cyp27a1*.

7
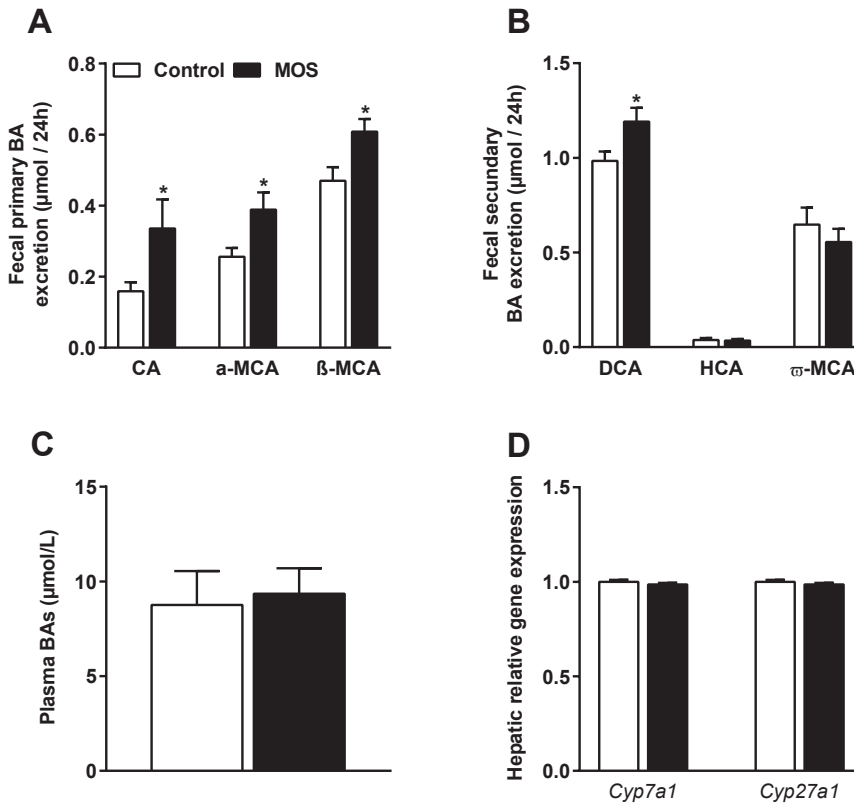
Figure 6. MOS increased fecal bile acid excretion. A) The fecal primary BAs cholic acid (CA), α-muricholic acid (α-MCA), β-muricholic acid (β-MCA), B) the fecal secondary hyocholic acid (HCA), deoxycholic acid (DCA), ω-muricholic acid (ω-MCA), C) plasma total BAs, and D) mRNA expression analysis of 7-α-hydroxylase (*Cyp7a1*) and sterol 27-hydroxylase (*Cyp27a1*) were determined in mice fed a WTD with or without MOS for 14 weeks. Open bars/circles represent the control group and closed bars/circles represent the MOS group. Values are presented as means ± SEM (n = 8–15 mice per group). * P<0.05 versus control.

DISCUSSION

Previous studies indicated that MOS decrease inflammation and plasma lipid levels [12–16]. Here, we tested the hypothesis that MOS reduces atherosclerosis development via these pathways. We found that *S. cerevisiae*-derived MOS indeed decreased the progression and severity of atherosclerosis in *E3L.CETP* mice. MOS reduced plasma cholesterol levels without affecting specific markers of systemic inflammation. Therefore, the decrease in atherosclerosis development after MOS supplementation can be explained by the cholesterol-lowering effect of MOS.

MOS supplementation resulted in a reduction in plasma non-HDL exposure by 21% and a decrease in total atherosclerotic lesion area in the aortic root by 54%. Similar reductions in plasma cholesterol and atherosclerotic lesion area have been achieved in *E3L.CETP* mice by statin treatment. For instance, low-dose atorvastatin treatment led to a reduction in plasma cholesterol levels of 19% in *E3L.CETP* mice, accompanied by a reduction of $\approx$50% in the total atherosclerotic lesion area in the aortic root [32]. In another study in *E3L.CETP* mice, rosuvastatin decreased plasma cholesterol by 25% and the total atherosclerotic lesion area by 62% [33]. In this paper, rosuvastatin reduced atherosclerosis beyond and independent of the reduction achieved by cholesterol lowering alone, which may be at least partly explained by its anti-inflammatory activity [34]. Interestingly, the magnitude of the decrease in plasma cholesterol level and atherosclerotic lesion area by statins and MOS are similar indicating that MOS may also have pleiotropic effects beyond cholesterol lowering in the reduction of atherosclerosis.

We found that MOS specifically reduced the type 5 atherosclerotic lesions. In humans, these lesions are characterised as advanced and vulnerable lesions, which are susceptible to plaque rupture and to develop other cardiovascular complications such as coronary heart disease or ischemic stroke [35,36]. In addition, MOS-supplemented mice displayed 29% more non-diseased segments compared to the control group, indicating that MOS decreased *de novo* lesion formation in the aortic arch. Given the strong effects of MOS on both plasma TC and atherosclerosis development, comparable to the effects of statins in *E3L.CETP* mice, dietary

7

MOS might present a novel approach in the prevention of atherosclerosis development and progression. It would be interesting to investigate whether MOS exerts its lipid-lowering effect when supplemented on top of statins.

MOS did not affect specific markers of systemic inflammation associated with atherosclerosis [31], despite having anti-inflammatory properties in previous studies [11–13]. However, we cannot exclude the possibility that MOS might have modulated other systemic immune markers or that it has affected the immune status more subtly or locally, for example within the atherosclerotic plaque.

Spring *et al.* have proposed that MOS binds type-1 fimbriae on pathogenic bacteria, preventing them from adhering to the intestinal mucosa and inducing an inflammatory trigger [17]. In the majority of previous studies, anti-inflammatory effects of MOS were observed after the application of pathogenic or pro-inflammatory stimuli, such as *E. Coli*, *Salmonella*, or LPS [11–13]. However, mice bred in our facility were kept under SPF conditions and therefore were not challenged with pathogenic stimuli. Whether a strong pathogenic stimulus is required to detect anti-inflammatory effects of MOS, remains to be further investigated.

Previous studies have shown that dietary MOS alters the gut microbiota, although these studies were mainly conducted in other species such as chickens [37,38], juvenile rainbow trout [39], or turkeys [40]. In the present study conducted in mice, MOS also interacted with the gut microbiota as shown by an increase in butyrate levels in cecum as well as an increased abundance of the phylum *Bacteroidetes* and a decrease in the phylum *Firmicutes*. However, since the β-diversity did not change, this suggests that MOS did not alter the microbial composition on a large scale. Notably, MOS induced the abundance of one specific identified species, *B. Ovatus*. This bacterium is a well-known mannan fermenter [41–43]. Therefore, we suggest that MOS served as a substrate for *B. Ovatus* to grow out. Interestingly, *B. Ovatus* also expresses bile salt hydrolases (BSH)[44,45] and accordingly is able to deconjugate primary BAs into secondary BAs. Compared to primary BAs, secondary BAs are less efficiently reabsorbed in the intestine and are relatively more excreted via the feces [18–20]. Indeed, MOS increased the fecal output of secondary BAs, likely via increasing the abundance of *B. Ovatus*.

Regulation of plasma TC levels and BA metabolism are tightly linked as cholesterol from plasma serves as substrate for *de novo* BA synthesis in the liver [46,47]. Increased fecal excretion of BAs thus requires increased production of BAs. *De novo* synthesis of BA in mice and humans predominantly involves the enzymes *Cyp7a1* and *Cyp27a1*. Since we did not observe differences in the expression of *Cyp7a1* and *Cyp27a1*, it seems likely that the increased activity of both genes was due to post-transcriptional regulation, alternative pathways involved in BA synthesis, or that other pathways in the enterohepatic circulation of BAs were affected.

In addition to increased secondary BA excretion, we also observed an increase in primary BA excretion after MOS supplementation. It is possible that MOS directly interacted with host cells involved in enterohepatic signalling, indirectly affecting recirculation of cholesterol or BAs, or that MOS acted as a BA sequestrant leading to reduced reabsorption of BAs. However, this seems unlikely since BA sequestrants usually result in increased plasma TG levels [48], which we did not observe in our study.

In literature, there are indications that the SCFA butyrate is associated with plasma cholesterol levels. In a previous study performed in mice, cecal infusion of butyrate increased hepatic cholesterol synthesis, suggesting that butyrate might elevate plasma cholesterol [49]. However, in another study performed in rats, hepatic cholesterol synthesis was reduced after ingestion of butyrate, albeit butyrate was given in combination with other SCFAs [50]. It remains to be determined whether increased cecal butyrate levels are involved in the cholesterol-lowering effect of MOS.

In conclusion, MOS decreased the progression of atherosclerosis up to 54% in *E3L.CETP* mice, which was largely explained by a reduction in plasma non-HDL cholesterol. The cholesterol-lowering effect of MOS was accompanied and likely explained by modulation of the gut microbiota, increased cecal butyrate levels, and increased fecal BA excretion.

7

ACKNOWLEDGEMENTS

REFERENCES

1.   WHO *WHO | The top 10 causes of death.*; World Health Organization, **2017**;

2.   Hansson, G. K.; Libby, P. The immune response in atherosclerosis: a double-edged sword. *Nat. Rev. Immunol.* **2006**, *6*, 508–519, doi:10.1038/nri1882.

3.   Hansson, G. K. Inflammation, atherosclerosis, and coronary artery disease. *N. Engl. J. Med.* **2005**, *352*, 1685–95, doi:10.1056/NEJMra043430.

4.   Libby, P. Inflammation in atherosclerosis. *Nature* **2002**, *420*, 868–74, doi:10.1038/nature01323.

5.   Epstein, F. H.; Ross, R. Atherosclerosis — An Inflammatory Disease. *N. Engl. J. Med.* **1999**, *340*, 115–126, doi:10.1056/NEJM199901143400207.

6.   Singh, R. B.; Mengi, S. A.; Xu, Y. J.; Arneja, A. S.; Dhalla, N. S. Pathogenesis of atherosclerosis: A multifactorial process. *Exp. Clin. Cardiol.* **2002**, *7*, 40–53.

7.   Abbott, D. W.; Martens, E. C.; Gilbert, H. J.; Cuskin, F.; Lowe, E. C. Coevolution of yeast mannan digestion: Convergence of the civilized human diet, distal gut microbiome, and host immunity. *Gut Microbes* **2015**, *6*, 334–339, doi:10.1080/19490976.2015.1091913.

8.   Torrecillas, S.; Montero, D.; Izquierdo, M. Improved health and growth of fish fed mannan oligosaccharides: potential mode of action. *Fish Shellfish Immunol.* **2014**, *36*, 525–44, doi:10.1016/j.fsi.2013.12.029.

9.   Berge, A. C.; Wierup, M. Nutritional strategies to combat Salmonella in mono-gastric food animal production. *animal* **2012**, *6*, 557–564, doi:10.1017/S1751731111002217.

10. Munyaka, P. M.; Echeverry, H.; Yitbarek, A.; Camelo-Jaimes, G.; Sharif, S.; Guenter, W.; House, J. D.; Rodriguez-Lecompte, J. C. Local and systemic innate immunity in broiler chickens supplemented with yeast-derived carbohydrates. *Poult. Sci.* **2012**, *91*, 2164–72, doi:10.3382/ps.2012-02306.

11. Wang, W.; Li, Z.; Han, Q.; Guo, Y.; Zhang, B.; D'inca, R. Dietary live yeast and mannan-oligosaccharide supplementation attenuate intestinal inflammation and barrier dysfunction induced by Escherichia coli in broilers. *Br. J. Nutr.* **2016**, *116*, 1878–1888,

7

doi:10.1017/S0007114516004116.

12. Che, T. M.; Johnson, R. W.; Kelley, K. W.; Van Alstine, W. G.; Dawson, K. A.; Moran, C. A.; Pettigrew, J. E. Mannan oligosaccharide modulates gene expression profile in pigs experimentally infected with porcine reproductive and respiratory syndrome virus. *J. Anim. Sci.* **2011**, *89*, 3016–29, doi:10.2527/jas.2010-3366.

13. Che, T. M.; Johnson, R. W.; Kelley, K. W.; Dawson, K. A.; Moran, C. A.; Pettigrew, J. E. Effects of mannan oligosaccharide on cytokine secretions by porcine alveolar macrophages and serum cytokine concentrations in nursery pigs. *J. Anim. Sci.* **2012**, *90*, 657–668, doi:10.2527/jas.2011-4310.

14. Yalcinkaya, I.; Guengoer, T.; Basalan, M.; Erdem, E. Mannan oligosaccharides (MOS) from Saccharomyces cerevisiae in broilers: Effects on performance and blood biochemistry. *TURKISH J. Vet. Anim. Sci.* **2008**, *32*, 43–48.

15. Sohail, M. U.; Ijaz, A.; Yousaf, M. S.; Ashraf, K.; Zaneb, H.; Aleem, M.; Rehman, H. Alleviation of cyclic heat stress in broilers by dietary supplementation of mannan-oligosaccharide and Lactobacillus-based probiotic: Dynamics of cortisol, thyroid hormones, cholesterol, C-reactive protein, and humoral immunity. *Poult. Sci.* **2010**, *89*, 1934–1938, doi:10.3382/ps.2010-00751.

16. M. Kannan, R. Karunakaran, V. Balakrishnan, T. G. P. Influence of Prebiotics Supplementation on Lipid Profile of Broilers. *Int. J. Poult. Sci.* **2005**, *4*, 994–997.

17. Spring, P.; Wenk, C.; Dawson, K. A.; Newman, K. E. The effects of dietary mannanoligosaccharides on cecal parameters and the concentrations of enteric bacteria in the ceca of Salmonella-challenged broiler chicks. *Poult. Sci.* **2000**, *79*, 205–211, doi:10.1093/ps/79.2.205.

18. Sayin, S. I.; Wahlström, A.; Felin, J.; Jäntti, S.; Marschall, H.-U.; Bamberg, K.; Angelin, B.; Hyötyläinen, T.; Orešič, M.; Bäckhed, F. Gut Microbiota Regulates Bile Acid Metabolism by Reducing the Levels of Tauro-beta-muricholic Acid, a Naturally Occurring FXR Antagonist. *Cell Metab.* **2013**, *17*, 225–235, doi:10.1016/j.cmet.2013.01.003.

19. St-Onge, M. P.; Farnworth, E. R.; Jones, P. J. H. Consumption of fermented and

nonfermented dairy products: Effects on cholesterol concentrations and metabolism. *Am. J. Clin. Nutr.* **2000**, *71*, 674–681.

20. Wahlström, A.; Sayin, S. I.; Marschall, H. U.; Bäckhed, F. Intestinal Crosstalk between Bile Acids and Microbiota and Its Impact on Host Metabolism. *Cell Metab.* **2016**, *24*, 41–50, doi:10.1016/j.cmet.2016.05.005.

21. Dietschy, J. M.; Turley, S. D.; Spady, D. K. Role of liver in the maintenance of cholesterol and low density lipoprotein homeostasis in different animal species, including humans. *J. Lipid Res.* **1993**, *34*, 1637–1659.

22. Out, C.; Groen, A. K.; Brufau, G. Bile acid sequestrants: more than simple resins. *Curr. Opin. Lipidol.* **2012**, *23*, 43–55, doi:10.1097/MOL.0b013e32834f0ef3.

23. Westerterp, M.; van der Hoogt, C. C.; de Haan, W.; Offerman, E. H.; Dallinga-Thie, G. M.; Jukema, J. W.; Havekes, L. M.; Rensen, P. C. N. Cholesteryl ester transfer protein decreases high-density lipoprotein and severely aggravates atherosclerosis in APOE*3-Leiden mice. *Arterioscler. Thromb. Vasc. Biol.* **2006**, *26*, 2552–9, doi:10.1161/01.ATV.0000243925.65265.3c.

24. de Haan, W.; van der Hoogt, C. C.; Westerterp, M.; Hoekstra, M.; Dallinga-Thie, G. M.; Princen, H. M. G.; Romijn, J. A.; Jukema, J. W.; Havekes, L. M.; Rensen, P. C. N. Atorvastatin increases HDL cholesterol by reducing CETP expression in cholesterol-fed APOE*3-Leiden.CETP mice. *Atherosclerosis* **2008**, *197*, 57–63, doi:10.1016/j.atherosclerosis.2007.08.001.

25. Wong, M. C.; van Diepen, J. A.; Hu, L.; Guigas, B.; de Boer, H. C.; van Puijvelde, G. H.; Kuiper, J.; van Zonneveld, A. J.; Shoelson, S. E.; Voshol, P. J.; Romijn, J. A.; Havekes, L. M.; Tamsma, J. T.; Rensen, P. C. N.; Hiemstra, P. S.; Berbée, J. F. P. Hepatocyte-specific IKKβ expression aggravates atherosclerosis development in APOE*3-Leiden mice. *Atherosclerosis* **2012**, *220*, 362–368, doi:10.1016/j.atherosclerosis.2011.06.055.

26. Bligh, E.; Dyer, W. a Rapid Method of Total Lipid Extraction and Purification. *Can. J. Biochem. Physiol.* **1959**, *37*, 911–917, doi:10.1139/o59-099.

27. Gevers, D.; Kugathasan, S.; Denson, L. A.; Vázquez-Baeza, Y.; Van Treuren, W.; Ren,

7

B.; Schwager, E.; Knights, D.; Song, S. J.; Yassour, M.; Morgan, X. C.; Kostic, A. D.; Luo, C.; González, A.; McDonald, D.; Haberman, Y.; Walters, T.; Baker, S.; Rosh, J.; Stephens, M.; Heyman, M.; Markowitz, J.; Baldassano, R.; Griffiths, A.; Sylvester, F.; Mack, D.; Kim, S.; Crandall, W.; Hyams, J.; Huttenhower, C.; Knight, R.; Xavier, R. J. The Treatment-Naive Microbiome in New-Onset Crohn's Disease. *Cell Host Microbe* **2014**, *15*, 382–392, doi:10.1016/j.chom.2014.02.005.

28.	Caporaso, J. G.; Kuczynski, J.; Stombaugh, J.; Bittinger, K.; Bushman, F. D.; Costello, E. K.; Fierer, N.; Peña, A. G.; Goodrich, J. K.; Gordon, J. I.; Huttley, G. A.; Kelley, S. T.; Knights, D.; Koenig, J. E.; Ley, R. E.; Lozupone, C. A.; McDonald, D.; Muegge, B. D.; Pirrung, M.; Reeder, J.; Sevinsky, J. R.; Turnbaugh, P. J.; Walters, W. A.; Widmann, J.; Yatsunenko, T.; Zaneveld, J.; Knight, R. QIIME allows analysis of high-throughput community sequencing data. *Nat. Methods* **2010**, *7*, 335–6, doi:10.1038/nmeth.f.303.

29.	Tomcik, K.; Ibarra, R. A.; Sadhukhan, S.; Han, Y.; Tochtrop, G. P.; Zhang, G. F. Isotopomer enrichment assay for very short chain fatty acids and its metabolic applications. *Anal. Biochem.* **2011**, *410*, 110–117, doi:10.1016/j.ab.2010.11.030.

30.	van Meer, H.; Boehm, G.; Stellaard, F.; Vriesema, A.; Knol, J.; Havinga, R.; Sauer, P. J.; Verkade, H. J. Prebiotic oligosaccharides and the enterohepatic circulation of bile salts in rats. *Am. J. Physiol. Gastrointest. Liver Physiol.* **2008**, *294*, G540-7, doi:10.1152/ajpgi.00396.2007.

31.	Merhi-Soussi, F.; Kwak, B. R.; Magne, D.; Chadjichristos, C.; Berti, M.; Pelli, G.; James, R. W.; MacH, F.; Gabay, C. Interleukin-1 plays a major role in vascular inflammation and atherosclerosis in male apolipoprotein E-knockout mice. *Cardiovasc. Res.* **2005**, *66*, 583–593, doi:10.1016/j.cardiores.2005.01.008.

32.	Verschuren, L.; Kleemann, R.; Offerman, E. H.; Szalai, A. J.; Emeis, S. J.; Princen, H. M. G.; Kooistra, T. Effect of low dose atorvastatin versus diet-induced cholesterol lowering on atherosclerotic lesion progression and inflammation in apolipoprotein E*3-Leiden transgenic mice. *Arterioscler. Thromb. Vasc. Biol.* **2005**, *25*, 161–167, doi:10.1161/01.ATV.0000148866.29829.19.

33.   Kleemann, R.; Princen, H. M. G.; Emeis, J. J.; Jukema, J. W.; Fontijn, R. D.; Horrevoets, A. J. G.; Kooistra, T.; Havekes, L. M. Rosuvastatin Reduces Atherosclerosis Development Beyond and Independent of Its Plasma Cholesterol – Lowering Effect in APOE * 3-Leiden Transgenic Mice. *Circulation* **2003**, *108*, 1368–1374, doi:10.1161/01. CIR.0000086460.55494.AF.

34.   Oesterle, A.; Laufs, U.; Liao, J. K. Pleiotropic Effects of Statins on the Cardiovascular System. *Circ. Res.* **2017**, *120*, 229–243, doi:10.1161/CIRCRESAHA.116.308537.

35.   Stary, H. C.; Chandler, A. B.; Dinsmore, R. E.; Fuster, V.; Glagov, S.; Insull, W.; Rosenfeld, M. E.; Schwartz, C. J.; Wagner, W. D.; Wissler, R. W. A Definition of Advanced Types of Atherosclerotic Lesions and a Histological Classification of Atherosclerosis. *Arterioscler. Thromb. Vasc. Biol.* **1995**, *15*.

36.   Bentzon, J. F.; Otsuka, F.; Virmani, R.; Falk, E. Mechanisms of Plaque Formation and Rupture. *Circ. Res.* **2014**, *114*.

37.   Pourabedin, M.; Xu, Z.; Baurhoo, B.; Chevaux, E.; Zhao, X. Effects of mannan oligosaccharide and virginiamycin on the cecal microbial community and intestinal morphology of chickens raised under suboptimal conditions. *Can. J. Microbiol.* **2014**, *60*, 255–66, doi:10.1139/cjm-2013-0899.

38.   Corrigan, A.; de Leeuw, M.; Penaud-Frézet, S.; Dimova, D.; Murphy, R. A. Phylogenetic and functional alterations in bacterial community compositions in broiler ceca as a result of mannan oligosaccharide supplementation. *Appl. Environ. Microbiol.* **2015**, *81*, 3460–70, doi:10.1128/AEM.04194-14.

39.   Gonçalves, A. T.; Gallardo-Escárate, C. Microbiome dynamic modulation through functional diets based on pre- and probiotics (mannan-oligosaccharides and *Saccharomyces cerevisiae*) in juvenile rainbow trout (*Oncorhynchus mykiss*). *J. Appl. Microbiol.* **2017**, *122*, 1333–1347, doi:10.1111/jam.13437.

40.   Corrigan, A.; Horgan, K.; Clipson, N.; Murphy, R. A. Effect of dietary prebiotic (mannan oligosaccharide) supplementation on the caecal bacterial community structure of turkeys. *Microb. Ecol.* **2012**, *64*, 826–36, doi:10.1007/s00248-012-0046-6.

7

41.   Gherardini, F. C.; Salyers, A. A. Purification and characterization of a cell-associated, soluble mannanase from Bacteroides ovatus. *J. Bacteriol.* **1987**, *169*, 2038–2043, doi:10.1128/JB.169.5.2038-2043.1987.

42.   Martens, E. C.; Lowe, E. C.; Chiang, H.; Pudlo, N. A.; Wu, M.; McNulty, N. P.; Abbott, D. W.; Henrissat, B.; Gilbert, H. J.; Bolam, D. N.; Gordon, J. I. Recognition and degradation of plant cell wall polysaccharides by two human gut symbionts. *PLoS Biol.* **2011**, *9*, e1001221, doi:10.1371/journal.pbio.1001221.

43.   Bågenholm, V.; Reddy, S. K.; Bouraoui, H.; Morrill, J.; Kulcinskaja, E.; Bahr, C. M.; Aurelius, O.; Rogers, T.; Xiao, Y.; Logan, D. T.; Martens, E. C.; Koropatkin, N. M.; Stålbrand, H. Galactomannan catabolism conferred by a polysaccharide utilisation locus of Bacteroides ovatus : enzyme synergy and crystal structure of a β-mannanase. *J. Biol. Chem.* **2016**, *292*, jbc.M116.746438, doi:10.1074/jbc.M116.746438.

44.   Masuda, N. Deconjugation of Bile Salts by Bacteroides and Clostridium. *Microbiol. Immunol.* **1981**, *25*, 1–11, doi:10.1111/j.1348-0421.1981.tb00001.x.

45.   SMITH, C. J.; ROCHA, E. R.; PASTER, B. J. The Medically Important Bacteroides spp. in Health and Disease. *Prokaryotes* **2006**, *7*, 381–427, doi:10.1007/0-387-30747-8_14.

46.   Li, T.; Chiang, J. Y. L. Bile acids as metabolic regulators. *Curr. Opin. Gastroenterol.* **2015**, *31*, 159–65, doi:10.1097/MOG.0000000000000156.

47.   Kuipers, F.; Bloks, V. W.; Groen, A. K. Beyond intestinal soap—bile acids in metabolic control. *Nat. Rev. Endocrinol.* **2014**, *10*, 488–498, doi:10.1038/nrendo.2014.60.

48.   Angelin, B.; Leijd, B.; Hultcrantz, R.; Einarsson, K. Increased turnover of very low density lipoprotein triglyceride during treatment with cholestyramine in familial hypercholesterolaemia. *J. Intern. Med.* **1990**, *227*, 201–6.

49.   den Besten, G.; Lange, K.; Havinga, R.; van Dijk, T. H.; Gerding, A.; van Eunen, K.; Müller, M.; Groen, A. K.; Hooiveld, G. J.; Bakker, B. M.; Reijngoud, D.-J. Gut-derived short-chain fatty acids are vividly assimilated into host carbohydrates and lipids. *Am. J. Physiol. Gastrointest. Liver Physiol.* **2013**, *305*, G900-10, doi:10.1152/ajpgi.00265.2013.

50.   Hara, H.; Haga, S.; Aoyama, Y.; Kiriyama, S. Short-chain fatty acids suppress cholesterol synthesis in rat liver and intestine. *J. Nutr.* **1999**, *129*, 942–8.

7

SUPPLEMENT

Table S1. Antibodies used for flow cytometry

Antibody	Fluorochrome	Dilution	Clone, supplier
CD45.2	FITC	1:100	104, BioLege
CD11b	Pacific Blue	1:150	M1/70, BioLegend
CD115-Biotin	n.a.	1:100	AFS98, eBioScience
Streptavidin	PeCy5	1:00	SAV, eBioScience
GR-1	PeCy7	1:1500	RB6-8C5
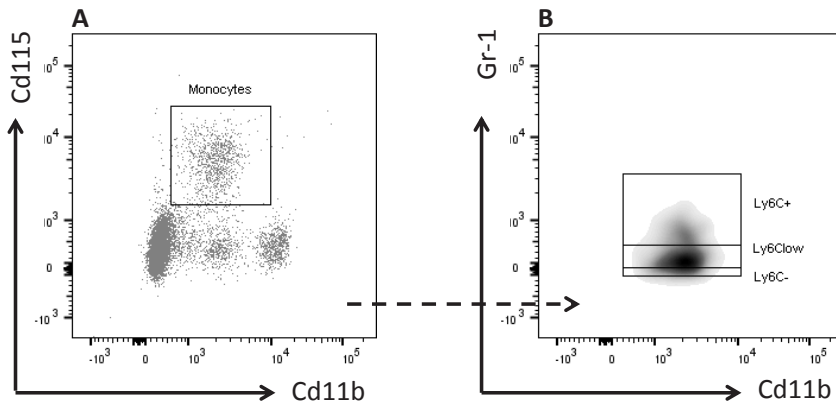
Figure S1. Gating strategy. Gating strategies for the analysis of total monocytes [A], Ly6C^{+}, Ly6C^{low}, and Ly6C^{-} monocyte subsets [B] in whole blood.
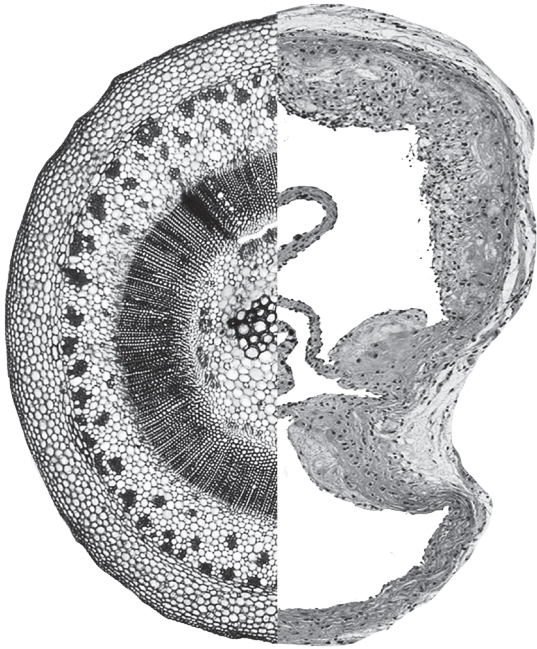
GENERAL
DISCUSSION

08

In this thesis, we aimed to understand the interplay between the indigestible carbohydrates inulin and mannan oligosaccharides (MOS), gut microbiota composition and function, and the development of cardiometabolic disease in mouse models. In this chapter, methods to map gut microbiota composition and function, factors that determine gut microbiota function, the role of the gut microbiota in the development of atherosclerosis, the translatability of mouse models in gut microbiota research, and implications for prebiotics will be discussed.

16S RIBOSOMAL RNA GENE V-REGION SEQUENCING OR WHOLE METAGENOME SHOTGUN SEQUENCING TO MAP GUT MICROBIOTA COMPOSITION?

The development of next generation sequencing has made it feasible to determine the bacterial composition at virtually any physical location, varying from ocean waters to human body surfaces and cavities. Currently, the 'golden standard' methods used to map gut microbiota composition are 16S rRNA gene amplicon sequencing and whole metagenome shotgun sequencing.

16S RIBOSOMAL RNA GENE SEQUENCING

The 16s rRNA gene is an approximately 1.5KBp gene that is unique to prokaryotes. The 16S rRNA gene is composed of highly conserved regions interspaced with nine variable regions named V1 to V9. A 16S rRNA V region can be amplified by PCR with primers that recognise the conserved flanking regions. The 16S rRNA variable regions are unique for specific genera [1], yielding clusters of similarity termed Operational Taxonomic Units (OTUs)[2,3]. A nearly complete 16S rRNA gene sequence is relatively easy to obtain for a novel bacterial isolate. This provides sufficient phylogenetic information to identify the isolate at least down to the genus level, thanks to the huge database of 16S rRNA gene sequence information that is publicly available and easily searchable [4]. 16S data lends itself to computational analytical techniques including diversity measures within (alpha) and between (beta) samples, which can be defined quantitatively (based on abundance) or qualitatively (based on presence/absence)[2]. Functional

8

annotation of microbiota communities after 16S sequencing is based on OTU assignment and linking this to databases with reference genomes. The presence of gene families in the microbiota communities are thus inferred based on the OTU assignment. Software tools for such "predictive metagenomics approaches" have been developed [5].

The fact that the 16S rRNA gene is unique to prokaryotes is an advantage in studying the host microbiome as this immediately eliminates host-derived and viral DNA contamination during the amplification and sequencing stage. In addition, important reasons to use 16S sequencing for the characterisation of gut microbiota composition, are its relatively low cost, fast turnaround time, and relative ease and availability of computational tools to analyse the data. A limitation of 16S rRNA sequencing is that a specific V-region often not uniquely identifies the species. Thus, taxonomic assignment will be of variable depth. Furthermore, additional functional analyses is not based on direct sequencing, but predicted based on the OTUs. Another disadvantage of 16S sequencing is the possibility that 16S rRNA genes are derived from horizontal gene transfer which may distort relationships between taxa in phylogenetic trees [6].

WHOLE METAGENOME SEQUENCING

Whole metagenome shotgun sequencing is based on full length DNA from the entire metagenome. Short read sequencing subsequently results in millions of short random DNA fragments that can then be assembled using reference genomes or used individually as markers for specific gut microbial organisms and their metabolic functions [2,7]. This results to the identification of microorganisms with augmented taxonomic resolution [8,9] as the entire genomes of organisms in the community become available for characterisation rather than the more limited single 16S rRNA gene.

While whole genome sequencing provides much more information, including genetically encoded functions of the gut microbiota, the extensive amount of sequence data obtained, however, also leads to a vast amount of challenges with regard to data processing, storage and analysis. For instance, the Illumina HiSeq 2500 platform can yield over 1 Tbp

of raw sequence data, which may even further increase during downstream processing and subsequent analysis. This also comes at much higher costs per sample since it may be necessary to sequence a metagenome with high coverage and thus less samples per run [3,10]. Whole genome sequencing also results in DNA sequences from other microorganisms such as viruses in a community. This may be an advantage or disadvantage based on the premise of the study. Nevertheless, these data need to be dealt with. However, it is expected that the high costs and the necessity of extensive advanced computational skills continue to decrease every year due to optimisation of short read next generation sequencing methods. Moreover, novel "long read" next generation sequencing techniques are in development that hold great promise for metagenomics analysis (reviewed in [11–13]).

The choice for 16S sequencing or whole metagenome sequencing approaches for microbiome analyses is usually dictated by the nature of the studies being conducted. Both of these sequencing methods have their advantages and disadvantages. In our experiments in **chapter 5** and **chapter 7**, we aimed to confirm that indigestible carbohydrates modulate gut microbiota composition. Our research questions required a method that provided enough detail to indicate major gut microbiota changes. We also aimed to perform the bioinformatics analyses in house at relatively low experimental costs. Therefore, in our studies 16S sequencing for the analysis of gut microbiota composition seemed sufficient. However, as shown in **chapter 5**, where 16S sequencing allowed us to identify specific genera that expressed properties that could explain some of our observations, whole genome sequencing will undoubtedly almost always provide additional detail and insight.

8

1H-NMR OR GC/LC-MS FOR THE IDENTIFICATION OF GUT MICROBIOTA FUNCTION?

DNA sequence analysis provides valuable information on the microbiota composition, from which the presence of potential gene families and biochemical pathways can be inferred. A more direct measure to determine the biochemical activities of the species that are present in the microbiota is analysis of the input metabolic substrates and output of bacterial metabolic products that are present in the feces and in the blood. Fecal/cecal metabolomics provides a complementary functional readout of microbial metabolism as well as its interaction with host and environmental factors [14]. The most commonly used methods for the large scale identification of metabolites (metabolomics) are either based on 1H-nuclear magnetic resonance (NMR) or on gas or liquid chromatography mass spectrometry (GC or LC-MS).

1H-NMR

1H-NMR is based on the principle that every proton behaves as a small magnet due to the fact that it has a spinning electrical charge. In a strong external magnetic field, these tiny magnets align and depending on their particular environment in the molecule require a certain amount of energy to be misaligned. This energy is transferred by a radio wave and can be measured. 1H-NMR can measure multiple metabolites in samples such as blood, serum/plasma, or cecal and fecal material [15]. NMR-based metabolite profiling is a well-established technique producing rapid, robust, and reproducible profiles without the need for extensive sample preparation. Identification of individual compounds is based on deconvolution of the measured spectra as well as 2D-NMR techniques. However, NMR is not an extremely sensitive method and the number of metabolites that can be detected in a given sample is around 70-80 depending on the matrix as well as the employed extraction techniques [16–18].

GC/LC-MS

GC/LC-MS analyses are based on molecular separation of a specific fraction of a sample by GC or LC followed by detection of the molecules employing MS. Sample preparation can be extensive depending on the type of compounds that is measured. Particularly absolute quantification using MS detection can be very cumbersome and usually involves spiking with stable isotope labelled internal standards. Although quantification can be cumbersome and is not as accurate as by 1H-NMR, vast numbers of metabolites (>1000) can be monitored and assessed by a single analysis. For targeted analysis of a specific class of compounds, such as fatty acids (FA) in blood and feces method choices usually depend on the expected concentrations and specific coverage of the available techniques.

The choice for either NMR or GC/LC-MS based analytical methods to measure metabolites associated with gut microbial activity and function is dependent upon the specific research question that needs to be addressed. For a rapid screen to determine whether overall activity differs between microbial communities, 1H-NMR based analyses likely suffices. However, when the question is whether a specific class of compounds is affected in blood, cecum, or feces, GC/LC-MS is likely the preferred method. In our research group, high fat/high cholesterol diets are used to induce obesity, insulin resistance and atherosclerosis. Therefore it is of particular interest to determine the spectrum of FA in the blood. Similarly, fermentation of the indigestible carbohydrates MOS and inulin by bacteria in the gut results in the production of short chain fatty acids (SCFA) in the large intestine. In order to have the ability to determine FA in blood, cecum, and feces with high specificity and sensitivity, we have setup a method using GC-MS for the characterisation of FA including SCFAs in blood, fecal and cecal samples (**chapter 2** and **chapter 3**).

8

SHORT-CHAIN FATTY ACIDS AS MARKERS FOR GUT MICROBIAL FUNCTION

Generally, and also in this thesis, the SCFAs acetate, propionate, and butyrate are measured as indication for gut microbiota function, since they are the main bacterial breakdown products of indigestible carbohydrates [19–21]. However, gut microbiota do more than the production of SCFAs. The gut microbiota contribute to the production and/or metabolism of a large spectrum of metabolites, including BAs, choline metabolites, vitamins, and lipids (reviewed in [20]), that differently may affect the gut microbiota itself, but also the host. Despite our global understanding of metabolite production by the gut microbiota that is used by the host, for many reasons, including the difficulty in culturing anaerobic bacteria, our knowledge of which bacterial species synthesise which metabolites is currently limited. Therefore, gut-bacteria-derived metabolites other than SCFAs need extensive research in the future in order to determine their relative contribution to health and disease. However, understanding the response of gut microbial communities to diet and other factors in order to predict gut microbiota function, presents a distinct set of challenges. Continued innovation in analysis tools to monitor microbial metabolic shifts and host interactions is needed, and especially to track these events under *in vivo* conditions. Although next-generation sequencing methods can provide an assembly of DNA sequences and insight into the competence of organisms to perform metabolic functions, these analysis' are not suitable for the provision of an overview on the functionality of particular gut bacteria under complex and dynamic environmental conditions. Metabolic profiling of biofluids (e.g. cecum content, plasma, or urine) that uses high-resolution spectroscopy offers additional information to some extent. In **chapter 5** and **chapter 7** we used both 16S rRNA gene sequencing and GC-MS metabolomics to identify the effect of inulin and MOS on gut microbiota composition and SCFA production. Although these two separate platforms provided useful compositional and functional information, the challenge for future research lies in optimising the computational capacity for co-analysis of these two (and other) analytical platforms in order to link gut microbiota composition to the produced metabolites.

WHAT DETERMINES GUT MICROBIOTA FUNCTION?

Microbial function is not only dependent on the individual separate microbial genera present in the microbiota but also on the interaction of the bacteria with each other, the host and the diet. Therefore, prebiotic feeding in one particular host or setting might lead to other results than when given to one another. Some important examples of the interaction of gut bacteria with their environment and how they determine microbial function will be discussed.

CROSS-FEEDING BETWEEN GUT BACTERIA

Co-culturing studies of different bacterial species have demonstrated that metabolites produced after fermentation of indigestible carbohydrates by one particular bacterium, may aid in the provision of substrates to support growth of other bacterial species, termed cross-feeding [22]. Cross-feeding can induce metabolic consequences that would not have been predicted simply by the substrate preferences of isolated bacteria [23]. For example, in a recent study only 8 of 55 bifidobacterial strains had the ability to degrade long-chain inulin. This leads to the suggestion that the observed blooming of *Bifidobacteria* by inulin *in vivo* is mainly due to cross-feeding of end-products released by other inulin-degrading gut bacteria [24]. Another example of cross-feeding was inferred from the increased production of butyrate by *Roseburia sp.* strain A2-183 when co-cultured with *B. adolescentis* L2-32. In plain culture medium, *Roseburia sp.* strain A2-183 is incapable of utilising lactate or to grow on fructo-oligosaccharides (FOS), while in co-culture with *B. adolescentis* L2-32 these bacteria are able to produce butyrate. Butyrate production observed in these *in vitro* co-culturing experiments is most likely due to cross-feeding on products released by partial hydrolysis of FOS from *B. Adolescnetis* [25]. In this thesis, we found increased abundance of *Allobaculum* and *Coprococcus* after feeding mice a high cholesterol diet supplemented with inulin (**chapter 5**). It remains possible that these genera did not thrive on inulin themselves but were increased in abundance due to cross-feeding.

8

SUBSTRATE COMPETITION BETWEEN GUT BACTERIA

Although we know little about the substrate preferences of the majority of the gut bacteria, it is not a surprise that prebiotics can affect non-target populations within the gut. For example, several studies have shown that inclusion of inulin as a dietary prebiotic increase proportions of *Bifidobacteria* in feces, while other studies also showed that inulin stimulate groups of bacteria other than *Bifidobacteria* in animal models [26,27]. Additionally, in *in vitro* gut simulations, two groups of *Clostridium*-related bacteria, and an added strain of *Roseburia inulinivorans*, were shown to be stimulated by inulin in a mixed fecal community [28]. We did not detect *Bifidobacteria* in mice that were fed with inulin in our studies (**chapter 5**), which makes it possible that the type of inulin in combination with cholesterol induced non-target populations within the gut.

BASELINE GUT MICROBIOTA COMPOSITION

Baseline gut microbiota composition may be another determinant for gut microbiota function. For instance, inulin is well-established to exert bifidogenic effects [29,30] and previous research illustrated that increased abundance of *Bifidobacteria* in the gut microbiota was associated with beneficial health parameters [31]. In **chapter 5,** we performed 16S rRNA gene sequencing analysis on cecal samples of the mice and we found that inulin had a profound effect on the microbiota composition [32]. However, we found that inulin mostly drove the growth of the genera *Allobaculum* and *Coprococcus*, while the growth of *Bifidobacteria* was not induced by inulin. In fact, quantification of the gut microbiota composition prior to inulin feeding revealed that *Bifidobacteria* could not be detected in ceca of these mice. It is therefore likely that we were not able to induce blooming of *Bifidobacteria* as they were not present in these mice. This proof-of-principle hypothesis is substantiated by a recent study in which blooming of another species, *Akkermansia Muciniphila*, depended on its initial baseline abundance [33], even though this study used probiotics and not prebiotics. It also remains possible that inulin in our hands differently affected bacterial substrate competition or induced cross-feeding leading to the outgrowth of other gut bacteria.

HOST-GUT-MICROBIOTA INTERACTIONS

Studies comparing the gut microbiome across inbred mouse lines have yielded evidence that host genetics can affect the gut microbiome. The relation between the composition of gut microbiota and the host genetic profile has been evidently demonstrated in murine models [34].

Maternal environment is one of the earliest factors that can have a profound effect on gut microbiota composition. Several studies have shown that genetically identical mice from the same mother and litter have a more comparable microbiome than mice from different litters, even though they may be housed in separate cages [34,35]. Furthermore, there is evidence that genetic polymorphisms help shape the gut microbiota [36]. This implicates that even minor differences in the genetic profile of mammals can play a tremendous role in shaping gut microbiota composition and therefore might affect gut microbiota function.

Another important driving force of shaping the microbiome is the immune system. The innate immune system plays an important part in shaping the community and environment of gut commensal microorganisms in order to be tolerated by the host and to be beneficial for metabolic activities [37]. For instance, gut microbiota dysbiosis has been reported in different mouse models of innate immune deficiency [38], such as in mice that lack the genes *Nod2* [39], *Nlrp6* [40], or *Tlr5* [41]. The other way around, in order for evolution of the mammalian immune system, a homeostatic relationships with the microbiota needs to be maintained (reviewed in [42]). The innate immune system might therefore promote the growth of beneficial gut bacteria and contribute to the preservation of a stable community of microorganisms while affecting their function.

8

DIET

Diet is one of the most important factors shaping gut microbial diversity. Gut bacteria do not only respond to indigestible carbohydrates that are ingested, but also to other dietary components such as lipids. Several independent studies revealed that one particular family of the *Firmicutes*, the *Erysipelotrichaceae*, alters in abundance in response to changes in the amount of dietary fat. For instance, after inducing obesity in mice by feeding them a 'Western-type' high fat diet

(HFD)(high in saturated and unsaturated fats), blooming occurred for specific members of the *Erysipelotrichaceae* family [43–45]. The relative abundance for these members declined when the HFD was changed again to the usual chow diet [43]. *Allobaculum* is a specific member of the *Erysipelotrichaceae* family. In **chapter 5** we fed *E3L.CETP* mice with a high cholesterol diet to induce hypercholesterolemia and we found an increase in the genus *Allobaculum* in inulin supplemented mice compared to controls. Apparently, *Allobaculum* does not only bloom on a HFD but also in the presence of hypercholesterolemic conditions. This is supported by evidence from a study of Martínez *et al.,* where they found that *Allobaculum* was mostly abundant in hypercholesterolemic hamsters [46]. It is therefore likely that the type and amount of dietary lipids are important mediators in shaping gut microbial composition, but also might play a role in gut microbiota function. For example, in **chapter 5** we fed *E3L.CETP* mice either a high cholesterol diet with 0.1% cholesterol or with 0.5% cholesterol supplemented without or with 10% inulin. The only difference between these two groups was the percentage of dietary cholesterol. In both studies, inulin did not beneficially affect hypercholesterolemia or atherosclerosis, but in the group that received 0.5% cholesterol, inulin led to early manifestations in liver inflammation which was not observed in the group that received 0.1% cholesterol with inulin. Therefore, it is important to keep in mind that diet is a major regulator in shaping the gut microbiota composition and unquestionably affect gut microbiota function.

METABOLIC ADAPTATION OF GUT BACTERIA

Many bacteria are well suited to metabolically adapt and grow on a variety of different substrates and produce a variety of different metabolites. For instance, *Roseburia inulini-vorans* is predominantly a butyrate producer, however during its growth on fucose, *Roseburia inulinivorans* can completely change its gene expression pattern, switching on genes that are capable of using fucose as an energy substrate, and producing propionate and propanol instead [47]. Similarly, *Ruminococcus obeum* produces acetate, lactate, and formate when grown on glucose, but additionally produces propionate while grown of fucose [48]. This indicates that gut bacteria can metabolically adapt depending on substrate availability and consequently

might also produce different metabolites. As we found increased production of SCFAs in both the inulin (**chapter 5**) and the MOS (**chapter 7**) studies, it remains rather difficult to determine whether the outgrowth of microbial genera in both studies are also the genera that are responsible for the produced SCFAs.

Thus, gut microbiota function can be determined by several factors other than gut microbiota composition alone, e.g. cross-feeding, substrate competition, baseline gut microbiota composition, host-gut-microbiota interactions, diet, and metabolic adaptation to various substrates. It is therefore expected that responses to prebiotics will vary in the context of these environmental factors. Although the interaction of gut microbiota between each other, the host and the diet will be difficult to study, it is a critical area in microbial research that needs further investigation.

IS THERE A ROLE FOR THE GUT MICROBIOTA IN ATHEROSCLEROSIS?

In the last two decades, the gut microbiota have been increasingly linked to metabolic and cardiovascular-related disorders such as atherosclerosis. There are several ways by which microbiota might be linked to and affect atherogenesis as will be discussed below.

THE INTERPLAY BETWEEN THE GUT MICROBIOTA, INFLAMMATION, AND ATHEROSCLEROSIS

Local or distant infections might cause a harmful inflammatory response that can aggravate plaque development or trigger plaque rupture. Previous studies supported this mechanism by findings of bacterial DNA in atherosclerotic plaques [49,50]. Furthermore, regardless of infection, local or systemic inflammation has been shown to trigger the immune system thereby activating inflammatory pathways leading to the production and release of pro-inflammatory cytokines and chemokines [51], which can aggravate the progression of atherosclerosis. In **chapter 5** and **chapter 7**, we have no indications of either changes in infection or local/systemic inflammation as mice were housed under specific-pathogen-free (SPF) conditions and markers of local plaque and systemic inflammation were unaffected. Whether inulin or MOS

8

altered the presence of systemic or local microbial components (e.g. LPS) remains unknown. Although the presence of bacterial DNA in atherosclerotic plaques is established and there is convincing data linking inflammatory signalling to atherosclerosis, evidence in humans remains scarce. Further clinical studies should therefore focus on whether treatment with antibiotics or fecal gut microbiota transplantation have beneficial effects. Importantly, obtaining such evidence might not be feasible owing to the long experimental duration, the risk of spreading antibiotic resistance, and might even further exacerbate the development of obesity and insulin resistance due to antibiotic side-effects when given prolonged or in early life [52].

THE INTERPLAY BETWEEN THE GUT MICROBIOTA, LIPIDS, AND ATHEROSCLEROSIS

There are indications that the gut microbiota affect lipid metabolism and subsequently atherosclerosis development. In subjects from the LifeLines-DEEP population cohort, a large-scale human study, it was found that the gut microbiota contribute to a substantial proportion of the variation found in blood lipids in humans [53]. They found that the family *Clostridiaceae/ Lachnospiracease* was specifically associated with low-density lipoproteins (LDL), while the family *Pasteurellaceae*, genus *Coprococcus*, and genus *Collinsella* species *Stercoris* showed strong association with triglyceride (TG) levels. Changes in either plasma LDL or TG levels are major risk factors for the development of atherosclerosis. Although we found an increase in the genus *Coprococcus* after a high cholesterol diet supplemented with inulin (**chapter 5**), we did not find any effect on plasma lipid levels and atherosclerosis development.

In contrast to inulin, in **chapter 7** we found that MOS significantly reduced plasma cholesterol levels and atherosclerosis development. Concomitantly, we identified an increase in the abundance of *Bacteroides Ovatus*. Currently, no other studies have identified an association between *Bacteroides Ovatus* and plasma lipid levels. Nevertheless, it may be possible that *Bacteroides Ovatus* is associated with altering plasma cholesterol levels via interactions with bile acids (BAs). For instance, specific BAs and their signalling pathways play important roles in cholesterol metabolism (reviewed in [54–56]) and atherosclerosis. Primary BAs that are synthesised in the liver end up in the terminal ileum where they can be mostly absorbed from

the terminal ileum. Another part will enter the colon and be modified by the gut microbiota expressing bile salt hydrolases (BSH) to yield so-called secondary BAs [56]. Indeed, *Bacteroides Ovatus* expresses BSH [44, 45] and accordingly is able to deconjugate primary BAs into secondary BAs. Some secondary BAs will be absorbed from the colon and, together with those absorbed from the ileum, transported to the liver for re-secretion into bile. This enterohepatic circulation of BAs contribute to the maintenance of the BA pool. When the BA pool is disturbed and leads to excess BA excretion via the feces, this loss can be compensated by hepatic *de novo* synthesis using cholesterol as a substrate [57,58]. In **chapter 7** we also found increased fecal excretion of BAs which may form an explanation for the reduced plasma cholesterol levels. It seems therefore plausible that interference with the gut microbiota in which BSH-activity and BA metabolism are affected, may eventually alter plasma cholesterol levels and as a result atherosclerosis development.

CAUSALLY LINK GUT MICROBIOTA TO ATHEROSCLEROSIS

When studying the microbiota and its direct role in disease, it is important to keep in mind Koch's postulates, which describe the criteria that are needed in order to determine a causative relationship between microorganisms and disease. As Koch's postulates were established in the late nineteenth century, one should now adapt these postulates and incorporate the substantial amount of knowledge on host-microorganism interactions. Alterations in the entire microbiome should be incorporated rather than only one specific pathogenic species. In order to determine whether the altered microbiota causes, or solely reflects, atherosclerosis in this thesis, a follow-up study is needed in which cecal content of the mice fed either inulin or MOS will be transferred to control mice. This will allow for prove of causality between the gut microbiota and the development of atherosclerosis.

8

ARE MOUSE STUDIES ON GUT MICROBIOTA TRANSLATIONAL TO HUMANS?

Much of the basic gut microbiota research is performed in mice. However, there are quite some differences between mice and humans. The gastrointestinal tract differs anatomically with for example a relatively short colon, a functional cecum and no appendix in mice compared to in humans [59]. In addition, physiological differences are substantial. For example, even on extreme diets wild type mice are quite resistant to atherosclerosis and overt type 2 diabetes [60,61].

Why do we still continue to use mice in research aiming for strategies to prevent and modulate human diseases? One of the reasons is that mice and humans share 99% of their genes and differ by 14% in genome size [62]. Furthermore, despite their vastly different overall body size, intestinal anatomy and diet (e.g. mice are coprophagous), the same phyla dominate the distal guts of mice and humans: *Firmicutes*, *Bacteroidetes*, and *Actinobacteria* [35]. However, a main reason to use mice is that mouse models are instrumental in assessing causality of complex gene-environment and host-microbiota interactions in a well-controlled manner. It is very difficult to study gut microbiota-host interactions in humans directly as human bacterial communities are influenced by a plethora of genetic and environmental factors. For example, in a recent study 126 intrinsic and extrinsic factors were found to be associated with inter-individual variation of the gut microbiota [63]. In fact, it is estimated that to adequately assess a relationship between metabolic disease and the intestinal microbiota while correcting for confounding factors, a study should contain at least 1700 subjects [64], which leads to a large variation that is difficult to correct for in human studies. However, even in well-controlled gut microbiota experiments using mouse models inter-study variations can occur due to confounding factors in the experimental setup. These variations include mouse breeding origin and housing, genetic background, maternal effects, and environmental conditions including diet, amount of (day)light, stress, and SPF conditions [59]. When setting up a new experiment, researchers therefore need to specifically take into account these possible study confounders.

To overcome these limitations, recently efforts have been initiated to standardise gut microbiota experiments. An example is the establishment of a standardised microbiota

in isobiotic mice that subsequently can be shared by different institutions performing gut microbiota research [42,65]. Although these efforts are still preliminary, they will increase reproducibility and comparability of experimental results between different studies, which is absolutely essential for progress in the gut microbiota research field.

PROBIOTICS, PREBIOTICS OR SYNBIOTICS?

SUPPLEMENTATION OF PROBIOTICS

Among the first strategies proposed to modulate gut microbiota was the administration of live microbes, probiotics. Some members of the gut bacteria are believed to promote health, whereas others may pose threats to health, particularly if they overgrow. Probiotics must possess specific properties in addition to conveying specific health benefits to the host. They need to stay viable and survive passage through the upper regions of the gastrointestinal tract and persist in the colon. They should be resistant to antagonistic, mutagenic, or pathogenic conditions in the gut. Also, the chosen microorganisms must be amenable to industrial processes and have to remain viable in the final supplemental/food product [66]. Even when probiotics fulfil the above mentioned criteria, there are limitations to the use of probiotics to promote health and/or prevent disease. A major limitation is that bacteria may exert completely different functions depending on environmental factors and the presence of other bacteria. It is therefore difficult to draw general conclusions about universal health effects of probiotics. Indeed, currently, few health claims for probiotics have been approved in Europe or the United States by the responsible regulatory agencies, e.g. European Food Safety Authority (EFSA) and US Food and Drug Administration (FDA). These limitations have not prevented numerous researchers and commercial companies to attribute therapeutic potential to probiotic microorganisms for obesity, insulin resistance syndrome, type 2 diabetes, and non-alcoholic fatty liver disease (NAFLD)(reviewed in [67]).

8

SUPPLEMENTATION OF PREBIOTICS

Prebiotics are defined as 'selectively fermentable ingredients that allow specific changes in the composition and/or activity of gastrointestinal microbiota that provide benefits to the host'. Multiple studies have reported the occurrence of study participants who respond to prebiotics (responders), whereas in other similar studies, the study participants failed to respond (non-responders) to the same prebiotic treatments [68–71]. This implies significant inter-individual variability in the response to dietary interventions. These responses likely depend on the taxonomic and functional composition of the gut microbiota. However, also other abiotic factors seem to play a role in the response to a given prebiotic. These include the nature of the digestive enzymes provided by the host, stomach and intestinal pH, and transit time, all of which can ultimately affect growth of bacterial members, even if a suitable growth substrate is provided [68]. As a practical strategy and future perspective, the introduction of multiple indigestible carbohydrates simultaneously or the combination of pre- and probiotics (synbiotics) may result in the enrichment and more diverse population of gut microbes.

SUPPLEMENTATION OF SYNBIOTICS

Synbiotics consist of a probiotic strain and a prebiotic substrate, in which the prebiotic is specifically intended to support the growth of the cognate probiotic [72]. One of the advantages of synbiotics is that such formulations could address the responder/non-responder phenomenon. To become established in the colon, a probiotic must not only secure nutrients and other growth factors but also outcompete the resident microbiota. By providing the probiotic organism with a niche opportunity in the form of a selectively fermentable prebiotic, the strain is given a competitive advantage. The most commonly used synbiotic combinations contain the probiotics *Lactobacilli* and *Bifidobacteria*, together with oligosaccharides, inulin, or fibers as the prebiotic component [73]. As we did not detect *Bifidobacteria* in cecum samples of *E3L.CETP* mice after feeding them with inulin (**chapter 5**), it remains to be investigated whether co-administration of inulin with *Bifidobacteria* would have resulted in different effects on plasma lipids and atherosclerosis development.

SUPPLEMENTATION OF SHORT-CHAIN FATTY ACIDS

Much of the beneficial effects of changes in gut microbiota composition on disease outcome are often attributed to the increased production of SCFAs. It therefore seems tempting and perhaps reasonably to supplement SCFAs directly instead of using probiotics or prebiotics. In fact, oral administration of SCFA has been associated with several beneficial effects. For example, oral administration with butyrate impairs atherogenesis by reducing plaque inflammation [74], protects against non-alcoholic steatohepatitis (NASH)[75], improves insulin sensitivity and increases energy expenditure [76], activates brown adipose tissue and reduces appetite via the gut-brain neural circuit [77]. It is important to consider the site of SCFA production to fully understand the biological effects of SCFA in humans. For instance, oral SCFA are rapidly absorbed in the proximal intestine and oxidised [78] and it is demonstrated that circulating concentrations of SCFAs, except for acetate, are toxic in high concentrations which might even lead to coma [79]. Therefore, is seems very important that either the right concentration of SCFA is administered in order to avoid toxic effects or that SCFAs are being produced in the distal gut after e.g. fermentation of prebiotics.

With prebiotic supplementation one assumes that fermentation of these indigestible carbohydrates takes only place in the distal part of the gut, the colon, where the gut microbiota resides. However, evidence also supports for a role of the gut microbiota in fermentation of e.g. inulin in the upper part of the GI tract [80]. This proximal site of fermentation might play an important role for the actual effect of inulin on host physiology and metabolism. For example, when inulin is fermented by gut bacteria in the colon, inulin is broken down into smaller pieces of fructose units [81]. In mice, the colon does not contain fructose receptors such as Glut5 (Slc2a5) compared to the small intestine [82]. The majority of the fructose formed after fermentation of inulin therefore abide in the colon. On the other hand, when inulin is fermented in the small intestine, fructose can be taken up directly by the fructose receptors, enter the bloodstream, and end up in e.g. the liver. Increased uptake of fructose is implicated in the development of metabolic diseases such as fructose-induced hypertension and NAFLD [83]. In **chapter 5**, we found that inulin both resulted in increased SCFA production in

8

cecum content, but also affected liver inflammation when combined with higher percentages (0.5%) of dietary cholesterol. Whether fermentation of inulin in our study took place in the small intestine and therefore resulted in increased uptake of fructose in the small intestine is not known.

Future studies should aim for the identification and validation of a role for synbiotics in health and disease. In order to study this, one could introduce an *in vivo* selection method that relies on the selection and isolation of strains whose abundance is significantly enriched in animals or study participants who had consumed a given prebiotic. When recombined as a synbiotic and introduced into a new host, these strains would be expected to colonise at greater levels than in the absence of the prebiotic. Furthermore, the site of fermentation of prebiotics and/or administration of SCFAs should be taken into account. This is a first step in the facilitation of understanding the specific effects of pre-, pro-, and synbiotics, and the processes involved in survival and the crosstalk mechanisms with the human host.

CONCLUSION

The studies described in this thesis increased our knowledge on the potential of the indigestible carbohydrates inulin and MOS in the modulation of the gut microbiota to affect the development of cardiometabolic disease. Specifically MOS induced beneficial effects on gut microbiota composition, atherosclerosis development and minor effects on the immune system. Although inulin did show prebiotic activity by changing gut microbiota composition and increasing the production of SCFAs, inulin adversely affected atherosclerosis development or led to manifestations of liver inflammation. The context in which the prebiotic is administered (e.g. mouse model, dietary background, concentration of the prebiotic) might be important factors that determine the actual effect of the prebiotic on cardiometabolic disease. Therefore, modulating cardiometabolic disease using indigestible carbohydrates suggest a promising strategy to further pursue but also warrants for some caution.

REFERENCES

1. Sanschagrin, S.; Yergeau, E. Next-generation Sequencing of 16S Ribosomal RNA Gene Amplicons. *J. Vis. Exp.* **2014**, doi:10.3791/51709.

2. Morgan, X. C.; Huttenhower, C. Chapter 12: Human microbiome analysis. *PLoS Comput. Biol.* **2012**, *8*, e1002808, doi:10.1371/journal.pcbi.1002808.

3. Kuczynski, J.; Lauber, C. L.; Walters, W. A.; Parfrey, L. W.; Clemente, J. C.; Gevers, D.; Knight, R. Experimental and analytical tools for studying the human microbiome. *Nat. Rev. Genet.* **2012**, *13*, 47–58, doi:10.1038/nrg3129.

4. DeSantis, T. Z.; Hugenholtz, P.; Larsen, N.; Rojas, M.; Brodie, E. L.; Keller, K.; Huber, T.; Dalevi, D.; Hu, P.; Andersen, G. L. Greengenes, a chimera-checked 16S rRNA gene database and workbench compatible with ARB. *Appl. Environ. Microbiol.* **2006**, *72*, 5069–72, doi:10.1128/AEM.03006-05.

5. Langille, M. G. I.; Zaneveld, J.; Caporaso, J. G.; McDonald, D.; Knights, D.; Reyes, J. A.; Clemente, J. C.; Burkepile, D. E.; Vega Thurber, R. L.; Knight, R.; Beiko, R. G.; Huttenhower, C. Predictive functional profiling of microbial communities using 16S rRNA marker gene sequences. *Nat. Biotechnol.* **2013**, *31*, 814–21, doi:10.1038/nbt.2676.

6. Zhi, X.-Y.; Zhao, W.; Li, W.-J.; Zhao, G.-P. Prokaryotic systematics in the genomics era. *Antonie Van Leeuwenhoek* **2012**, *101*, 21–34, doi:10.1007/s10482-011-9667-x.

7. Segata, N.; Boernigen, D.; Tickle, T. L.; Morgan, X. C.; Garrett, W. S.; Huttenhower, C. Computational meta'omics for microbial community studies. *Mol. Syst. Biol.* **2013**, *9*, 666, doi:10.1038/msb.2013.22.

8. Tyson, G. W.; Chapman, J.; Hugenholtz, P.; Allen, E. E.; Ram, R. J.; Richardson, P. M.; Solovyev, V. V.; Rubin, E. M.; Rokhsar, D. S.; Banfield, J. F. Community structure and metabolism through reconstruction of microbial genomes from the environment. *Nature* **2004**, *428*, 37–43, doi:10.1038/nature02340.

9. Qin, J.; Li, R.; Raes, J.; Arumugam, M.; Burgdorf, K. S.; Manichanh, C.; Nielsen, T.; Pons, N.; Levenez, F.; Yamada, T.; Mende, D. R.; Li, J.; Xu, J.; Li, S.; Li, D.; Cao, J.;

8

Wang, B.; Liang, H.; Zheng, H.; Xie, Y.; Tap, J.; Lepage, P.; Bertalan, M.; Batto, J.-M.; Hansen, T.; Le Paslier, D.; Linneberg, A.; Nielsen, H. B.; Pelletier, E.; Renault, P.; Sicheritz-Ponten, T.; Turner, K.; Zhu, H.; Yu, C.; Li, S.; Jian, M.; Zhou, Y.; Li, Y.; Zhang, X.; Li, S.; Qin, N.; Yang, H.; Wang, J.; Brunak, S.; Doré, J.; Guarner, F.; Kristiansen, K.; Pedersen, O.; Parkhill, J.; Weissenbach, J.; Antolin, M.; Artiguenave, F.; Blottiere, H.; Borruel, N.; Bruls, T.; Casellas, F.; Chervaux, C.; Cultrone, A.; Delorme, C.; Denariaz, G.; Dervyn, R.; Forte, M.; Friss, C.; van de Guchte, M.; Guedon, E.; Haimet, F.; Jamet, A.; Juste, C.; Kaci, G.; Kleerebezem, M.; Knol, J.; Kristensen, M.; Layec, S.; Le Roux, K.; Leclerc, M.; Maguin, E.; Melo Minardi, R.; Oozeer, R.; Rescigno, M.; Sanchez, N.; Tims, S.; Torrejon, T.; Varela, E.; de Vos, W.; Winogradsky, Y.; Zoetendal, E.; Bork, P.; Ehrlich, S. D.; Wang, J. A human gut microbial gene catalogue established by metagenomic sequencing. *Nature* **2010**, *464*, 59–65, doi:10.1038/nature08821.

10. Sims, D.; Sudbery, I.; Ilott, N. E.; Heger, A.; Ponting, C. P. Sequencing depth and coverage: Key considerations in genomic analyses. *Nat. Rev. Genet.* **2014**, *15*, 121–132, doi:10.1038/nrg3642.

11. Ku, H.-J.; Lee, J.-H. Development of a novel long-range 16S rRNA universal primer set for metagenomic analysis of gastrointestinal microbiota in newborn infants. *J. Microbiol. Biotechnol.* **2014**, *24*, 812–22.

12. Koren, S.; Phillippy, A. M. One chromosome, one contig: complete microbial genomes from long-read sequencing and assembly. *Curr. Opin. Microbiol.* **2015**, *23*, 110–120, doi:10.1016/J.MIB.2014.11.014.

13. Frank, J. A.; Pan, Y.; Tooming-Klunderud, A.; Eijsink, V. G. H.; McHardy, A. C.; Nederbragt, A. J.; Pope, P. B. Improved metagenome assemblies and taxonomic binning using long-read circular consensus sequence data. *Sci. Rep.* **2016**, *6*, 25373, doi:10.1038/srep25373.

14. Zierer, J.; Long, T.; Telenti, A.; Spector, T.; Menni, C. The fecal metabolome as a functional readout of the gut microbiome. *Consort. METabolomics Stud. Sci. Meet.* **2016**, doi:10.1038/s41588-018-0135-7.

15. Jacobs, D. M.; Deltimple, N.; van Velzen, E.; van Dorsten, F. A.; Bingham, M.; Vaughan, E. E.; van Duynhoven, J. 1H NMR metabolite profiling of feces as a tool to assess the impact of nutrition on the human microbiome. *NMR Biomed.* **2008**, *21*, 615–626, doi:10.1002/nbm.1233.

16. Kim, H. K.; Kostidis, S.; Choi, Y. H. NMR Analysis of Fecal Samples. In; Humana Press, New York, NY, **2018**; pp. 317–328.

17. Verhoeven, A.; Slagboom, E.; Wuhrer, M.; Giera, M.; Mayboroda, O. A. Automated quantification of metabolites in blood-derived samples by NMR. *Anal. Chim. Acta* **2017**, *976*, 52–62, doi:10.1016/J.ACA.2017.04.013.

18. Kostidis, S.; Addie, R. D.; Morreau, H.; Mayboroda, O. A.; Giera, M. Quantitative NMR analysis of intra- and extracellular metabolism of mammalian cells: A tutorial. *Anal. Chim. Acta* **2017**, *980*, 1–24, doi:10.1016/J.ACA.2017.05.011.

19. den Besten, G.; van Eunen, K.; Groen, A. K.; Venema, K.; Reijngoud, D.-J.; Bakker, B. M. The role of short-chain fatty acids in the interplay between diet, gut microbiota, and host energy metabolism. *J. Lipid Res.* **2013**, *54*, 2325–40, doi:10.1194/jlr.R036012.

20. Nicholson, J. K.; Holmes, E.; Kinross, J.; Burcelin, R.; Gibson, G.; Jia, W.; Pettersson, S. Host-Gut Microbiota Metabolic Interactions. *Science (80-.).* **2012**, *336*, 1262–1267, doi:10.1126/science.1223813.

21. Roy, C. C.; Kien, C. L.; Bouthillier, L.; Levy, E. Short-Chain Fatty Acids: Ready for Prime Time? *Nutr. Clin. Pract.* **2006**, *21*, 351–366, doi:10.1177/0115426506021004351.

22. Flint, H. J.; Duncan, S. H.; Scott, K. P.; Louis, P. Interactions and competition within the microbial community of the human colon: links between diet and health. *Environ. Microbiol.* **2007**, *9*, 1101–1111, doi:10.1111/j.1462-2920.2007.01281.x.

23. Hoek, M. J. A. van; Merks, R. M. H. Emergence of microbial diversity due to cross-feeding interactions in a spatial model of gut microbial metabolism. *BMC Syst. Biol.* **2017**, *11*, 56, doi:10.1186/s12918-017-0430-4.

24. Rossi, M.; Corradini, C.; Amaretti, A.; Nicolini, M.; Pompei, A.; Zanoni, S.; Matteuzzi,

8

D. Fermentation of fructooligosaccharides and inulin by bifidobacteria: a comparative study of pure and fecal cultures. *Appl. Environ. Microbiol.* **2005**, *71*, 6150–8, doi:10.1128/AEM.71.10.6150-6158.2005.

25.   Duncan, S. H.; Scott, K. P.; Ramsay, A. G.; Harmsen, H. J. M.; Welling, G. W.; Stewart, C. S.; Flint, H. J. Effects of alternative dietary substrates on competition between human colonic bacteria in an anaerobic fermentor system. *Appl. Environ. Microbiol.* **2003**, *69*, 1136–42.

26.   Apajalahti, J. H. A.; Kettunen, H.; Kettunen, A.; Holben, W. E.; Nurminen, P. H.; Rautonen, N.; Mutanen, M. Culture-independent microbial community analysis reveals that inulin in the diet primarily affects previously unknown bacteria in the mouse cecum. *Appl. Environ. Microbiol.* **2002**, *68*, 4986–95.

27.   Kleessen, B.; Hartmann, L.; Blaut, M. Oligofructose and long-chain inulin: influence on the gut microbial ecology of rats associated with a human faecal flora. *Br. J. Nutr.* **2001**, *86*, 291–300.

28.   Duncan, S. H.; Scott, K. P.; Ramsay, A. G.; Harmsen, H. J. M.; Welling, G. W.; Stewart, C. S.; Flint, H. J. Effects of alternative dietary substrates on competition between human colonic bacteria in an anaerobic fermentor system. *Appl. Environ. Microbiol.* **2003**, *69*, 1136–42.

29.   Petry, N.; Egli, I.; Chassard, C.; Lacroix, C.; Hurrell, R. Inulin modifies the bifido-bacteria population, fecal lactate concentration, and fecal pH but does not influence iron absorption in women with low iron status. *Am. J. Clin. Nutr.* **2012**, *96*, 325–31, doi:10.3945/ajcn.112.035717.

30.   Kolida, S.; Meyer, D.; Gibson, G. R. A double-blind placebo-controlled study to establish the bifidogenic dose of inulin in healthy humans. *Eur. J. Clin. Nutr.* **2007**, *61*, 1189–1195, doi:10.1038/sj.ejcn.1602636.

31.   Meyer, D.; Stasse-Wolthuis, M. The bifidogenic effect of inulin and oligofructose and its consequences for gut health. *Eur. J. Clin. Nutr.* **2009**, *63*, 1277–89, doi:10.1038/ejcn.2009.64.

32. Fan, C.-H.; Cao, J.-H.; Zhang, F.-C. The prebiotic inulin as a functional food - a review. *Eur. Rev. Med. Pharmacol. Sci.* **2016**, *20*, 3262–5.

33. Zhang, L.; Carmody, R. N.; Kalariya, H. M.; Duran, R. M.; Moskal, K.; Poulev, A.; Kuhn, P.; Tveter, K. M.; Turnbaugh, P. J.; Raskin, I.; Roopchand, D. E. Grape proanthocyanidin-induced intestinal bloom of Akkermansia muciniphila is dependent on its baseline abundance and precedes activation of host genes related to metabolic health. *J. Nutr. Biochem.* **2018**, *56*, 142–151, doi:10.1016/j.jnutbio.2018.02.009.

34. Benson, A. K.; Kelly, S. A.; Legge, R.; Ma, F.; Low, S. J.; Kim, J.; Zhang, M.; Oh, P. L.; Nehrenberg, D.; Hua, K.; Kachman, S. D.; Moriyama, E. N.; Walter, J.; Peterson, D. A.; Pomp, D. Individuality in gut microbiota composition is a complex polygenic trait shaped by multiple environmental and host genetic factors. *Proc. Natl. Acad. Sci.* **2010**, *107*, 18933–18938, doi:10.1073/pnas.1007028107.

35. Ley, R. E.; Bäckhed, F.; Turnbaugh, P.; Lozupone, C. a; Knight, R. D.; Gordon, J. I. Obesity alters gut microbial ecology. *Proc. Natl. Acad. Sci. U. S. A.* **2005**, *102*, 11070–11075, doi:10.1073/pnas.0504978102.

36. Kovacs, A.; Ben-Jacob, N.; Tayem, H.; Halperin, E.; Iraqi, F. A.; Gophna, U. Genotype Is a Stronger Determinant than Sex of the Mouse Gut Microbiota. *Microb. Ecol.* **2011**, *61*, 423–428, doi:10.1007/s00248-010-9787-2.

37. Levy, M.; Thaiss, C. A.; Elinav, E. Metagenomic cross-talk: the regulatory interplay between immunogenomics and the microbiome. *Genome Med.* **2015**, *7*, 120, doi:10.1186/s13073-015-0249-9.

38. Thaiss, C. A.; Levy, M.; Suez, J.; Elinav, E. The interplay between the innate immune system and the microbiota. *Curr. Opin. Immunol.* **2014**, *26*, 41–8, doi:10.1016/j.coi.2013.10.016.

39. Petnicki-Ocwieja, T.; Hrncir, T.; Liu, Y.-J.; Biswas, A.; Hudcovic, T.; Tlaskalova-Hogenova, H.; Kobayashi, K. S. Nod2 is required for the regulation of commensal microbiota in the intestine. *Proc. Natl. Acad. Sci.* **2009**, *106*, 15813–15818, doi:10.1073/pnas.0907722106.

8

40.   Elinav, E.; Strowig, T.; Kau, A. L.; Henao-Mejia, J.; Thaiss, C. A.; Booth, C. J.; Peaper, D. R.; Bertin, J.; Eisenbarth, S. C.; Gordon, J. I.; Flavell, R. A. NLRP6 inflammasome regulates colonic microbial ecology and risk for colitis. *Cell* **2011**, *145*, 745–57, doi:10.1016/j.cell.2011.04.022.

41.   Vijay-Kumar, M.; Aitken, J. D.; Carvalho, F. A.; Cullender, T. C.; Mwangi, S.; Srinivasan, S.; Sitaraman, S. V; Knight, R.; Ley, R. E.; Gewirtz, A. T. Metabolic syndrome and altered gut microbiota in mice lacking Toll-like receptor 5. *Science* **2010**, *328*, 228–31, doi:10.1126/science.1179721.

42.   Hooper, L. V; Littman, D. R.; Macpherson, A. J. Interactions between the microbiota and the immune system. *Science* **2012**, *336*, 1268–73, doi:10.1126/science.1223490.

43.   Turnbaugh, P. J.; Bäckhed, F.; Fulton, L.; Gordon, J. I. Diet-induced obesity is linked to marked but reversible alterations in the mouse distal gut microbiome. *Cell Host Microbe* **2008**, *3*, 213–23, doi:10.1016/j.chom.2008.02.015.

44.   Turnbaugh, P. J.; Ridaura, V. K.; Faith, J. J.; Rey, F. E.; Knight, R.; Gordon, J. I. The effect of diet on the human gut microbiome: a metagenomic analysis in humanized gnotobiotic mice. *Sci. Transl. Med.* **2009**, *1*, 6ra14, doi:10.1126/scitranslmed.3000322.

45.   Zhang, C.; Zhang, M.; Wang, S.; Han, R.; Cao, Y.; Hua, W.; Mao, Y.; Zhang, X.; Pang, X.; Wei, C.; Zhao, G.; Chen, Y.; Zhao, L. Interactions between gut microbiota, host genetics and diet relevant to development of metabolic syndromes in mice. *ISME J.* **2010**, *4*, 232–41, doi:10.1038/ismej.2009.112.

46.   Martínez, I.; Wallace, G.; Zhang, C.; Legge, R.; Benson, A. K.; Carr, T. P.; Moriyama, E. N.; Walter, J. Diet-induced metabolic improvements in a hamster model of hypercholesterolemia are strongly linked to alterations of the gut microbiota. *Appl. Environ. Microbiol.* **2009**, *75*, 4175–84, doi:10.1128/AEM.00380-09.

47.   Scott, K. P.; Martin, J. C.; Campbell, G.; Mayer, C. D.; Flint, H. J. Whole-genome transcription profiling reveals genes up-regulated by growth on fucose in the human gut bacterium "Roseburia inulinivorans." *J. Bacteriol.* **2006**, *188*, 4340–4349, doi:10.1128/JB.00137-06.

48.   Reichardt, N.; Duncan, S. H.; Young, P.; Belenguer, A.; McWilliam Leitch, C.; Scott, K. P.; Flint, H. J.; Louis, P. Phylogenetic distribution of three pathways for propionate production within the human gut microbiota. *ISME J.* **2014**, *8*, 1323–35, doi:10.1038/ismej.2014.14.

49.   Ott, S. J.; El Mokhtari, N. E.; Musfeldt, M.; Hellmig, S.; Freitag, S.; Rehman, A.; Kühbacher, T.; Nikolaus, S.; Namsolleck, P.; Blaut, M.; Hampe, J.; Sahly, H.; Reinecke, A.; Haake, N.; Günther, R.; Krüger, D.; Lins, M.; Herrmann, G.; Fölsch, U. R.; Simon, R.; Schreiber, S. Detection of Diverse Bacterial Signatures in Atherosclerotic Lesions of Patients With Coronary Heart Disease. *Circulation* **2006**, *113*, 929–937, doi:10.1161/CIRCULATIONAHA.105.579979.

50.   Koren, O.; Spor, A.; Felin, J.; Fak, F.; Stombaugh, J.; Tremaroli, V.; Behre, C. J.; Knight, R.; Fagerberg, B.; Ley, R. E.; Backhed, F. Human oral, gut, and plaque microbiota in patients with atherosclerosis. *Proc. Natl. Acad. Sci.* **2011**, *108*, 4592–4598, doi:10.1073/pnas.1011383107.

51.   Akira, S.; Uematsu, S.; Takeuchi, O. Pathogen Recognition and Innate Immunity. *Cell* **2006**, *124*, 783–801, doi:10.1016/j.cell.2006.02.015.

52.   Cox, L. M.; Blaser, M. J. Antibiotics in early life and obesity. *Nat. Rev. Endocrinol.* **2015**, *11*, 182–90, doi:10.1038/nrendo.2014.210.

53.   Fu, J.; Bonder, M. J.; Cenit, M. C.; Tigchelaar, E. F.; Maatman, A.; Dekens, J. A. M.; Brandsma, E.; Marczynska, J.; Imhann, F.; Weersma, R. K.; Franke, L.; Poon, T. W.; Xavier, R. J.; Gevers, D.; Hofker, M. H.; Wijmenga, C.; Zhernakova, A. The Gut Microbiome Contributes to a Substantial Proportion of the Variation in Blood Lipids. *Circ. Res.* **2015**, *117*, 817–24, doi:10.1161/CIRCRESAHA.115.306807.

54.   Kuipers, F.; Stroeve, J. H. M.; Caron, S.; Staels, B. Bile acids, farnesoid X receptor, atherosclerosis and metabolic control. *Curr. Opin. Lipidol.* **2007**, *18*, 289–97, doi:10.1097/MOL.0b013e3281338d08.

55.   Hageman, J.; Herrema, H.; Groen, A. K.; Kuipers, F. A role of the bile salt receptor FXR in atherosclerosis. *Arterioscler. Thromb. Vasc. Biol.* **2010**, *30*, 1519–28, doi:10.1161/

8

ATVBAHA.109.197897.

56.   De Boer, J. F.; Bloks, V. W.; Verkade, E.; Heiner-Fokkema, M. R.; Kuipers, F. New insights in the multiple roles of bile acids and their signalling pathways in metabolic control. *Curr. Opin. Lipidol.* **2018**, *29*, 194–202.

57.   Li, T.; Chiang, J. Y. L. Bile acids as metabolic regulators. *Curr. Opin. Gastroenterol.* **2015**, *31*, 159–65, doi:10.1097/MOG.0000000000000156.

58.   Kuipers, F.; Bloks, V. W.; Groen, A. K. Beyond intestinal soap—bile acids in metabolic control. *Nat. Rev. Endocrinol.* **2014**, *10*, 488–498, doi:10.1038/nrendo.2014.60.

59.   Nguyen, T. L. A.; Vieira-Silva, S.; Liston, A.; Raes, J. How informative is the mouse for human gut microbiota research? *Dis. Model. Mech.* **2015**, *8*, 1–16, doi:10.1242/dmm.017400.

60.   Lee, Y. T.; Lin, H. Y.; Chan, Y. W. F.; Li, K. H. C.; To, O. T. L.; Yan, B. P.; Liu, T.; Li, G.; Wong, W. T.; Keung, W.; Tse, G. Mouse models of atherosclerosis: a historical perspective and recent advances. *Lipids Health Dis.* **2017**, *16*, 12, doi:10.1186/s12944-016-0402-5.

61.   Kennedy, A. J.; Ellacott, K. L. J.; King, V. L.; Hasty, A. H. Mouse models of the metabolic syndrome. *Dis. Model. Mech.* **2010**, *3*, 156–66, doi:10.1242/dmm.003467.

62.   Chinwalla, A. T.; Cook, L. L.; Delehaunty, K. D.; Fewell, G. A.; Fulton, L. A.; Fulton, R. S.; Graves, T. A.; Hillier, L. W.; Mardis, E. R.; McPherson, J. D.; Miner, T. L.; Nash, W. E.; Nelson, J. O.; Nhan, M. N.; Pepin, K. H.; Pohl, C. S.; Ponce, T. C.; Schultz, B.; Thompson, J.; Trevaskis, E.; Waterston, R. H.; Wendl, M. C.; Wilson, R. K.; Yang, S.-P.; An, P.; Berry, E.; Birren, B.; Bloom, T.; Brown, D. G.; Butler, J.; Daly, M.; David, R.; Deri, J.; Dodge, S.; Foley, K.; Gage, D.; Gnerre, S.; Holzer, T.; Jaffe, D. B.; Kamal, M.; Karlsson, E. K.; Kells, C.; Kirby, A.; Kulbokas, E. J.; Lander, E. S.; Landers, T.; Leger, J. P.; Levine, R.; Lindblad-Toh, K.; Mauceli, E.; Mayer, J. H.; McCarthy, M.; Meldrim, J.; Meldrim, J.; Mesirov, J. P.; Nicol, R.; Nusbaum, C.; Seaman, S.; Sharpe, T.; Sheridan, A.; Singer, J. B.; Santos, R.; Spencer, B.; Stange-Thomann, N.; Vinson, J. P.; Wade, C. M.; Wierzbowski, J.; Wyman, D.; Zody, M. C.; Birney, E.; Goldman,

N.; Kasprzyk, A.; Mongin, E.; Rust, A. G.; Slater, G.; Stabenau, A.; Ureta-Vidal, A.; Whelan, S.; Ainscough, R.; Attwood, J.; Bailey, J.; Barlow, K.; Beck, S.; Burton, J.; Clamp, M.; Clee, C.; Coulson, A.; Cuff, J.; Curwen, V.; Cutts, T.; Davies, J.; Eyras, E.; Grafham, D.; Gregory, S.; Hubbard, T.; Hunt, A.; Jones, M.; Joy, A.; Leonard, S.; Lloyd, C.; Matthews, L.; McLaren, S.; McLay, K.; Meredith, B.; Mullikin, J. C.; Ning, Z.; Oliver, K.; Overton-Larty, E.; Plumb, R.; Potter, S.; Quail, M.; Rogers, J.; Scott, C.; Searle, S.; Shownkeen, R.; Sims, S.; Wall, M.; West, A. P.; Willey, D.; Williams, S.; Abril, J. F.; Guigó, R.; Parra, G.; Agarwal, P.; Agarwala, R.; Church, D. M.; Hlavina, W.; Maglott, D. R.; Sapojnikov, V.; Alexandersson, M.; Pachter, L.; Antonarakis, S. E.; Dermitzakis, E. T.; Reymond, A.; Ucla, C.; Baertsch, R.; Diekhans, M.; Furey, T. S.; Hinrichs, A.; Hsu, F.; Karolchik, D.; Kent, W. J.; Roskin, K. M.; Schwartz, M. S.; Sugnet, C.; Weber, R. J.; Bork, P.; Letunic, I.; Suyama, M.; Torrents, D.; Zdobnov, E. M.; Botcherby, M.; Brown, S. D.; Campbell, R. D.; Jackson, I.; Bray, N.; Couronne, O.; Dubchak, I.; Poliakov, A.; Rubin, E. M.; Brent, M. R.; Flicek, P.; Keibler, E.; Korf, I.; Batalov, S.; Bult, C.; Frankel, W. N.; Carninci, P.; Hayashizaki, Y.; Kawai, J.; Okazaki, Y.; Cawley, S.; Kulp, D.; Wheeler, R.; Chiaromonte, F.; Collins, F. S.; Felsenfeld, A.; Guyer, M.; Peterson, J.; Wetterstrand, K.; Copley, R. R.; Mott, R.; Dewey, C.; Dickens, N. J.; Emes, R. D.; Goodstadt, L.; Ponting, C. P.; Winter, E.; Dunn, D. M.; von Niederhausern, A. C.; Weiss, R. B.; Eddy, S. R.; Johnson, L. S.; Jones, T. A.; Elnitski, L.; Kolbe, D. L.; Eswara, P.; Miller, W.; O'Connor, M. J.; Schwartz, S.; Gibbs, R. A.; Muzny, D. M.; Glusman, G.; Smit, A.; Green, E. D.; Hardison, R. C.; Yang, S.; Haussler, D.; Hua, A.; Roe, B. A.; Kucherlapati, R. S.; Montgomery, K. T.; Li, J.; Li, M.; Lucas, S.; Ma, B.; McCombie, W. R.; Morgan, M.; Pevzner, P.; Tesler, G.; Schultz, J.; Smith, D. R.; Tromp, J.; Worley, K. C.; Lander, E. S.; Abril, J. F.; Agarwal, P.; Alexandersson, M.; Antonarakis, S. E.; Baertsch, R.; Berry, E.; Birney, E.; Bork, P.; Bray, N.; Brent, M. R.; Brown, D. G.; Butler, J.; Bult, C.; Chiaromonte, F.; Chinwalla, A. T.; Church, D. M.; Clamp, M.; Collins, F. S.; Copley, R. R.; Couronne, O.; Cawley, S.; Cuff, J.; Curwen, V.; Cutts, T.; Daly, M.; Dermitzakis, E. T.; Dewey, C.; Dickens, N. J.; Diekhans, M.;

Dubchak, I.; Eddy, S. R.; Elnitski, L.; Emes, R. D.; Eswara, P.; Eyras, E.; Felsenfeld, A.; Flicek, P.; Frankel, W. N.; Fulton, L. A.; Furey, T. S.; Gnerre, S.; Glusman, G.; Goldman, N.; Goodstadt, L.; Green, E. D.; Gregory, S.; Guigó, R.; Hardison, R. C.; Haussler, D.; Hillier, L. W.; Hinrichs, A.; Hlavina, W.; Hsu, F.; Hubbard, T.; Jaffe, D. B.; Kamal, M.; Karolchik, D.; Karlsson, E. K.; Kasprzyk, A.; Keibler, E.; Kent, W. J.; Kirby, A.; Kolbe, D. L.; Korf, I.; Kulbokas, E. J.; Kulp, D.; Lander, E. S.; Letunic, I.; Li, M.; Lindblad-Toh, K.; Ma, B.; Maglott, D. R.; Mauceli, E.; Mesirov, J. P.; Miller, W.; Mott, R.; Mullikin, J. C.; Ning, Z.; Pachter, L.; Parra, G.; Pevzner, P.; Poliakov, A.; Ponting, C. P.; Potter, S.; Reymond, A.; Roskin, K. M.; Sapojnikov, V.; Schultz, J.; Schwartz, M. S.; Schwartz, S.; Searle, S.; Singer, J. B.; Slater, G.; Smit, A.; Stabenau, A.; Sugnet, C.; Suyama, M.; Tesler, G.; Torrents, D.; Tromp, J.; Ucla, C.; Vinson, J. P.; Wade, C. M.; Weber, R. J.; Wheeler, R.; Winter, E.; Yang, S.-P.; Zdobnov, E. M.; Waterston, R. H.; Whelan, S.; Worley, K. C.; Zody, M. C. Initial sequencing and comparative analysis of the mouse genome. *Nature* **2002**, *420*, 520–562, doi:10.1038/nature01262.

63.   Zhernakova, A.; Kurilshikov, A.; Bonder, M. J.; Tigchelaar, E. F.; Schirmer, M.; Vatanen, T.; Mujagic, Z.; Vila, A. V.; Falony, G.; Vieira-Silva, S.; Wang, J.; Imhann, F.; Brandsma, E.; Jankipersadsing, S. A.; Joossens, M.; Cenit, M. C.; Deelen, P.; Swertz, M. A.; Weersma, R. K.; Feskens, E. J. M.; Netea, M. G.; Gevers, D.; Jonkers, D.; Franke, L.; Aulchenko, Y. S.; Huttenhower, C.; Raes, J.; Hofker, M. H.; Xavier, R. J.; Wijmenga, C.; Fu, J. Population-based metagenomics analysis reveals markers for gut microbiome composition and diversity. *Science (80-.).* **2016**, *352*, 565–569, doi:10.1126/science.aad3369.

64.   Falony, G.; Joossens, M.; Vieira-Silva, S.; Wang, J.; Darzi, Y.; Faust, K.; Kurilshikov, A.; Bonder, M. J.; Valles-Colomer, M.; Vandeputte, D.; Tito, R. Y.; Chaffron, S.; Rymenans, L.; Verspecht, C.; De Sutter, L.; Lima-Mendez, G.; Dhoe, K.; Jonckheere, K.; Homola, D.; Garcia, R.; Tigchelaar, E. F.; Eeckhaudt, L.; Fu, J.; Henckaerts, L.; Zhernakova, A.; Wijmenga, C.; Raes, J. Population-level analysis of gut microbiome

variation. *Science (80-.).* **2016**, *352*, 560–564, doi:10.1126/science.aad3503.

65.   Legrand, N.; Ploss, A.; Balling, R.; Becker, P. D.; Borsotti, C.; Brezillon, N.; Debarry, J.; de Jong, Y.; Deng, H.; Di Santo, J. P.; Eisenbarth, S.; Eynon, E.; Flavell, R. A.; Guzman, C. A.; Huntington, N. D.; Kremsdorf, D.; Manns, M. P.; Manz, M. G.; Mention, J. J.; Ott, M.; Rathinam, C.; Rice, C. M.; Rongvaux, A.; Stevens, S.; Spits, H.; Strick-Marchand, H.; Takizawa, H.; van Lent, A. U.; Wang, C.; Weijer, K.; Willinger, T.; Ziegler, P. Humanized Mice for Modeling Human Infectious Disease: Challenges, Progress, and Outlook. *Cell Host Microbe* **2009**, *6*, 5–9.

66.   Ziemer, C. J.; Gibson, G. R. An overview on the functional food concept: prospectives and applied researches in probiotics, prebiotics and synbiotics. *Int. Dairy J.* **1998**, *8*, 473–479, doi:10.18006/2016.4(3S).273.278.

67.   Delzenne, N. M.; Neyrinck, A. M.; Bäckhed, F.; Cani, P. D. Targeting gut microbiota in obesity: effects of prebiotics and probiotics. *Nat. Rev. Endocrinol.* **2011**, *7*, 639–646, doi:10.1038/nrendo.2011.126.

68.   Martínez, I.; Kim, J.; Duffy, P. R.; Schlegel, V. L.; Walter, J. Resistant starches types 2 and 4 have differential effects on the composition of the fecal microbiota in human subjects. *PLoS One* **2010**, *5*, e15046, doi:10.1371/journal.pone.0015046.

69.   Korpela, K.; Flint, H. J.; Johnstone, A. M.; Lappi, J.; Poutanen, K.; Dewulf, E.; Delzenne, N.; de Vos, W. M.; Salonen, A. Gut Microbiota Signatures Predict Host and Microbiota Responses to Dietary Interventions in Obese Individuals. *PLoS One* **2014**, *9*, e90702, doi:10.1371/journal.pone.0090702.

70.   Lappi, J.; Salojärvi, J.; Kolehmainen, M.; Mykkänen, H.; Poutanen, K.; de Vos, W. M.; Salonen, A. Intake of Whole-Grain and Fiber-Rich Rye Bread Versus Refined Wheat Bread Does Not Differentiate Intestinal Microbiota Composition in Finnish Adults with Metabolic Syndrome. *J. Nutr.* **2013**, *143*, 648–655, doi:10.3945/jn.112.172668.

71.   Dewulf, E. M.; Cani, P. D.; Claus, S. P.; Fuentes, S.; Puylaert, P. G. B.; Neyrinck, A. M.; Bindels, L. B.; de Vos, W. M.; Gibson, G. R.; Thissen, J.-P.; Delzenne, N. M. Insight into the prebiotic concept: lessons from an exploratory, double blind intervention

8

study with inulin-type fructans in obese women. *Gut* **2013**, *62*, 1112–21, doi:10.1136/gutjnl-2012-303304.

72. Kolida, S.; Gibson, G. R. Synbiotics in health and disease. *Annu. Rev. Food Sci. Technol.* **2011**, *2*, 373–93, doi:10.1146/annurev-food-022510-133739.

73. Pandey, K. R.; Naik, S. R.; Vakil, B. V. Probiotics, prebiotics and synbiotics- a review. *J. Food Sci. Technol.* **2015**, *52*, 7577–7587, doi:10.1007/s13197-015-1921-1.

74. Aguilar, E. C.; Leonel, A. J.; Teixeira, L. G.; Silva, A. R.; Silva, J. F.; Pelaez, J. M. N.; Capettini, L. S. A.; Lemos, V. S.; Santos, R. A. S.; Alvarez-Leite, J. I. Butyrate impairs atherogenesis by reducing plaque inflammation and vulnerability and decreasing NFκB activation. *Nutr. Metab. Cardiovasc. Dis.* **2014**, *24*, 606–13, doi:10.1016/j.numecd.2014.01.002.

75. Jin, C. J.; Sellmann, C.; Engstler, A. J.; Ziegenhardt, D.; Bergheim, I. Supplementation of sodium butyrate protects mice from the development of non-alcoholic steatohepatitis (NASH). *Br. J. Nutr.* **2015**, *114*, 1745–1755, doi:10.1017/S0007114515003621.

76. Gao, Z.; Yin, J.; Zhang, J.; Ward, R. E.; Martin, R. J.; Lefevre, M.; Cefalu, W. T.; Ye, J. Butyrate improves insulin sensitivity and increases energy expenditure in mice. *Diabetes* **2009**, *58*, 1509–17, doi:10.2337/db08-1637.

77. Li, Z.; Yi, C.-X.; Katiraei, S.; Kooijman, S.; Zhou, E.; Chung, C. K.; Gao, Y.; van den Heuvel, J. K.; Meijer, O. C.; Berbée, J. F. P.; Heijink, M.; Giera, M.; Willems van Dijk, K.; Groen, A. K.; Rensen, P. C. N.; Wang, Y. Butyrate reduces appetite and activates brown adipose tissue via the gut-brain neural circuit. *Gut* **2017**, gutjnl-2017-314050, doi:10.1136/gutjnl-2017-314050.

78. Braden, B.; Adams, S.; Duan, L. P.; Orth, K. H.; Maul, F. D.; Lembcke, B.; Hör, G.; Caspary, W. F. The [13C]acetate breath test accurately reflects gastric emptying of liquids in both liquid and semisolid test meals. *Gastroenterology* **1995**, *108*, 1048–55.

79. Clausen, M. R.; Mortensen, P. B.; Bendtsen, F. Serum levels of short-chain fatty acids in cirrhosis and hepatic coma. *Hepatology* **1991**, *14*, 1040–1045, doi:S0270913991003026 [pii].

80.   Loh, G.; Eberhard, M.; Brunner, R. M.; Hennig, U.; Kuhla, S.; Kleessen, B.; Metges, C. C. Inulin alters the intestinal microbiota and short-chain fatty acid concentrations in growing pigs regardless of their basal diet. *J. Nutr.* **2006**, *136*, 1198–202, doi:136/5/1198 [pii].

81.   Ricca, E.; Calabrò, V.; Curcio, S.; Iorio, G. The State of the Art in the Production of Fructose from Inulin Enzymatic Hydrolysis. *Crit. Rev. Biotechnol.* **2007**, *27*, 129–145, doi:10.1080/07388550701503477.

82.   Yue, F.; Cheng, Y.; Breschi, A.; Vierstra, J.; Wu, W.; Ryba, T.; Sandstrom, R.; Ma, Z.; Davis, C.; Pope, B. D.; Shen, Y.; Pervouchine, D. D.; Djebali, S.; Thurman, R. E.; Kaul, R.; Rynes, E.; Kirilusha, A.; Marinov, G. K.; Williams, B. A.; Trout, D.; Amrhein, H.; Fisher-Aylor, K.; Antoshechkin, I.; DeSalvo, G.; See, L.-H.; Fastuca, M.; Drenkow, J.; Zaleski, C.; Dobin, A.; Prieto, P.; Lagarde, J.; Bussotti, G.; Tanzer, A.; Denas, O.; Li, K.; Bender, M. A.; Zhang, M.; Byron, R.; Groudine, M. T.; McCleary, D.; Pham, L.; Ye, Z.; Kuan, S.; Edsall, L.; Wu, Y.-C.; Rasmussen, M. D.; Bansal, M. S.; Kellis, M.; Keller, C. A.; Morrissey, C. S.; Mishra, T.; Jain, D.; Dogan, N.; Harris, R. S.; Cayting, P.; Kawli, T.; Boyle, A. P.; Euskirchen, G.; Kundaje, A.; Lin, S.; Lin, Y.; Jansen, C.; Malladi, V. S.; Cline, M. S.; Erickson, D. T.; Kirkup, V. M.; Learned, K.; Sloan, C. A.; Rosenbloom, K. R.; Lacerda de Sousa, B.; Beal, K.; Pignatelli, M.; Flicek, P.; Lian, J.; Kahveci, T.; Lee, D.; James Kent, W.; Ramalho Santos, M.; Herrero, J.; Notredame, C.; Johnson, A.; Vong, S.; Lee, K.; Bates, D.; Neri, F.; Diegel, M.; Canfield, T.; Sabo, P. J.; Wilken, M. S.; Reh, T. A.; Giste, E.; Shafer, A.; Kutyavin, T.; Haugen, E.; Dunn, D.; Reynolds, A. P.; Neph, S.; Humbert, R.; Scott Hansen, R.; De Bruijn, M.; Selleri, L.; Rudensky, A.; Josefowicz, S.; Samstein, R.; Eichler, E. E.; Orkin, S. H.; Levasseur, D.; Papayannopoulou, T.; Chang, K.-H.; Skoultchi, A.; Gosh, S.; Disteche, C.; Treuting, P.; Wang, Y.; Weiss, M. J.; Blobel, G. A.; Cao, X.; Zhong, S.; Wang, T.; Good, P. J.; Lowdon, R. F.; Adams, L. B.; Zhou, X.-Q; Pazin, M. J.; Feingold, E. A.; Wold, B.; Taylor, J.; Mortazavi, A.; Weissman, S. M.; Stamatoyannopoulos, J. A.; Snyder, M. P.; Guigo, R.; Gingeras, T. R.; Gilbert, D. M.; Hardison, R. C.; Beer, M. A.; Ren, B.;

8

Mouse ENCODE Consortium A comparative encyclopedia of DNA elements in the mouse genome. *Nature* **2014**, *515*, 355–364, doi:10.1038/nature13992.

83.   Douard, V.; Ferraris, R. P. The role of fructose transporters in diseases linked to excessive fructose intake. *J. Physiol.* **2013**, *591*, 401–414, doi:10.1113/jphysiol.2011.215731.
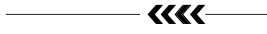
8

ADDENDUM

09

SUMMARY

Cardiometabolic disease such as obesity, type 2 diabetes, and atherosclerosis, are a leading cause of morbidity and mortality in the Western world. Two important risk factors for the development of cardiometabolic disease are hyperlipidemia and inflammation. Recently, evidence strongly indicates a role for the gut microbiota in the development of cardiometabolic disease. Therapeutic approaches are therefore aimed at modifying the gut microbiota composition and function to beneficially affect the development of cardiometabolic disease and its underlying risk factors. A potential candidate to modify gut microbiota composition are indigestible carbohydrates, or prebiotics. In this thesis, we aimed to understand the interplay between various indigestible carbohydrates, gut microbiota composition and function, and the development of obesity, type 2 diabetes, and atherosclerosis.

Chapter 1 serves as a general introduction in which hyperlipidemia and inflammation are introduced as the two main risk factors for cardiometabolic disease. More specifically, the role of the gut microbiota composition, function, and dysfunction (or dysbiosis) will be discussed as modifiable risk factors in the development of cardiometabolic disease. A tool to modify the gut microbiota composition and function and dietary interventions with indigestible carbohydrates are discussed in further detail. Finally, the importance of methods to quantify gut microbiota function is illustrated.

Since we exploit the use of high fat and high cholesterol diets in the development of cardiometabolic disease, it is important to have the ability to determine blood lipid composition. As the various fatty acids play distinct roles in health and disease, methods that can specifically determine the fatty acid profile are needed for fundamental and clinical studies. **Chapter 2** describes a method to determine the medium- and long chain fatty acid composition of blood of mice using gas chromatography-mass spectrometry (GC-MS) analysis. This method quantitatively monitors fatty acid composition using a combination of pentafluorobenzyl bromide (PFBBr) derivatization, internal standards (IS), and electron-capture negative ionisation (ECNI) in a comprehensive, sensitive, and accurate manner.

In addition, we explore the use of indigestible carbohydrates to modulate microbiota composition and function. Microbial function can be determined by measuring the products

9

261

after microbial fermentation of indigestible carbohydrates, short-chain fatty acids (SCFAs). **Chapter 3** describes a method to determine SCFAs in blood, cecum, and feces samples using GC-MS analysis. By applying the combination of PFBBr derivatization, IS, and ECNI, this method represents a fast, reliable, and reproducible method for the separation and quantification of SCFAs in various mouse-derived samples which can be further exploited for quantification of SCFAs in human studies.

In **chapter 4**, we studied the effect of the indigestible carbohydrate and prebiotic inulin on accelerated atherosclerosis development after placement of a perivascular cuff around the femoral artery of the mice. Previous studies indicated a beneficial role of inulin on inflammation and hyperlipidemia. However, the effect of inulin on atherosclerosis development has not been extensively studied yet. Male APOE*3-Leiden (*E3L*) mice were fed a high-cholesterol diet without or supplemented with inulin for 5 weeks and underwent perivascular cuff surgery in week 3 of the experiment. The combination of this well-established mouse model for human-like lipid metabolism and perivascular cuff placement around the femoral artery, enables us to specifically study the short-term effect of inulin on inflammatory-driven atherosclerosis development. In contrast to our hypothesis, inulin aggravated accelerated atherosclerosis development in these mice, which was accompanied by adverse lesion composition and outward vascular remodelling. Inulin did not affect blood monocyte composition, suggesting that the aggravated atherosclerosis development was driven by the significantly increased plasma cholesterol levels.

In **chapter 5**, we shifted our focus from short-term effects of inulin on atherosclerosis development to long-term atherosclerosis development in a lipid-driven atherosclerotic mouse model. Female APOE*3-Leiden.CETP (*E3L.CETP*) mice were fed a moderate high (0.1%) or high (0.5%) cholesterol diet without or supplemented with inulin for 11 weeks. By combining the use of female *E3L.CETP* mice and different cholesterol-enriched diets, we were able to specifically study the long-term effects of inulin on lipid-driven atherosclerosis development. Inulin combined with a high cholesterol diet clearly showed prebiotic activity, but did not affect plasma cholesterol levels or atherosclerosis development. Surprisingly, inulin combined with

a high (0.5%) cholesterol diet resulted in mild hepatic inflammation. Inulin with a moderate high (0.1%) cholesterol diet did not result in liver inflammation. It was therefore concluded that, although inulin is widely acknowledged as a prebiotic with favourable effects on lipid metabolism and cardiovascular disease, inulin clearly not always exerts beneficial effects.

In **chapter 6**, we switched our attention from a well-known prebiotic to the relatively unknown indigestible carbohydrate MOS, which have great potential to modify gut microbiota composition, inflammation, and hyperlipidemia. MOS have proven effective at improving growth performance, while also reducing inflammation and hyperlipidemia. However, beneficial effects of MOS on inflammation have been shown mainly in the intestines. As obesity is associated with chronic low-grade inflammation that predominantly manifests in extra-intestinal adipose tissue, we aimed to determine the effect of MOS on inflammation in mesenteric white adipose tissue (mWAT) and liver. In addition, we determined the effect of MOS on whole-body glucose tolerance in both lean and high-fat diet (HFD)-induced obese mice. It was found that MOS slightly altered immune cell composition in mWAT and liver of lean mice, but MOS did not ameliorate HFD-induced glucose intolerance or inflammation. Our data therefore indicate extra-intestinal modulatory properties of MOS on immune composition as reported in previous studies. However, the effects are relatively modest.

MOS have proven effective at improving growth performance, while also reducing hyperlipidemia and inflammation in livestock. As atherosclerosis is accelerated both by hyper-lipidemia and inflammation, **chapter 7** describes the effect of dietary MOS on atheroscle-rosis development in hyperlipidemic *E3L.CETP* mice. Mice were fed a high cholesterol diet, with or without MOS for 14 weeks. This study revealed that MOS decreased the onset of atherosclerosis development, via lowering of plasma cholesterol levels. Furthermore, MOS modified the gut microbiota composition and function as was observed by increased cecal butyrate levels and fecal bile acid (BA) excretion. We therefore concluded that MOS presumably decreased atherosclerosis development and lowered plasma cholesterol levels via interactions with the gut microbiota.

In **chapter 8**, the results of this thesis and the value of our research regarding

9

methods to map gut microbiota composition and function, SCFAs as a marker for gut microbial function, factors that determine gut microbiota function, the role of the gut microbiota in the development of atherosclerosis, the translatability of mouse models in gut microbiota research, and implications for prebiotics are discussed. Taken together, the studies described in this thesis increased our knowledge on the potential of various indigestible carbohydrates in the modulation of the gut microbiota to affect the development of cardiometabolic disease, suggesting a promising strategy to further pursue with some caution.

9
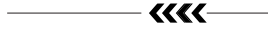
NEDERLANDSE SAMENVATTING

Cardiometabole ziekten zoals obesitas, type 2 diabetes en slagaderverkalking (atherosclerose) zijn een belangrijke oorzaak van morbiditeit en mortaliteit in de Westerse Wereld. Twee belangrijke risicofactoren voor het ontstaan van cardiometabole ziekten zijn hyperlipidemie en ontsteking. Ook bacteriën die zich huisvesten in ons darmstelsel kunnen een belangrijke rol kunnen spelen bij het ontstaan en het verloop van cardiometabole ziekten. Daarom wordt veel onderzoek gedaan om niet alleen de samenstelling, maar ook de functie van de darm-bacteriehuishouding dusdanig te veranderen dat het ontstaan van cardiometabole ziekten wordt voorkomen. Vezels, voor de mens onverteerbare koolhydraten, vormen een primaire voedingsbron voor darmbacteriën en zijn daarom een belangrijk potentieel middel om de samenstelling en functie van de darmbacteriën te veranderen. Dit proefschrift heeft als doel om de wisselwerking tussen verschillende onverteerbare koolhydraten, de samenstelling en functie van de darmbacteriën, en het ontstaan en verloop van cardiometabole ziekten zoals obesitas, type 2 diabetes, en atherosclerose beter te begrijpen.

In **hoofdstuk 1** worden hyperlipidemie en ontsteking geïntroduceerd als twee belangrijke risicofactoren voor het ontstaan van cardiometabole ziekte. Nadruk wordt gelegd op de darmbacteriën als risicofactor in de ontwikkeling van cardiometabole ziekten. De samenstelling, de functie en verstoring van een gezonde darmbacteriehuishouding worden hierin belicht. Om het belang van het veranderen van de darmbacteriehuishouding in cardi-ometabole ziekten te benadrukken, wordt het nut van dieetinterventies middels onverteerbare koolhydraten in meer detail uitgelegd. Tenslotte wordt het belang van goede technische analytische methoden uitgelicht om metabolieten in feces te meten omdat deze metabolieten de functie van de darmbacteriën weerspiegelen.

Het onderzoek wat beschreven wordt in dit proefschrift maakt gebruik van vetrijke en cholesterolrijke diëten om cardiometabole pathologie in muizen op te wekken. Het is bekend dat verscheidene vetzuren een verschillende rol kunnen spelen in ziekte en gezondheid. Daarom is het belangrijk voor fundamentele- en klinische studies om de juiste meetmethoden in huis te hebben om ook het vetzuurprofiel van het bloed in kaart te brengen. **Hoofdstuk 2** beschrijft een methode die de samenstelling van middellange- en lange keten vetzuren in het bloed van

muizen kan bepalen met behulp van gaschromatografie-massaspectrometrie (GC-MS). Deze methode wordt gekenmerkt door het gebruik van pentafluorbenzylbromide (PFBBr), interne standaarden (IS) en negatieve ionen voor elektronvangst (ECNI). Deze combinatie van kenmerken maakt deze methode geschikt om vetzuren op een volledige, gevoelige en nauwkeurige manier kwantitatief in kaart te brengen.

Tevens waren wij geïnteresseerd in het effect van koolhydraten, die door de mens niet kunnen worden verteerd, op de functie van de darmbacteriën. Een belangrijke functie van darmbacteriën is het verteren van deze koolhydraten, waarbij korte keten vetzuren (SCFAs) vrij komen. **Hoofdstuk 3** beschrijft een methode om SCFAs in bloed, dikke darm en in feces te meten met behulp van GC-MS. Ook deze methode maakt gebruik van PFBBr, IS, en ECNI en is een snelle, betrouwbare en reproduceerbare methode voor de scheiding en kwantificatie van SCFAs in verschillende monsters afkomstig uit fundamenteel muizenonderzoek. Bovendien kan deze methode ook toegepast worden in humaan onderzoek.

In **hoofdstuk 4** hebben we de korte termijn effecten van de onverteerbare koolhydraat inuline op de ontwikkeling van atherosclerose bestudeerd. Eerdere studies lieten al zien dat dit prebioticum een gunstig effect had op ontsteking en hyperlipidemie. Het effect van inuline op de ontwikkeling van atherosclerose is echter nog beperkt onderzocht. Mannelijke APOE*3-Leiden (*E3L*) muizen werden gedurende 5 weken lang gevoed met een hoog cholesterol dieet mét of zonder de aanvulling van inuline. *E3L* muizen op een hoog cholesterol dieet lijken wat betreft lipiden metabolisme en atherosclerose ontwikkeling sterk op de mens. Om versnelde atherosclerose in deze muizen te induceren, ondergingen de muizen een operatie in week 3 waarbij een manchet rond de dijbeenslagader van de muizen werd geplaatst. Bij dit versnelde atherosclerose proces speelt ontsteking een belangrijke rol. In tegenstelling tot onze hypothese dat inuline atherosclerose zou verminderen, kwam uit het onderzoek in **hoofdstuk 4** naar voren dat inuline het proces van atherosclerose verergerd had. Dit ging gepaard met grotere, ontstoken laesies en een grotere diameter van het bloedvat. Tot onze verrassing had inuline geen effect op de samenstelling van immuun cellen in het bloed, maar verhoogde wel het cholesterol niveau in het bloed. Dit geeft aan dat de verergering van atherosclerose hoogstwaarschijnlijk

NEDERLANDSE SAMENVATTING

een gevolg was van een verhoogde cholesterol niveau.

In **hoofdstuk 5** richtten we ons op de lange termijneffecten van inuline op de ontwikkeling van atherosclerose. Vrouwelijke APOE *3-Leiden.CETP (*E3L.CETP*) muizen werden gevoed met een matig hoog (0.1%) of hoog (0.5%) cholesterol dieet mét of zonder aanvulling van inuline. Met deze studie opzet ontwikkelen deze muizen in een periode van 11 weken atherosclerose rond het kleppengebied in het hart, wat overeenkomt met "natuurlijke" atherosclerose die ook in de mens wordt gezien en voornamelijk een gevolg is van het hoge lipidenniveau in het bloed. Uit dit onderzoek kwam naar voren dat inuline in combinatie met een hoog (0.5%) cholesterol dieet een duidelijke prebiotische activiteit liet zien, maar verder geen effect had op het lipiden niveau in het bloed of op de ontwikkeling van atherosclerose. Inuline in combinatie met dit hoge cholesterol (0.5%) dieet resulteerde zelfs in milde lever-ontsteking. Inuline gecombineerd met een matig hoog (0.1%) cholesterol dieet liet ook geen effect op plasma lipiden zien, maar had daarentegen geen nadelige gevolgen op ontsteking in de lever. Hoewel inuline dus wordt erkend als een prebioticum met gunstige effecten op het lipidenmetabolisme en cardiovaculaire aandoeningen, lieten onze experimenten duidelijk iets anders zien en kan geconcludeerd worden dat inuline niet altijd gunstig is.

In **hoofdstuk 6** hebben we onze aandacht verlegd van een erkend prebioticum naar een relatief onbekende onverteerbare koolhydraat met potentie om effect te hebben op de darmbacteriehuishouding, ontsteking en hyperlipidemie. Eerdere studies toonden aan dat MOS effectief zijn bij het verbeteren van de groei van dieren in de veehouderij, terwijl daarnaast een vermindering van ontsteking en hyperlipidemie werd waargenomen. De gevonden gunstige effecten van MOS op ontsteking lijken voornamelijk een gevolg van effecten op het darmstelsel. Echter zijn er ook aanwijzingen dat MOS buiten de darmen gunstige effecten kunnen uitoefenen. Omdat obesitas gepaard gaat met ontsteking die zich voornamelijk buiten de darmen manifesteert, hebben we het effect van MOS onderzocht op obesitas-gerelateerde ontsteking in extra-intestinaal metabool weefsel zoals vetweefsel en de lever. Daarnaast hebben we ook gekeken naar de effecten van MOS op glucosetolerantie. Obesitas induceerden we middels een hoog vet dieet (HFD) en vervolgens onderzochten we de effecten van MOS op

9

ontsteking in zowel slanke muizen als in muizen met obesitas. Wij vonden dat MOS de samen-stelling van de immuuncellen binnen het mesenteriale witte vetweefsel (mWAT) en de lever van vooral magere muizen enigszins veranderde. Echter werden er geen effecten gevonden van MOS op het verbeteren van glucosetolerantie. Ondanks het feit dat de gevonden effecten relatief bescheiden zijn, concludeerden wij dat MOS de potentie heeft om ontsteking in weefsel buiten het darmstelsel te moduleren.

Zowel hyperlipidemie als ontsteking spelen een belangrijke rol in atherosclerose. In **hoofdstuk 7** onderzochten wij het effect van MOS op de ontwikkeling van atherosclerose in vrouwelijke *E3L.CETP* muizen. Deze muizen werden 14 weken lang gevoed met een hoog cholesterol dieet, mét of zonder toevoeging van MOS. Dit onderzoek liet zien dat MOS de ontwikkeling van atherosclerose reduceerde middels verlaging van het cholesterol niveau in het bloed. Daarnaast lieten MOS een sterke verandering zien op de darmbacteriehuishouding en op de activiteit van de darmbacteriën. Dit laatste bleek uit een verhoging van de SCFA butyraat in de dikke darm en een verhoogde uitscheiding van galzuren in de feces. Uit dit onderzoek kan daarom geconcludeerd worden dat MOS de ontwikkeling van atherosclerose en plasma cholesterol niveaus verlagen via interacties met de darmbacteriën en effecten op plasma cholesterol.

De belangrijkste resultaten die beschreven staan in dit proefschrift worden bediscussi-eerd in **hoofdstuk 8**. Het belang van het gebruik van methoden om de microbiota compositie en functie in kaart te brengen, factoren die de functie van de microbiota bepalen, de rol van de microbiota in de ontwikkeling van atherosclerose, de vertaalbaarheid van muismodel-len in microbiota onderzoek en de implicaties van prebiotica worden eveneens besproken. Samenvattend hebben de studies in dit proefschrift onze kennis vergroot over de potentie van verschillende onverteerbare koolhydraten in het moduleren van de darmbacteriehuishouding om de ontwikkeling van cardiometabole ziekten te beïnvloeden. Dit is een veelbelovende strategie waarbij enige voorzichtigheid is geboden.

9

CURRICULUM VITAE

Lisa Rianne Hoving werd geboren op 5 december 1987 in Groningen. In 2005 behaalde zij haar havo diploma aan de Dr. Nassau College Quintus in Assen. In datzelfde jaar begon zij met de studie Verpleegkunde aan Hogeschool Windesheim in Zwolle, waarvan zij in 2006 haar propedeuse behaalde. Kort daarna verhuisde Lisa naar Maastricht om daar te beginnen als verzorgende in de thuiszorg. Dit heeft zij van 2006 tot 2013 voortgezet.

In 2007, na een kort oriëntatiejaar inclusief het behalen van de TOEFL iBT Engels op Malta, begon zij aan de studie Gezondheidswetenschappen aan de Universiteit van Maastricht met als afstuurrichtingen Bewegingswetenschappen en Bioregulatie. Tijdens deze opleiding heeft Lisa verscheidene stages gelopen waaronder een onderzoeksstage in Australië aan de University of Sydney. Tevens werd zij tijdens haar studie ingeloot als excellente student voor het Honours Programma 'International Health' dat parallel liep aan de studie Gezondheidswetenschappen. Haar externe afstudeeronderzoek volbracht zij aan Wageningen University & Research (WUR) waar zij onderzoek deed naar de effecten van flavonoïden op energie absorptie en metabolisme in de dunne darm.

Als logisch gevolg van het onderzoek in Wageningen, vervolgde Lisa na het behalen van haar Master of Science (MSc) diploma in 2013 haar weg richting promotieonderzoek op de afdeling Humane Genetica van het Leids Universitair Medisch Centrum in Leiden, onder begeleiding van Prof. Dr. Ko Willems van Dijk en Dr. Vanessa van Harmelen. Haar PhD project was onderdeel van het consortium IN-CONTROL dat gefinancierd werd door Cardiovasculair Onderzoek Nederland (CVON). Het promotieonderzoek, waarvan de resultaten staan beschreven in dit proefschrift, werd afgerond in 2018 en verdedigd in januari 2019.

9
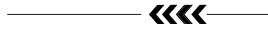
LIST OF
PUBLICATIONS

Hoving LR, Langenberg M, Franke-Fayard B, Chevalley SC, Ramaser J, Janse C, van Harmelen V, Willems van Dijk K, Roestenberg M. Malaria liver stage and blood stage infection is determined by liver and plasma cholesterol. *In preparation*

Hoving LR, Katiraei S, Pronk A, Heijink M, Vonk KKD, Amghar-el Bouazzaoui F, Vermeulen R, Drinkwaard L, Giera M, van Harmelen V, Willems van Dijk K. The prebiotic inulin modulates gut microbiota but does not ameliorate atherosclerosis in hypercholesterolemic APOE*3-Leiden.CETP mice. *Scientific Reports. 2018;8(1)*

Hoving LR, Katiraei S, Heijink M, Pronk A, van der Wee-Pals L, Streefland T, Giera M, Willems van Dijk K, van Harmelen V. Dietary mannan oligosaccharides modulate gut microbiota, increase fecal bile acid excretion, and decrease plasma cholesterol and atherosclerosis development. *Molecular Nutrition and Food Research. 2018;62(10)*

Hoving LR, van der Zande HJP, Pronk A, Guigas B, Willems van Dijk K, van Harmelen V. Dietary yeast-derived mannan oligosaccharides have immune-modulatory properties but do not improve high fat diet-induced obesity and glucose intolerance. *PLoS One. 2018;13(5)*

Hoving LR, Heijink M, van Harmelen V, van Dijk KW, Giera M. GC-MS analysis of medium- and long-chain fatty acids in blood samples. *Methods in Molecular Biology. 2018;1730:257-265*

Hoving LR, Heijink M, van Harmelen V, van Dijk KW, Giera M. GC-MS analysis of short-chain fatty acids in feces, cecum content, and blood Samples. *Methods in Molecular Biology. 2018;1730:247-256*

Hoving LR, de Vries MR, de Jong RCM, Katiraei S, Pronk A, Quax PHA, van Harmelen V, Willems van Dijk K. The prebiotic inulin aggravates accelerated atherosclerosis in hypercholesterolemic APOE*3-Leiden Mice. *Nutrients. 2018;10:172*

9

Katiraei S, **Hoving LR**, van Beek L, Mohamedhoesein S, Carlotti F, van Diepen JA, Rensen PCN, Netea MG, Willems van Dijk K, Berbée JFP, van Harmelen V. BMT decreases HFD-induced weight gain associated with decreased preadipocyte number and insulin secretion. *Plos One. 2017;12(4)*

Konings J, **Hoving LR**, Ariëns RS, Hethershaw EL, Ninivaggi M, Hardy LJ, de Laat B, Ten Cate H, Philippou H, Govers-Riemslag JW. The role of activated coagulation factor XII in overall clot stability and fibrinolysis. *Thrombosis Research. 2015;136(2):474-480*

van der Stelt I, Hoek-van den Hil EF, Swarts JJM, Vervoort JJM, **Hoving L**, Skaltsounis L, Lemonakis N, Andreadou I, van Schothorst EM, Keijer J. Nutraceutical oleuropein supplementation prevents high fat diet-induced adiposity in mice. *Journal of Functional Foods. 2015;14:702-715*

9
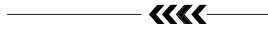
DANKWOORD

Dit proefschrift zou niet tot stand zijn gekomen zonder de betrokkenheid van velen. Daarom wil ik iedereen, ieder op zijn eigen wijze, bedanken voor hun waardevolle toevoeging.

Allereerst mijn promotor Prof. Dr. Willems van Dijk en co-promotor Dr. V.J.A. van Harmelen. Beste **Ko**, ik wil je bedanken voor je rust en vertrouwen die mij alle ruimte hebben gegeven om mijzelf te kunnen ontwikkelen binnen het onderzoek. Beste **Vanessa**, bedankt dat je 4 jaar lang mijn kamergenoot en de meest fijne co-promotor was die ik me kon wensen!

Mijn directe collega's, oftewel de lipido's. **Amanda**, bedankt voor je zorgzaamheid en droge grappen die de lange dagen op het PDC een eitje/uitje maakten. **Saeed**, bedankt voor het zijn van mijn directe PhD-microbiota-compagnon! Bedankt **Mattijs**, **Lianne**, **Sam**, **Jan**, **Ayze** en **Fatiha**, naast een fijne tijd op het lab heb ik met jullie mogen genieten van de leuke uitjes buiten het werk om. Tot slot **Dorina**, thanks for being my supportive (HG- and sports) friend!

Voorts wil ik ook alle andere mensen bedanken met wie ik samen gepubliceerd heb of die mij hierbij hebben bijgestaan. **Martin**, **Marieke**, en **Dick-Paul** van CPM, bedankt dat jullie mij op een basale en leuke manier kennis hebben laten maken met de wondere wereld van GC-MS. Collega's van de afdeling Parasitologie, met geen enkele afdeling heb ik zo nauw samengewerkt: **Bruno** en **Patrick**, bedankt voor de ontspannen en leuke sfeer tijdens de verschillende (mannan) studies. **Marijke**, mijn malaria-maatje, bedankt voor de prettige en gesmeerde samenwerking waarin twee specialismen met elkaar samensmolten. Bedankt **Meta**, **Blandine**, **Sev**, **Chris**, **Shahid**, **Jai**, **Hermelijn**, **Alice** en **Arifa** voor alle fijne kneepjes van het Parasitologie-vak en de aantal spannende (althans dat vond ik) malaria-uurtjes op het PDC. Alle collega's van **Lab Endo** en **Lab Meijer** wil ik bedanken voor de waardevolle bijdragen tijdens werkbesprekingen en gezellige koffiepauzes. **Lisanne**, ik had me geen betere paranimf-maatje kunnen wensen; ik ben blij dat ik jou heb mogen leren kennen. **Jimmy**, bedankt voor je wijze adviezen en de momenten dat ik mij zo nu en dan ook een PhD student van jou voelde. **Trea**, **Lianne** en **Isabel**, bedankt voor jullie geduld, analytische inzichten en goedlachse gesprekken op zowel het lab als op het PDC!

De afgelopen jaren heb ik het voorrecht gehad om een aantal studenten te mogen begeleiden, wat ik tot op de dag van vandaag één van de leukste dingen vond om te doen tijdens mijn promotietraject. **Lizette**, **Rosalie**, **Isabel**, en **Thomas**, bedankt voor de fijne tijd en dat jullie mij ook elke dag wat nieuws leerden.

Graag wil ik alle mensen bedanken van andere afdelingen en organisaties die mij hebben geholpen of gesteund gedurende mijn promotietraject. Collega's van het **PDC**: bedankt voor al jullie goede zorgen! De 3e verdieping inclusief het HG secretariaat, mijn tweede huis: bedankt voor alle wisselende gesprekken in de labs, de wandelgangen en tijdens de HG borrels. Ook alle **studenten in het lab**, bedankt voor jullie frisse blik en het harde werken. Leden van de **MGC-commissie 2016**: bedankt voor de geweldige commissie-ervaring tijdens de MGC workshop in Dortmund! Collega's uit het **CVON IN-CONTROL consortium**, bedankt voor de goede samenwerking en uitwisselingen van expertise tijdens de meetings en daarbuiten. Bedankt **Jettie**, voor je zorgzame en verhelderende loopbaan-inzichten. **Malou**, bedankt voor je geduld, je kundigheid, en je out-of-the-box mentaliteit tijdens het ontwerpen van mijn boekje. Je hebt er echt iets heel moois van gemaakt!

Vriendinnetjes! **Geerte**, a.k.a. Barrie: naast dat je een goede vriendin bent, bedankt dat je mijn WUR-LUMC buddy was! Praten over koetjes, kalfjes en ons hart kunnen luchten waren de momenten die het (LUMC)leven mooi maakten. **Paula**, ik ben zo dankbaar dat we onze Ozzie vriendschap na 6 stille jaren weer hebben voortgezet! **Iris** en **Maria**, ik ben blij dat wij nog steeds vriendinnetjes zijn na alle mooie tijden in Maastricht. Paranimfen / vriendinnetjes: **Hilde**, het lief en leed dat wij deelden tijdens Artikel 9 cursus ging verder dan gedrevenheid en ambities; wat heeft geleid tot een hele mooie, pure en zeer dierbare vriendschap. **Kelly**, bedankt dat je de afgelopen 4 jaar mijn inuline-redder-in-nood, mijn wandelende agenda en mijn rosé(bier)-genootje/vriendinnetje was en nog steeds bent!

Tot slot mijn lieve familie en schoonfamilie, ik ben enorm trots en dankbaar dat ik altijd bij jullie terecht kan voor onvoorwaardelijke steun, een moment van rust, liefde, gezelligheid en om de drukke stad even in te ruilen voor het nuchtere 'down-to-earth' plattelandsleven.

Lieve **Daan**, mijn beste maatje, mijn grootste steun, en allerliefste vriend! Jij hebt alles van heel dichtbij meegemaakt, stond altijd voor mij klaar en telkens was je weer even trots. Er zijn ontelbaar veel dingen waar ik je voor zou willen bedanken, maar vooral bedankt voor al je goede zorgen, je vertrouwen, je steun, je begrip, geduld en heel veel liefde de afgelopen 4 jaar!

Liefs
lisa

9